



Forschungszentrum Karlsruhe
in der Helmholtz-Gemeinschaft

Wissenschaftliche Berichte
FZKA 6979

Experiments on the Oxidation of Boron Carbide at High Temperatures

**M. Steinbrück, A. Meier, U. Stegmaier,
L. Steinbock**

**Institut für Materialforschung
Programm Nukleare Sicherheitsforschung**

Mai 2004

Forschungszentrum Karlsruhe

in der Helmholtz-Gemeinschaft

Wissenschaftliche Berichte

FZKA 6979

Experiments on the Oxidation of Boron Carbide at High Temperatures

M. Steinbrück, A. Meier, U. Stegmaier, L. Steinbock

Institut für Materialforschung

Programm Nukleare Sicherheitsforschung

Forschungszentrum Karlsruhe GmbH, Karlsruhe

2004

Impressum der Print-Ausgabe:

**Als Manuskript gedruckt
Für diesen Bericht behalten wir uns alle Rechte vor**

**Forschungszentrum Karlsruhe GmbH
Postfach 3640, 76021 Karlsruhe**

**Mitglied der Hermann von Helmholtz-Gemeinschaft
Deutscher Forschungszentren (HGF)**

ISSN 0947-8620

urn:nbn:de:0005-069792

OXIDATION VON BORKARBID BEI HOHEN TEMPERATUREN

ZUSAMMENFASSUNG

Borkarbid wird weltweit in verschiedenen Kernreaktoren als Absorbermaterial in Steuerstäben eingesetzt. Während eines hypothetischen schweren Störfalls führen eutektische Wechselwirkungen zwischen B_4C und den umgebenden Hüllrohren aus rostfreiem Stahl schon bei Temperaturen um 1200 °C und somit weit unterhalb der Schmelztemperaturen der einzelnen Komponenten zur Bildung von Schmelzphasen. Das so freigelegte Absorbermaterial sowie gebildete B_4C /Metall-Schmelzen sind dem Dampf im Reaktor ausgesetzt. Die Oxidation von Borkarbid ist stark exotherm und führt zur Bildung von gasförmigen Reaktionsprodukten, wie H_2 , CO , CO_2 and CH_4 , die u. a. die Spaltproduktchemie beeinflussen.

Es wurden umfangreiche Versuchsserien zum Oxidationsverhalten von Borkarbid bei hohen Temperaturen durchgeführt. Vier unterschiedliche B_4C Probenmaterialien wurden unter unterschiedlichen dampfhaltigen Atmosphären im Temperaturbereich zwischen 800 und 1600 °C untersucht. Im Unterschied zu bisher publizierten Daten bei niedrigeren Temperaturen, die auf der Auswertung von Masseänderungen der Proben basieren, wurden in den hier vorgestellten Untersuchungen massenspektrometrisch ermittelte Gasfreisetzungsraten zur Bestimmung der Oxidationskinetik herangezogen.

Die Oxidation von Borkarbid wird bestimmt durch die Bildung einer flüssigen oberflächlichen Boroxidschicht, die als Diffusionsbarriere wirkt, und deren Reaktion mit Dampf unter Bildung von flüchtigen Borsäuren bzw. deren direkter Verdampfung bei Temperaturen oberhalb 1500 °C . Bildung und Verbrauch von B_2O_3 ergeben insgesamt eine paralineare Reaktionskinetik. Bei den für schwere Störfälle typischen Bedingungen (Temperatur, Dampfangebot) stellt sich aber schon kurz nach Initiierung der Oxidation eine lineare Oxidationsrate ein.

Diese ist stark beeinflusst von den thermohydraulischen Umgebungsbedingungen, insbesondere von Dampf rate und Dampfpartialdruck. Die Eigenschaften der B_4C -Proben selbst haben nur einen vergleichsweise geringen Einfluss auf die Oxidationskinetik.

Bei den gewählten Versuchsbedingungen wurden nur sehr geringe Mengen Methan gebildet, welches einen großen Einfluss auf die Chemie des Spaltprodukts Jod hat. Thermochemische Rechnungen bestätigten, dass Methan nur bei Temperaturen unterhalb 800 °C bevorzugt gebildet wird.

Dieser Bericht aktualisiert und ersetzt den im Rahmen des EU-Programms COLOSS (5. Rahmenprogramm 2000-2003) erstellten internen Bericht SAM-COLOSS-P026.

ABSTRACT

Boron carbide is widely used as neutron absorbing control rod material in Western Boiling Water Reactors (BWR) and Russian RBMKs and VVERs and some Pressurised Water Reactors (PWR). During a hypothetical severe accident the B₄C reacts with the surrounding stainless steel cladding forming eutectic melts at temperatures above 1200 °C which is far below the melting temperatures of all components. The remaining uncovered absorber material as well as the B₄C/metal mixtures may be exposed to the steam in the reactor core. The oxidation of boron carbide is highly exothermic and produces various gaseous reaction products like H₂, CO, CO₂ and CH₄ which may affect the fission product chemistry.

Extensive test series were performed to study the oxidation behaviour of boron carbide at high temperatures. Four types of B₄C specimens with quite different properties were investigated under various atmospheres in the temperature range between 800 and 1600 °C. In contrast to most of the data published so far mainly at lower temperatures which are based on the evaluation of mass changes, gas production data were used to determine the oxidation kinetics of B₄C in steam.

The oxidation kinetics of boron carbide are determined by the formation of a liquid boron oxide barrier diffusion layer and its loss due to the reaction with surplus steam to form volatile boric acids and/or direct evaporation at temperatures above 1500 °C. The overall reaction kinetics are parabolic. Under the conditions typical for severe accidents (high temperatures and steam flow rates) linear oxidation kinetics establishes soon after initiation of the oxidation.

The oxidation kinetics are strongly influenced by the surrounding conditions, in particular by the steam flow rate and the steam partial pressure. On the other hand, the properties of the B₄C sample itself have only a limited effect on the oxidation.

Only very low amounts of methane - which is of interest for the fission gas chemistry due to the formation of organic iodine - were produced in these tests. The highest methane release was measured at the lowest test temperatures in agreement with thermo-chemical pre-test calculations.

This report updates and replaces the internal report SAM-COLOSS-P026 published as one deliverable of the EC COLOSS program (5th Framework Program 2000-2003).

CONTENTS

1	Introduction.....	1
2	Experimental set-up	2
3	Test conduct.....	5
4	Specimens.....	6
5	Experimental results.....	12
5.1	Transient test series	12
5.2	Isothermal test series.....	14
5.2.1	Framatome pellets	14
5.2.2	CODEX pellets.....	23
5.2.3	ESK pellets	24
5.2.4	ESK powder	28
5.2.5	Comparative views	29
5.3	Tests under varying atmosphere	33
5.4	Further tests.....	36
6	Thermo-chemical equilibrium calculations	37
7	Summary, discussion and conclusions	38
	Acknowledgements	41
	References	42
	Appendix	44
A1	Test parameters of experiments on B ₄ C oxidation in the BOX rig (chronological order).....	45
A2	Essential results of isothermal experiments on B ₄ C oxidation in the BOX rig	49
A3	Conversion from H ₂ volume rates into reaction rates	52
A4	Figures A1 – A64: Test protocols	53

LIST OF TABLES

Table 1:	Relative intensities of the MS signals of all gaseous species measured and used for quantitative analyses	4
Table 2:	B ₄ C specimens used in BOX experiments	7
Table 3:	Chemical composition of the B ₄ C specimens in mass-%	7
Table 4:	Release of hydrogen and carbon dioxide during complete oxidation of a small B ₄ C specimen. Expected results based on Equation 2.	37
Table A1:	Test parameters of experiments on B ₄ C oxidation in the BOX rig (chronological order)	45
Table A2:	Essential results of isothermal experiments on B ₄ C oxidation in the BOX rig	49
Table A3:	Geometric surface of the specimens and conversion factors from volume into specific molar hydrogen release rates	52

LIST OF FIGURES

Figure 1:	BOX Rig for the investigation of the oxidation kinetics of B ₄ C	3
Figure 2:	Injection of steam into the empty reaction tube and its measurement by the mass spectrometer during the commissioning tests	3
Figure 3:	B ₄ C specimen support for scoping tests (top) and improved version (bottom)	4
Figure 4:	B ₄ C powder specimen in a shallow zirconia crucible	5
Figure 5:	Typical test conduct of a transient test from 800 to 1500 °C	5
Figure 6:	Typical test conduct of an isothermal test, here: at 1100 °C	6
Figure 7:	X-ray diffraction pattern of the B ₄ C specimens	8
Figure 8:	Cumulative pore volume and pore size distribution in pellet samples	9
Figure 9:	Optical microscopy images of the three types of B ₄ C absorber pellets investigated	10
Figure 10:	SEM images of the three types of B ₄ C absorber pellets investigated	11
Figure 11:	Gas release during transient oxidation of a B ₄ C pellet in argon steam atmosphere	12
Figure 12:	Dependence of hydrogen release rate (as a measure for the B ₄ C oxidation rate) on temperature: a) linear scale; b) Arrhenius type diagram	13
Figure 13:	Gas release during transient oxidation of B ₄ C pellets in steam and steam/hydrogen. Argon was used as carrier gas in all tests.	14
Figure 14:	Comparison of two transient oxidation tests with/without isothermal pre-phase at 800 °C	15
Figure 15:	Gas release during isothermal oxidation of Framatome pellets	15
Figure 16:	Ion currents measured by mass spectrometer: a) at mass 62 indicating formation of orthoboric acid H ₃ BO ₃ , b) at masses 18 and 40 showing MS performance during the tests	16
Figure 17:	Gas release during isothermal oxidation of Framatome pellets at low steam injection rates	17
Figure 18:	Ion currents measured by mass spectrometer: a) at mass 62 indicating formation of orthoboric acid H ₃ BO ₃ , b) at masses 18 and 40 showing MS performance during the tests	18
Figure 19:	Appearance of Framatome B ₄ C pellets after isothermal tests (first series) at the indicated temperatures	19
Figure 20:	B ₄ C specimens after isothermal oxidation in steam: SEM images of the pellet surfaces (40x)	20

Figure 21: B ₄ C specimens after isothermal oxidation in steam: SEM images of the pellet surfaces (160x)	21
Figure 22: B ₄ C specimens after isothermal oxidation in steam: SEM images of the pellet surfaces (1600x)	22
Figure 23: X-ray diffraction patterns of Framatome pellets after tests at 800 and 1400 °C in comparison with an as-received specimen	23
Figure 24: Gas release during isothermal oxidation of CODEX pellets	24
Figure 25: Ion currents measured by mass spectrometer: a) at mass 62 indicating formation of orthoboric acid H ₃ BO ₃ , b) at masses 18 and 40 showing MS performance during the tests	24
Figure 26: Gas release during isothermal oxidation of ESK pellets	25
Figure 27: Ion currents measured by mass spectrometer: a) at mass 62 indicating formation of orthoboric acid H ₃ BO ₃ , b) at masses 18 and 40 showing MS performance during the tests	26
Figure 28: Gas release during isothermal oxidation of ESK pellets at low steam flow	26
Figure 29: Ion current measured by mass spectrometer: a) at mass 62 indicating formation of orthoboric acid H ₃ BO ₃ , b) at masses 18 and 40 showing MS performance during the tests at low steam flow rates	26
Figure 30: Formation and relocation of superficial boron oxide at dense ESK pellets. a) bottom surface after isothermal tests at high steam flow; b) bottom surface after isothermal tests at low steam flow; c) shell surface after tests at 800 and 1400 °C at low steam flow	27
Figure 31: Gas release during isothermal oxidation of ESK powder	28
Figure 32: Ion current measured by mass spectrometer: a) at mass 62 indicating formation of orthoboric acid H ₃ BO ₃ , b) at masses 18 and 40 showing MS performance during the tests	28
Figure 33: Hydrogen release during isothermal oxidation of the various specimens	29
Figure 34: Hydrogen release during isothermal oxidation of the various specimens at 1200 °C showing 1) peak oxidation rates for porous specimens after initiation of steam injection and 2) dependence of oxidation rate on steam flow	30
Figure 35: Integral release of H ₂ , CO, CO ₂ and CH ₄ during 30 min isothermal oxidation in steam in dependence on temperature.	31
Figure 36: Hydrogen release during isothermal oxidation of various B ₄ C specimens in flowing steam/argon mixture at 800 °C	31
Figure 37: Integral mass change of B ₄ C specimens after 30 min oxidation in a flowing steam/argon mixture in dependence on temperature	32
Figure 38: Pre-test mass (black), post-test mass (red), B ₂ O ₃ formed, recalculated from the hydrogen release data (green), and B ₂ O ₃ remaining in the specimen, calculated as the difference between post-test mass and	

oxidised B ₄ C (blue) for the various specimens in dependence on temperature	33
Figure 39: Oxidation of Framatome B ₄ C pellets under changing steam/hydrogen atmosphere at 800 and 1200 °C.	34
Figure 40: Detailed results of test Box00921 at 800 °C: a) methane release, b) ratio between carbon dioxide and carbon monoxide release rates	34
Figure 41: Oxidation of B ₄ C pellets at 1200 °C in flowing Ar/steam; left: varying steam flow rate, right: varying argon flow rate.	35
Figure 42: Influence of steam flow rate (left) and argon flow rate (right) on the oxidation kinetics of B ₄ C at 1200 °C	35
Figure 43: Mass change of a B ₄ C pellet during heat-up to 1350 °C in pure argon	36
Figure 44: Thermo-chemical calculations: a) equilibrium composition of 1 B ₄ C and 10 H ₂ O in dependence on temperature, b) ratio of the carbon containing species CH ₄ /(CO+CO ₂) in dependence on temperature and inlet gas composition	37
Figure 45: Dependence of the equilibrium composition of 1 B ₄ C and 10 H ₂ O on system pressure at 1000 °C (left) and 1500 °C (right)	38
Figure 46: Oxidation of B ₄ C at high temperatures: comparison of recent FZK results with literature data obtained at different steam partial pressures	39
Figure 47: Oxidation of B ₄ C at high temperatures: comparison of recent FZK results with literature data obtained at different steam partial pressures (Arrhenius diagram)	40
Figure 48: Ratio of boron oxide remained in the specimen and boron oxide totally produced during isothermal tests with Framatome pellets	40
Figure A1-A64: Test conduct and main results of the MS measurements	54-117

1 Introduction

Boron carbide is widely used as neutron absorbing control rod material in Western Boiling Water Reactors (BWR) and Russian RBMKs and VVERs. Additionally, in French Pressurised Water Reactors (PWR) it is used together with Ag-In-Cd alloy in so-called hybrid control rods [1]. During a hypothetical severe accident the B₄C reacts with the surrounding SS cladding forming eutectic melts at temperatures above 1200 °C [2-4] which is far below the melting temperatures of all components. The remaining uncovered absorber material as well as the B₄C/metal mixtures may be exposed to the steam in the reactor core.

The oxidation of B₄C by steam is highly exothermic and produces 6-7 times the amount of hydrogen as the oxidation of the same mass of Zircaloy. Furthermore, gaseous carbon- and boron-containing species are formed which may affect the fission product chemistry in the containment, e.g. for the release of organic iodine compounds.

The following chemical reactions are thought to play a role during oxidation of boron carbide:



Surplus steam then reacts with the liquid boron oxide to form more volatile boric acids:



At higher temperatures, also direct evaporation of boron oxide is possible:



Currently, only a few data sets on the oxidation kinetics of boron carbide are available, most of them obtained at temperatures ≤ 1000 °C [5-8]. Only Gogotsi [9] and Sato [10] published results on the oxidation of hot-pressed B₄C pellets up to temperatures of 1200 and 1300 °C, respectively. The results of all these tests are mostly based on the evaluation of mass changes. They vary in a wide range and are strongly dependent on the material composition and physical form of the B₄C (pellets or powder) and in particular on the test conditions. No data exist on the oxidation behaviour of sintered B₄C pellets, typical for French PWR design.

Therefore, a separate-effects test program on boron carbide oxidation (BOX) up to 1600 °C was conducted at Forschungszentrum Karlsruhe (FZK) within the COLOSS project of the Euratom 5th Framework Programme. It is closely related to the FZK bundle tests QUENCH-07 [13] and QUENCH-09 [17] with a B₄C control rod and the French Phebus FPT-3 test [14] as well as with the separate-effects test programme at IPSN, France. This report describes

the results of the extensive experimental work performed with the BOX Rig. The results obtained by tests performed in a thermal balance are published in another FZKA report [11].

2 Experimental set-up

A new experimental set-up designed for the B₄C oxidation tests (BOX Rig) was put into operation in the first year of the project. The BOX Rig ([Figure 1](#)) consists of

- A gas supply system for Ar, H₂ and steam (0-4 mol/h each), consisting of two gas flow controllers, one liquid flow controller and a so-called controlled evaporator mixer unit (CEM), where the liquid water was evaporated and mixed with the non-condensable gas. The whole system is delivered by Bronkhorst High-Tech B.V.
- A tube furnace with maximum temperatures of 1700 °C, with an alumina reaction tube (inner diameter: 32 mm, length: 600 mm) and molybdenum heaters, delivered by HTM Reetz GmbH Berlin.
- A quadrupole mass spectrometer (MS) Balzers GAM 300.

The off-gas tube from the furnace to the MS (SS, inner diameter: 6 mm, length: 2,7 m) is heated to about 150 °C to prevent steam condensation. The mass spectrometer allows the quantitative analysis of all gaseous reaction products. In particular, the hydrogen release rate was used in most of the tests as a continuous measure for the reaction kinetics. [Table 1](#) summarises the relative intensities of all MS peaks of the species measured and indicates which masses were used for quantitative analysis. CO and N₂ have their main peaks at the same mass 28. Therefore, it had to be assumed, that nitrogen is completely absent in the system. Furthermore, there is an overlapping of peaks from CO₂ and boric acid at mass 44. This may lead to erroneous measurements of CO and CO₂. That is why only the hydrogen signal is used for quantitative analysis of the oxidation kinetics.

The mass spectrometer is calibrated for H₂, CO, CO₂, and CH₄ with certificated 95%Ar-5%gas mixtures. The Bronkhorst supply system for steam and gas was used for steam calibration. All parts of the system are computer controlled by a LabView program especially written for the BOX Rig.

The commissioning tests were performed successfully. The steam flow rate can be regulated sufficiently well and is measured accurately by the MS ([Figure 2](#)). Problems arising from the condensation of boric acids in the off-gas system have been at least partially solved by heating the off-gas pipes and periodically cleaning the whole off-gas system with steam. Nevertheless, there has been the tendency for blockage of the off-gas system and the capillary tube of the mass spectrometer during tests at temperatures ≥ 1400 °C.

For first scoping tests, the specimens were kept in a normal alumina boat in the reaction tube. Strong interactions between the B₄C pellets and the Al₂O₃ were observed for temperatures above 1400 °C. Furthermore, the pellets showed an axially inhomogeneous oxidation due to the inhomogeneous steam flow along the specimens. Therefore, the sample support was changed 1) by using an yttria disc as sample support and 2) by sawing off the wall of the alumina boat directed to the steam flow ([Figure 3](#)).

The powder specimens were kept in a small flat crucible as shown in Figure 4.

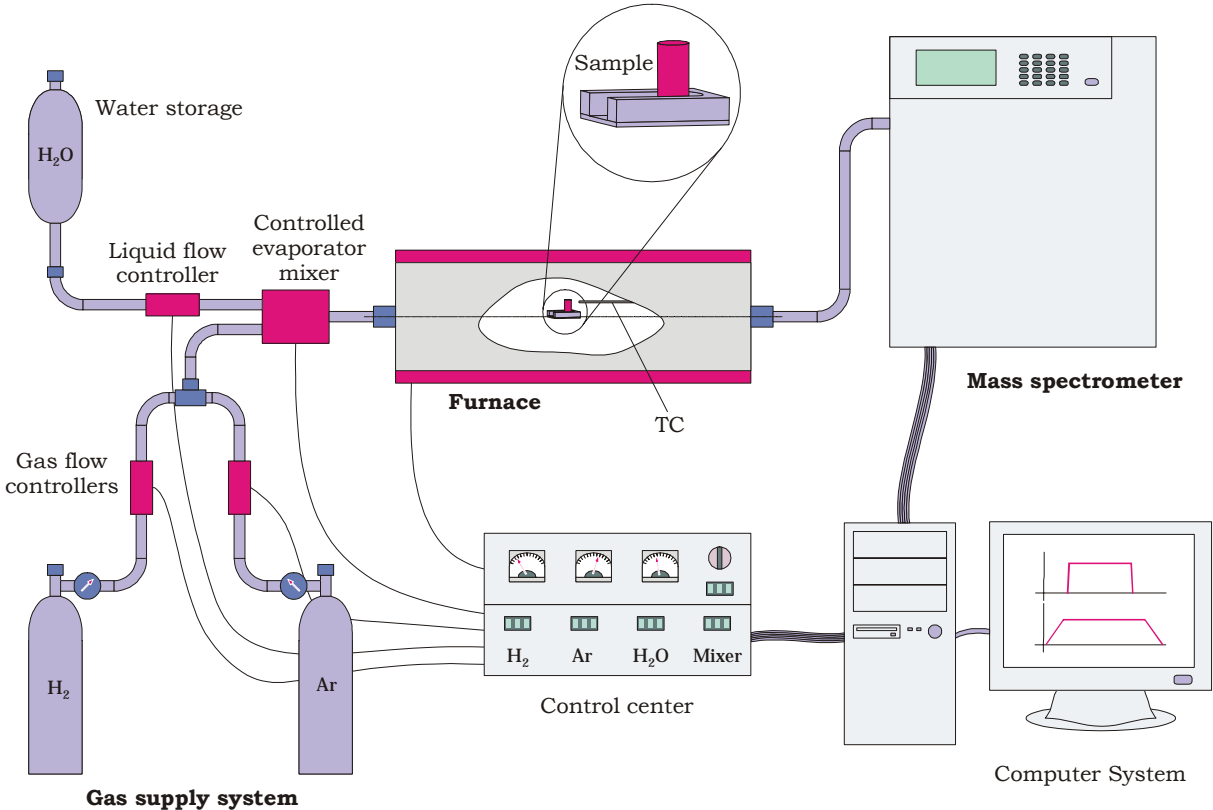


Figure 1: BOX Rig for the investigation of the oxidation kinetics of B₄C

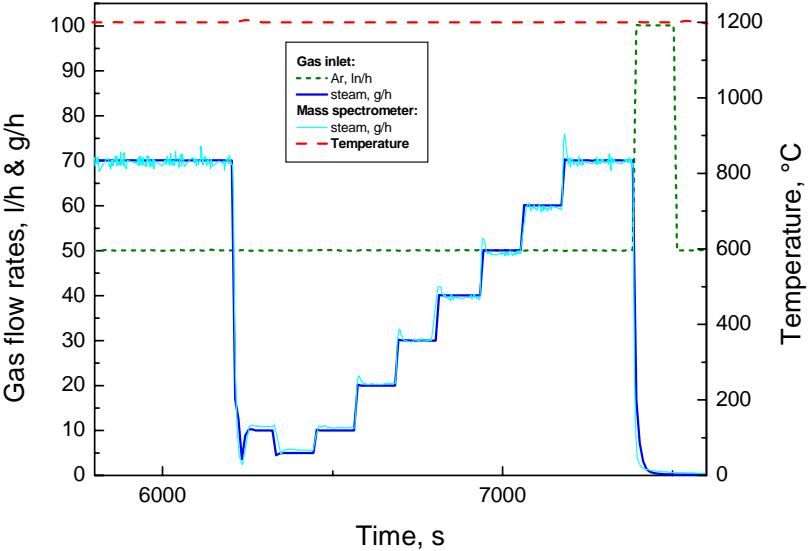


Figure 2: Injection of steam into the empty reaction tube and its measurement by the mass spectrometer during the commissioning tests

Table 1: Relative intensities of the MS signals of all gaseous species measured and used for quantitative analyses

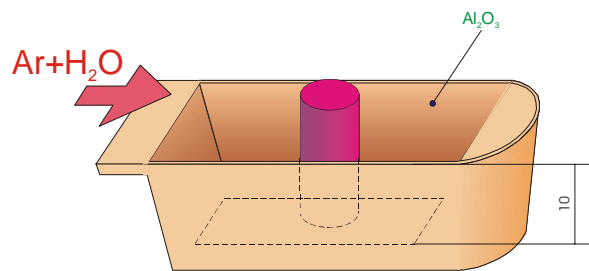
	1	2	12	13	14	15	16	17	18	20	22	28	29	32	40	44	45, 62 ...
H ₂	2	100															
H ₂ O	2	<1					2	26	100								
CO			6		1		3					100	1				
CO ₂			10				16				2	13				100	
(N ₂) ¹					14							100	1				
CH ₄	16		3	8	16	85	100	1									
O ₂														100			
Ar										23					100		
BA ²																!	x

1 not measured

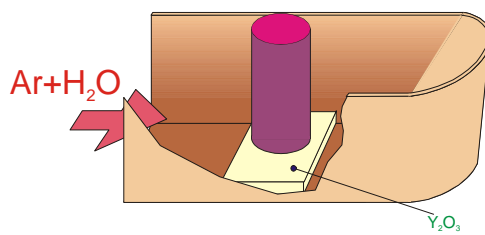
2 boric acids



considered for quantitative analysis



First test series



New test series

Figure 3: B₄C specimen support for scoping tests (top) and improved version (bottom)

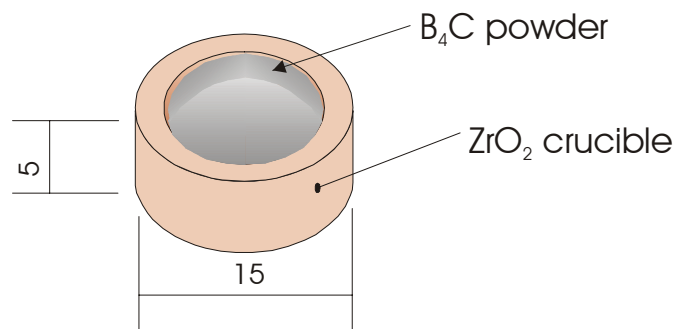


Figure 4: B₄C powder specimen in a shallow zirconia crucible

3 Test conduct

The specimens were usually heated in an inert atmosphere (50 l/h argon at normal conditions, i.e. 0 °C and 1 bar) up to the desired starting temperature for the transient or isothermal oxidation. Then, the steam injection was switched on, usually with a flow rate of 30 g/h resulting in a steam partial pressure of 42755 Pa. At the end of the oxidation period, the steam flow was switched off and the argon flow increased to 100 l/h to accelerate the gas exchange from oxidising to inert atmosphere under which the specimens were cooled. Figures 5 and 6 show as examples typical test conducts for transient and isothermal experiments, respectively. The injected steam mass flow rates were in a large surplus in comparison to the amount of steam consumed by the oxidation reaction, as can be seen from both the steam curves (injected, off-gas) in the diagrams. A small deviation of the outlet steam flow rate from the inlet rate was observed only at the beginning of the test and at the highest temperatures, when the oxidation rate was very high. Thus, no steam starvation was expected to occur during these tests.

The heating rate during the heat-up phase and in the transient tests was 20 K/min.

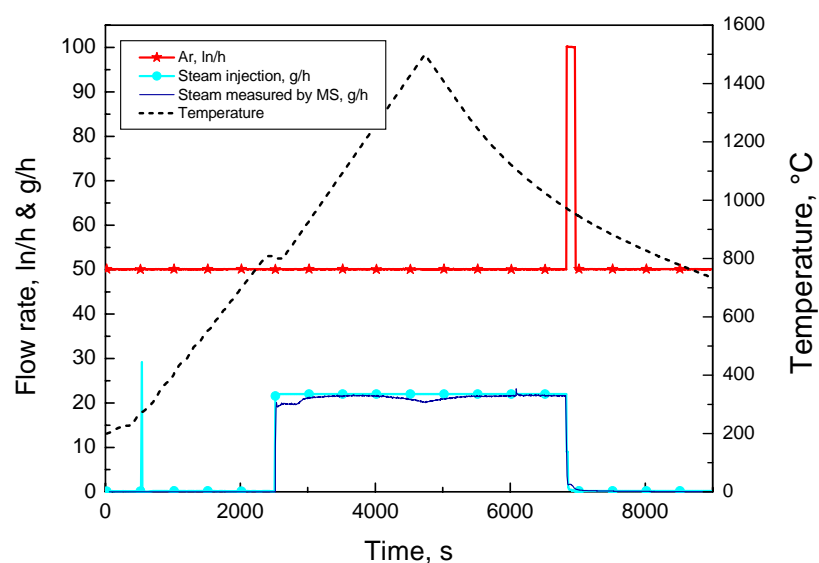


Figure 5: Typical test conduct of a transient test from 800 to 1500 °C

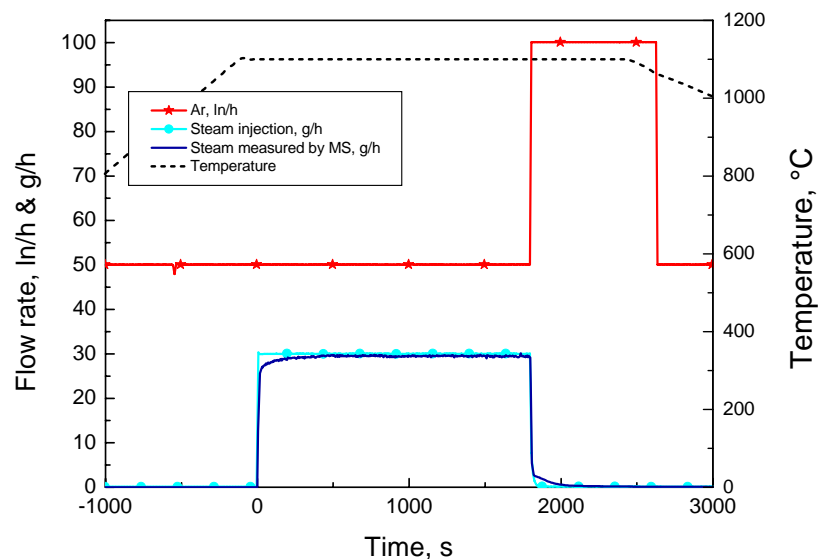


Figure 6: Typical test conduct of an isothermal test, here: at 1100 °C

4 Specimens

Four types of B_4C specimens were investigated: 1) commercial pellets used in French PWRs (Framatome), 2) pellets of Russian origin used in the CODEX tests at AEKI Budapest with boron carbide control rod (CODEX), 3) dense absorber pellets without open porosity obtained by Elektroschmelzwerk Kempten, Germany (ESK) and 4) B_4C powder as formerly used in German BWRs and obtained by the same company (ESK powder). The different species were chosen to investigate the influence of the sample (state, geometry, density, porosity etc.) on the oxidation behaviour. [Table 2](#) summarises the main properties of the different samples.

For **chemical analysis** of the impurities the specimens were crushed in a boron carbide mortar, dissolved by microwave digestion under pressure in HNO_3/HF and analysed by inductively coupled plasma optical emission spectroscopy (ICP-OES). The carbon content was analysed by combustion method. The results are summarised in [Table 3](#). The boron and the silicon concentration could not be analysed due to restrictions in the method, therefore, the boron concentration given in Table 3 is calculated as the difference between the sum of all analysed elements and 100 %. The CODEX pellets contain a relatively high amount of impurities, especially of aluminium and stainless steel components.

Further on, X-ray diffraction was used to identify the **crystallographic phase composition** of the specimens. [Figure 7](#) summarises the results. As expected, the rhombohedral B_4C phase is the main phase in all specimens. A small amount of free carbon was detected in the CODEX specimen. A very few peaks of small intensity could not assigned to a known phase.

Table 2: B₄C specimens used in BOX experiments

	Pellet Framatome	Pellet CODEX	Pellet ESK*	Powder ESK
diameter	7.47 mm	7.5 mm	12.25 mm	10.95 mm
height	14.0 mm	10.3 mm	9.4 mm	3.0 mm
mass	≈ 1.1 g	≈ 0.82 g	≈ 2.6 g	≈ 0.46 g
density	1.8 g/cm ³	1.8 g/cm ³	2.34 g/cm ³	1.6 g/cm ³
geometric surface	3.724 · 10 ⁻⁴ m ²	2.87 · 10 ⁻⁴ m ²	4.8 · 10 ⁻⁴ m ²	0.942 · 10 ⁻⁴ m ²
volume	6.136 · 10 ⁻⁷ m ³	4.55 · 10 ⁻⁷ m ³	1.11 · 10 ⁻⁶ m ³	2.825 · 10 ⁻⁷ m ³
surface/volume	607 m ⁻¹	631 m ⁻¹	432 m ⁻¹	333 m ⁻¹
BET surface specific, total	3.5-4.0 m ² /g 4 m ²			0.07 m ² /g 0.03 m ²
pore volume mean pore size	160 mm ³ /g ca. 5 μm	110 mm ³ /g ca. 5 μm	5 mm ³ /g < 1 μm	
grain size				14 mesh and finer
supplier	Framatome	Russia	ESK	ESK

* mean values, exact values are given in the appendix, [Table A3](#)

Table 3: Chemical composition of the B₄C specimens in mass-%

Specimen → Element ↓	FRAMATOME	CODEX	ESK	ESK powder
C	22.27 ± 0.02	18.81 ± 0.07	21.83 ± 0.33	20.99 ± 0.09
Al	0.0829 ± 0.0006	0.343 ± 0.010	0.0070 ± 0.0006	0.0166 ± 0.0001
Ba	0.00048 ± 0.00004	0.00054 ± 0.00005	0.00003 ± 0.00001	0.00034 ± 0.00001
Ca	0.0269 ± 0.0015	0.0646 ± 0.0002	0.0133 ± 0.0009	0.0197 ± 0.0003
Cr	0.0014 ± 0.0001	0.232 ± 0.002	0.0008 ± 0.00005	0.00025 ± 0.00001
Fe	0.110 ± 0.001	1.538 ± 0.004	0.058 ± 0.001	0.0307 ± 0.0001
K	0.0011 ± 0.0006	0.0008 ± 0.00003	0.00044 ± 0.00012	0.0017 ± 0.0001
Ni	0.0048 ± 0.0003	0.1139 ± 0.0007	0.00089 ± 0.00015	0.00038 ± 0.00001
Ti	0.0069 ± 0.0011	0.0351 ± 0.0002	0.0225 ± 0.0009	0.0110 ± 0.0004
Σ impurities	0.23	2.33	0.10	0.08
rest (B)	77.50	78.86	78.07	78.93
ratio B/C	3.5	4.2	3.6	3.8

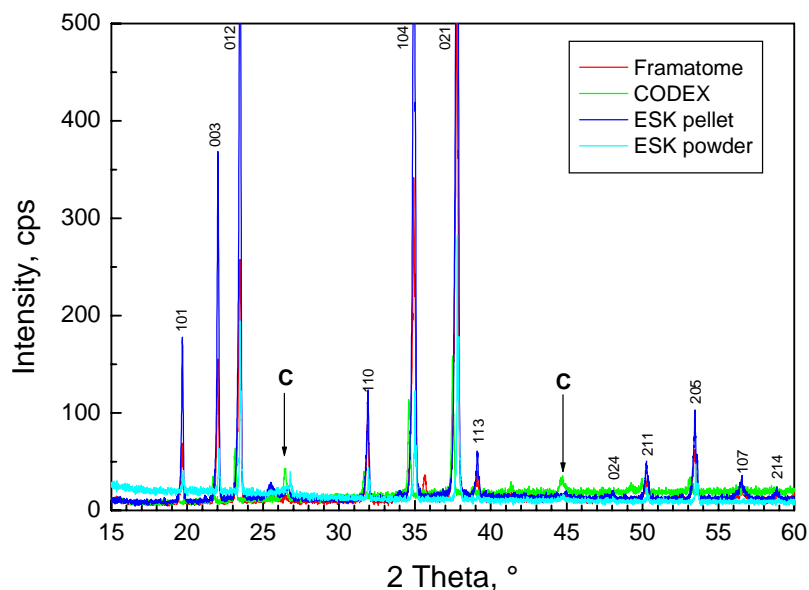


Figure 7: X-ray diffraction pattern of the B_4C specimens

First test results indicated that the free surface of the specimens should have a considerable influence on the oxidation kinetics. Therefore, the **BET adsorption technique** was used to determine the reactive surface of the powder and the Framatome pellets. The results are indicated in Table 2. Whereas the obtained value for the powder is reliable, the measured BET surfaces of the pellet were widely scattering due to limitations of the method regarding solid samples; so the value for the pellet has to be treated with caution.

Hence, the **Hg-porosimetry** was used to characterise the pore volume and distribution of the pellet specimens. The Framatome pellets have the highest porosity of 28.2 %, but a marked peak of the pore radius between 5 and 10 μm . The porosity of the CODEX sample is comparable with 19.5 %, but [Figure 8](#) shows a much broader distribution of the pore size. The porosity of the ESK pellet is considerably lower (1.3 %), the mean pore size is less than 1 μm .

Finally, a number of images of polished cross sections of the various pellets were taken by optical microscopy and scanning electron microscopy (SEM) with secondary and back-scattered electrons (SE, BSE). A selection of such images is compiled in [Figures 9-10](#). These images confirm the results obtained by various methods discussed above and impressively show the very different microstructure of the three kinds of pellets investigated. The Framatome pellets have a very uniform microstructure; the open porosity is clearly visible. On the other hand, the microstructure of the CODEX pellets is very irregular and dominated by large porous grains. The SEM-BSE image (Figure 10) shows a relatively high amount of metal impurity phases, indicated by the light spots. Besides, the B_4C phase composition seems to vary within the specimen as could be indicated by the variation of grey tones in the OM images (Figure 9). The ESK pellets again have a very uniform microstructure with smaller, obviously closed pores and no signs of impurity phases.

Altogether, the samples investigated have quite different microstructures whose influence on the oxidation kinetics could be analysed during the test series. Most of the experiments were

performed using the Framatome pellets which were used as a reference material. Thus, isothermal tests have been performed between 800 and 1600 °C in 100 K steps using Framatome samples. The test program for the other specimens was restricted to experiments at 800, 1000, 1200, and 1400 °C.

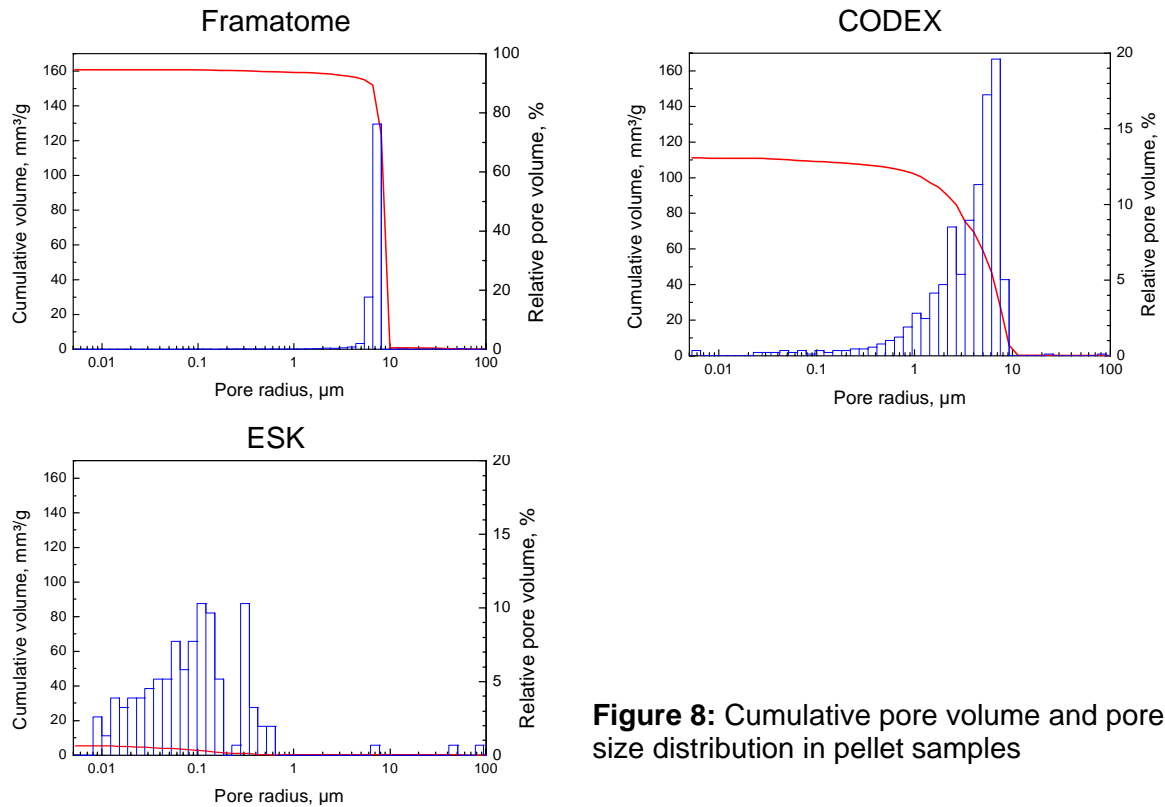
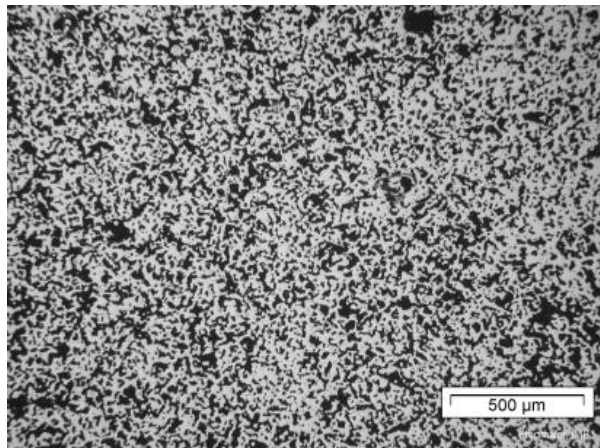
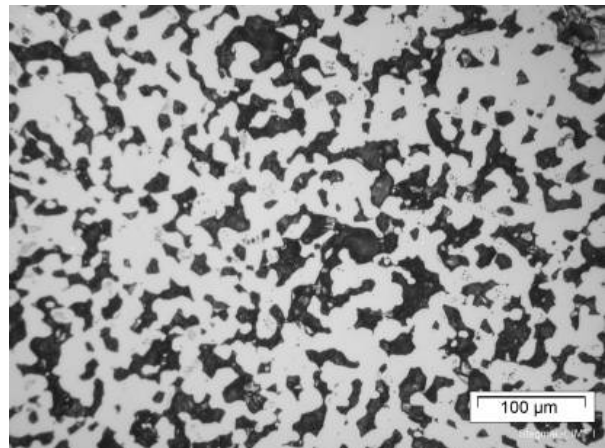


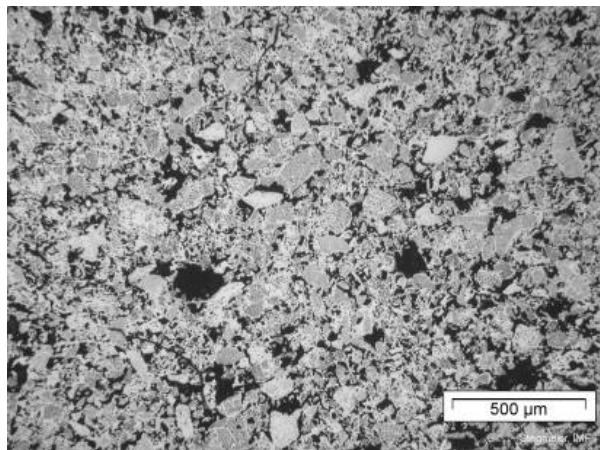
Figure 8: Cumulative pore volume and pore size distribution in pellet samples



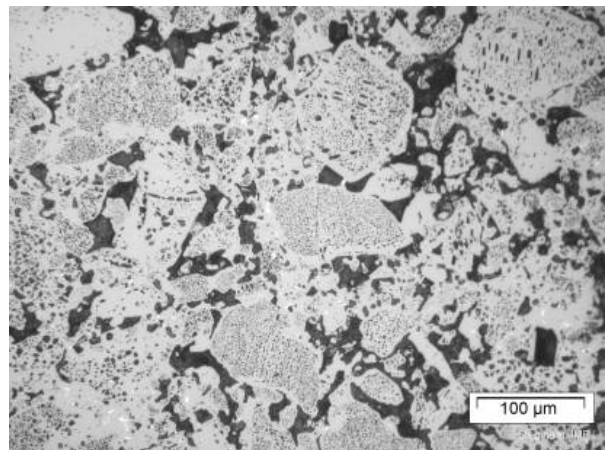
Framatome, 35x



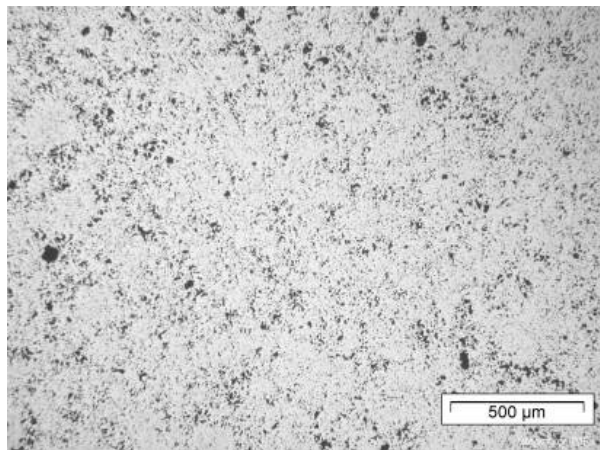
Framatome, 140x



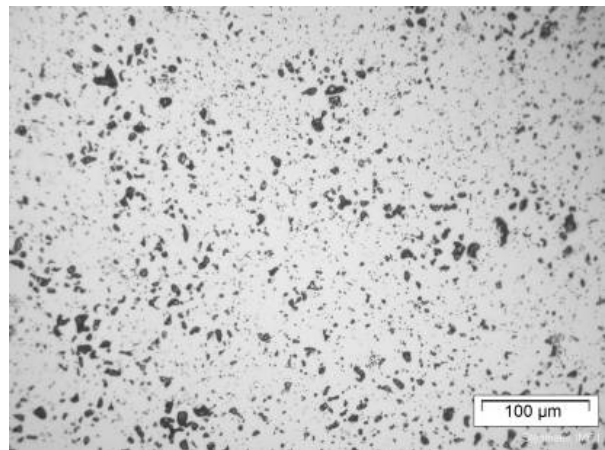
CODEX, 35x



CODEX, 140x



ESK, 35x



ESK, 140x

Figure 9: Optical microscopy images of the three types of B₄C absorber pellets investigated

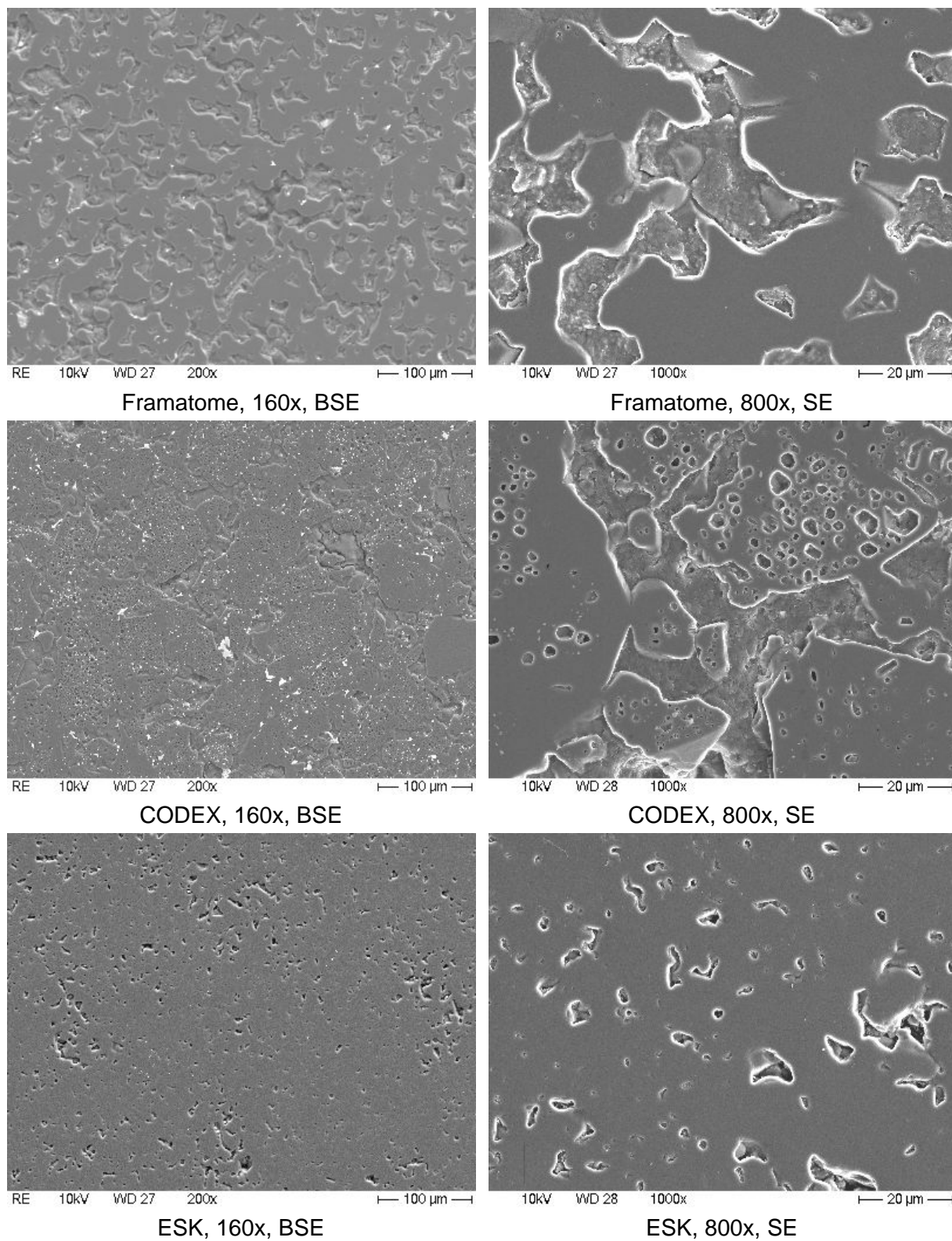


Figure 10: SEM images of the three types of B₄C absorber pellets investigated

5 Experimental results

5.1 Transient test series

Six transient tests with Framatome pellets were performed in order to get an idea on the reaction behaviour of B_4C in argon/steam and argon/steam/hydrogen in the temperature range of interest between 800 and 1500 °C. The main test parameters, conduct and gas release data of all tests are compiled in the appendix of this report.

Figure 11 shows a typical example of the gas release during a transient test. The main gaseous reaction products are hydrogen, carbon monoxide and carbon dioxide, as it is expected from equations 1-2. Methane was produced, only to a lesser extent, at the beginning of the oxidation phase at the lowest temperatures. Taking the hydrogen release rate as a measure of the oxidation rate, one could recognise from Figure 11 a strong oxidation peak immediately after steam inlet. Then, the oxidation rate remains roughly constant during heat-up of the pellet up to temperatures of about 1200 °C, before, at higher temperatures the rate accelerates again with increasing temperature. The first peak could be caused 1) by enhanced oxidation of the bare pellet surface before a barrier layer has been established and 2) by a change of the reactive surface at the beginning of the test, e.g. due to plugging of open pores.

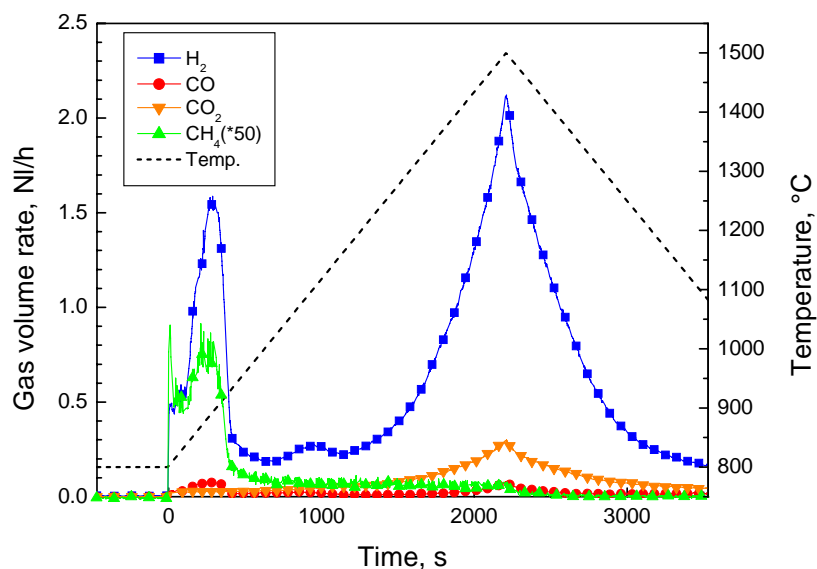


Figure 11: Gas release during transient oxidation of a B_4C pellet in argon steam atmosphere

Figures 12 a,b illustrate the dependence of the oxidation rate on temperature in more detail. They show a complex behaviour with an intermediate peak at about 1100 °C at lower temperatures, before an exponential Arrhenius type temperature dependence indicating thermal activation of the oxidation reaction is established starting at about 1270 °C.

Two tests were performed in steam hydrogen mixtures to investigate the influence of the oxygen potential on the composition of the off-gas mixture: one with comparable flow rates of steam and hydrogen and one with a surplus of hydrogen. The gas release rates measured in

these tests are shown in [Figure 13](#) in comparison with the results of the experiments in pure steam/argon mixture. The hydrogen injection clearly leads to a shift in the CO/CO₂ equilibrium towards CO. The methane release rate is only slightly influenced by the composition of the atmosphere; the reduced methane rate during the test with excess hydrogen is rather caused by a reduced overall oxidation rate due to the lower steam flow rate (7.5 vs. 25 g/h).

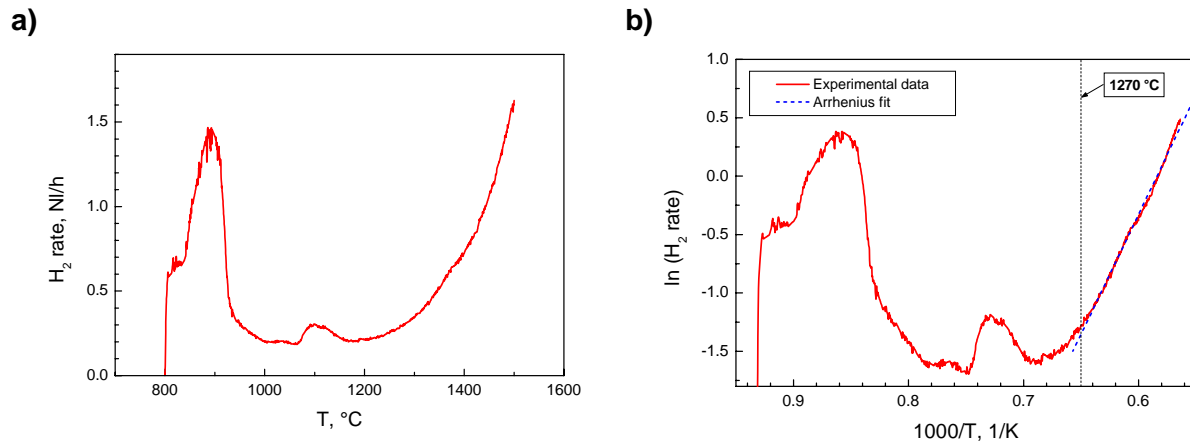


Figure 12: Dependence of hydrogen release rate (as a measure for the B₄C oxidation rate) on temperature: a) linear scale; b) Arrhenius type diagram

Figure 13 also illustrates the excellent reproducibility of the tests. Even the slightly lower hydrogen release during test Box00816 (red curve in Figure 13a) could be explained. In that test the pellet specimen tipped over during charging, which caused a slightly decreased effective surface of the specimen.

Finally, one test was performed where the temperature transient was started after equilibrium during oxidation at 800 °C had been established, in order to separate transient from initial effects. The steam flow rate was slightly different in the two tests shown in [Figure 14](#) (22 l/h in Box 00821 vs. 30 l/h in Box10406), thus one could not directly compare both tests, but the diagram gives a clear indication that the two peaks at about 900 °C and 1100 °C occur independently of the initial conditions.

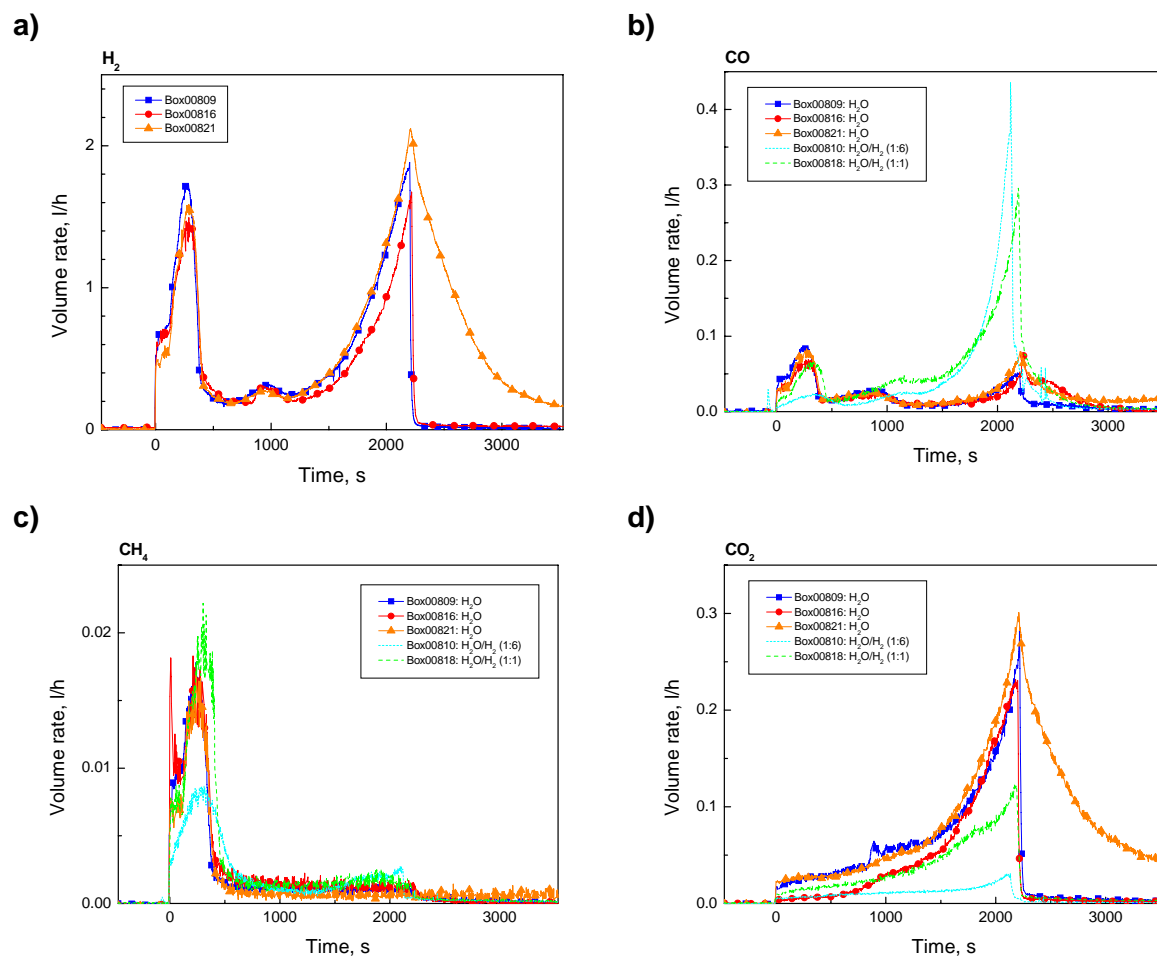


Figure 13: Gas release during transient oxidation of B₄C pellets in steam and steam/hydrogen. Argon was used as carrier gas in all tests.

Test Box10406 was a kind of combined isothermal/transient test and is therefore a good opportunity to switch over to the next chapter.

5.2 Isothermal test series

More than 40 tests on the isothermal oxidation of B₄C were performed with different species under various boundary conditions. In this chapter essential results of that experimental work is presented. The test conditions and results of all isothermal tests are compiled in the appendix of the report. The majority of the tests were performed for 30 minutes at temperatures between 800 and 1400 °C under a flowing argon/steam mixture resulting in a steam partial pressure of 42755 Pa. This automated procedure allowed easily to compare various tests with each other.

5.2.1 Framatome pellets

Most of the tests were performed with Framatome pellets. These pellets were chosen as reference material because firstly they are presently used in French nuclear reactors and secondly such kind of specimens are also used in SET on control rod degradation [12], out-

of-pile QUENCH bundle tests [13, 17] well as in the in-pile experiment PHEBUS-FPT3 [14]. The following diagrams are preferably based on results of the 3rd test series, which was performed after some improvements of the test rig and the sample support, as described in chapter 2.

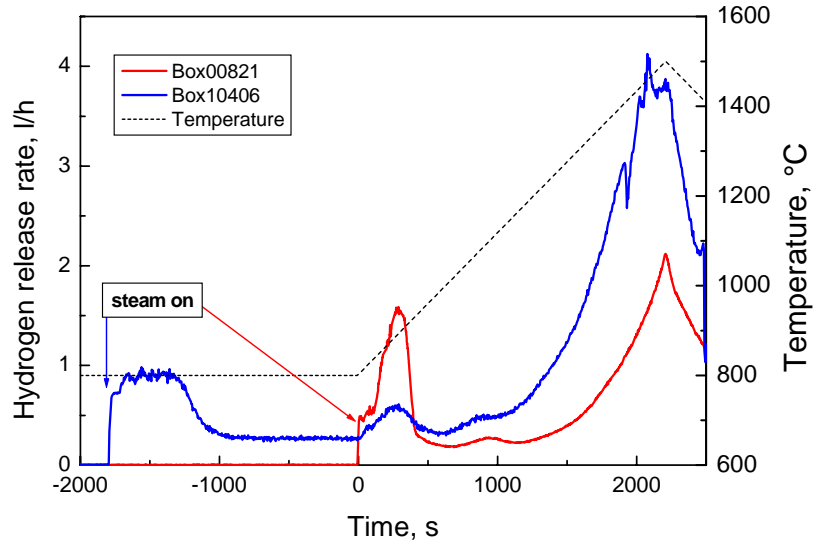


Figure 14: Comparison of two transient oxidation tests with/without isothermal pre-phase at 800 °C

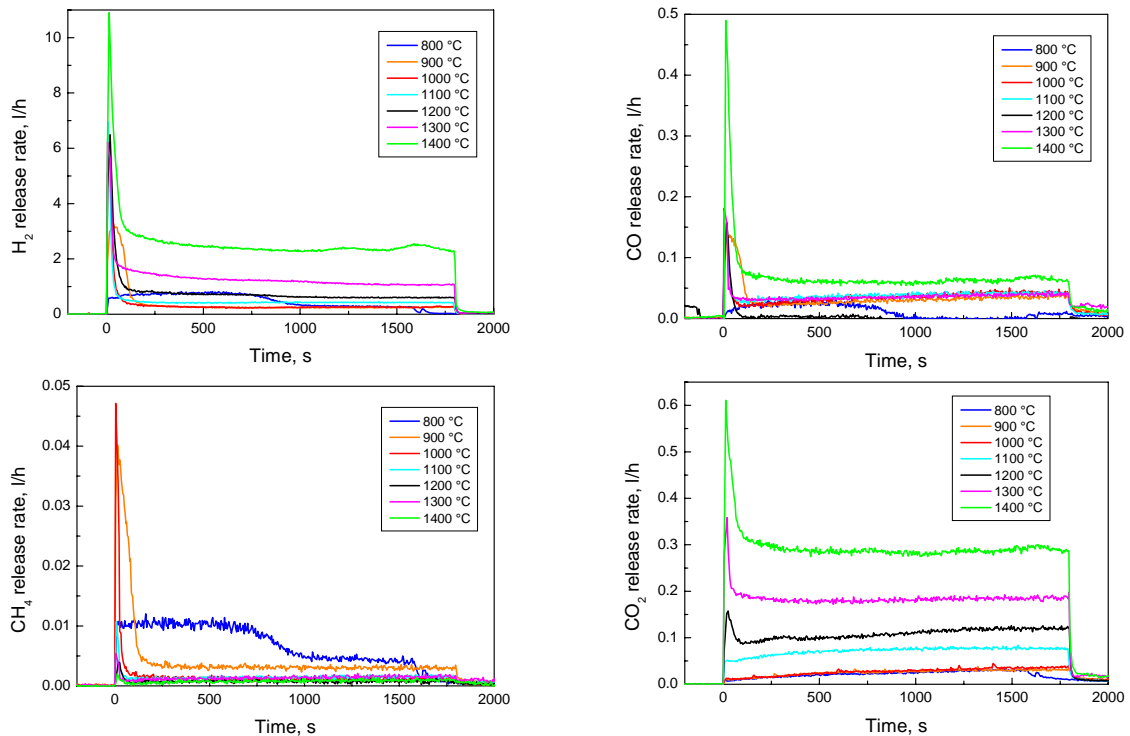


Figure 15: Gas release during isothermal oxidation of Framatome pellets

Figure 15 shows the results of the mass spectroscopic analysis of the gaseous oxidation products. There is the clear tendency for an increasing release of hydrogen, carbon monoxide (irregularities were caused by mass spectrometer malfunction) and carbon dioxide

with increasing temperature. On the other hand, the highest - but nevertheless low (pay attention to the scales!) - methane production was measured at the lowest temperature.

Obviously, the oxidation of the (porous) pellets takes place in two steps: A first peak in the production of gases, and therefore, in the oxidation rate is followed by more or less constant oxidation kinetics after a few minutes. Only at 800 °C the transition from higher to lower rates was observed after about 12 minutes. An explanation for that behaviour will be given in the discussion chapter.

Besides the non-condensable gases some masses assigned to boric acids (amu 43, 45, 62) were measured by the mass spectrometer. Boric acids are products of the reaction of B_2O_3 with steam which is believed to play a significant role in the overall oxidation kinetics. Boric acid production could only be measured qualitatively due to a missing calibration method and partial condensation in the off-gas system. Nevertheless, [Figure 16a](#) indicates that an enhanced production of orthoboric acid H_3BO_3 is starting at 1100 °C.

[Figure 16b](#) shows the ion currents at mass 18 and 40 belonging to steam and argon as a measure for the overall performance of the mass spectrometer during the tests. Obviously, the measuring condition kept constant during the tests, only during the tests at 1200 and 1300 °C a slight decrease of the ion current at both masses indicates a slight decrease of the pressure in the mass spectrometer.

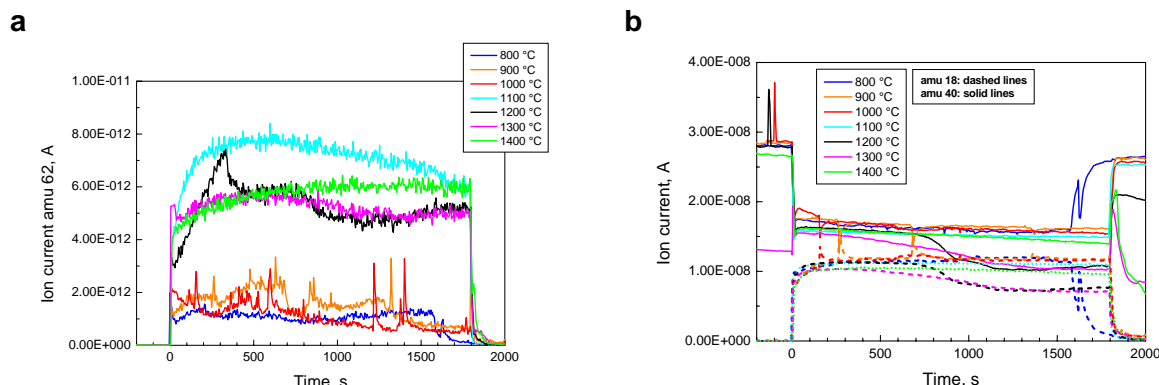


Figure 16: Ion currents measured by mass spectrometer: a) at mass 62 indicating formation of orthoboric acid H_3BO_3 , b) at masses 18 and 40 showing MS performance during the tests

After various discussions with modellers, another test series was performed with tenfold lower steam flow rates (3 g/h instead of 30 g/h). The results of the off-gas analysis is summarised in [Figure 17](#). The test at 800 °C was run one hour in order to reach at least roughly an equilibrium state. The initial peaks in gas release are considerably broader as the ones in the tests with higher steam flow rates and it took more time to reach a constant oxidation rate. Furthermore, the absolute values of gas release are about four times lower in the test series with reduced steam injection.

[Figure 18](#) again shows additional results obtained by the MS measurement. Boric acid formation increases with temperature during the steam injection, but the values are by approx. one order of magnitude lower than in the test series with higher steam rates. The

right diagram in Figure 18 shows some instabilities of the mass spectrometer during the test at 1400 °C, the other tests run very well.

Post-test examinations

Figure 19 shows the appearance of Framatome pellets after isothermal tests at 800, 1200, and 1600 °C during the first series. The mass loss after 30 minutes oxidation at 1600 °C is obvious. It should be mentioned that the consumption of the pellet and therefore the reduction of the diameter of the cylindrical specimens was almost perfectly uniform in later tests after improvement of the sample support (Fig. 3). Post-test examinations were performed with all specimens of the first isothermal series. SEM images were taken from the surface of the pellets at various magnifications. Figures 20-22 give an overview on the appearance of the specimens after tests between 800 and 1600 °C in comparison with a fresh B₄C pellet.

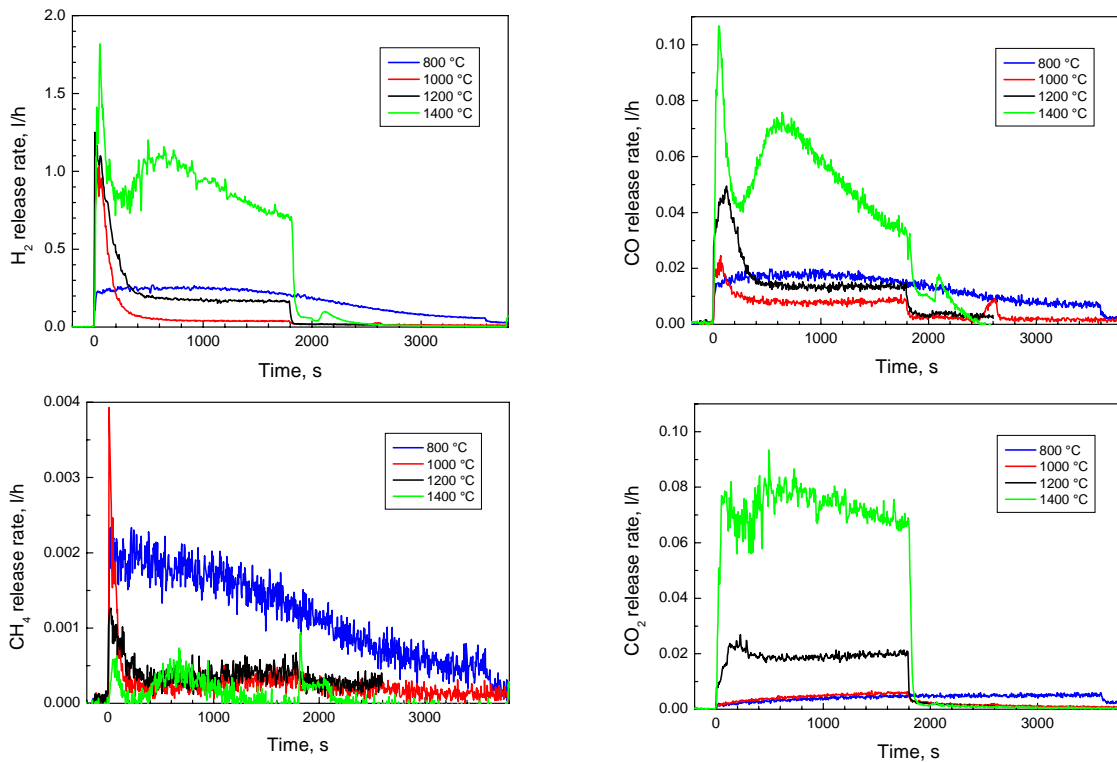


Figure 17: Gas release during isothermal oxidation of Framatome pellets at low steam injection rates

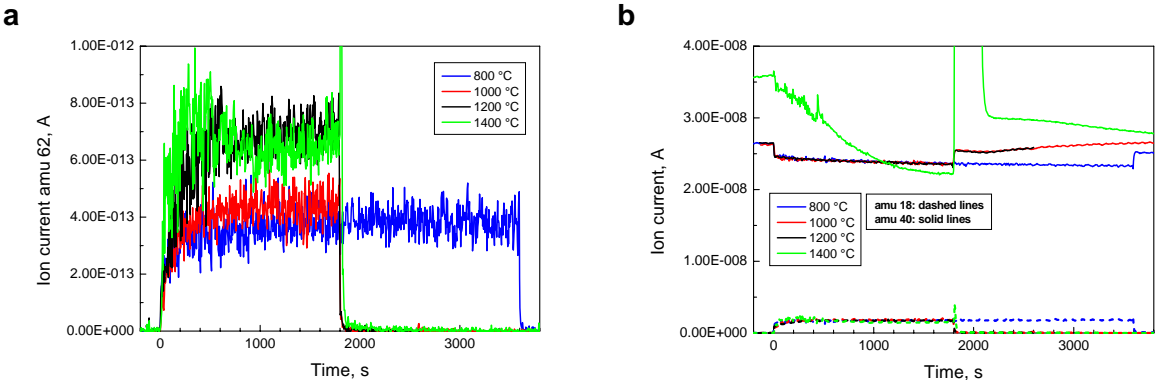
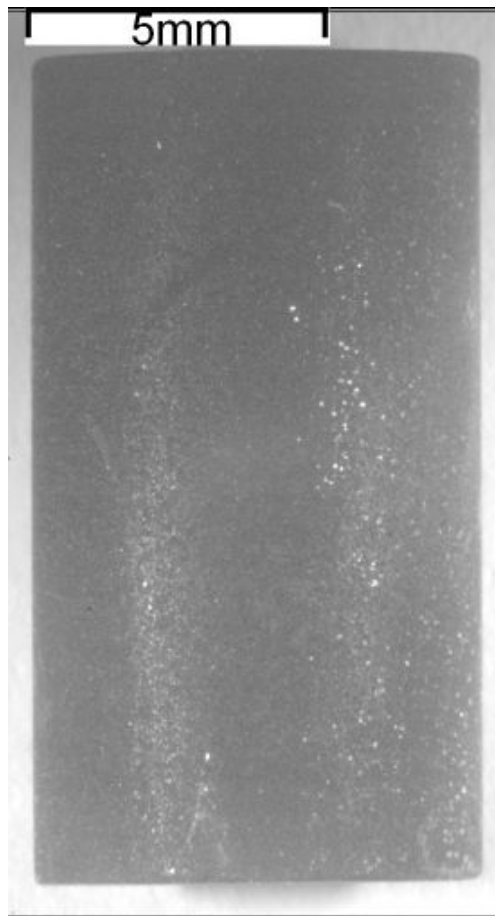
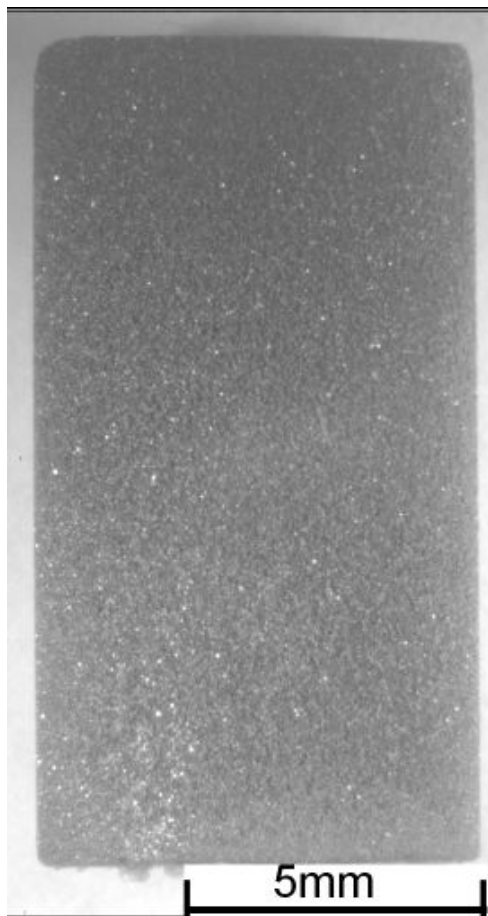


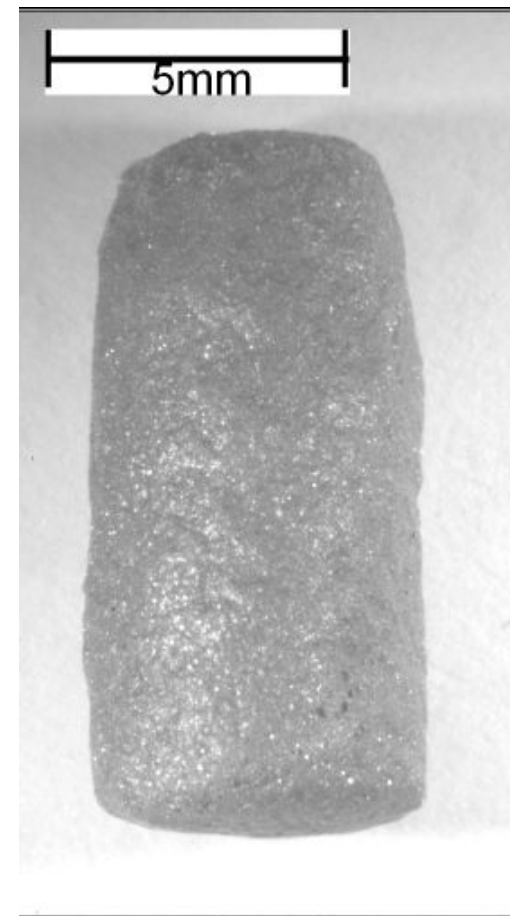
Figure 18: Ion currents measured by mass spectrometer: a) at mass 62 indicating formation of orthoboric acid H_3BO_3 , b) at masses 18 and 40 showing MS performance during the tests



30 min, 800 °C



30 min, 1200 °C



30 min, 1600 °C

Figure 19: Appearance of Framatome B₄C pellets after isothermal tests (first series) at the indicated temperatures

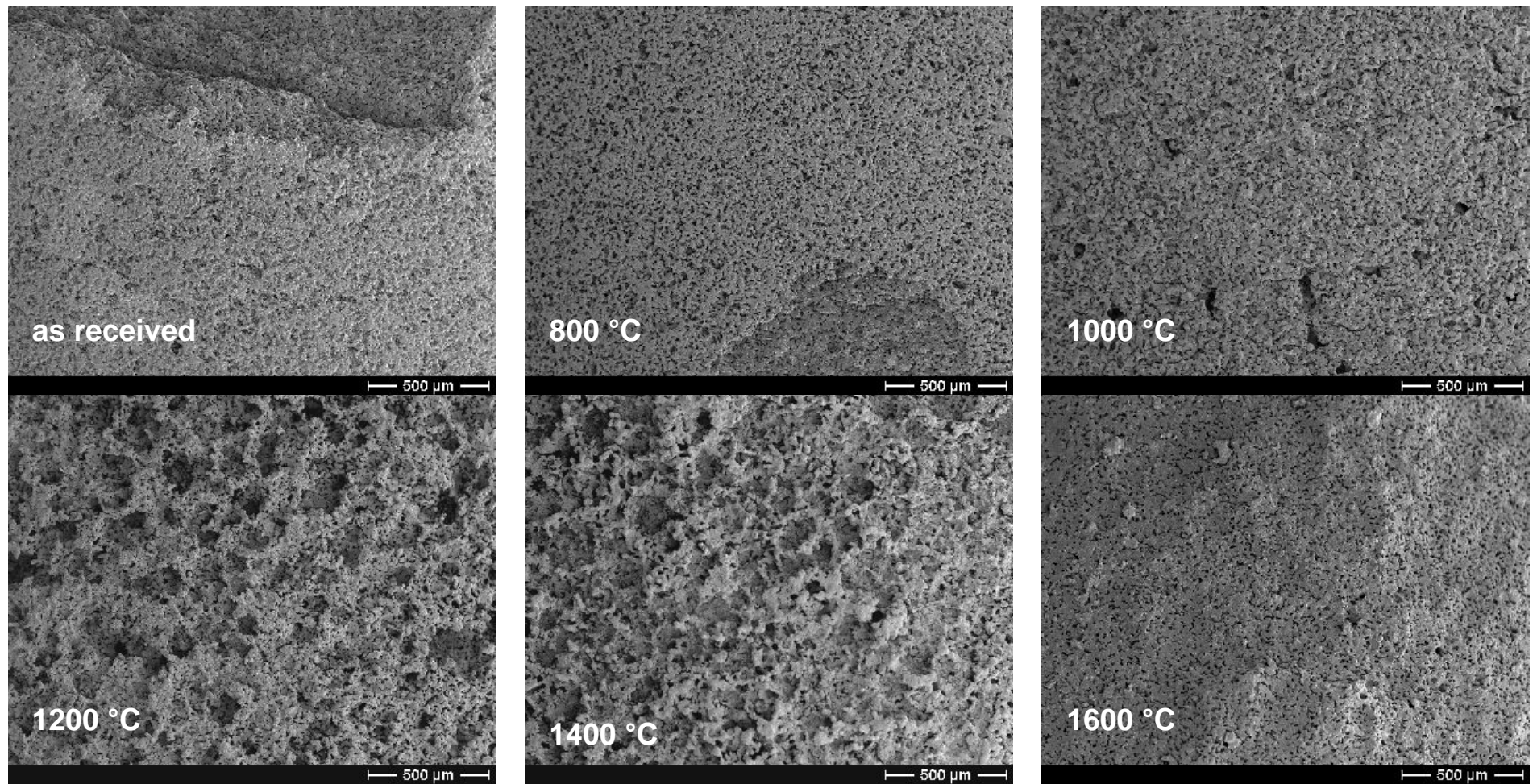


Figure 20: B₄C specimens after isothermal oxidation in steam: SEM images of the pellet surfaces (40x)

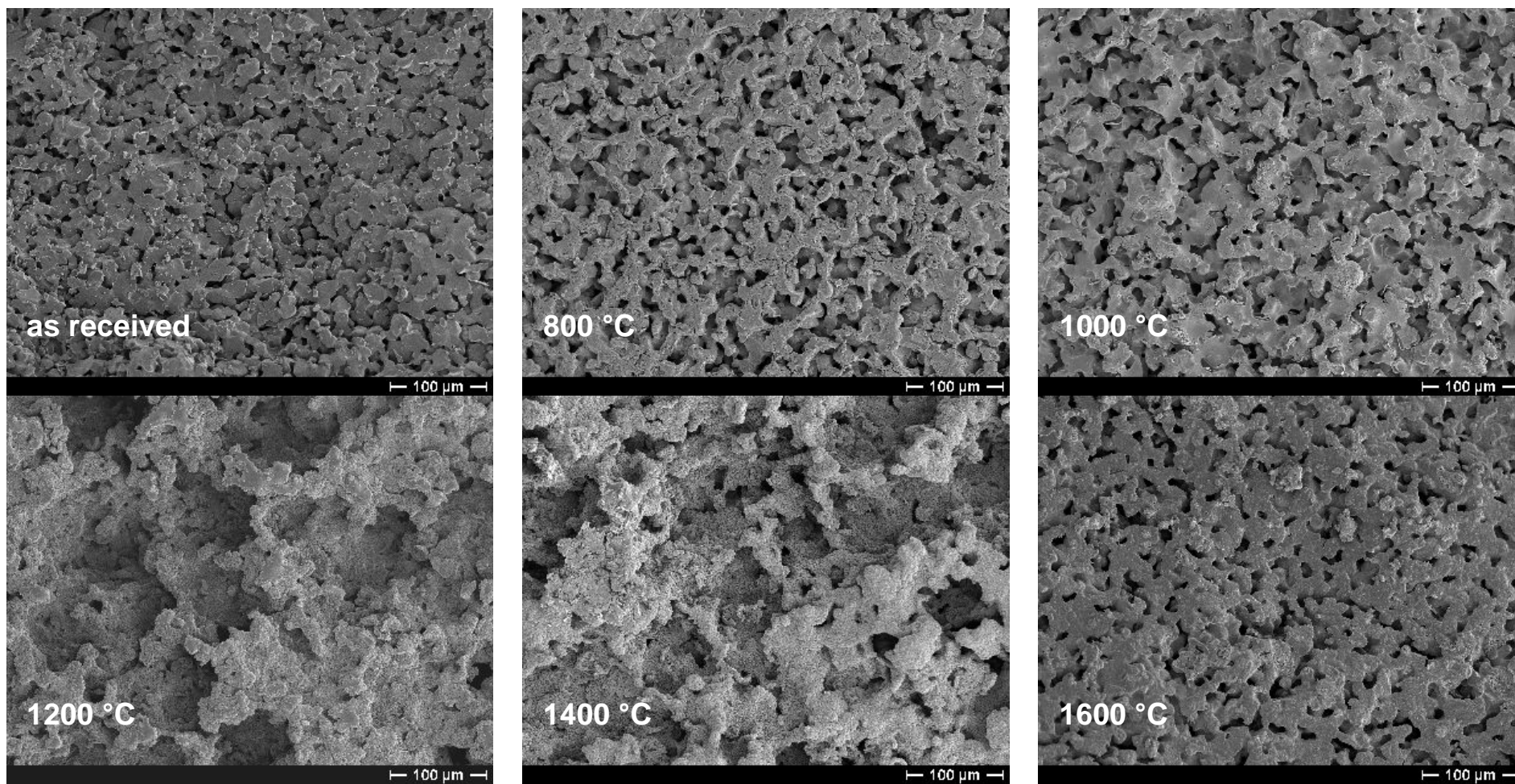


Figure 21: B₄C specimens after isothermal oxidation in steam: SEM images of the pellet surfaces (160x)

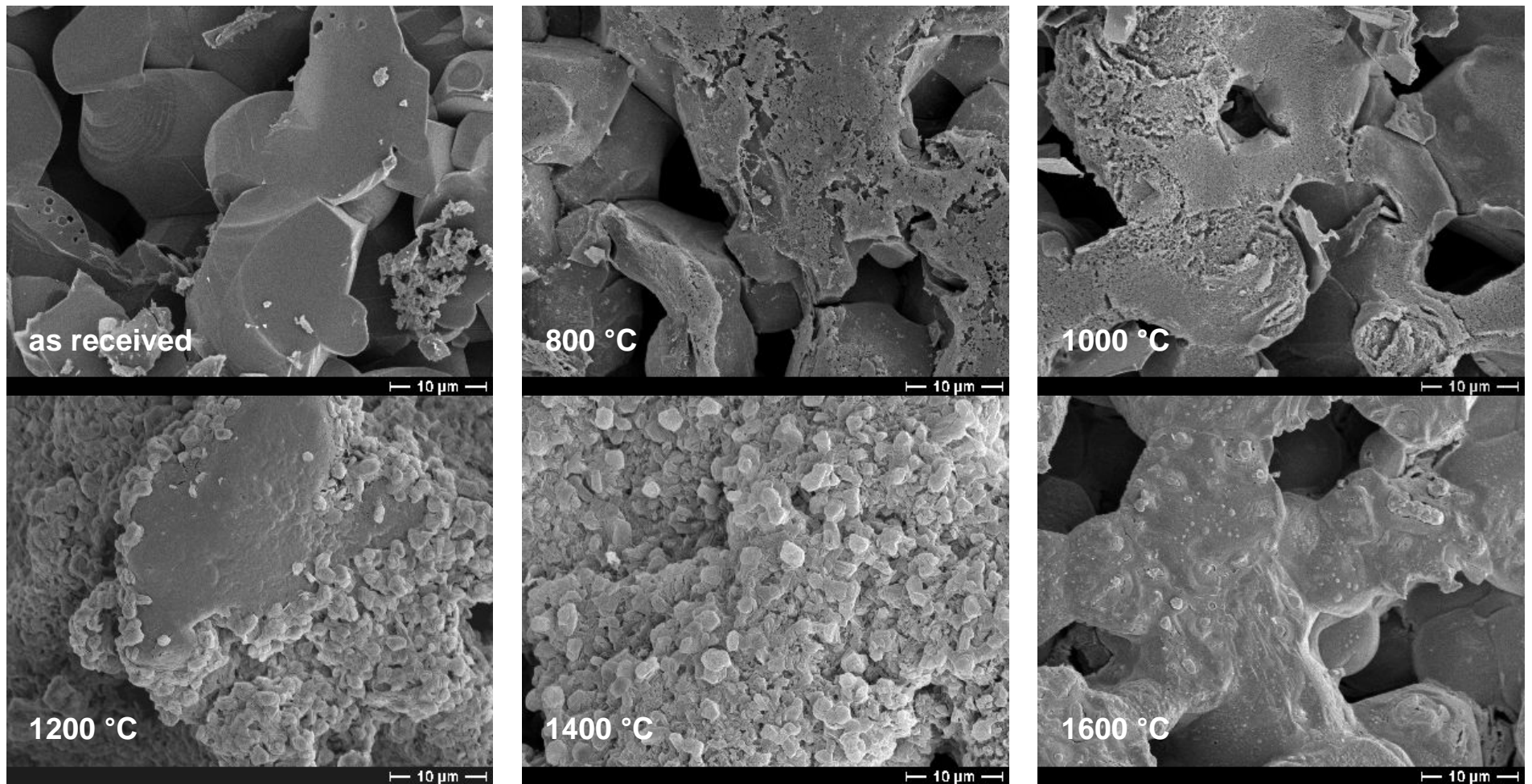


Figure 22: B₄C specimens after isothermal oxidation in steam: SEM images of the pellet surfaces (1600x)

The SEM images show an increasing roughness of the surface and porosity with rising temperatures up to 1400 °C; the surface at 1600 °C looks like molten at the high temperature. Furthermore, an irregular surface coating on the specimens after tests at 800 and 1000 °C and light, 1-5 µm sized crystallites covering the surface of the pellets after tests at 1200 and 1400 °C are visible at the highest magnification. The former may be residuals of a B₂O₃ scale formed during oxidation, the origin of the latter could not be solved so far.

Post-test diffraction diagrams after the isothermal tests at 800 and 1400 °C (Figure 23) confirm the preferred deposition of boric acid (as a reaction product of B₂O₃ with air humidity) in the test at the lower temperatures.

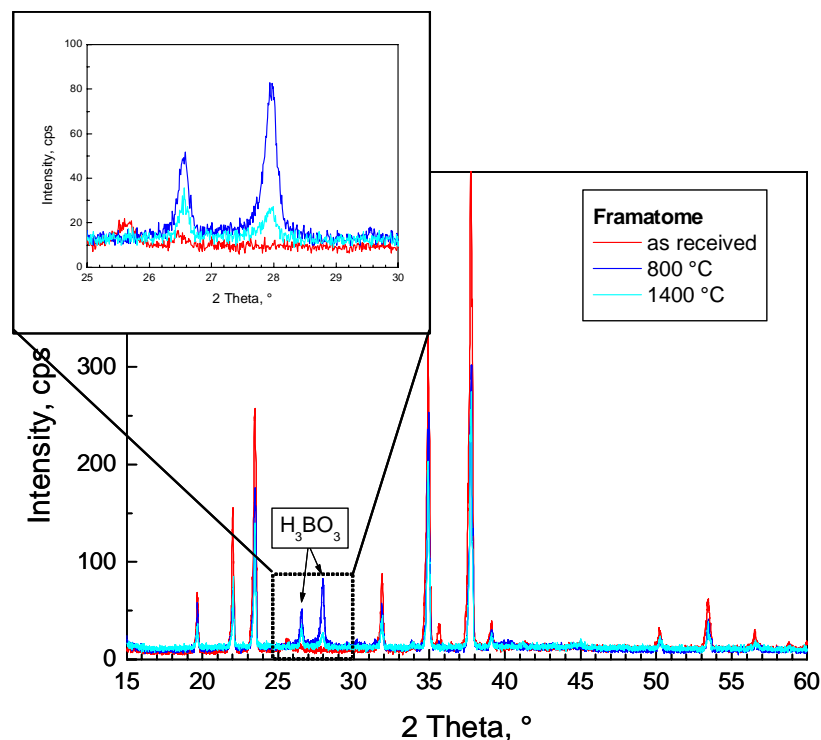


Figure 23: X-ray diffraction patterns of Framatome pellets after tests at 800 and 1400 °C in comparison with an as-received specimen

5.2.2 CODEX pellets

These pellets were produced in Russia and used in the Hungarian CODEX tests on the degradation of small VVER type bundles with B₄C control rod. The properties of the CODEX pellets are comparable to the Framatome pellets, as it is described in chapter 4, but the pore size distribution is broader and the impurity content is significantly higher.

Figure 24 shows a quite similar behaviour with respect to the gas release obtained with the CODEX specimens. During the test at 1200 °C the steam injection was interrupted for 90 seconds, therefore, the test was prolonged by that time.

Experimental results

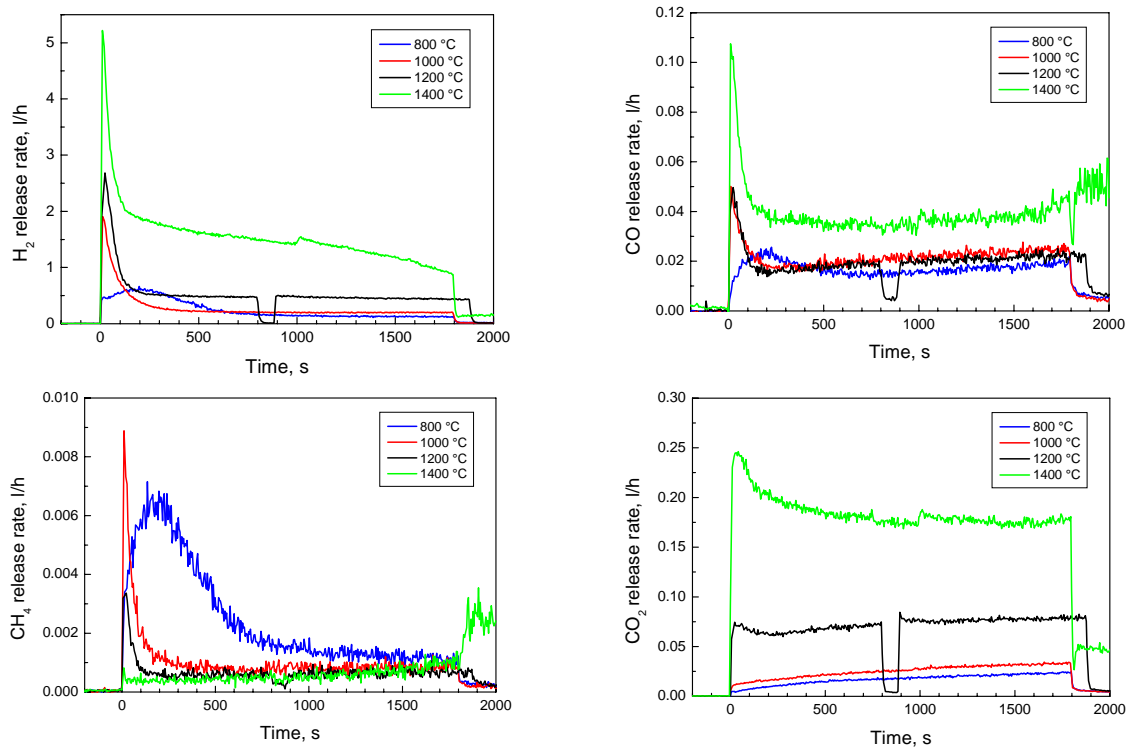


Figure 24: Gas release during isothermal oxidation of CODEX pellets

The formation of boric acid was also seen in that test series. The capillary of the mass spectrometer was increasingly plugged during the test at 1400 °C as it is shown in [Figure 25b](#). Therefore, the results of that test have to be taken with care at least in the second half of the experiment.

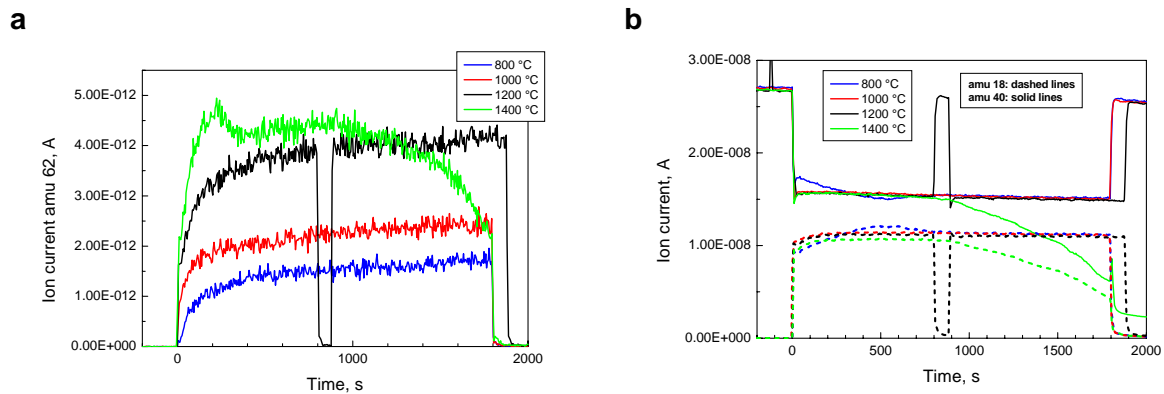


Figure 25: Ion currents measured by mass spectrometer: a) at mass 62 indicating formation of orthoboric acid H₃BO₃, b) at masses 18 and 40 showing MS performance during the tests

5.2.3 ESK pellets

ESK pellets were chosen for comparison reasons especially because of their high purity and high density without open porosity. These kind of pellets were used as absorber pellets in the Italian PEC reactor, a Liquid Metal Fast Reactor (cooled by sodium) of 116 MW thermal

power under construction by ENEA. Its construction was stopped by the government after a referendum on nuclear energy matters in 1988.

Figure 26 demonstrates a quite different oxidation behaviour of these dense pellets especially at begin of the steam injection. The initial peak of gas release and thus oxidation rate is considerably smaller than for the porous Framatome and CODEX pellets. The somewhat unsteady shape of the hydrogen curve and the signal at mass 62 obtained in the test at 1400 °C is caused by a partial blockage of the MS capillary starting at 450 s as can be seen in **Figure 27b**.

For comparison with the porous Framatome pellets, a second test series was conducted at low steam flow rates (3 g/h). Only a comparatively small initial peak of the gas release was observed also in these tests as can be seen in **Figure 28**. The oxidation rates are significantly lower than for the tests at higher steam flow rates with ESK pellets. The test at 800 °C was run one hour; the diagrams show only the results of the first 30 minutes because steady state condition had already established at that time. The experiments under low steam rates run perfectly with respect to the MS performance as can be seen from **Figure 29**.

X-ray diffraction of the surface of the ESK pellets showed smaller H_3BO_3 peaks in comparison with the Framatome pellets for the 800 °C sample and no boric acid peaks at all for the 1400 °C sample.

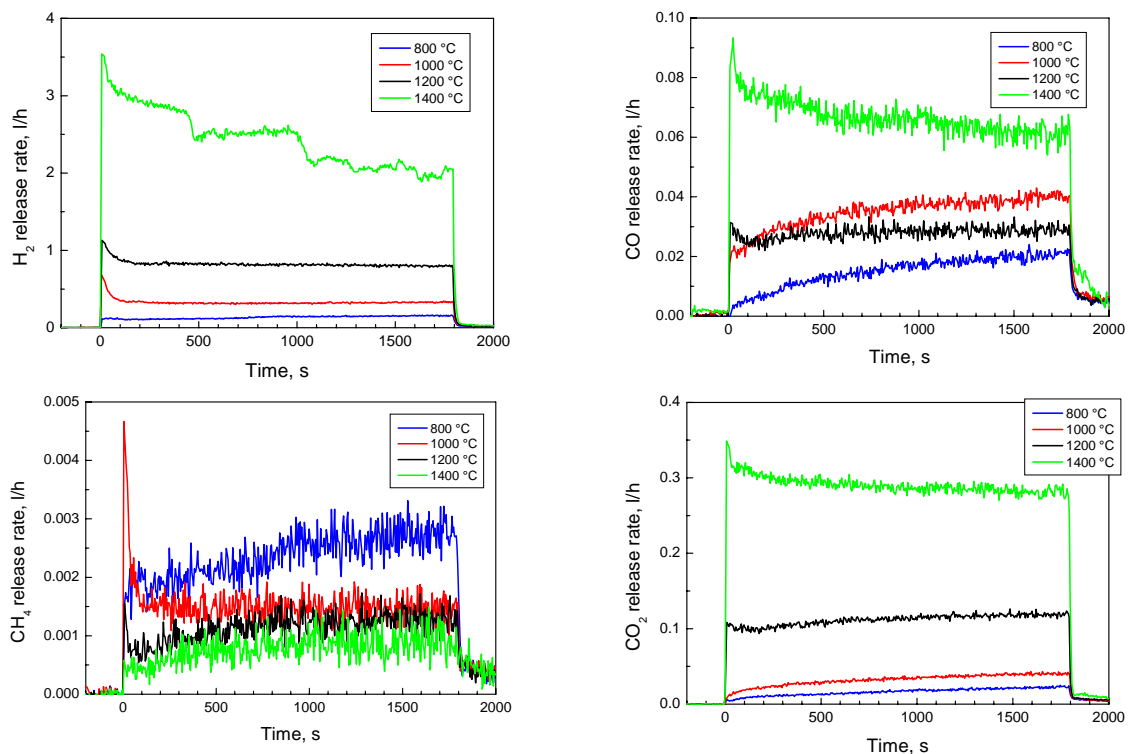


Figure 26: Gas release during isothermal oxidation of ESK pellets

SEM images of the bottom surface and the shell surface of ESK pellets after tests at different temperatures indicate relocation of superficial boron oxide especially during tests at lower temperatures (**Figure 30 a-c**). Such relocation processes were not observed at Framatome pellets where the open porosity seems to absorb the liquid boron oxide.

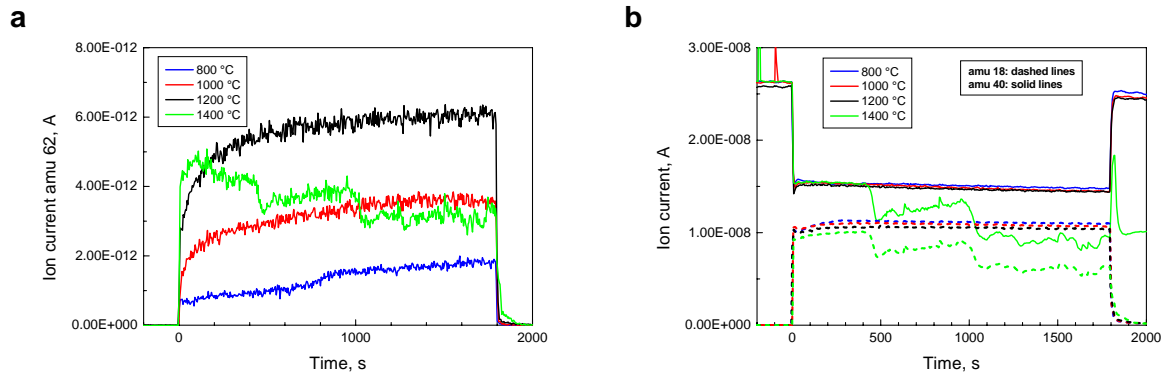


Figure 27: Ion currents measured by mass spectrometer: a) at mass 62 indicating formation of orthoboric acid H_3BO_3 , b) at masses 18 and 40 showing MS performance during the tests

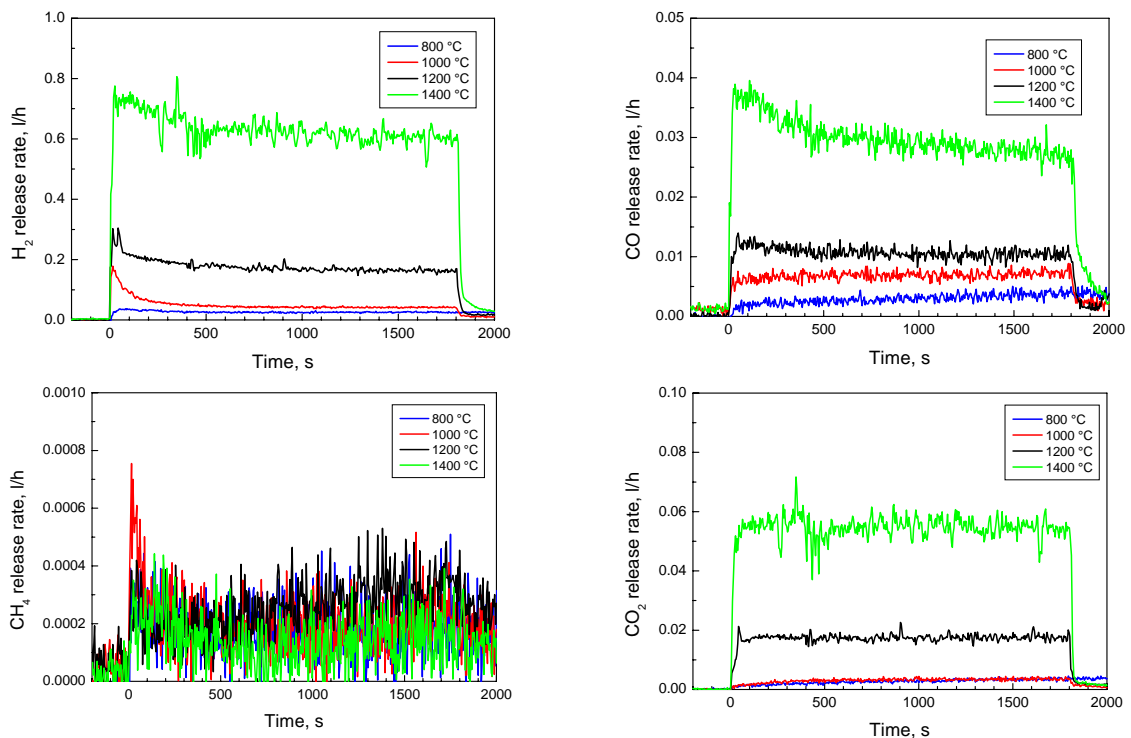


Figure 28: Gas release during isothermal oxidation of ESK pellets at low steam flow

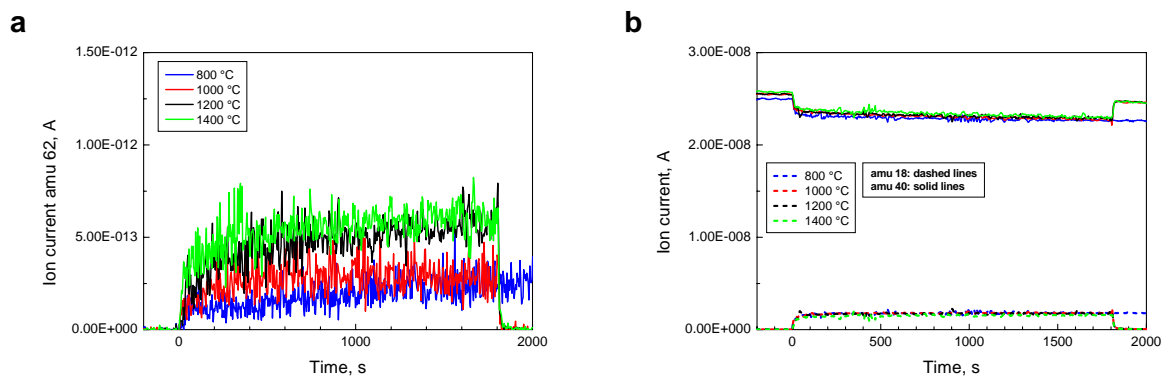


Figure 29: Ion current measured by mass spectrometer: a) at mass 62 indicating formation of orthoboric acid H_3BO_3 , b) at masses 18 and 40 showing MS performance during the tests at low steam flow rates

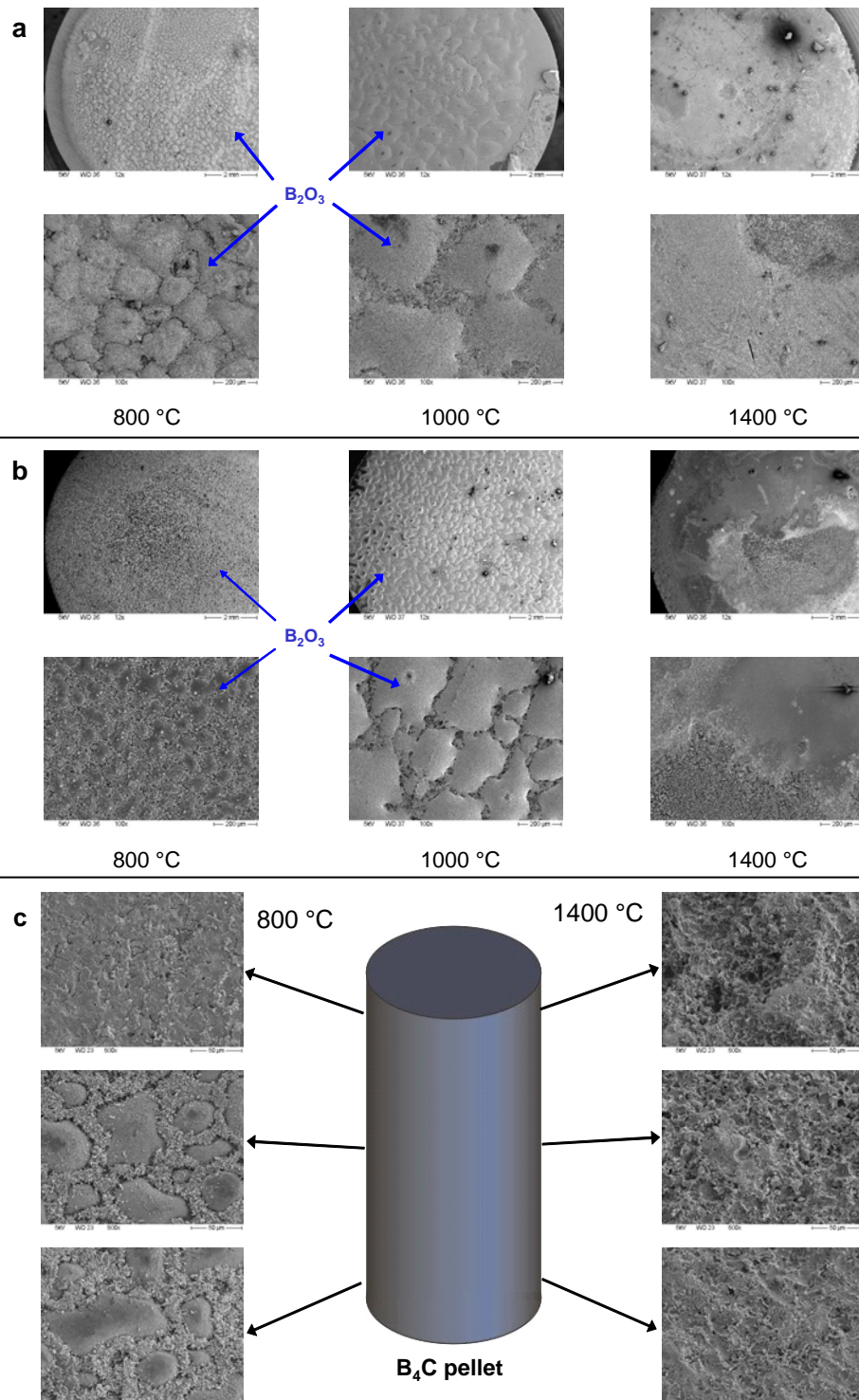


Figure 30: Formation and relocation of superficial boron oxide at dense ESK pellets. a) bottom surface after isothermal tests at high steam flow; b) bottom surface after isothermal tests at low steam flow; c) shell surface after tests at 800 and 1400 °C at low steam flow

5.2.4 ESK powder

Finally, a B₄C powder formerly used in German Boiling Water Reactors (BWR) was investigated in view of its oxidation behaviour in steam.

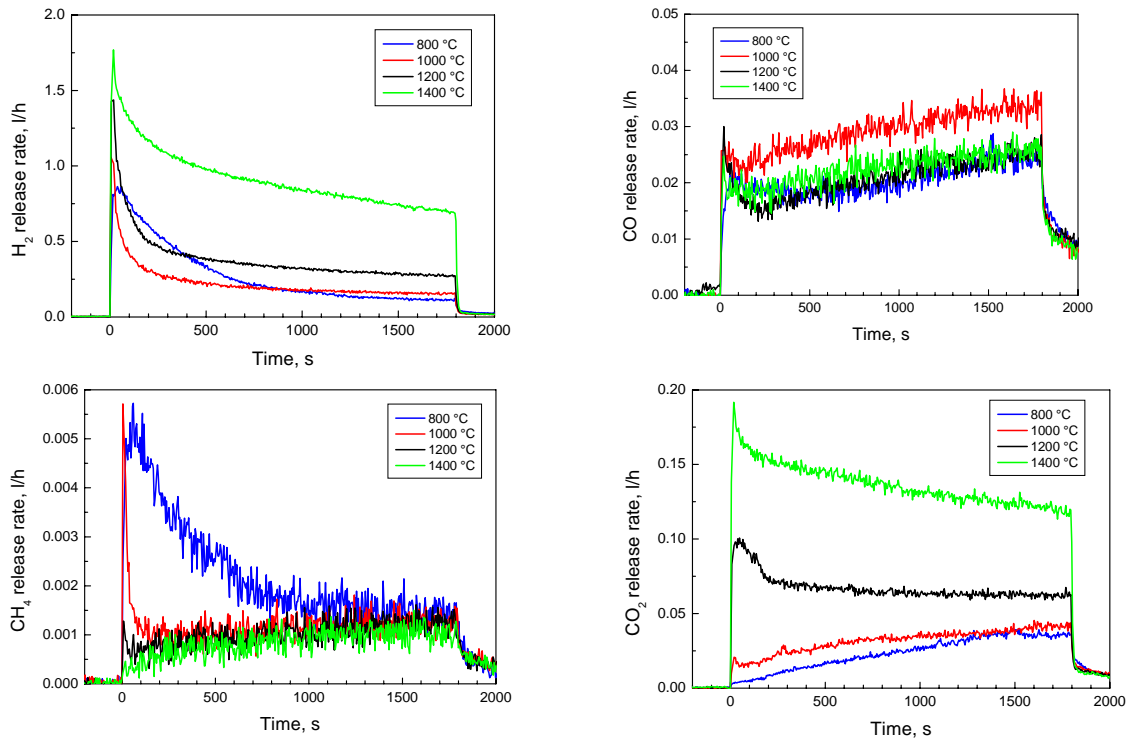


Figure 31: Gas release during isothermal oxidation of ESK powder

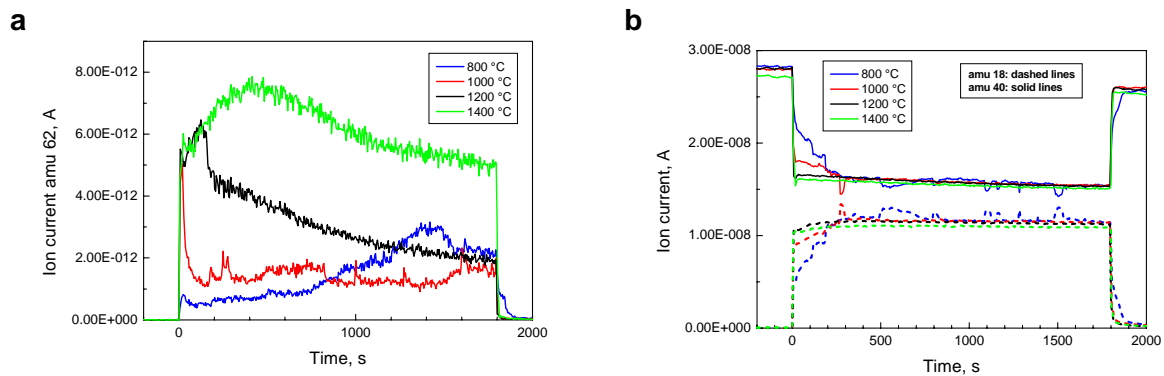


Figure 32: Ion current measured by mass spectrometer: a) at mass 62 indicating formation of orthoboric acid H₃BO₃, b) at masses 18 and 40 showing MS performance during the tests

Figures 31 and 32 summarise the results of that test series. The separation between the two phases (initial peak and plateau) is not so sharp as in the tests with pellets. The unsteady ion currents shown in Figure 32 do not seem to have a negative effect on the results of the gas analyses.

5.2.5 Comparative views

In this chapter some diagrams are presented which compare data from the various test series. This may be useful for evaluation of the overall results and give some indication which mechanisms are important for modelling.

First, the hydrogen release rates referred to the accessible geometric surface of the specimens are put together at the different temperatures. [Figure 33](#) and in more detail for the test series at 1200 °C [Figure 34](#), offer interesting insights into the mechanism of the B₄C oxidation.

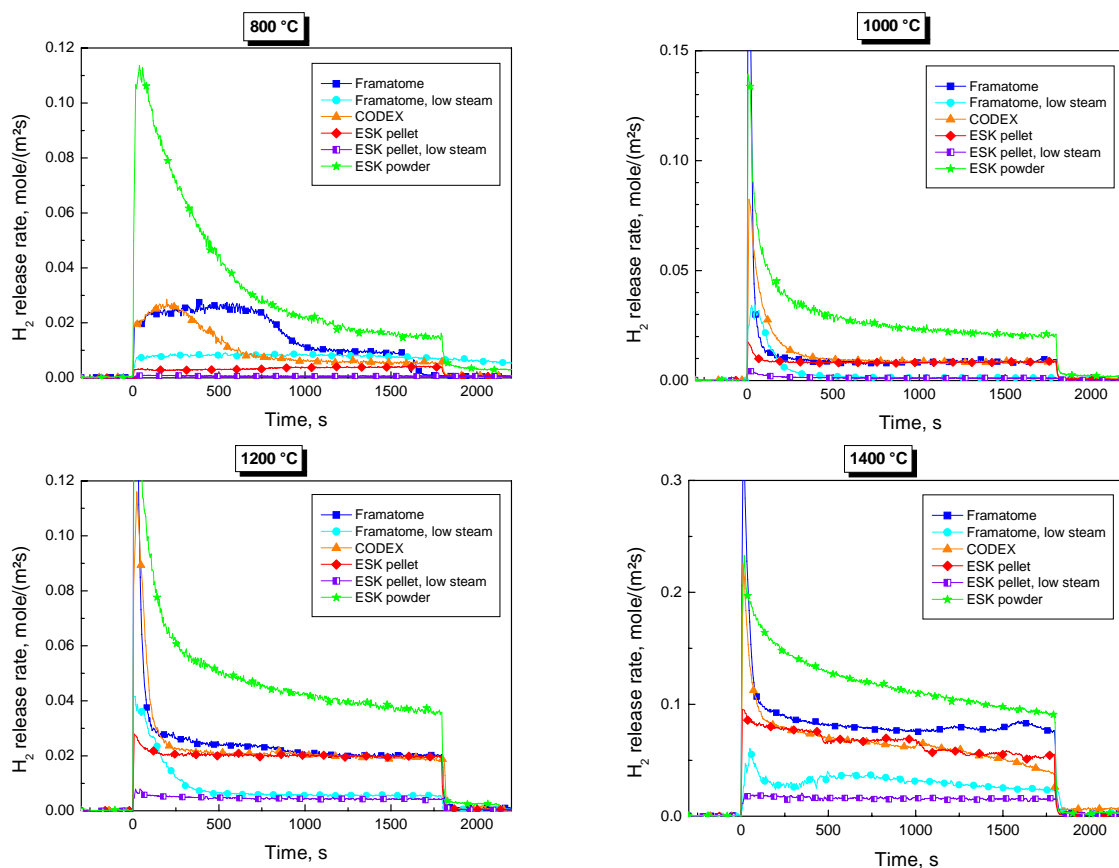


Figure 33: Hydrogen release during isothermal oxidation of the various specimens

Obviously, the initial peak hydrogen production (oxidation rate) is tightly correlated with the porosity of the sample. Strongly increased hydrogen rates after switching on the steam injection is only observed for the porous pellets and the powder. A more or less constant level of the oxidation rate is established soon and is, at least for the pellets, only dependent on the steam flow rate or more generally on the thermal hydraulic boundary conditions. Apparently, the porous specimens initially have a higher active surface leading to increased oxidation rates. The formed liquid boron oxide fills or clogs up pores and only the geometric surface is available for steam access during the plateau phase. During that phase, the oxidation rate is controlled by the transport of the boric acids formed by the reaction of B₂O₃ and steam (Eqs. 4-5) or at higher temperatures (>1500 °C) by direct evaporation of boron oxide (Eq. 6).

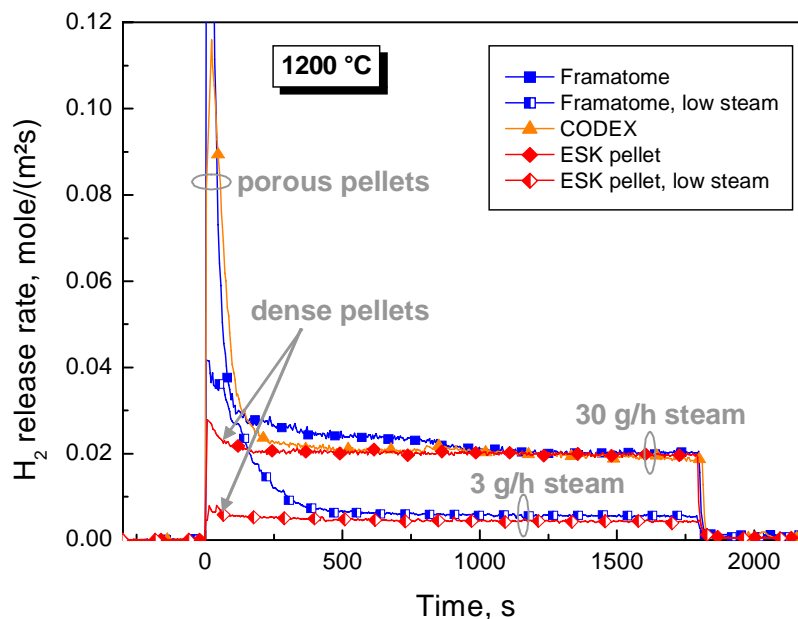


Figure 34: Hydrogen release during isothermal oxidation of the various specimens at 1200 °C showing 1) peak oxidation rates for porous specimens after initiation of steam injection and 2) dependence of oxidation rate on steam flow

The somewhat different behavior of the powder can be easily explained by the larger porosity which delivers a higher surface than the geometric one to which the data are referred to and which is not completely filled by liquid B_2O_3 during the duration of the test. Surface effects may also explain the behaviour at 800 °C and the strong differences during the initial phase of the tests. The striking difference of the oxidation rates of Framatome and ESK pellets at 800 °C and at low steam rate is certainly caused by the different porosities of these specimens. Apparently, the open pores are not plugged by the low amount of boron oxide formed at the low temperature and low steam flow rate, leading to a significant higher active surface of the porous specimen. The slight differences for the 1400 °C tests may be caused by MS problems due to the enhanced production of boric acids, as it was already explained above.

Figure 35 compiles the integral gas release data of all tests taken from Table A2. These data should not be overrated because they do not take into account the different sample surfaces and do not judge the quality of the data. Nevertheless, the diagrams clearly show some tendencies. The hydrogen and carbon dioxide production increase with increasing temperature, the highest methane release was measured at the lowest test temperature, and for CO no clear dependency on temperature is visible.

Many tests have been performed at 800 °C with the various species. The behaviour of the specimens during oxidation at that temperature seems to be more complex than at higher temperatures. So, it takes more time to reach an equilibrium plateau of the oxidation rate. An oscillating gas release rate was observed in some of the tests with Framatome pellets at 800 °C. Figure 36 gives an overview of the hydrogen release rates during all tests performed at 800 °C. Again, a closer look onto these data suggests an important influence of the porosity of the specimens on the initial oxidation rates. Later on, the hydrogen release rates get nearer to each other. Furthermore, the diagram illustrates that the reproducibility of the test results obtained under the same boundary conditions is excellent. On the other hand,

small changes in the conditions may significantly influence the results, as it is demonstrated by the test Box00906 where the argon flow rate accidentally was reduced from 50 to 25 l/h leading to a steam partial pressure of 0.55 instead of 0.43 bar.

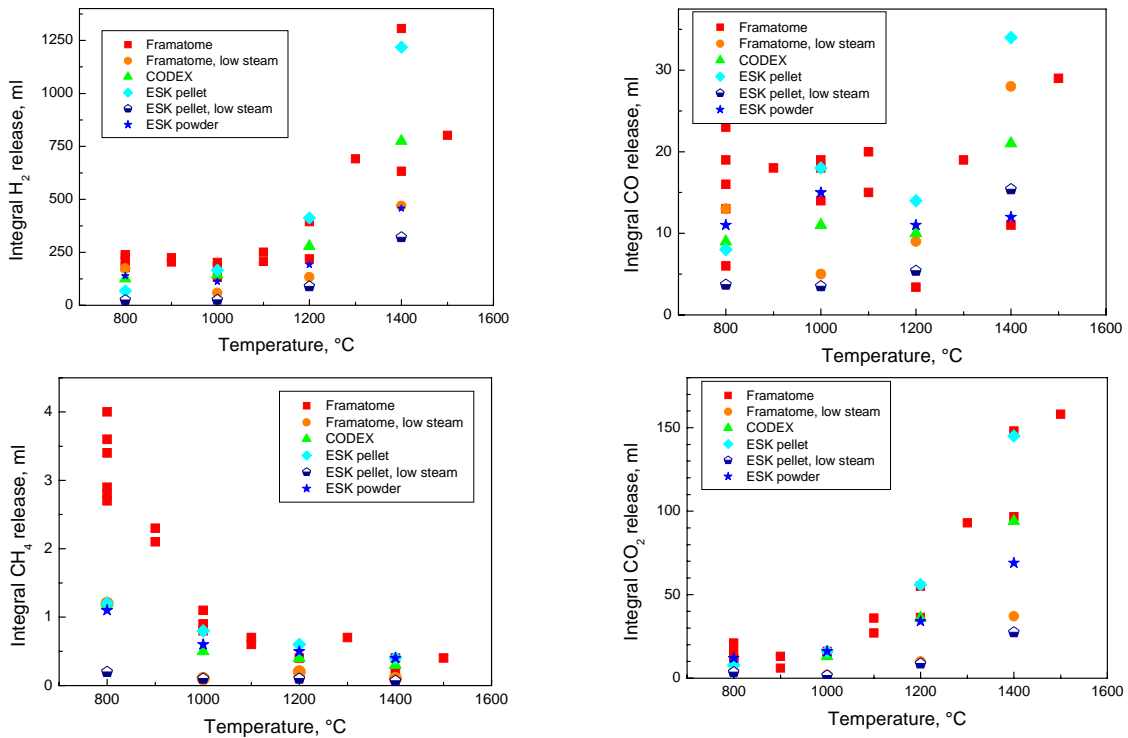


Figure 35: Integral release of H₂, CO, CO₂ and CH₄ during 30 min isothermal oxidation in steam in dependence on temperature.

Note: The tests with the Framatome/ESK pellets at 800 °C and low steam flow took 60 min!

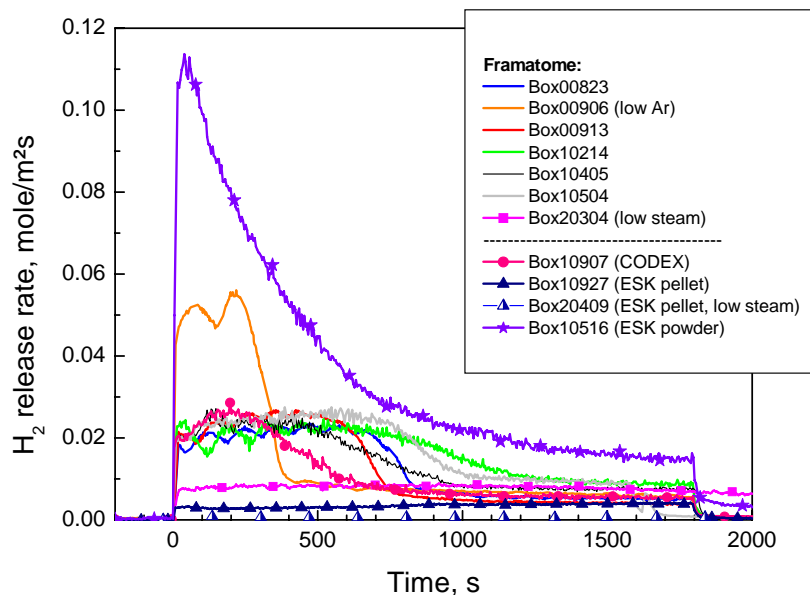


Figure 36: Hydrogen release during isothermal oxidation of various B₄C specimens in flowing steam/argon mixture at 800 °C

Figure 37 summarises the integral mass change of the specimens which was measured in all tests. At 800 °C most of the specimens gained mass due to the formation of boron oxide B_2O_3 remaining in the pores or at the surface of the sample. At higher temperatures the boron oxide increasingly reacts with steam to form volatile boric acids or directly evaporates leading to a mass loss of the specimens. Furthermore, one can draw some conclusions by comparing the results of the various species. The ESK pellets without open porosity do not gain mass even at the lower temperatures and the powder sample with the highest porosity experiences the highest increase in mass up to 1200 °C. This is probably correlated with the capability to absorb liquid boron oxide.

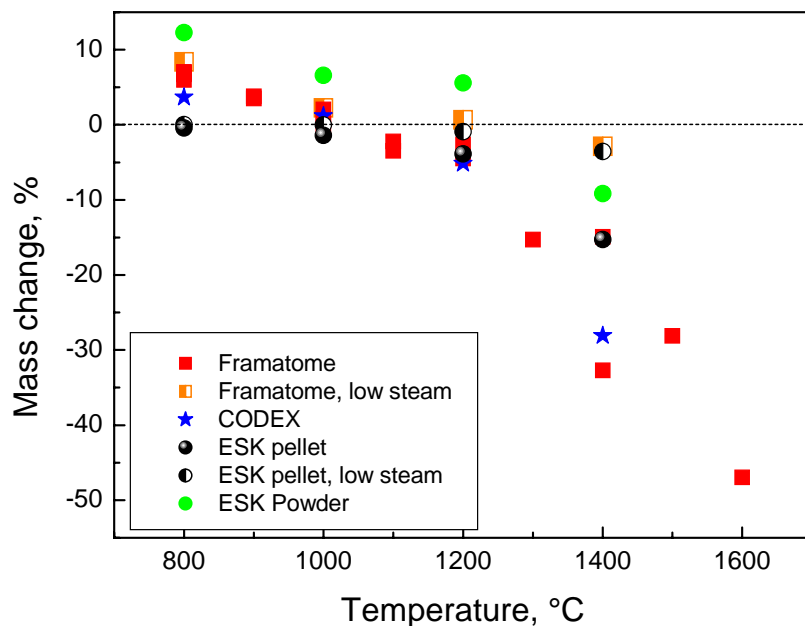


Figure 37: Integral mass change of B_4C specimens after 30 min oxidation in a flowing steam/argon mixture in dependence on temperature

Note: The tests with the Framatome/ESK pellets at 800 °C and low steam flow took 60 min!

Figure 38 illustrates this behaviour in more detail. The B_2O_3 production (green bars) increases with increasing temperature for all specimens, but the boron oxide remaining in the specimen at the end of the test (blue bars) is quite different for the various specimens. The dense pellet does not absorb liquid B_2O_3 at all; the powder absorbs considerable masses of the liquid reaction product.

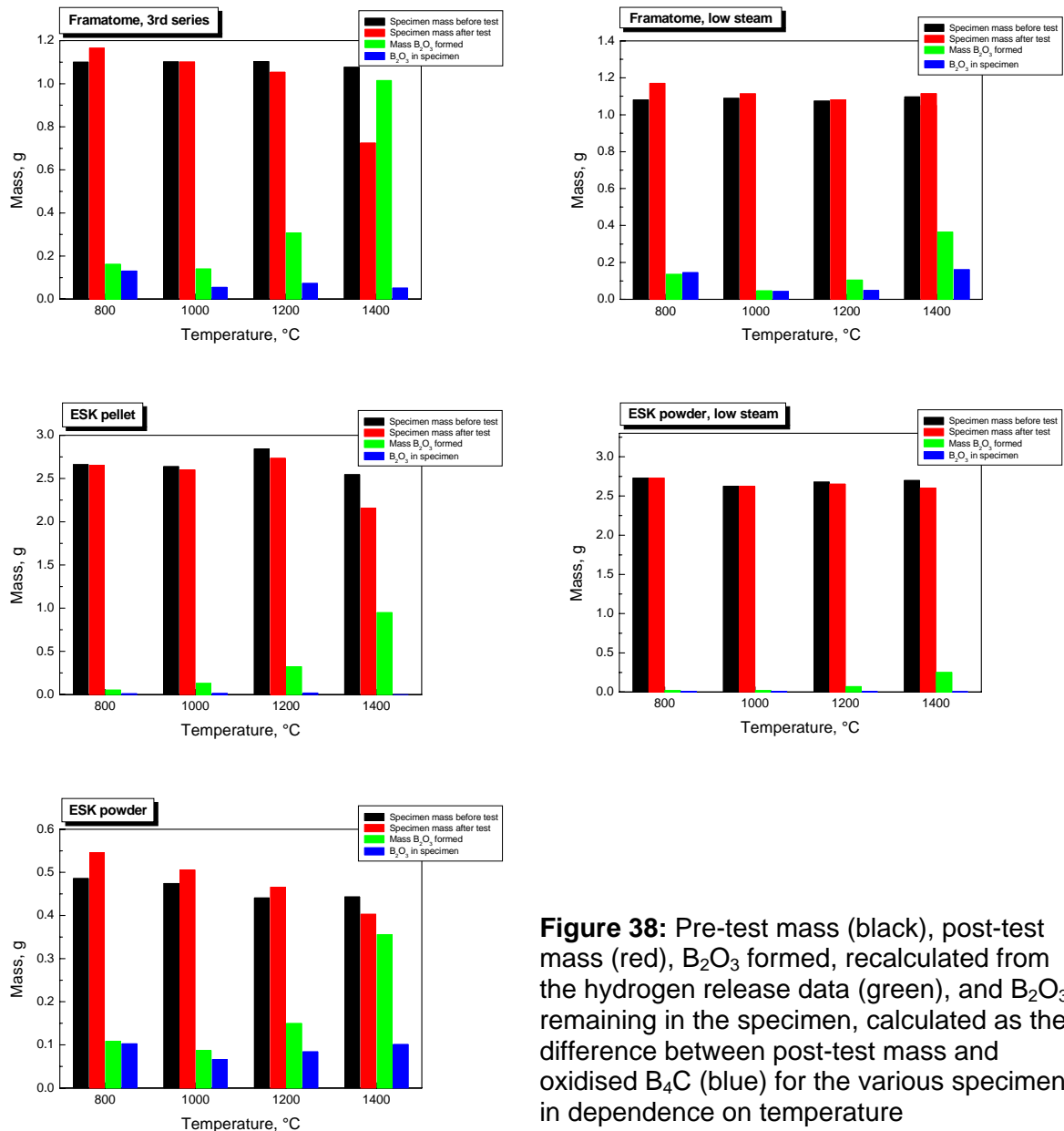


Figure 38: Pre-test mass (black), post-test mass (red), B₂O₃ formed, recalculated from the hydrogen release data (green), and B₂O₃ remaining in the specimen, calculated as the difference between post-test mass and oxidised B₄C (blue) for the various specimens in dependence on temperature

5.3 Tests under varying atmosphere

Some tests were performed at constant temperature under changing atmosphere to investigate the effect of atmosphere on the oxidation kinetics and on the off-gas composition. In particular, it was of interest whether the production of methane can be forced by atmospheres with a high content of hydrogen and thus low oxygen potential.

Two tests were conducted with stepwise changes from pure steam (+Ar) to almost pure hydrogen (+Ar) atmosphere at 800 and at 1200 °C as it is shown in [Figure 39](#).

Experimental results

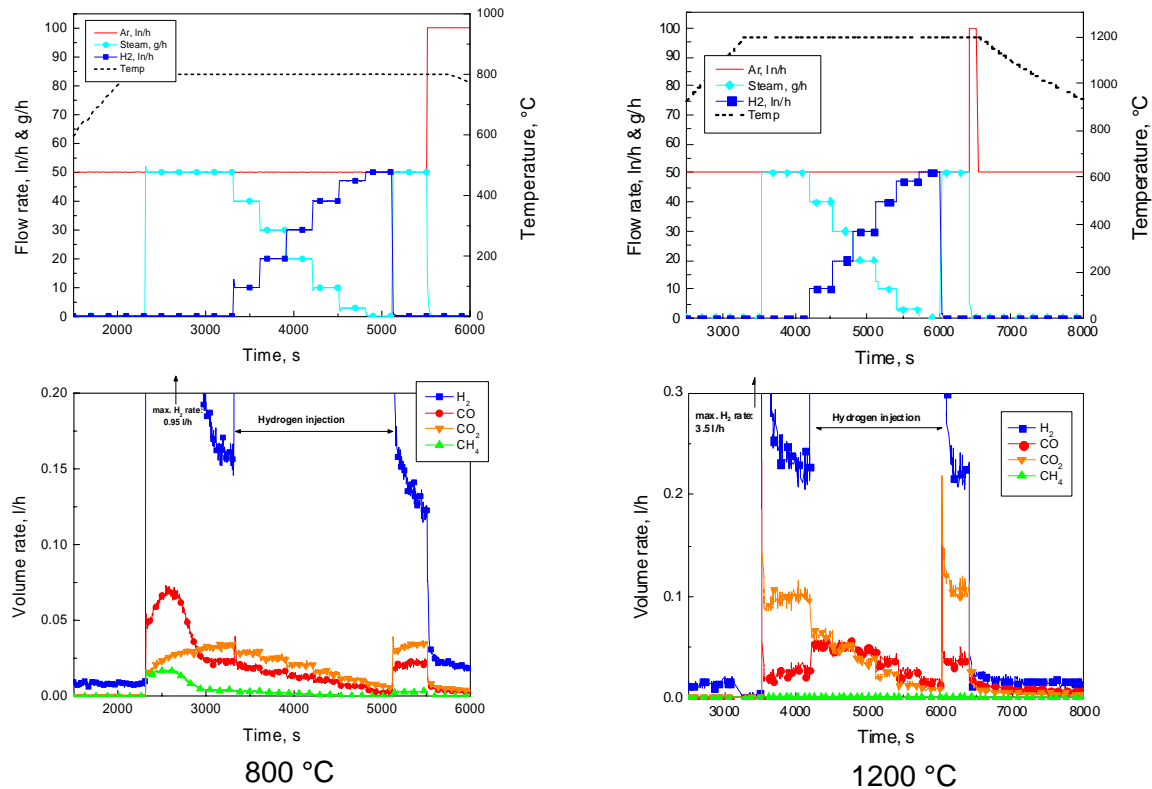


Figure 39: Oxidation of Framatome B₄C pellets under changing steam/hydrogen atmosphere at 800 and 1200 °C.

The upper diagrams show the test conditions (gas injection and temperature), the lower ones results of the mass spectroscopic gas measurements.

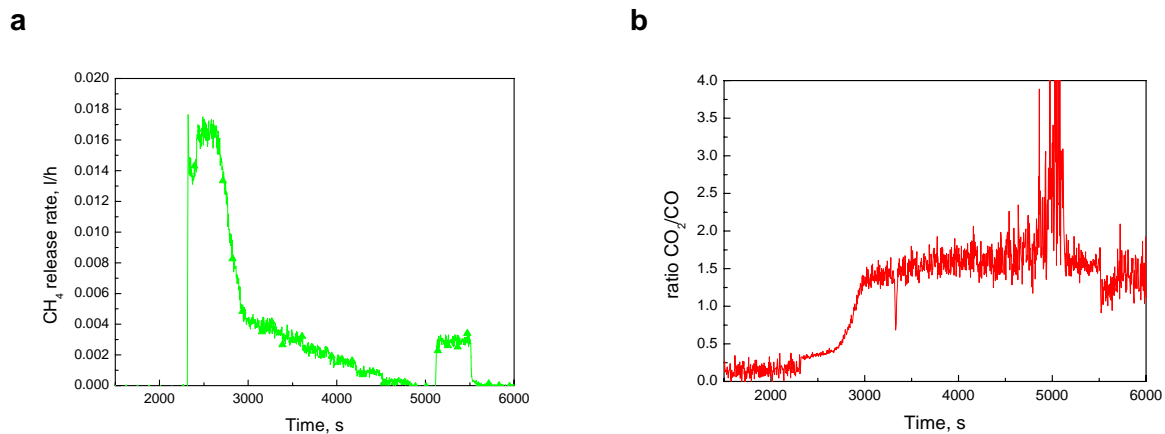


Figure 40: Detailed results of test Box00921 at 800 °C: a) methane release, b) ratio between carbon dioxide and carbon monoxide release rates

The reduction of the steam flow rate led to a decrease of the carbon containing species CO, CO₂, and CH₄, thus indicating a decrease in the oxidation rate. The change in the oxygen potential did not significantly influence the relative composition of the off-gas, as can be seen in [Figure 40](#) in more detail for the test at 800 °C.

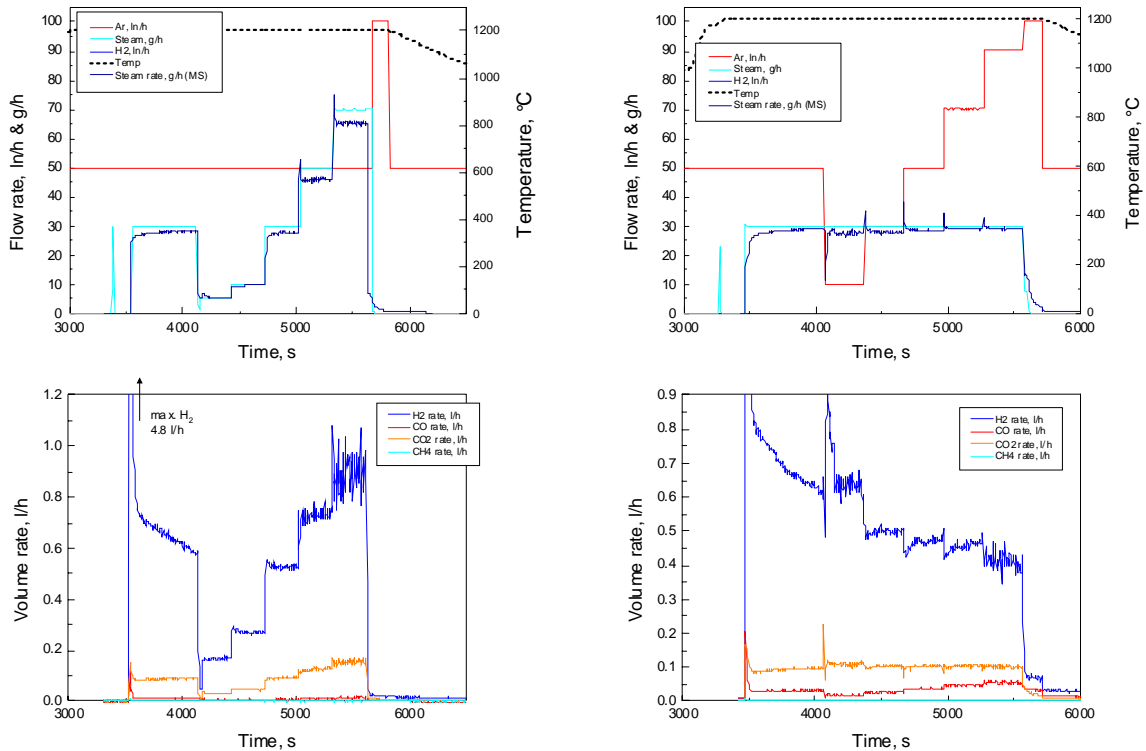


Figure 41: Oxidation of B₄C pellets at 1200 °C in flowing Ar/steam; left: varying steam flow rate, right: varying argon flow rate.

The upper diagrams show the test conditions (gas injection and temperature), the lower ones results of the mass spectroscopic gas measurements.

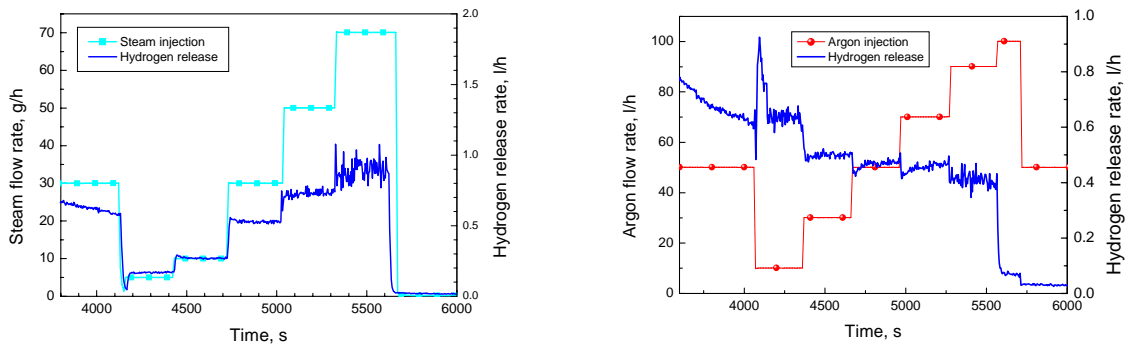


Figure 42: Influence of steam flow rate (left) and argon flow rate (right) on the oxidation kinetics of B₄C at 1200 °C

Figures 41 and 42 show the results of two tests with stepwise changing steam (Box10115) and argon (Box10126) atmosphere. The increase of the steam flow rate by one order of magnitude (steam partial pressure 0.11→0.64 bar) enhances the oxidation rate - here shown as hydrogen release rate - by a factor of five. On the other hand, the increase of the argon flow rate by an order of magnitude (steam partial pressure 0.79→0.27 bar) causes only a decrease of the oxidation rate by about 30 %. These results indicate that the oxidation rate of boron carbide is strongly influenced by the steam flow rate and to a smaller degree by the steam partial pressure.

Additional tests with varying steam partial pressures at different temperatures were performed on request of modellers in order to allow better determination of model

parameters. They are listed in Table A1 and test conducts as well as MS results are compiled in appendix A4. Special tests with varying argon/steam flow rates and constant steam partial pressure surprisingly showed no clear correlation between flow rates and oxidation rates (see also Table A1 and appendix A4).

5.4 Further tests

In this chapter the results of two tests will be presented which do not fit into the preceding ones, but which give some further information on the experimental procedure.

First, one test was performed with a thin B_4C disc which was completely oxidised at $1400\text{ }^\circ\text{C}$ to proof the mass balance in the BOX tests. The test conduct and gas release are shown in the appendix (test Box10914). [Table 4](#) gives an overview on the results obtained. There is a good correspondence between the gas release measured by mass spectrometer and the calculated values based on the mass of the specimen and using Equation 2. But it has to be mentioned once more, that the balance between hydrogen release and carbon containing gases was not met in the majority of the tests, probably due to problems with overlapping MS signals.

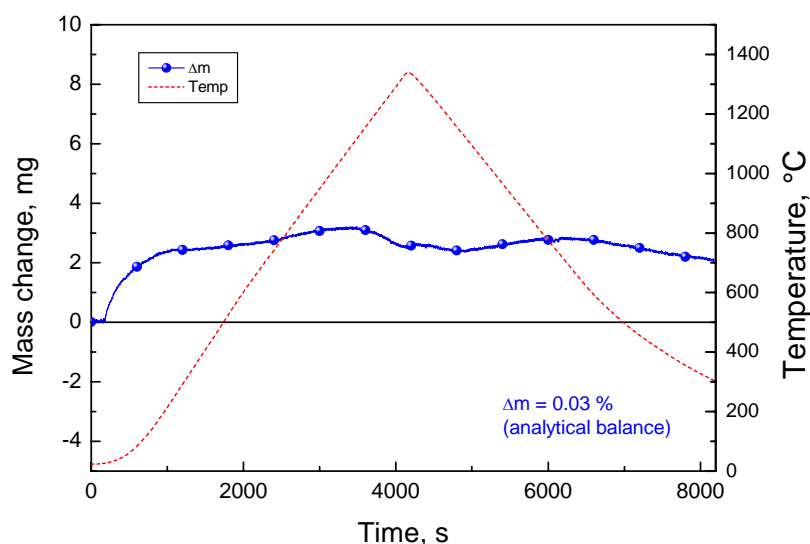


Figure 43: Mass change of a B_4C pellet during heat-up to $1350\text{ }^\circ\text{C}$ in pure argon

In another test, a Framatome pellet was heated up to $1350\text{ }^\circ\text{C}$ in pure argon in a thermal balance to analyse the amount of humidity in the specimen which could influence the oxidation process. [Figure 43](#) shows that the mass of the pellet remained practically unchanged during the test ($\Delta m = +0.03\%$) indicating that the specimens were free of surface impurities.

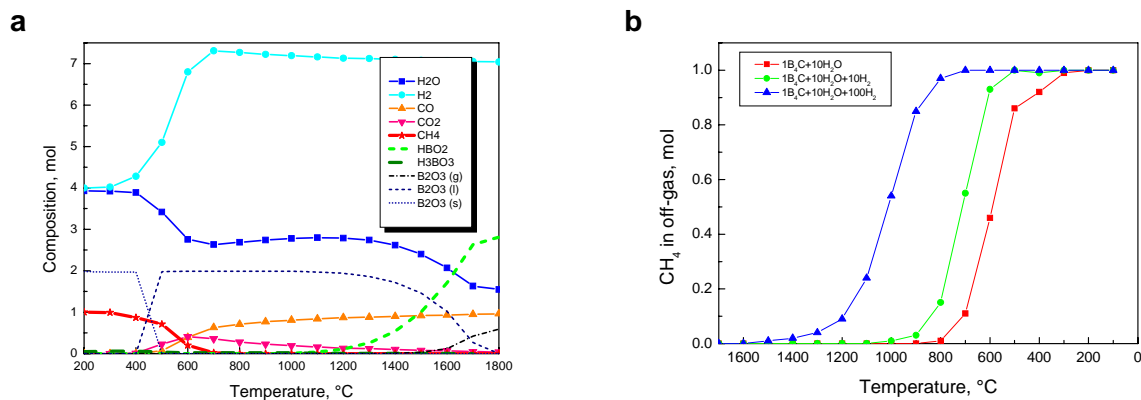
Table 4: Release of hydrogen and carbon dioxide during complete oxidation of a small B₄C specimen. Expected results based on Equation 2.

	Measured	Expected
Specimen mass	0.0317 g	
H₂ release	0.0048 mol	0.0046 mol
CO₂ release	0.00058 mol	0.00057 mol

6 Thermo-chemical equilibrium calculations

Thermo-chemical pre-test calculations were performed using the equiTherm 5.0 software [15] with the built-in Barin data base for pure substances. The oxidation of B₄C in steam-containing environments can be mainly described by the chemical reactions given in chapter 1 with B₂O₃, H₂, as well as CO, CO₂ and CH₄ as primary reaction products. Further on, the boric oxide will react with steam to produce various types of boric acids (HBO₂, H₃BO₃, (HBO₂)₃) and/or directly evaporates.

According to the calculations, CO production (equation 1) is preferred at higher temperatures. This is in contradiction with the experimental results where the CO₂ release is predominating. A significant methane production which is of interest due to its potential influence on the iodine fission product chemistry is only obtained at low temperatures (<700 °C). [Figure 44](#) additionally shows that the transition temperature from preferred CO/CO₂ to CH₄ production depends on the oxygen potential in the gas mixture. At temperatures above 1200 °C and 1500 °C considerable amounts of gaseous metaboric acid HBO₂ and boric oxide B₂O₃, respectively, are calculated to evaporate. There is only a minor influence of the system pressure on the composition of the reaction products ([Figure 45](#)).

**Figure 44:** Thermo-chemical calculations: a) equilibrium composition of 1 B₄C and 10 H₂O in dependence on temperature, b) ratio of the carbon containing species CH₄/(CO+CO₂) in dependence on temperature and inlet gas composition

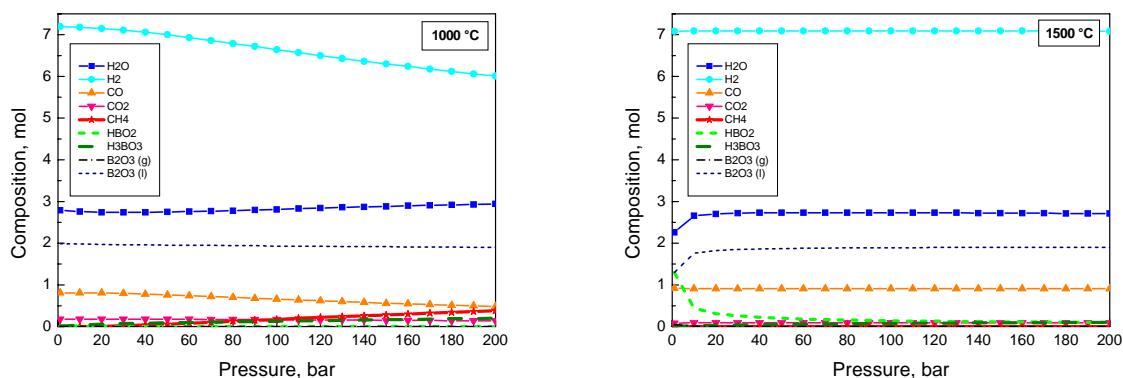


Figure 45: Dependence of the equilibrium composition of 1 B₄C and 10 H₂O on system pressure at 1000 °C (left) and 1500 °C (right)

7 Summary, discussion and conclusions

Extensive test series were performed to study the oxidation behaviour of boron carbide at high temperatures. Four types of B₄C specimens with quite different properties were investigated under various atmospheres in the temperature range between 800 and 1600 °C. In contrast to most of the B₄C oxidation data published in the past where the mass change was analysed, the release rates of the gaseous reaction products was the main measured variable in our tests.

The oxidation kinetics of B₄C in steam at the temperatures of interest are supposed to be determined by at least two processes: (1) The formation of liquid B₂O₃ which covers the surface and acts as a diffusion barrier for the starting materials and products of the reaction, and (2) the evaporation of B₂O₃ and the products of its reaction with steam, mainly boric acids. The former process which is only dependent on temperature follows a parabolic kinetics whereas the latter one which is depending on temperature and surrounding conditions, especially on the steam flow rate, is thought to be of linear kinetics giving altogether parabolic oxidation kinetics. The two competitive processes lead to an equilibrium thickness of the oxide scale which acts as a diffusion barrier for the species which take part in the oxidation reaction.

Another modelling approach takes into account the surface reaction kinetics and mass transport in the gas phase as rate determining steps of the oxidation process [18].

Under the conditions chosen in the tests a constant reaction rate was established soon after initiation of the oxidation which was accompanied by a peak reaction rate. On the one hand, the initiation phase strongly differed from specimen type to specimen type, on the other hand the oxidation rates corresponded to each other during the second, constant phase under the same boundary conditions. It is assumed that due to different open porosities of the various specimens the active surface differs at begin of the reaction. The formation of liquid boron oxide soon causes the plugging of the pores, thus allowing only oxidation at the outer (geometric) surface of the samples and leading to comparable results obtained with the

various pellet types. Only at low oxidation rates, i.e. at low temperatures and low steam flow rates, the porosity of the specimens influences the oxidation rate for longer times.

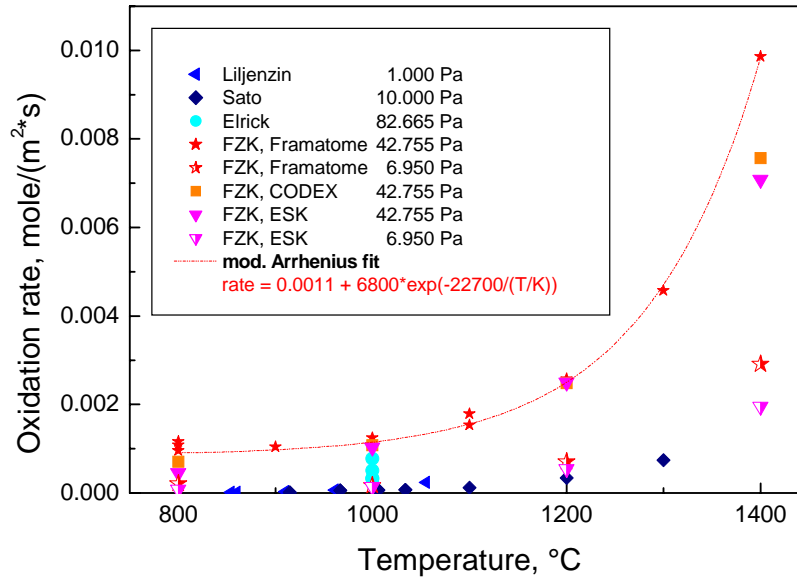


Figure 46: Oxidation of B_4C at high temperatures: comparison of recent FZK results with literature data obtained at different steam partial pressures

The oxidation rate is strongly dependent on the steam flow rate. This is one of the reasons why the literature data on the oxidation of B_4C are widely scattering and why one cannot directly compare the recent results with literature results. [Figure 46](#) compares FZK oxidation rates based on the hydrogen release data during the plateau phase and referring to the geometric surface of the pellets with literature data. The FZK data usually were obtained at higher steam partial pressures and rates and are therefore above the mainstream of the data known from literature. The FZK data obtained at lower steam flow rates are comparable with Sato's results. The equation for the dependence of the oxidation rate on temperature given in [Figure 46](#) is only valid for the conditions of this test series and must not be generalised.

[Figure 47](#) presents the same data and additionally recent data obtained in the VERDI test rig at IRSN (France) [16] in an Arrhenius type diagram showing that different boundary condition do not only affect the absolute values but also the "activation energy" of the oxidation. Elrick's data [5] were obtained during one test where several specimens were located at various axial positions in a tube furnace along the steam flow. The VERDI data have been produced at the highest steam partial pressures and flow rates. [Figure 48](#) may deliver another explanation for differences in results based on mass change and based on gas release measurements. Especially at the lower temperatures, a considerable amount of boron oxide remains in the specimens; therefore, data based on mass change evaluation could underestimate the oxidation rate.

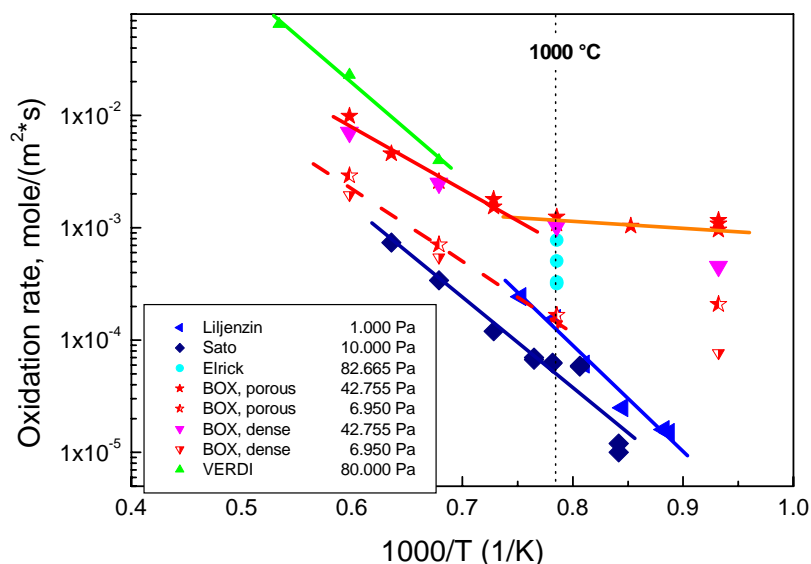


Figure 47: Oxidation of B_4C at high temperatures: comparison of recent FZK results with literature data obtained at different steam partial pressures (Arrhenius diagram)

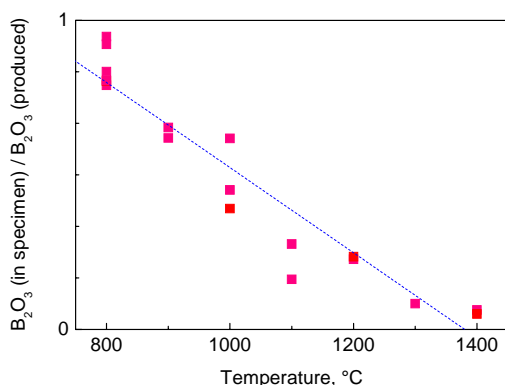


Figure 48: Ratio of boron oxide remained in the specimen and boron oxide totally produced during isothermal tests with Framatome pellets

A thermally activated temperature dependence following an exponential (Arrhenius type) equation is only obtained for temperatures above 1270 °C as was shown in the transient tests and confirmed by the isothermal experiments. At lower temperatures, the dependence on temperature is much more complex due to the mechanisms described above and demands modelling work for explanation.

Besides hydrogen, the main gaseous reaction products of the oxidation of B_4C in water vapour containing atmosphere were carbon monoxide CO and carbon dioxide CO_2 . Only small amounts of methane CH_4 were released even during the tests at 800 °C, the release rates further decreased with increasing temperature to almost zero above 1000 °C. This is in agreement with the thermo-chemical calculations which gave considerable methane production only below 800 °C. The difference between the experimental and calculated CO/ CO_2 ratio cannot be explained so far. Presently, it could not be excluded that CO/ CO_2 composition changes on the way from the hot furnace to "cold" mass spectrometer.

Finally, one can say that a lot of data are now available for modelling. It was shown that the boundary conditions have a strong influence on the oxidation process and thus have to be

included in the models. On the other hand, the properties of the specimens itself affect the oxidation kinetics only to a limited extent.

Acknowledgements

The experimental work described in this report was co-financed by the European Commission under the Euratom Fifth Framework Programme on Nuclear Fission Safety 1998-2002.

We are grateful to the Elektroschmelzwerk Kempten (now Wacker Chemie GmbH, Werk Kempten) who made available B₄C pellets and powder free of charge. The chemical analyses of the various materials used were performed by the Analytical Department of the Institute for Materials Research I at FZK (Dr. Adelhelm), which is acknowledged here. Furthermore, we want to thank Dr. Leiste (FZK/IMF-I) for delivering X-ray diffractograms of the specimens for phase analysis and Mrs. Offermann (FZK/IMF-III) for carrying out the BET and Hg porosimetry measurements. Finally, we thank Dr. Haste (PSI, Villingen) for the careful review of the report.

References

- [1] Y. Kawada
Reactors and materials of nuclear elements containing Boron
Note Technique SEMAR 98/67, IPSN Cadarache, May 1998
- [2] P. Hofmann, M. Markiewicz, J. Spino
Reaction behaviour of B₄C absorber material with stainless steel and Zircaloy in severe LWR accidents
Report KfK 4598, Kernforschungszentrum Karlsruhe, July 1989
- [3] L. Belovsky et al.
Chemical interaction in B₄C-filled control rod segments above 1000 °C under transient conditions
5th International Conference on Nuclear Engineering ICONE5, paper 2148, Nice, France, May 26-29, 1997
- [4] F. Nagase, H. Uetsuka, T. Otomo
Chemical interactions between B₄C and stainless steel at high temperatures
J. Nucl. Mat. 52, 245 (1997)
- [5] R.M. Elrick et al.
Boron carbide - steam reactions with caesium hydroxide and caesium iodide at 1270 K in an Inconel 600 system
Report NUREG/CR-4963, 1987
- [6] L.M. Litz
Oxidation of boron carbide by air, water, and air-water mixtures at elevated temperatures
J. Electrochem. Soc. 110, 921-925 (1963)
- [7] R.E. Woodley
The reaction of boronated graphite with water vapor
Carbon 7, 609-613 (1969)
- [8] J.O. Liljenzin et al.
The influence of chemistry on melt core accidents
Final report of the NKA Project ATKI-150, September 1990
- [9] G.A. Gogotsi, Y.L. Groushevsky, O.B. Dashevskaya
Complex investigations of hot-pressed boron carbide
L. Less-Common Metals 117, 225-230 (1986)

-
- [10] T. Sato et al.
Oxidation of non-oxide ceramics by water vapour at high temperatures
Fac. Eng., Tohoku Univ., Sendai, Japan. Zairyo 37(412), 77-82 (1988)
- [11] W. Krauss, G. Schanz, H. Steiner
TG-Rig Tests (Thermal Balance) on the Oxidation of B₄C. Basic Experiments, Modelling and Evaluation Approach
Report FZKA 6883, October 2003
- [12] M. Steinbrück, A. Meier, U. Stegmaier
Degradation and oxidation of B₄C control rod segments.
Report FZKA 6980, 2004
- [13] M. Steinbrück et al.
Results of the B₄C Control Rod Test QUENCH-07
Report FZKA 6746, 2004
- [14] B. Clement, G. Repetto
Test Protocol for the Phebus FP Test FPT-3 (as for January 2001)
Note Technique SEMAR 01/01, IPSN Cadarache, January 2001
- [15] I. Barin, W. Schmidt, G. Eriksson
equiTherm V 5.0 for Windows
Scienceware-VCH Software, 1996
- [16] F. Bertrand, O. Marchand, G. Repetto
B₄C control rod oxidation during a severe accident in a PWR reactor. Separate effect and integral tests analysis for modelling purpose with the ICARE/CATARE code
10th International Topical Meeting on Nuclear Reactor Thermal Hydraulics (NURETH-10), Seoul, Korea, October 5-9, 2003
- [17] M. Steinbrück et al.
Results of the QUENCH-09 Experiment with a B₄C Control Rod
Report FZKA 6829, 2004
- [18] M.S. Veshchunov, private communication

Appendix

- A1 Test parameters of experiments on B₄C oxidation in the BOX rig (chronological order)**
- A2 Essential results of isothermal experiments on B₄C oxidation in the BOX rig**

Table A1: Test parameters of experiments on B₄C oxidation in the BOX rig (chronological order)

Test	Specimen	Crucible	Ar, ln/h	H ₂ , ln/h	H ₂ O, g/h	T, °C	Remarks
00809	Framatome	Al ₂ O ₃	50	0	22.5	800-1500	
00810	Framatome	Al ₂ O ₃	50	50	7.5	800-1500	
00816	Framatome	Al ₂ O ₃	50	0	22	800-1500	MS determination of B containing species
00817	-	-	50	0-50	0-70	1200	MS determination of B containing species, test H ₂ and steam supply
00818	Framatome	Al ₂ O ₃	50	30	25	800-1500	
00821	Framatome	Al ₂ O ₃	50	0	22	800-1500-800	heat-up and cool-down in steam
00823	Framatome	Al ₂ O ₃	50	0	30	800	1 st test of the isothermal series
00824	Framatome	Al ₂ O ₃	50	0	30	1000	
00825	Framatome	Al ₂ O ₃	50	0	30	1200	
00828	Framatome	Al ₂ O ₃	50	0	30	1400	
00829	Framatome	Al ₂ O ₃	50	0	30	1600	blockage of off-gas pipe
00906	Framatome	Al ₂ O ₃	25	0	30	800	repetition of test 00823
00913	Framatome	Al ₂ O ₃	50	0	30	800	repetition of test 00823
00921	Framatome	Al ₂ O ₃	50	0-50	50-0	800	variable H ₂ /steam ratio
00927	Framatome	Al ₂ O ₃	50	0-50	50-0	1200	variable H ₂ /steam ratio
00928	Framatome	Al ₂ O ₃	50	0	30	1500	MS problems?
01207	Framatome	Al ₂ O ₃	50	0	5-70	1200	NEW SAMPLE SUPPORT , variable steam rate

Appendix

Test	Specimen	Crucible	Ar, ln/h	H ₂ , ln/h	H ₂ O, g/h	T, °C	Remarks
01208	Framatome	Al ₂ O ₃	10-100	0	30	1200	variable argon rate
10115	Framatome	Al ₂ O ₃ +Y ₂ O ₃	50	0	5-70	1200	variable steam rate, repetition of test 01207
10126	Framatome	Al ₂ O ₃ +Y ₂ O ₃	10-100	0	30	1200	variable Ar rate, repetition of test 01208
10213	Framatome	Al ₂ O ₃ +Y ₂ O ₃	50	0-90	30	1200	variable H ₂ rate, negative MS values
10214	Framatome	Al ₂ O ₃ +Y ₂ O ₃	50	0	30	800	negative MS values
10216	Framatome	Al ₂ O ₃ +Y ₂ O ₃	50	0	30	900	negative MS values
10219	Framatome	Al ₂ O ₃ +Y ₂ O ₃	50	0	30	1000	
10220	Framatome	Al ₂ O ₃ +Y ₂ O ₃	50	0	30	1100	reaction tube leaking
10405	Framatome	Al ₂ O ₃ +Y ₂ O ₃	50	0	30	800	
10406	Framatome	Al ₂ O ₃ +Y ₂ O ₃	50	0	30	800-1500	off-gas pipe blocked during cool-down phase
10504	Framatome	Al ₂ O ₃ +Y ₂ O ₃	50	0	30	800	8 MM OFF-GAS TUBING, off-gas temp too low, bad MS signal for steam
10511	Framatome	Al ₂ O ₃ +Y ₂ O ₃	50	0	30	900	
10514	Framatome	Al ₂ O ₃ +Y ₂ O ₃	50	0	30	1000	
10516	ESK powder	ZrO ₂ (4% Y ₂ O ₃)	50	0	30	800	1 st powder test
10529	ESK powder	ZrO ₂ (4% Y ₂ O ₃)	50	0	30	1000	
10530	ESK powder	ZrO ₂ (4% Y ₂ O ₃)	50	0	30	1200	
10531	ESK powder	ZrO ₂ (4% Y ₂ O ₃)	50	0	30	1400	
10605a	Framatome	Al ₂ O ₃ +Y ₂ O ₃	50	0	30	1100	
10606	Framatome	Al ₂ O ₃ +Y ₂ O ₃	50	0	30	1200	negative MS values

Appendix

Test	Specimen	Crucible	Ar, ln/h	H ₂ , ln/h	H ₂ O, g/h	T, °C	Remarks
10607	Framatome	Al ₂ O ₃ +Y ₂ O ₃	50	0	30	1300	
10611	Framatome	Al ₂ O ₃ +Y ₂ O ₃	50	0	30	1400	
10612	Framatome	Al ₂ O ₃ +Y ₂ O ₃	50	0	30	1500	blockade of off-gas pipe
10907	CODEX	Al ₂ O ₃ +Y ₂ O ₃	50	0	30	800	1 st CODEX test
10910	CODEX	Al ₂ O ₃ +Y ₂ O ₃	50	0	30	1000	
10911	CODEX	Al ₂ O ₃ +Y ₂ O ₃	50	0	30	1200	
10912	CODEX	Al ₂ O ₃ +Y ₂ O ₃	50	0	30	1400	
10913	-	Al ₂ O ₃ +Y ₂ O ₃	20-50	25 %	0-70	1200	purification of BOX Rig, adjustment of calibration factors for steam and H ₂
10914	thin disc	Al ₂ O ₃ +Y ₂ O ₃	50	0	30	1400	complete oxidation of a small specimen to adjust H and C balance
10927	ESK pellet	Al ₂ O ₃ +Y ₂ O ₃	50	0	30	800	1 st Test with dense 1/2 ESK Pellet
11001	ESK pellet	Al ₂ O ₃ +Y ₂ O ₃	50	0	30	1000	
11002	ESK pellet	Al ₂ O ₃ +Y ₂ O ₃	50	0	30	1200	
11004	ESK pellet	Al ₂ O ₃ +Y ₂ O ₃	50	0	30	1400	
20304	Framatome	Al ₂ O ₃ +ZrO ₂	50	0	3	800	1 st test with low steam rate
20305	Framatome	Al ₂ O ₃ +ZrO ₂	50	0	3	1000	
20306	Framatome	Al ₂ O ₃ +ZrO ₂	50	0	3	1200	
20307	Framatome	Al ₂ O ₃ +ZrO ₂	50	0	3	1400	MS capillary blocked

Appendix

Test	Specimen	Crucible	Ar, ln/h	H ₂ , ln/h	H ₂ O, g/h	T, °C	Remarks
20313	Framatome	Al ₂ O ₃ +ZrO ₂	50	0	3	1400	repetition of test 20307
20409	ESK pellet	Al ₂ O ₃ +ZrO ₂	50	0	3	800	1 st test with ESK pellet at low steam rate
20410	ESK pellet	Al ₂ O ₃ +ZrO ₂	50	0	3	1000	
20411	ESK pellet	Al ₂ O ₃ +ZrO ₂	50	0	3	1200	
20416	ESK pellet	Al ₂ O ₃ +ZrO ₂	50	0	3	1400	
30509	ESK pellet	Al ₂ O ₃ +ZrO ₂	15-300	0	3-60	1200	IBRAE proposal, varying flow rate, p _{H2O} constant
30512a	ESK pellet	Al ₂ O ₃ +ZrO ₂	15-300	0	3-60	1000	IBRAE proposal, varying flow rate, p _{H2O} constant
30512c	ESK pellet	Al ₂ O ₃ +ZrO ₂	15-300	0	3-60	1400	IBRAE proposal, varying flow rate, p _{H2O} constant
30520	ESK pellet	Al ₂ O ₃ +ZrO ₂	50	0	5-70	1000	varying steam flow rate
30521	ESK pellet	Al ₂ O ₃ +ZrO ₂	50	0	5-70	1200	varying steam flow rate
30524	ESK pellet	Al ₂ O ₃ +ZrO ₂	50	0	5-70	1000	varying steam flow rate

Table A2: Essential results of isothermal experiments on B₄C oxidation in the BOX rig

Test	Specimen	T °C	H ₂ _{max} l/h	H ₂ _{const} l/h	H ₂ _{integral} ml	CO _{integral} ml	CO ₂ _{integr} ml	CH ₄ _{integr} ml	Δm %	Ox. rate mole/m ² s	Remarks
00823	Framatome	800	0.7	0.15	184	16	16	2.7	+6.8	0.00062	1 st series
00906	Framatome	800	1.6	0.2	223	19	12	3.6	+7.0	0.00083	1 st series, repetition of test 00823, low Ar
00913	Framatome	800	0.8	0.12	178	13	11	2.8	+7.0	0.00050	1 st series, repetition of test 00823
10214	Framatome	800	0.73	0.26	239	-	-	2.9	+6.7	0.0011	2 nd series, negative MS values
10405	Framatome	800	0.81	0.23	208	23	21	4.0	+5.6	0.00096	3 rd series
10504	Framatome	800	0.82	0.28	236	6	11	3.4	+6.9	0.0012	3 rd series, off-gas temp too low, bad MS signal for steam
20304	Framatome	800	0.25	(0.05)	174	13	4	1.2	+8.4	(0.00021)	low steam, 1 h!
10216	Framatome	900	3.67	0.25	224	-	(6.5)	2.1	+3.5	0.0010	2 nd series, negative MS values
10511	Framatome	900	3.31	0.25	205	18	13	2.3	+3.8	0.0010	3 rd series
00824	Framatome	1000	4.7	0.14	132	14	14	0.8	+2.1	0.00058	1 st series
10219	Framatome	1000	5.69	0.3	203	18	16	1.1	+0.8	0.0013	2 nd series
10514	Framatome	1000	5.68	0.26	180	19	14	0.9	-0.1	0.0011	3 rd series
20305	Framatome	1000	1.02	0.04	59	5	2	0.1	+2.3	0.00017	low steam
10220	Framatome	1100	3.25	0.37	207	15	27	0.6	-3.5	0.0015	2 nd series, reaction tube

Appendix

Test	Specimen	T °C	H ₂ _{max} l/h	H ₂ _{const} l/h	H ₂ _{integral} ml	CO _{integral} ml	CO ₂ _{integr} ml	CH ₄ _{integr} ml	Δm %	Ox. rate mole/m ² s	Remarks
											leaking
10605a	Framatome	1100	6.90	0.43	251	20	36	0.7	-2.2	0.0018	3 rd series
00825	Framatome	1200	6.2	0.35	219	3.4	36	0.4	-2.6	0.0015	1 st series
10606	Framatome	1200	6.49	0.62	395	-	55	0.4	-4.5	0.0026	3 rd series, negative MS values
20306	Framatome	1200	1.25	0.17	134	9	10	0.2	+0.7	0.00071	low steam
10607	Framatome	1300	6.23	1.10	691	(19)	93	0.7	-15.3	0.0046	3 rd series
00828	Framatome	1400	6.4	1	633	11	97	0.2	-14.9	0.00420	1 st series
10611	Framatome	1400	10.90	2.37	1306	35	148	0.4	-32.7	0.0099	3 rd series
20307	Framatome	1400	-	-	-	-	-	-	-2.9	-	low steam, MS failure
20313	Framatome	1400	1.82	(0.70)	469	28	37	0.1	1.5	(0.0029)	low steam
00928	Framatome	1500	3.5	1.1	802	29	158	0.4	-28.1	0.0046	1 st series, MS problems?
00829	Framatome	1600	9.4						-47.0	-	1 st series, blockage of off-gas pipe
10907	CODEX	800	0.66	0.13	126	9	9	1.2	+3.7	0.00070	
10910	CODEX	1000	1.91	0.2	144	11	13	0.5	+1.2	0.0011	
10911	CODEX	1200	2.68	0.46	279	10	36	0.4	-5.2	0.0025	
10912	CODEX	1400	5.2	1.4	775	(21)	(94)	(0.3)	-28.1	0.0076	
10927	ESK pellet	800	0.16	0.14	68	8	8	1.2	-0.4	0.00045	

Appendix

Test	Specimen	T °C	H ₂ _{max} l/h	H ₂ _{const} l/h	H ₂ _{integral} ml	CO _{integral} ml	CO ₂ _{integr} ml	CH ₄ _{integr} ml	Δm %	Ox. rate mole/m ² s	Remarks
20409	ESK pellet	800	0.036	0.024	25	4	4	0.2	0.011	0.000077	low steam
11001	ESK pellet	1000	0.68	0.32	166	18	16	0.8	-1.4	0.0010	
20410	ESK pellet	1000	0.18	0.042	26	4	2	0.1	-0.011	0.00014	low steam
11002	ESK pellet	1200	1.13	0.81	413	14	56	0.6	-3.9	0.0025	
20411	ESK pellet	1200	0.31	0.17	90	5	9	0.1	-0.9	0.00054	low steam
11004	ESK pellet	1400	3.54	2.1	1219	34	145	0.4	-15.3	0.0071	
20416	ESK pellet	1400	0.78	0.61	321	15	28	0.1	-3.6	0.0020	low steam
10516	ESK powder	800	0.86	(0.12)	139	11	12	1.1	+12.3	0.0020	
10529	ESK powder	1000	1.06	0.16	112	15	16	0.6	+6.6	0.0026	
10530	ESK powder	1200	1.44	0.29	192	11	34	0.5	+5.6	0.0048	
10531	ESK powder	1400	1.77	(0.74)	458	12	69	0.4	-9.2	0.0122	
10914	Framatome thin disc	1400	1.75	-	121	(3)	19	(0.3)	-100		complete oxidation of a small specimen

A3 Conversion from H₂ volume rates into reaction rates

As already mentioned before, the oxidation reaction rates given in this report are based on the hydrogen release rates, assuming the formation of CO₂ is the main reaction (equation 2), and referred to the geometric surface of the specimens. The cylinder surface less the surface of the bottom was used for the pellets and only the circular surface of the ZrO₂ crucible for the powder specimens. The ESK pellets originally were too large for the BOX Rig, therefore, they were cut in two pieces. The exact dimensions of the resulting (half) pellets are specified in [Table A3](#).

The gas flow rates given in the diagrams and tables of this report are referred to normal conditions, i.e. 0 °C and 1 bar, thus the molar volume of all gases (injected and measured) is 22.4 l/mol.

The hydrogen release rates were converted by the following equation:

$$[\text{H}_2 \text{ release rate in l/h}] = [\text{H}_2 \text{ release rate in mole/m}^2\text{s}] \times F_{\text{H}_2} \quad (\text{A1})$$

The oxidation rates referred to the molar amount of consumed boron carbide is calculated by equation 5.

$$[\text{H}_2 \text{ release rate in l/h}] = [\text{B}_4\text{C oxidation rate in mole/m}^2\text{s}] \times F_{\text{B}_4\text{C}} \quad (\text{A2})$$

with $F_{\text{B}_4\text{C}} = 8 \times F_{\text{H}_2}$

Table A3: Geometric surface of the specimens and conversion factors from volume into specific molar hydrogen release rates

Specimen	A, m ²	F _{H₂}
Framatome	$3.72 \cdot 10^{-4}$	30.03
CODEX	$2.87 \cdot 10^{-4}$	23.14
ESK powder	$0.94 \cdot 10^{-4}$	7.60
ESK 10927	$4.80 \cdot 10^{-4}$	38.71
ESK 11001	$4.82 \cdot 10^{-4}$	38.87
ESK 11002	$5.03 \cdot 10^{-4}$	40.56
ESK 11004	$4.60 \cdot 10^{-4}$	37.09
ESK 20409	$4.91 \cdot 10^{-4}$	39.59
ESK 20410	$4.72 \cdot 10^{-4}$	38.06
ESK 20411	$4.76 \cdot 10^{-4}$	38.38
ESK 20416	$4.85 \cdot 10^{-4}$	39.11
ESK 30520	$4.68 \cdot 10^{-4}$	37.74
ESK 30521	$4.89 \cdot 10^{-4}$	39.43

A4 Figures A1 – A64: Test protocols

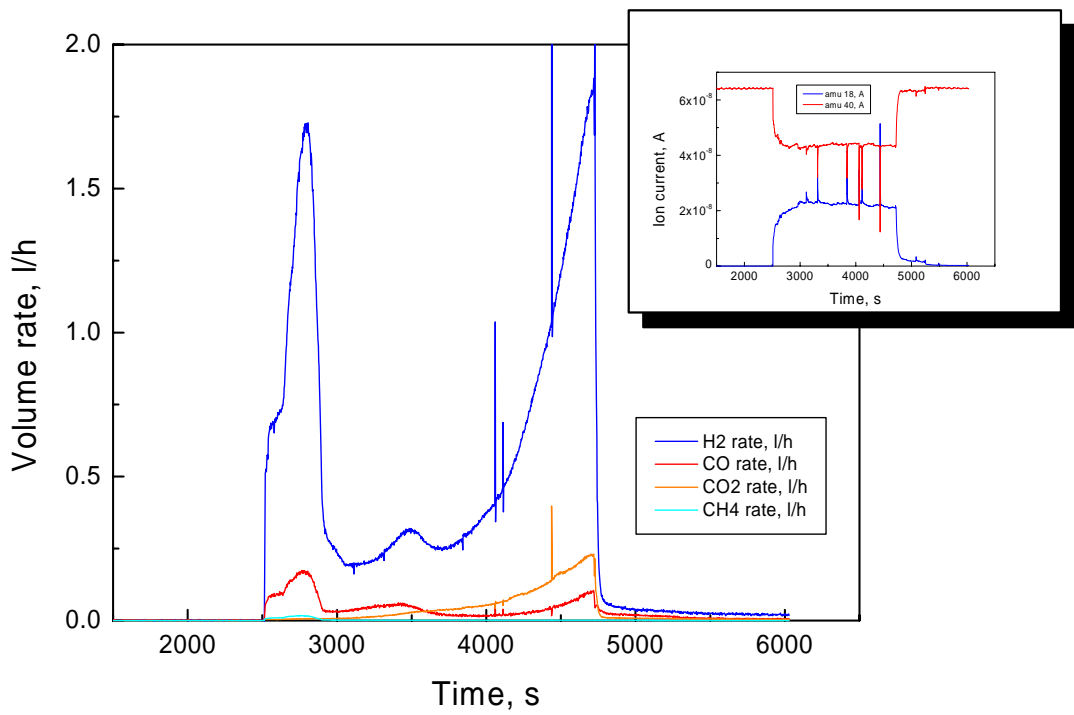
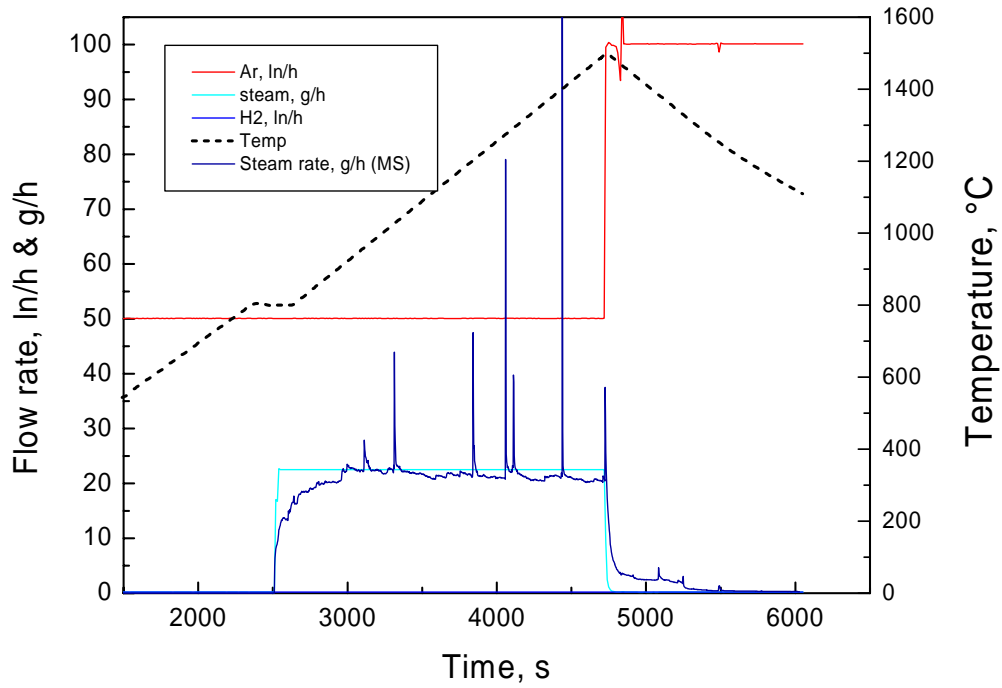
On the following pages the test conduct and main results obtained by mass spectrometer of all tests performed are compiled in chronological order.

For each experiment one diagram (the upper one) shows temperatures and gas input. Mostly, the steam (and hydrogen if it was injected) rate measured by MS is shown additionally for comparison in this diagram.

The lower diagram presents the results of the MS measurements for H₂, CO, CO₂ and CH₄. Additionally, a small diagram shows the ion currents measured at masses 18 and 40, representing the major input gases steam and argon. From that diagram one can see, if the test run well. A simultaneous decrease of the ion currents of steam and argon is an indication for a (partial) blockade of the MS capillary which was sometimes seen during tests at higher temperatures. For such tests the data have to be considered carefully and only taken "half-quantitatively".

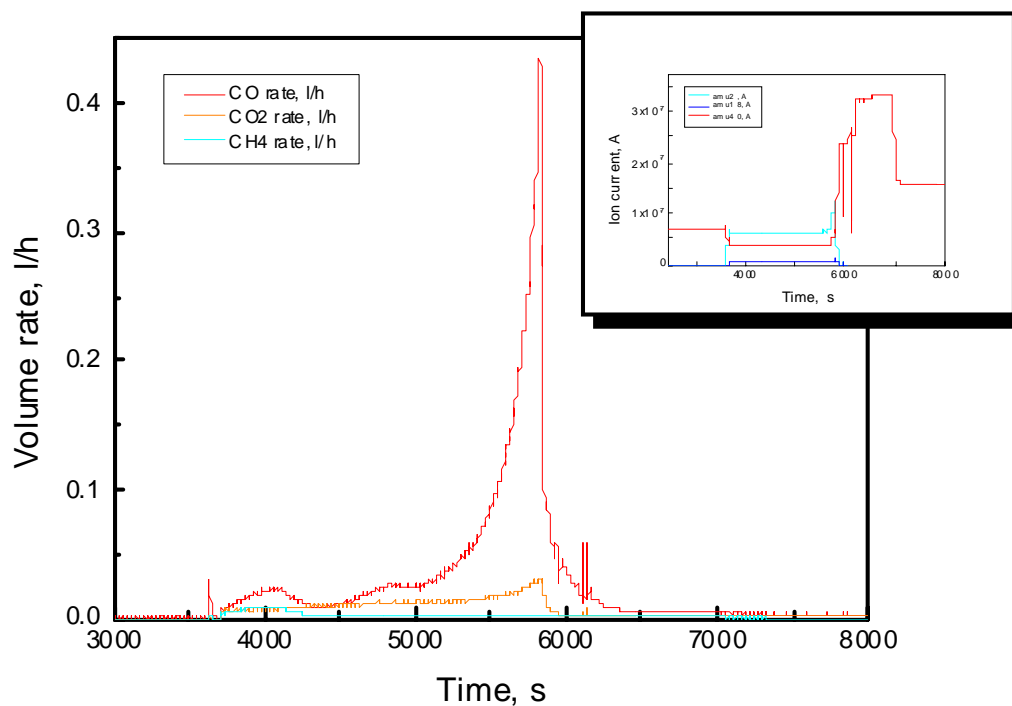
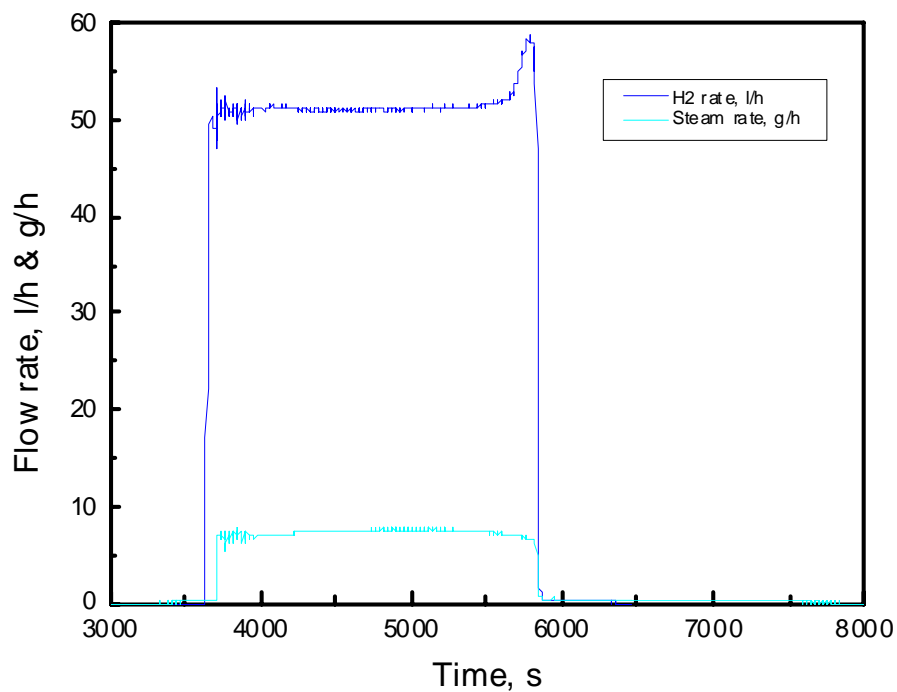
Test Box00809:

Transient oxidation between 800 and 1500 °C of a Framatome B₄C pellet in steam



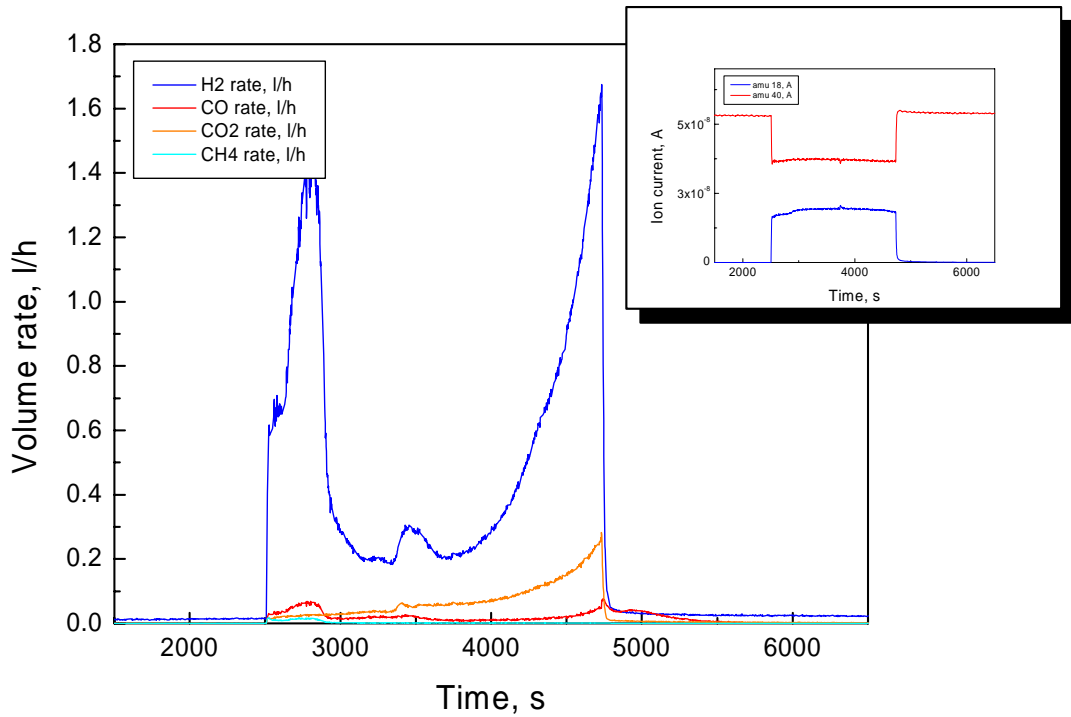
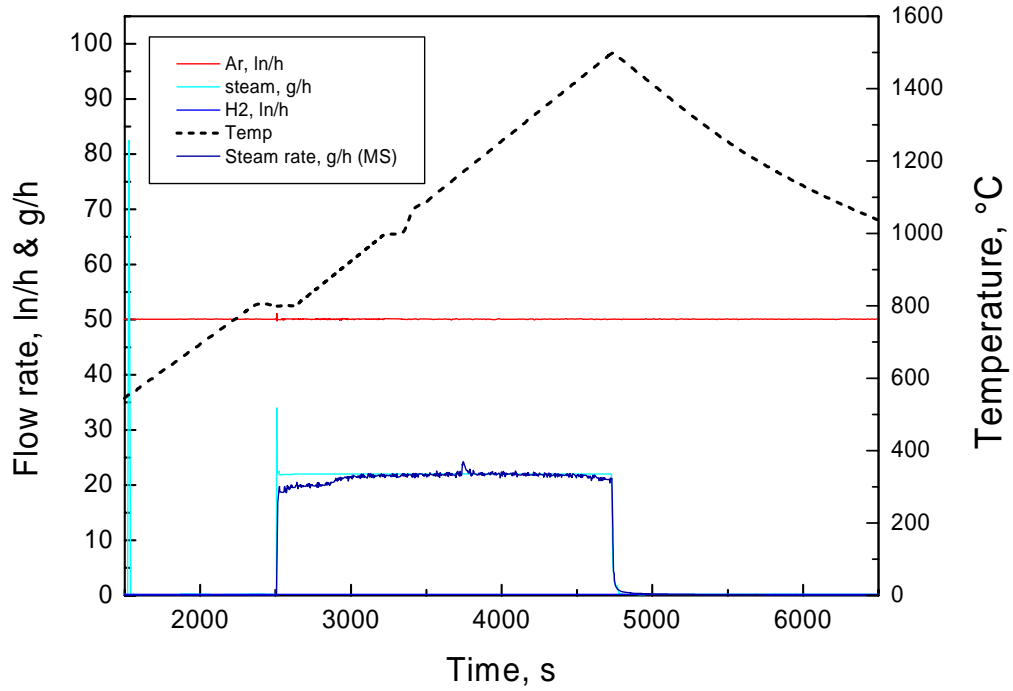
Test Box00810:

Transient oxidation between 800 and 1500 °C of
a Framatome pellet B_4C in steam/hydrogen mixture



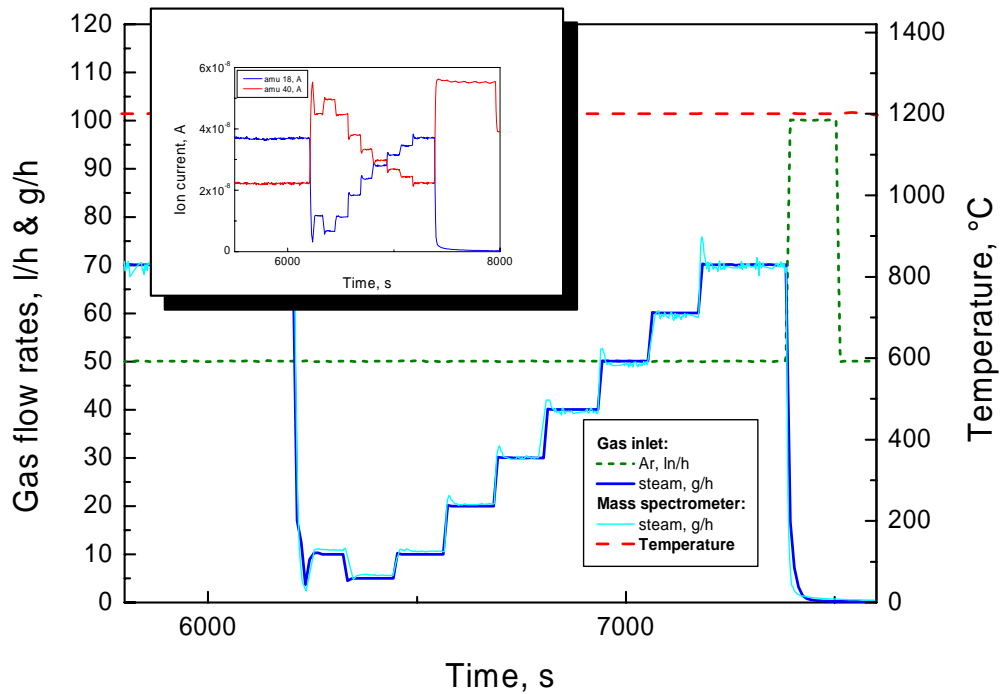
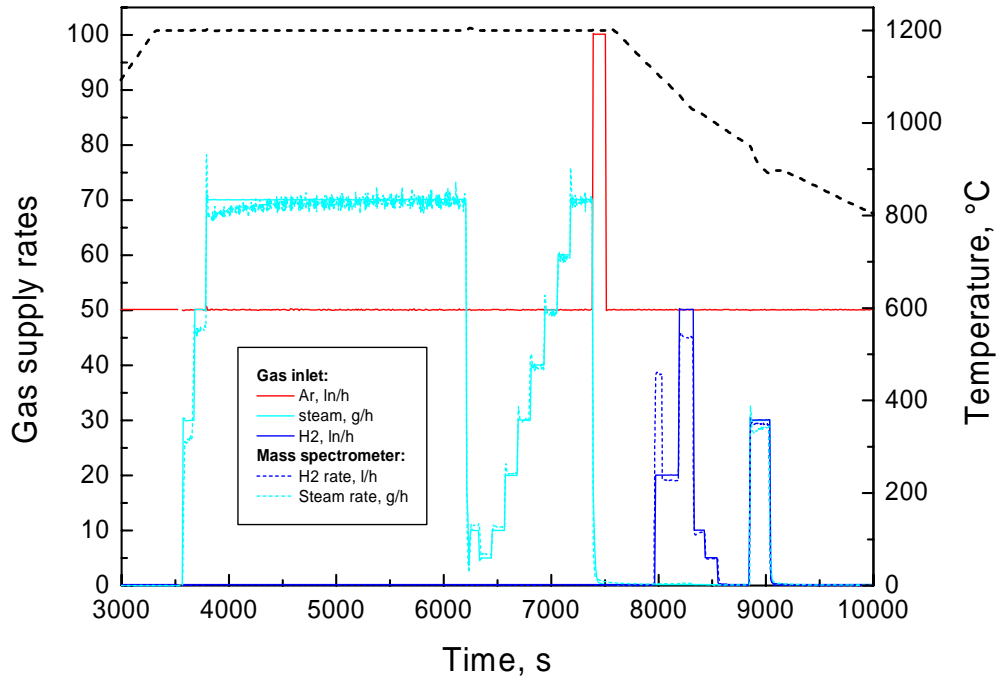
Test Box00816:

Transient oxidation between 800 and 1500 °C of a Framatome B₄C pellet in steam



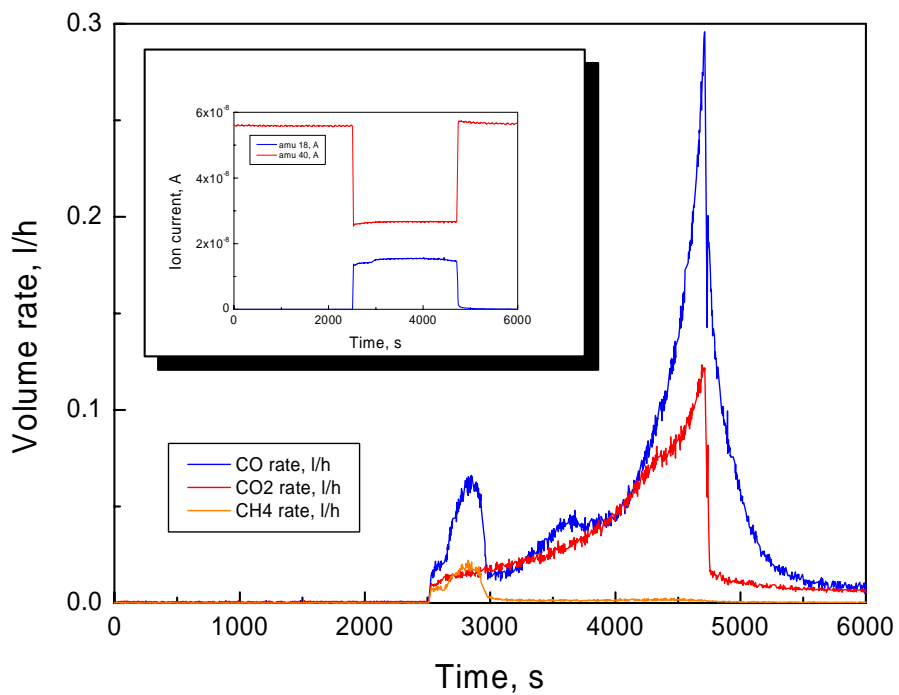
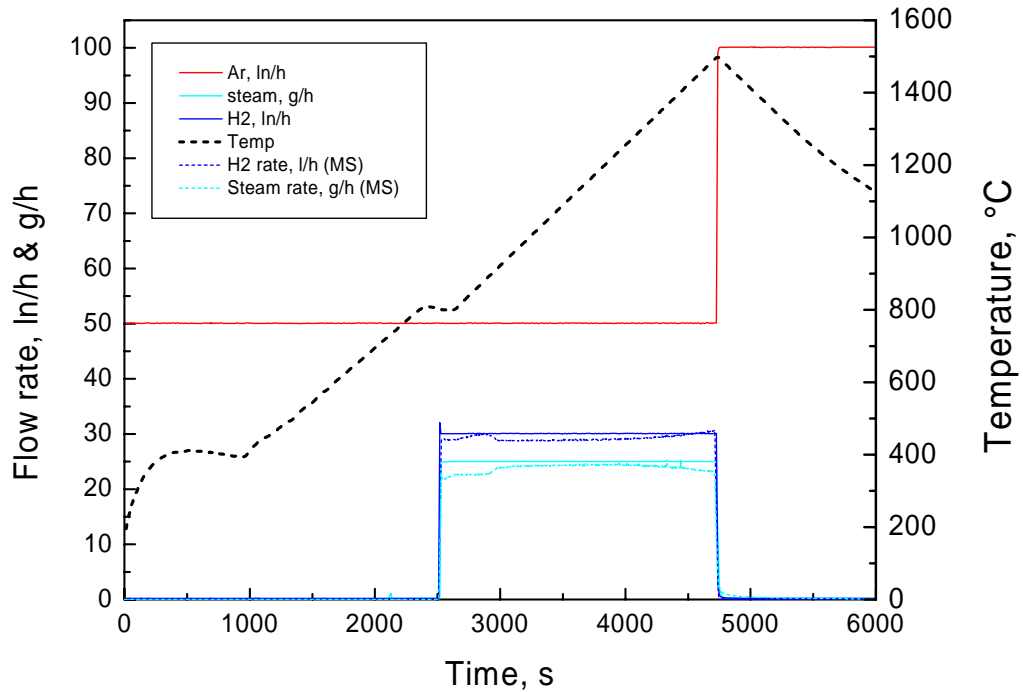
Test Box00817:

Purification of the gas tubes (from boric acid) and test of the steam and hydrogen supply



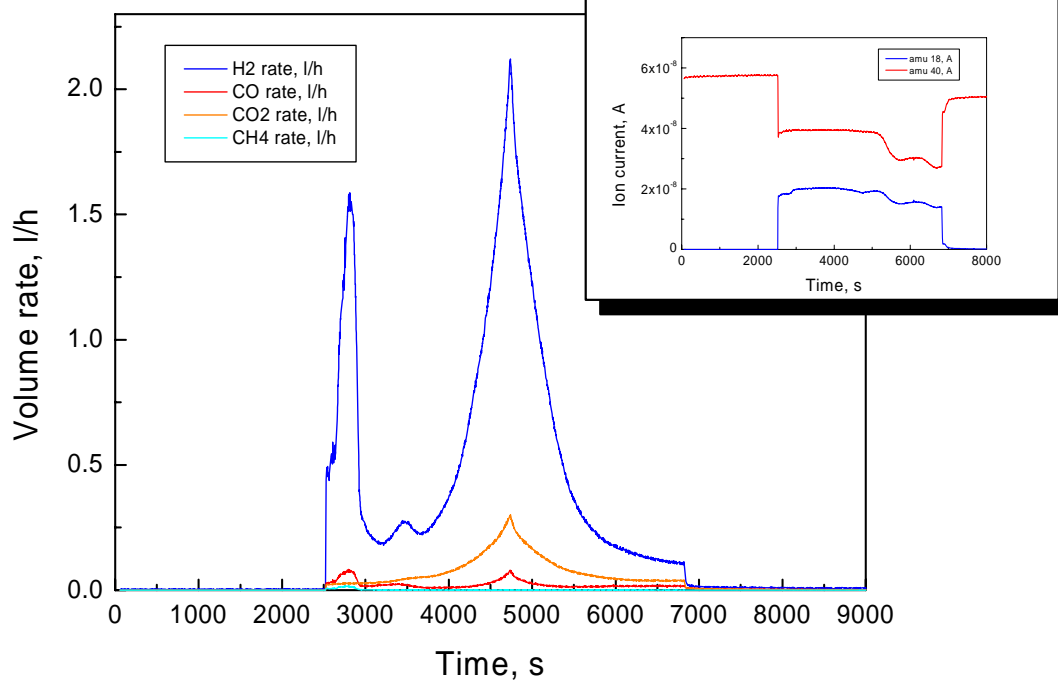
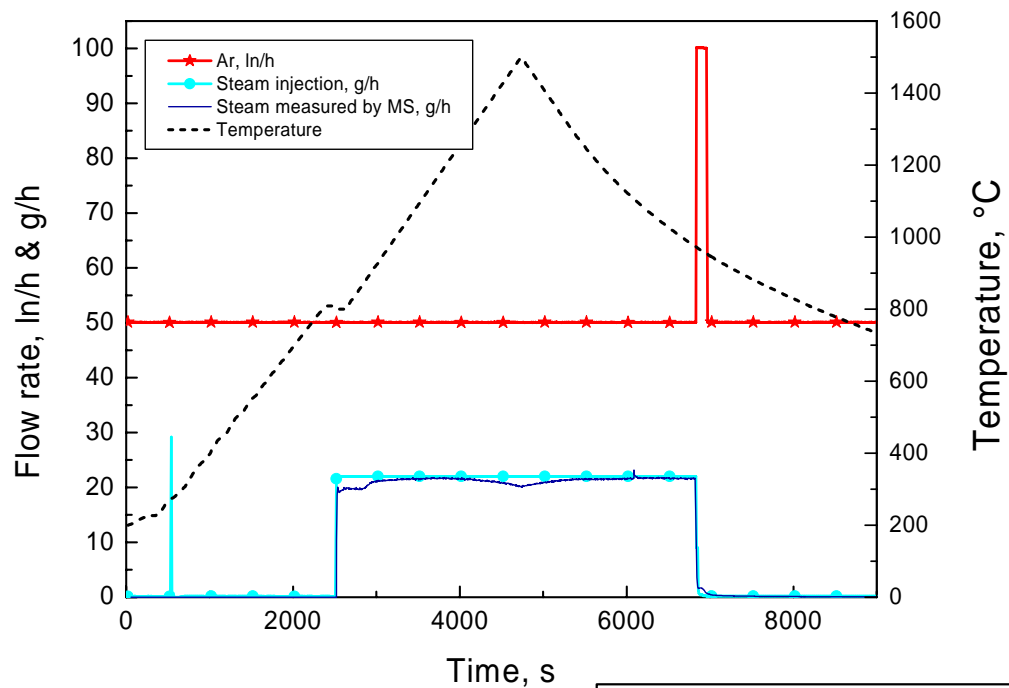
Test Box00818:

Transient oxidation between 800 and 1500 °C of a Framatome B₄C pellet in steam/hydrogen



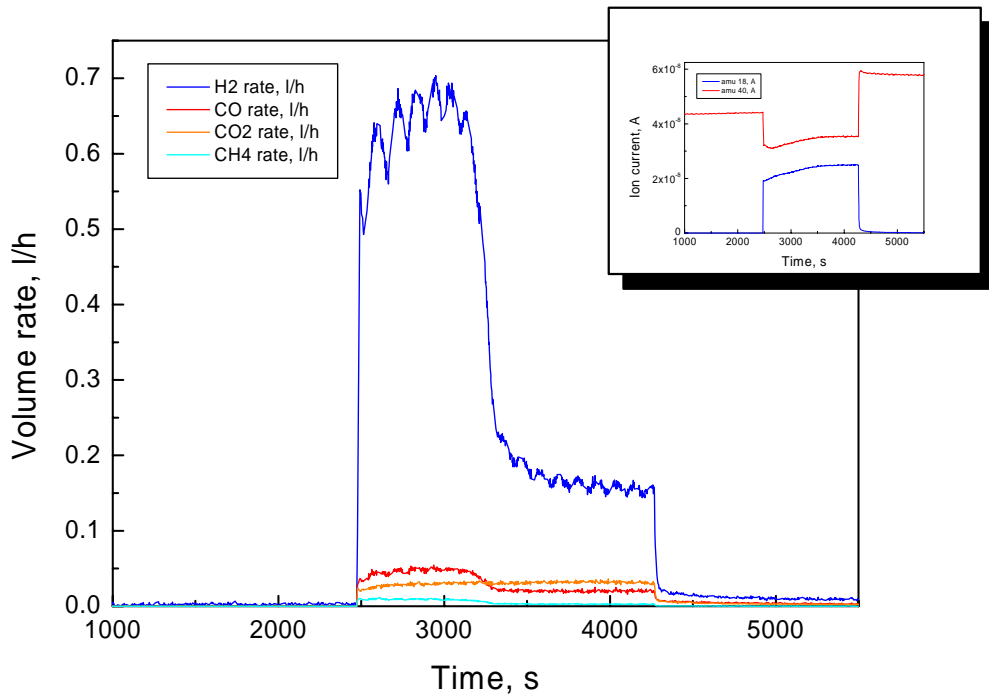
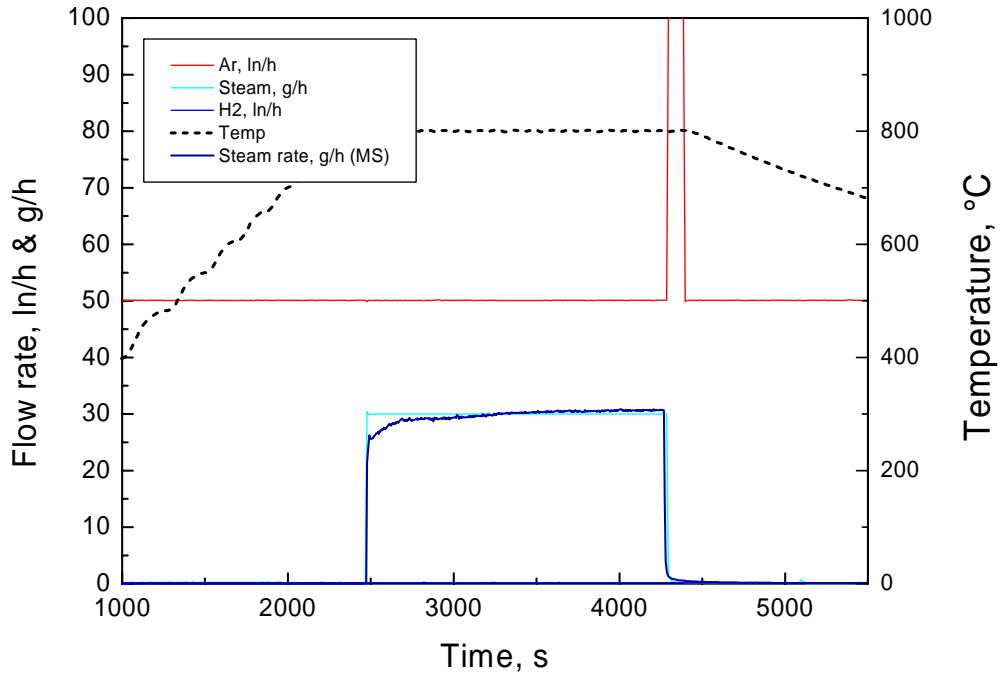
Test Box00821:

Transient oxidation between 800 and 1500 °C of
a Framatome B₄C pellet in steam



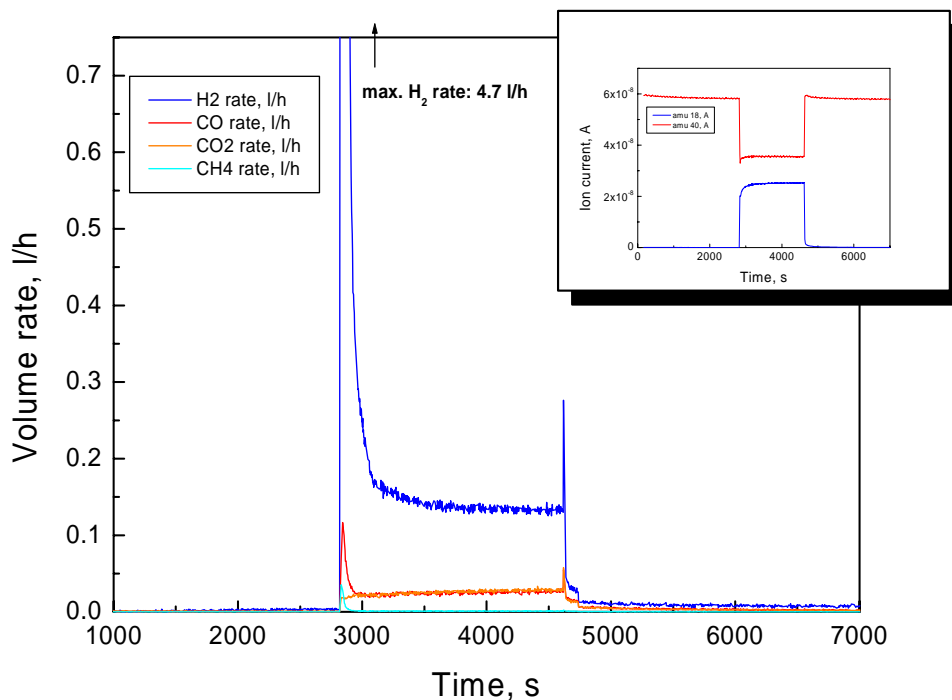
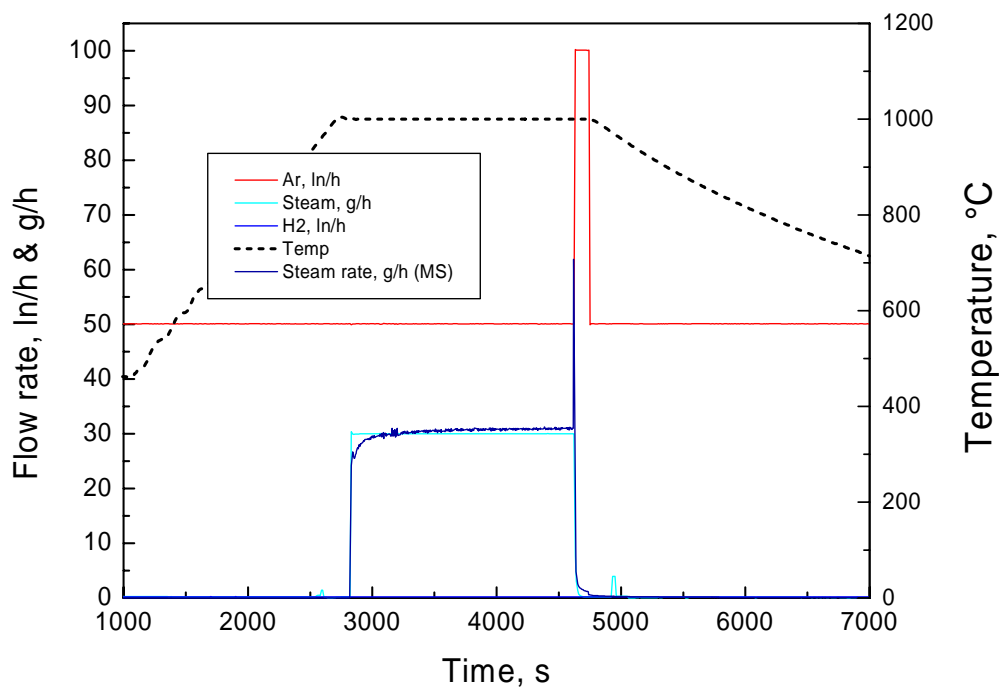
Test Box00823:

Isothermal oxidation of a Framatome B₄C pellet in Ar/steam at 800 °C



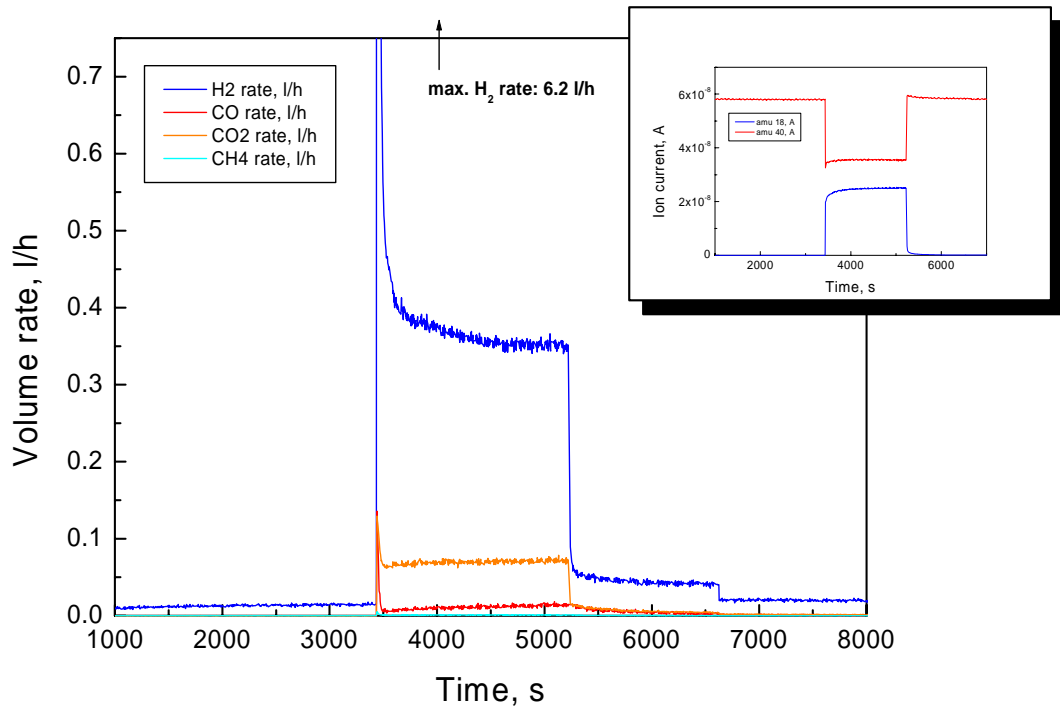
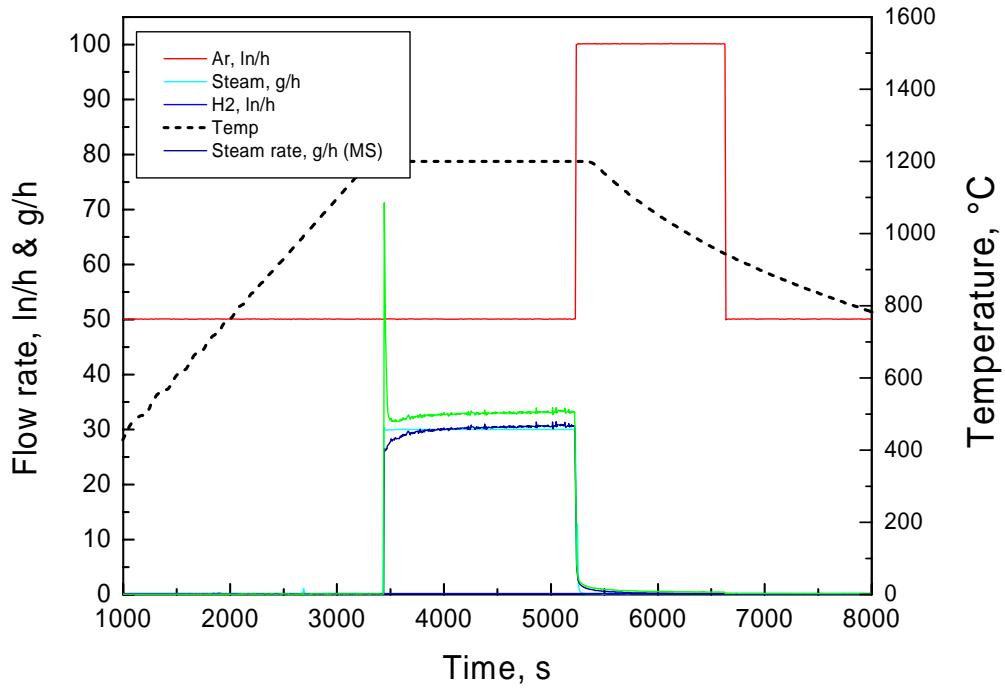
Test Box00824:

Isothermal oxidation of a Framatome B₄C pellet in Ar/steam at 1000 °C



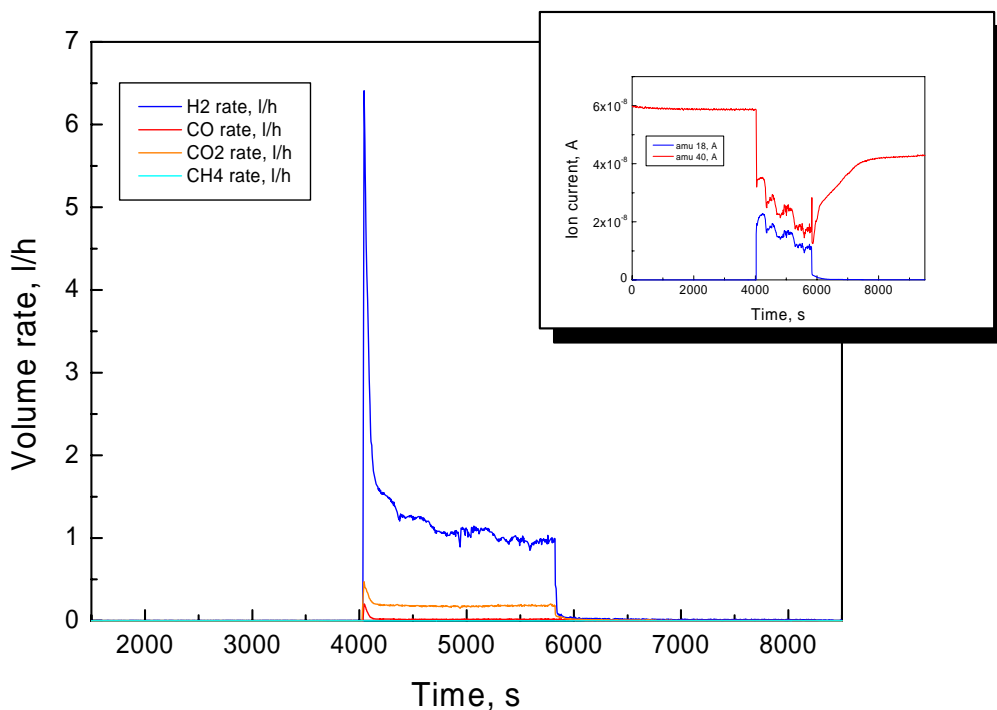
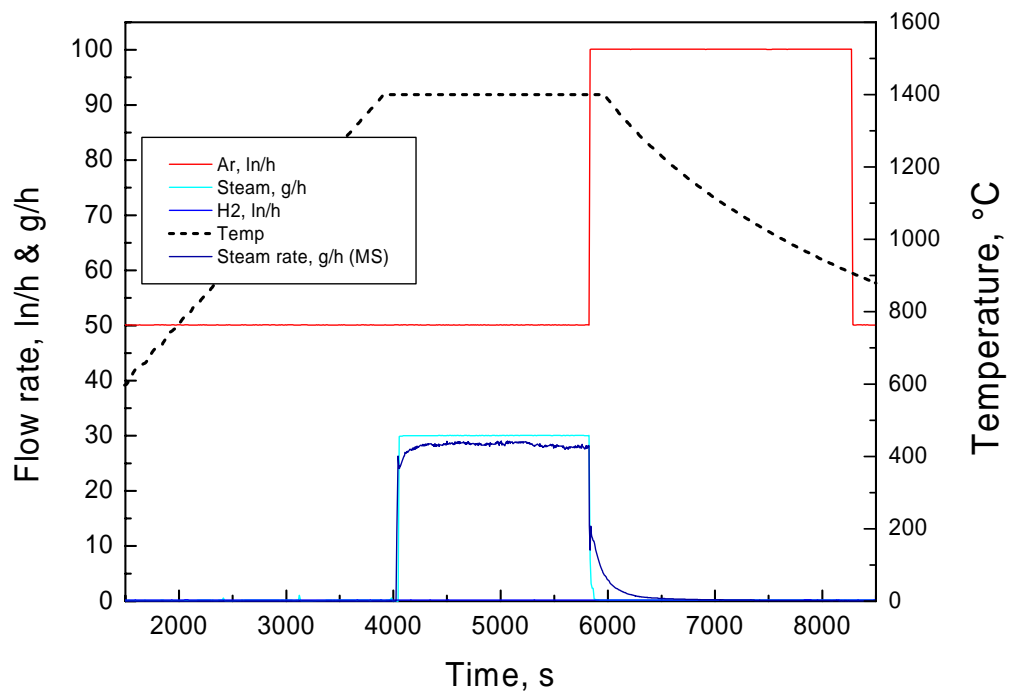
Test Box00825:

Isothermal oxidation of a Framatome B₄C pellet in Ar/steam at 1200 °C



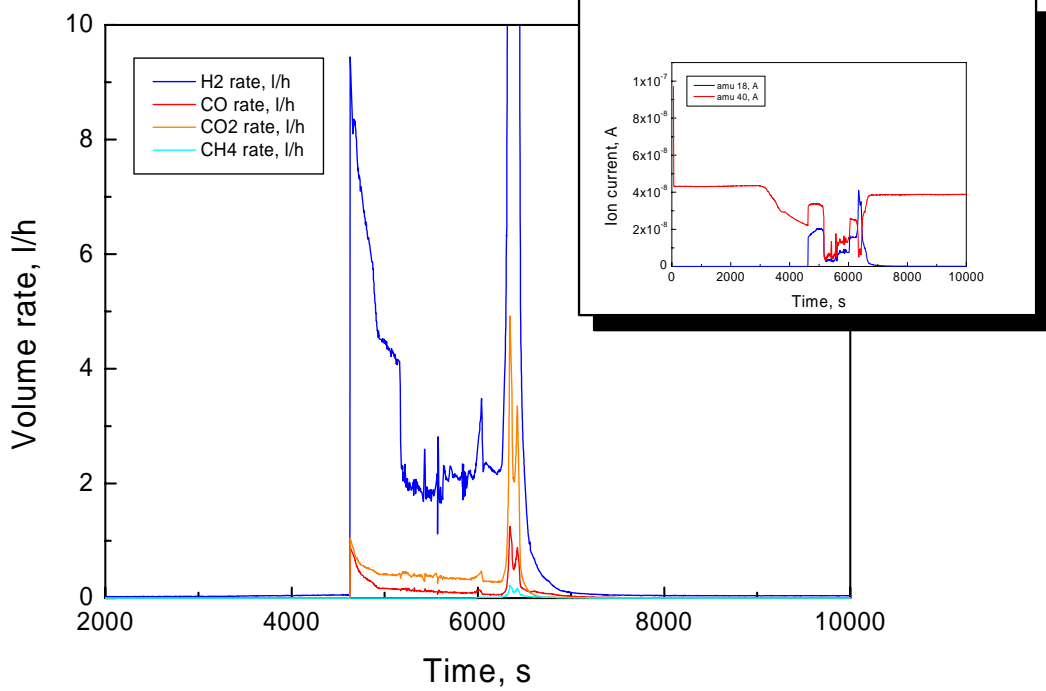
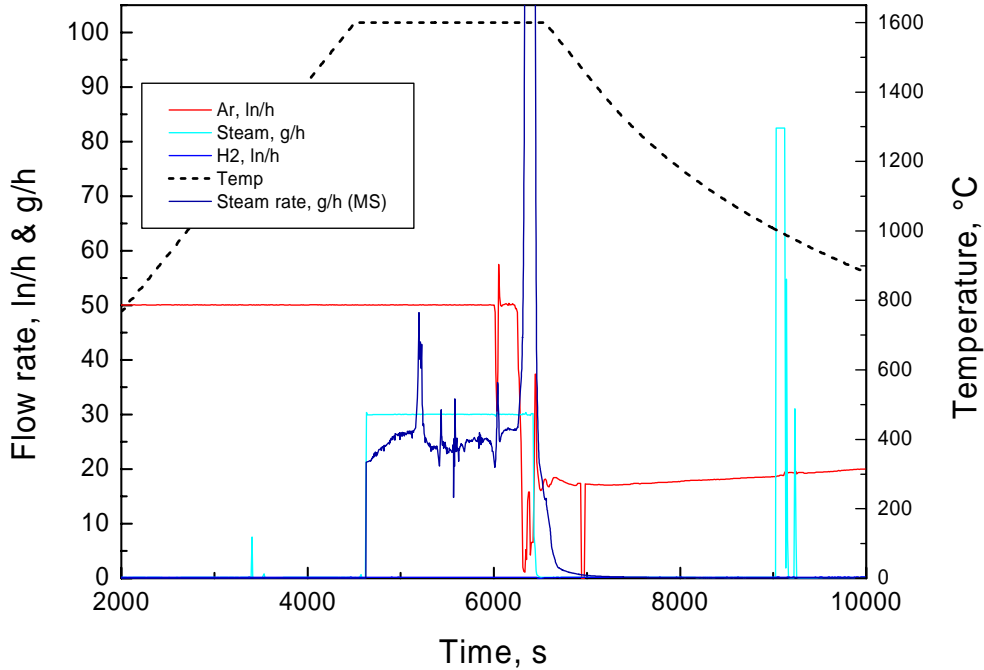
Test Box00828:

Isothermal oxidation of a Framatome B₄C pellet in Ar/steam at 1400 °C

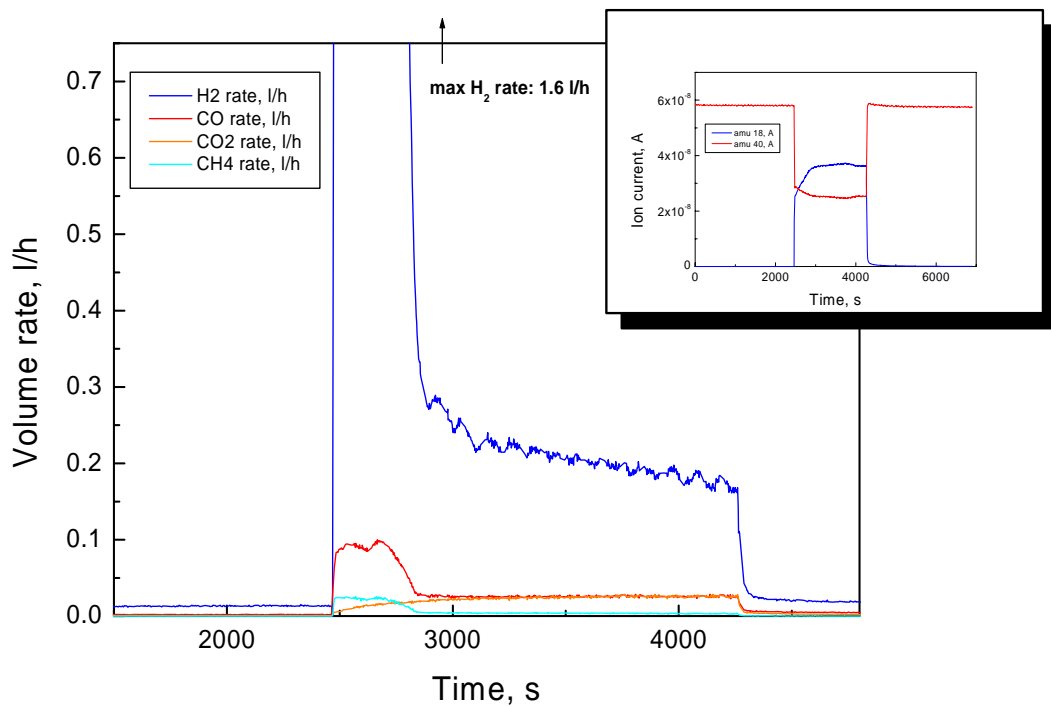
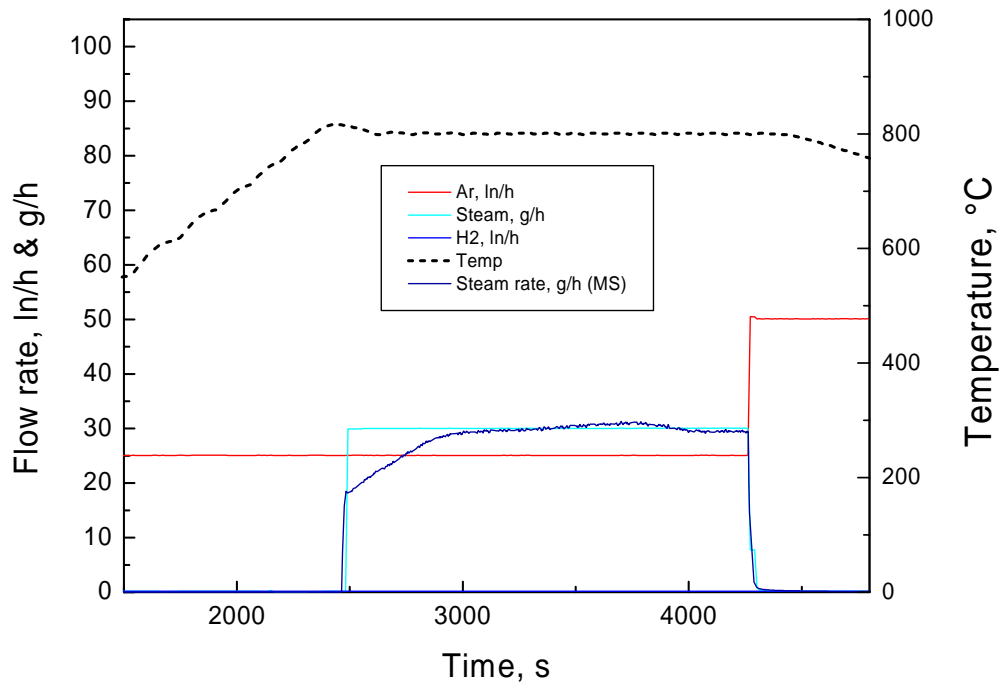


Test Box00829:

Isothermal oxidation of a Framatome B_4C pellet
in Ar/steam at 1600 °C

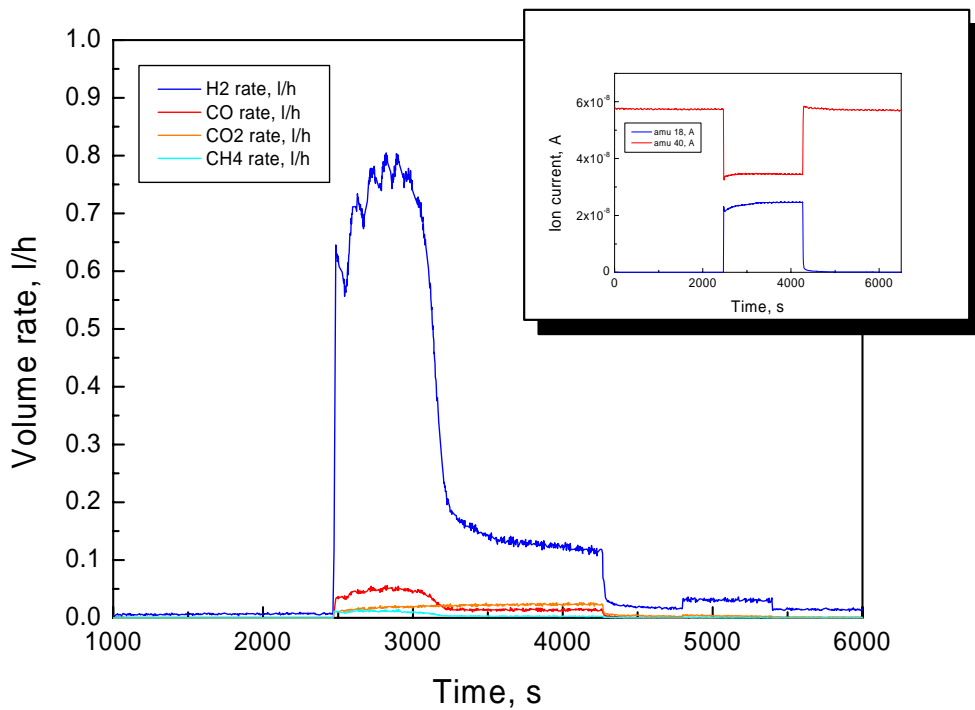
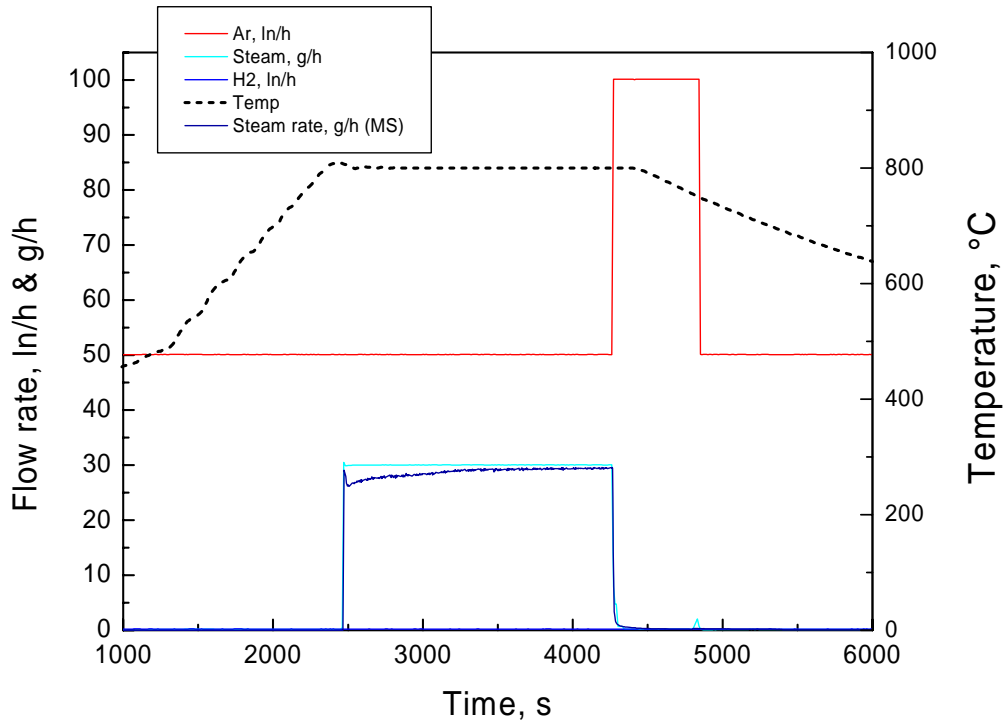


Test Box00906: Isothermal oxidation of a Framatome B₄C pellet in Ar/steam at 800 °C



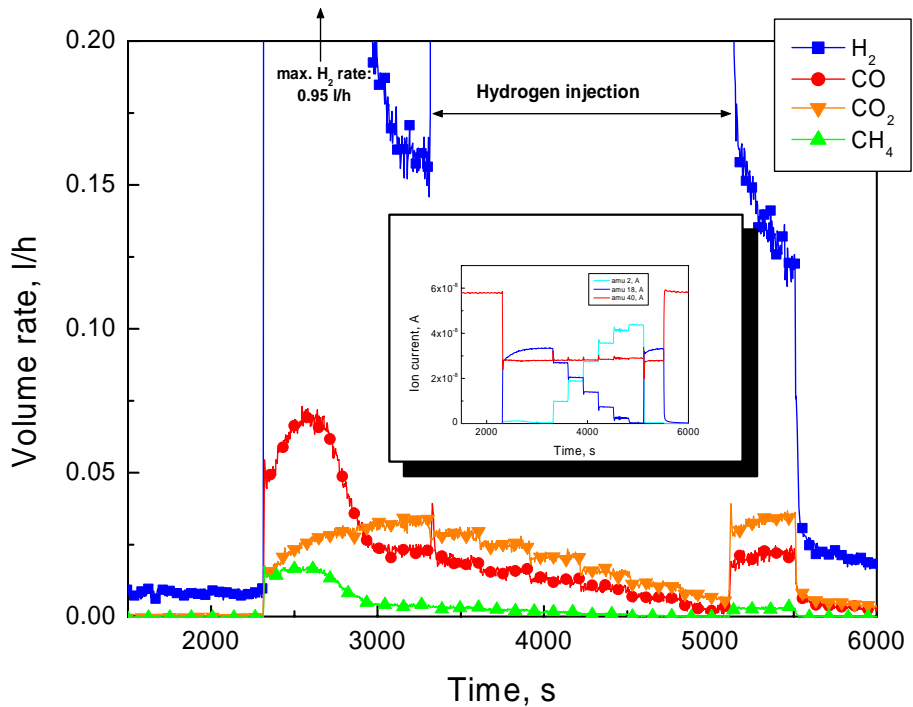
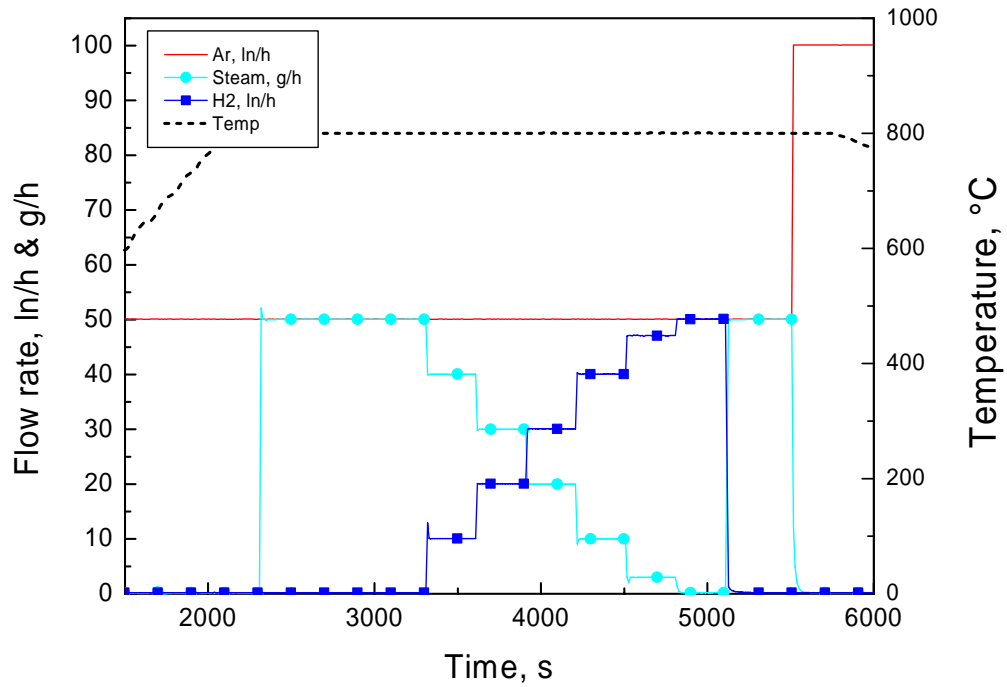
Test Box00913:

Isothermal oxidation of a Framatome B₄C pellet in Ar/steam at 800 °C



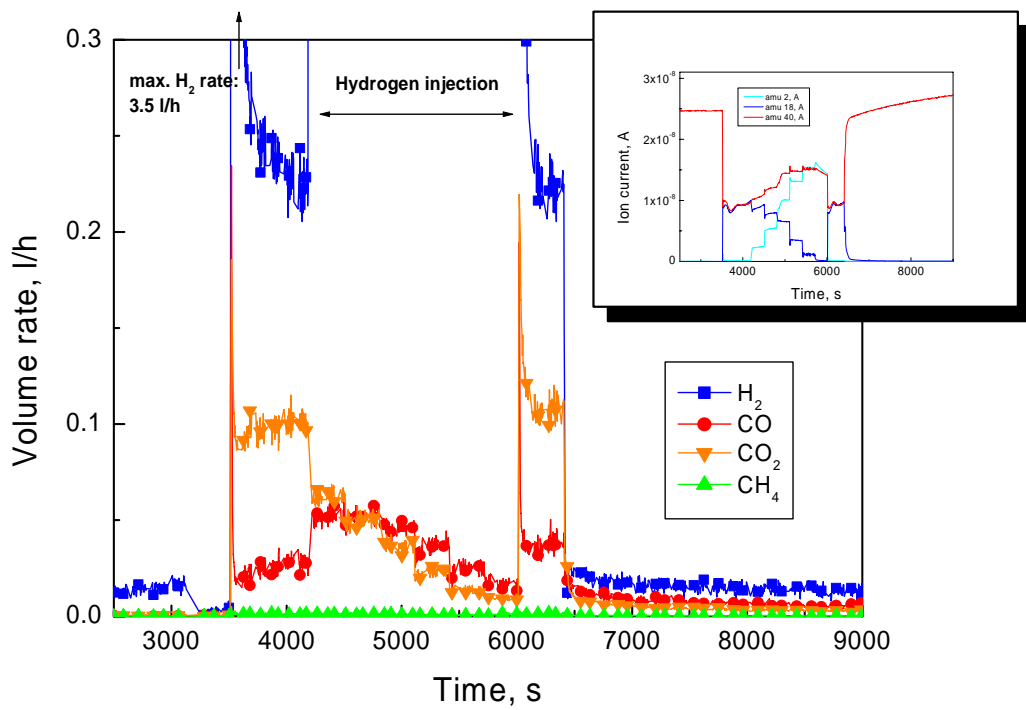
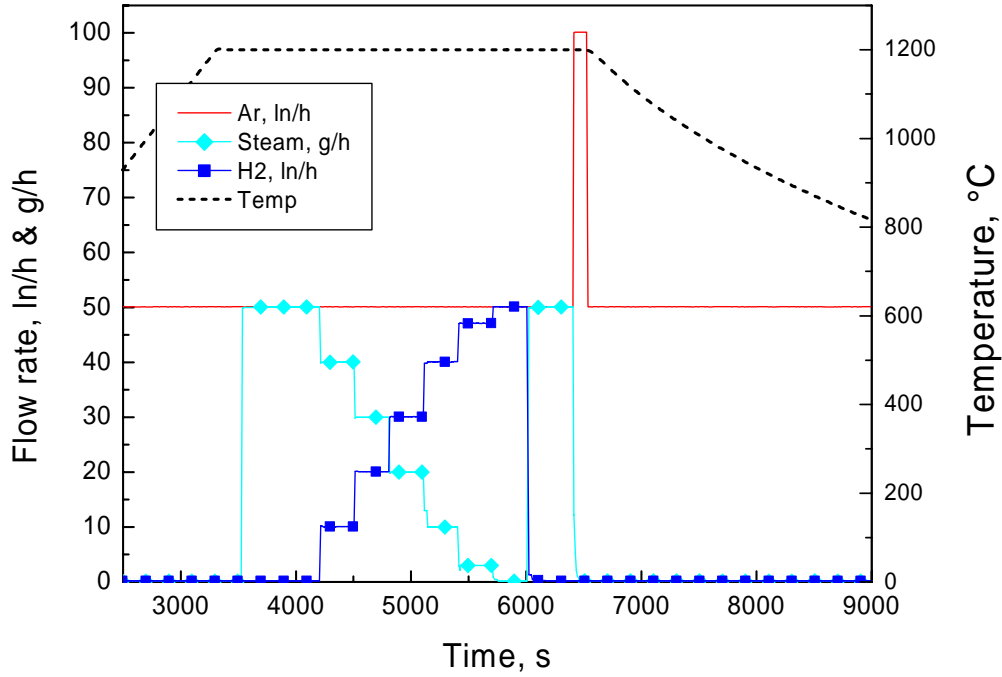
Test Box00921:

Oxidation of a Framatome B₄C pellet at 800 °C under varying hydrogen/steam atmosphere



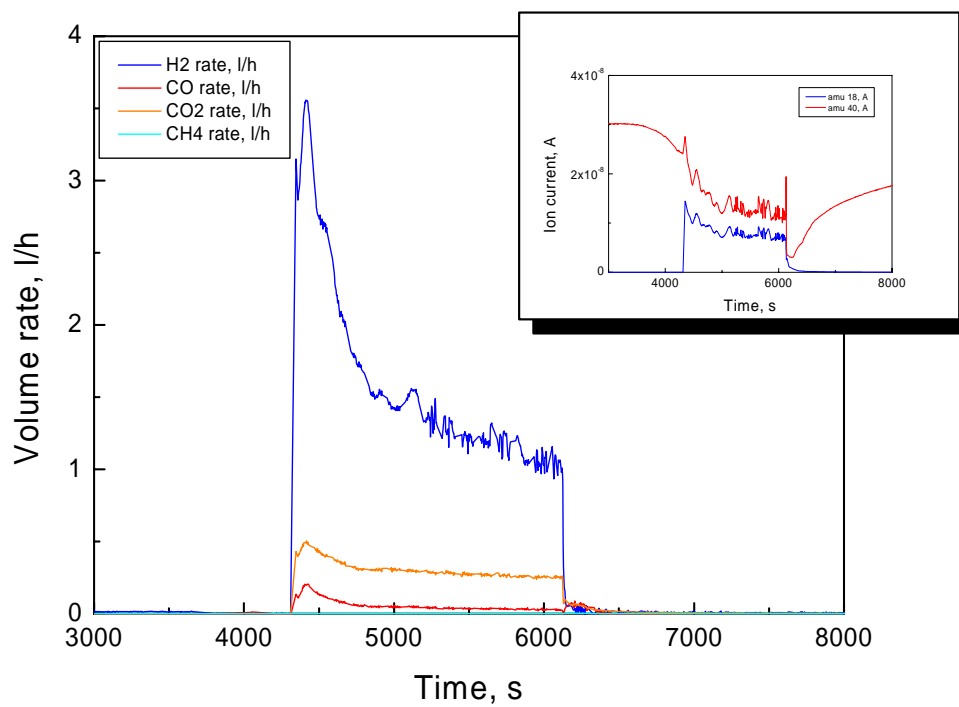
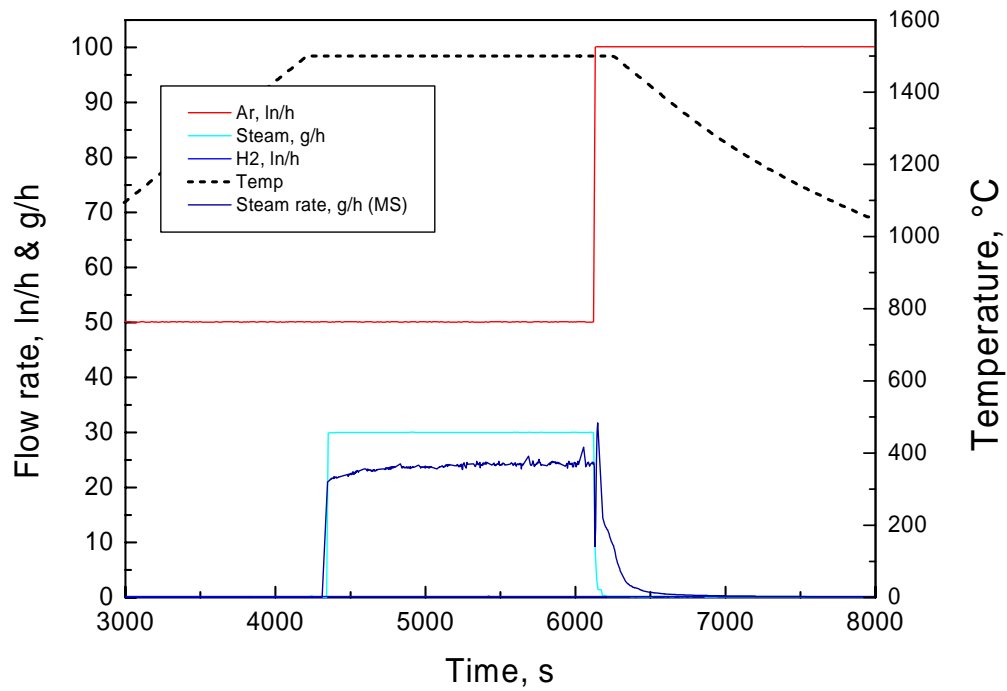
Test Box00927:

Oxidation of a Framatome B₄C pellet at 1200 °C under varying hydrogen/steam atmosphere



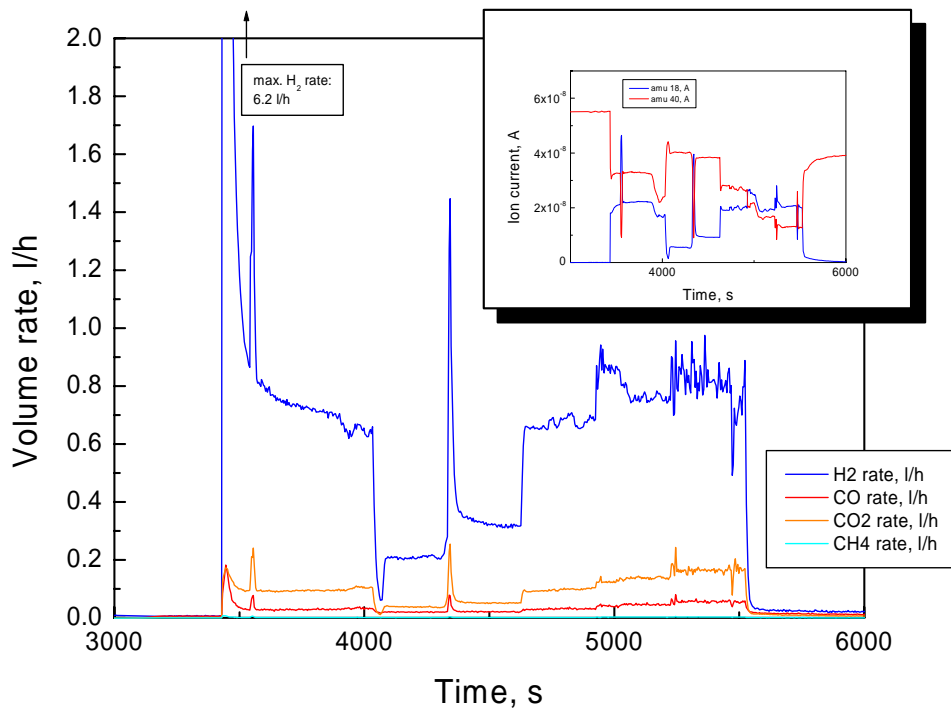
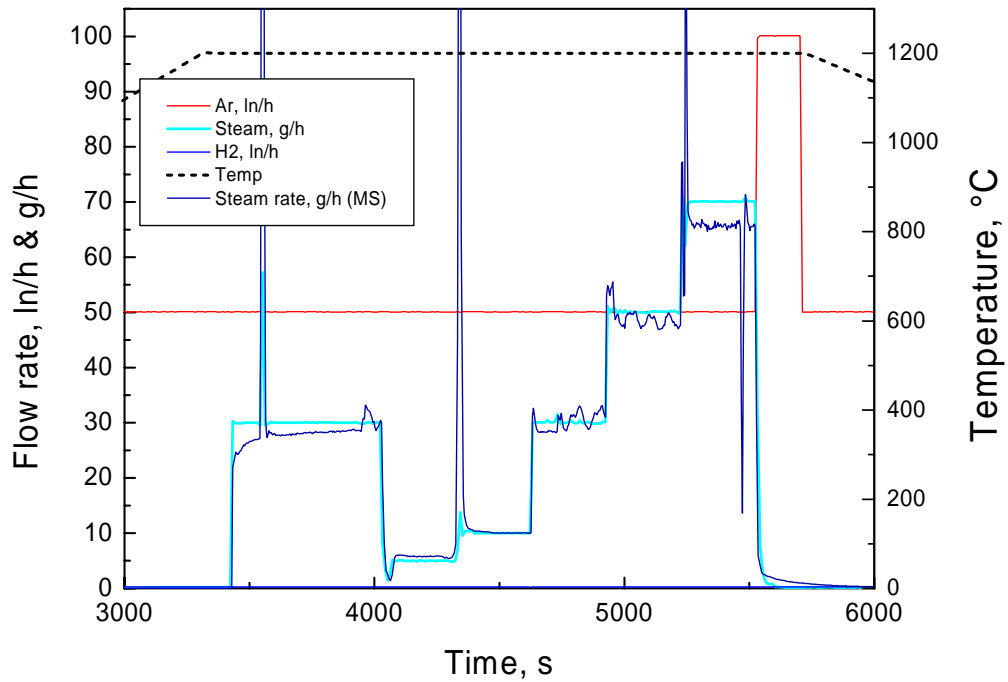
Test Box00928:

Isothermal oxidation of a Framatome B₄C pellet
in Ar/steam at 1500 °C



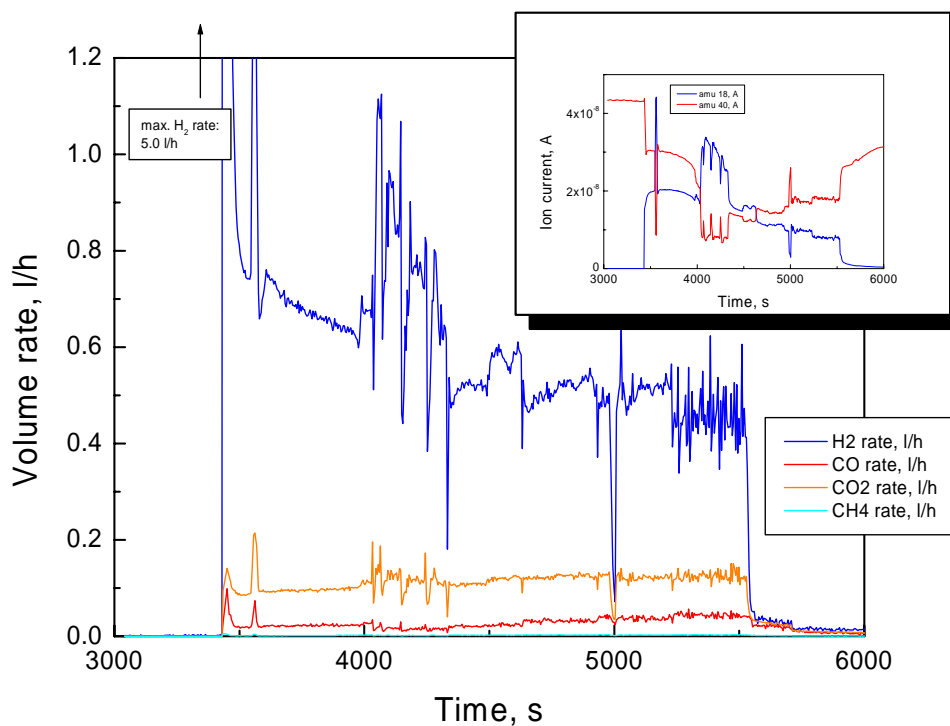
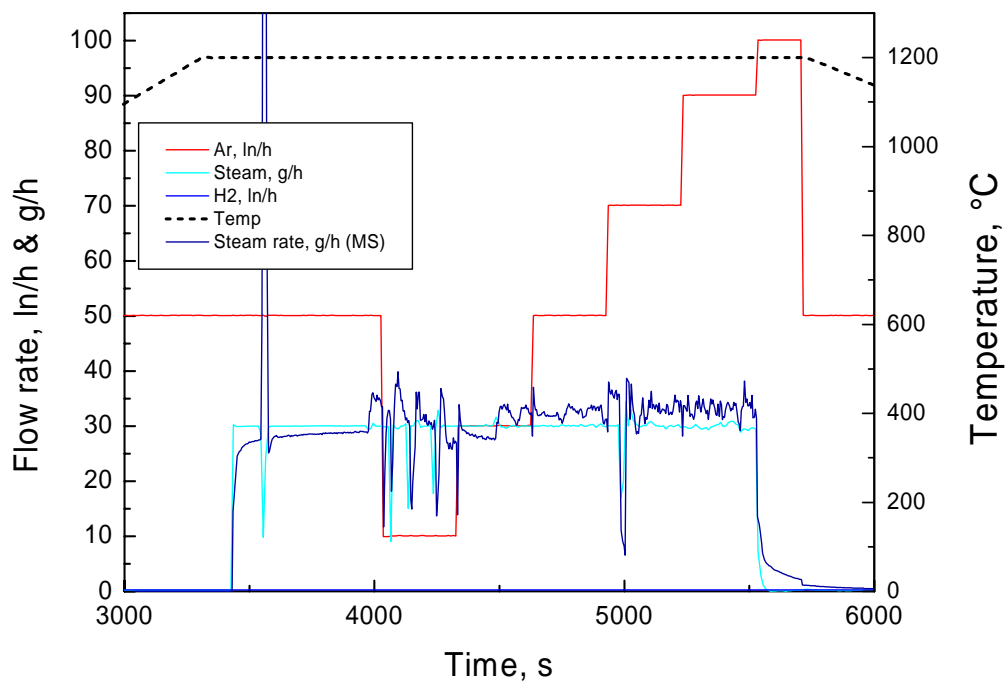
Test Box01207:

Oxidation of a Framatome B₄C Pellet at 1200 °C under Ar/steam; Variation of the steam flow rate



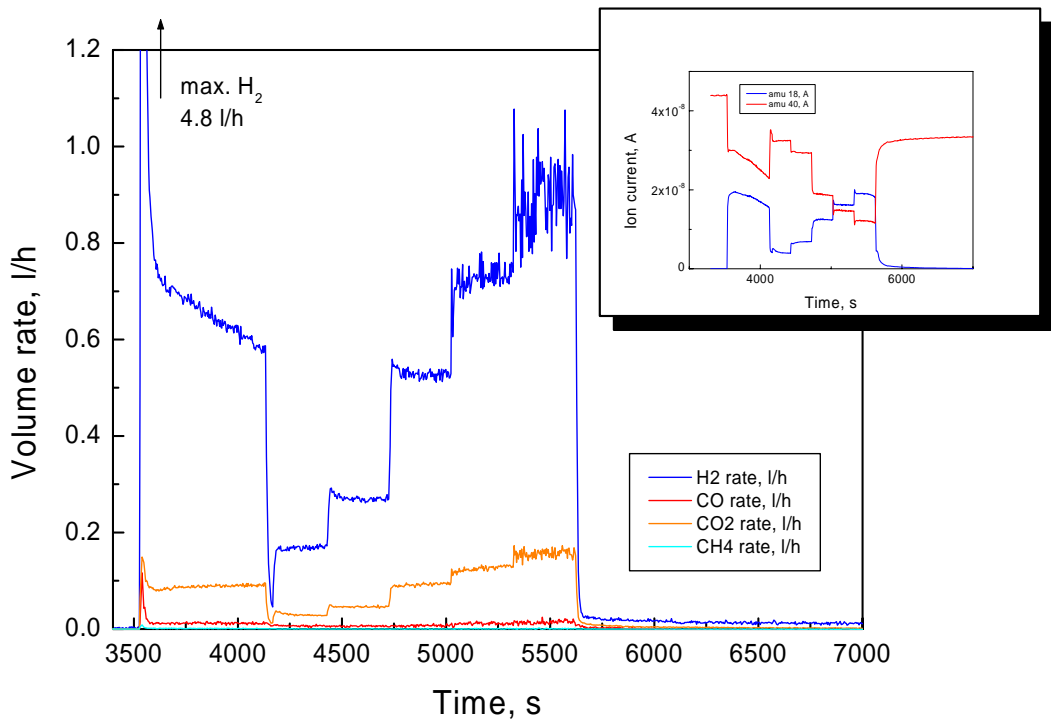
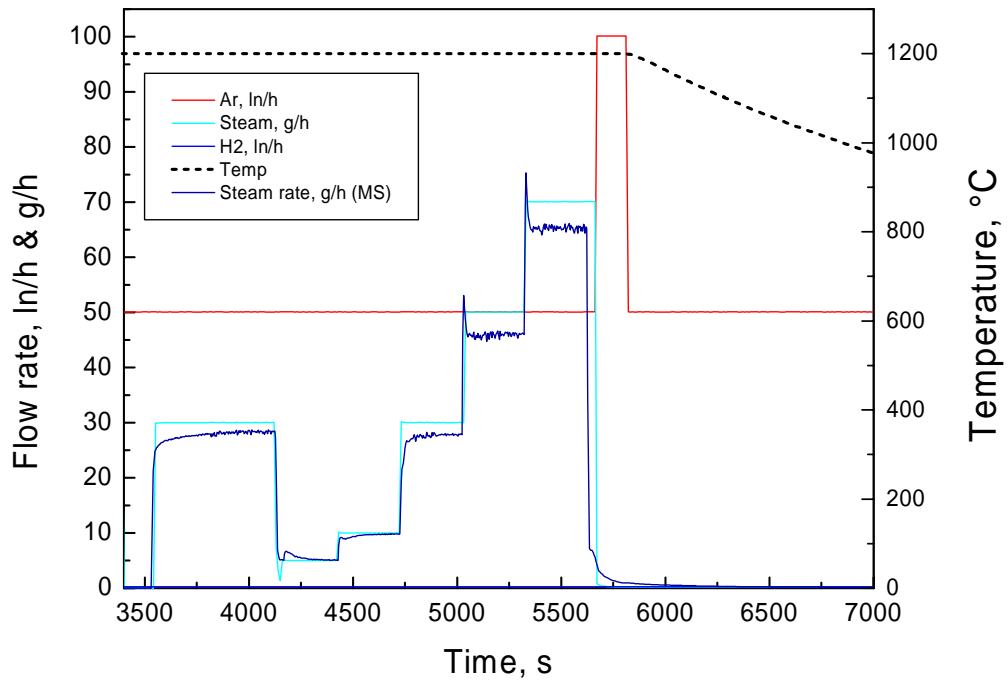
Test Box01208:

Oxidation of a Framatome B₄C Pellet at 1200 °C
under Ar/steam; Variation of the argon flow rate



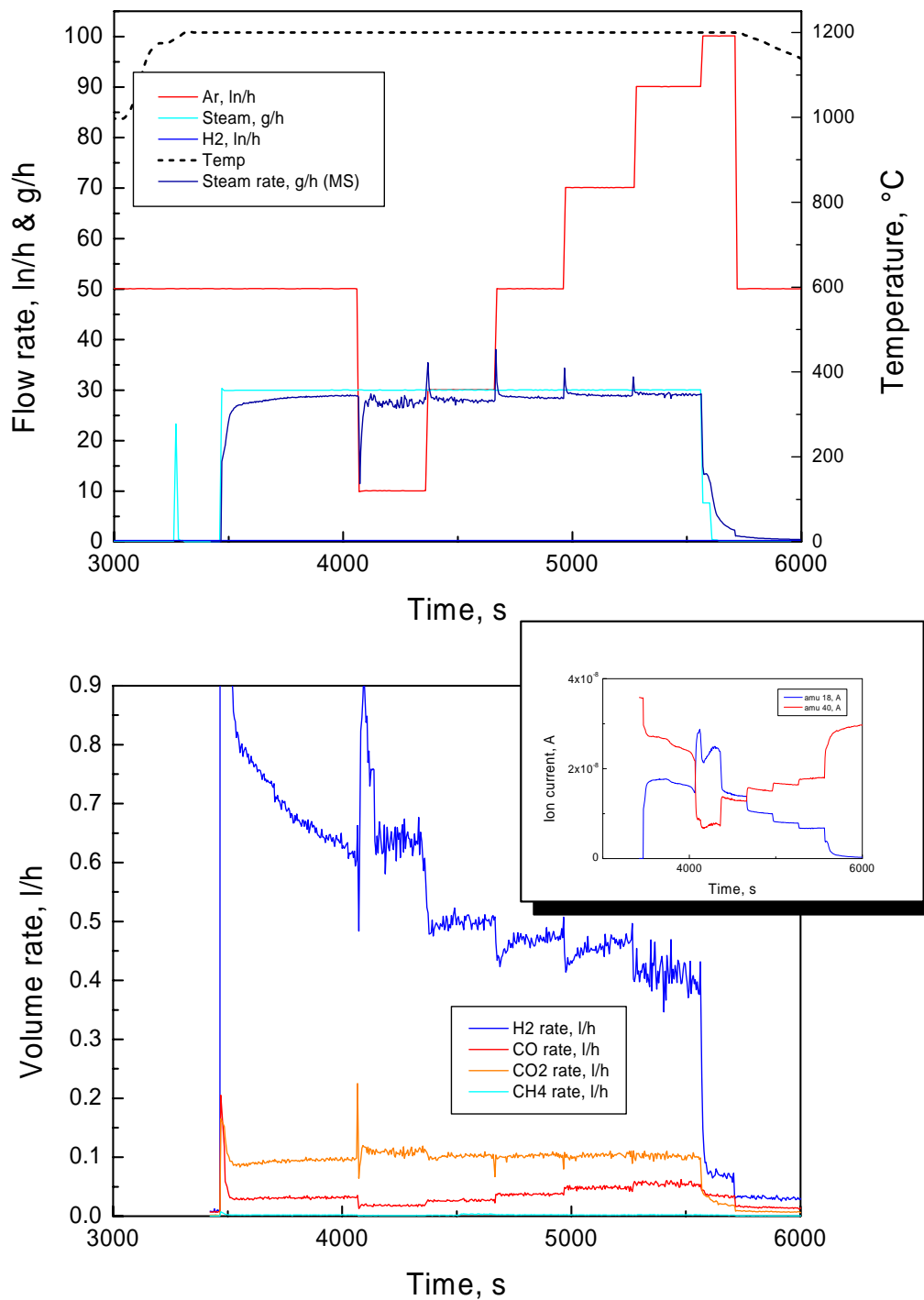
Test Box10115:

Oxidation of a Framatome B₄C Pellet at 1200 °C under Ar/steam; Variation of the steam flow rate



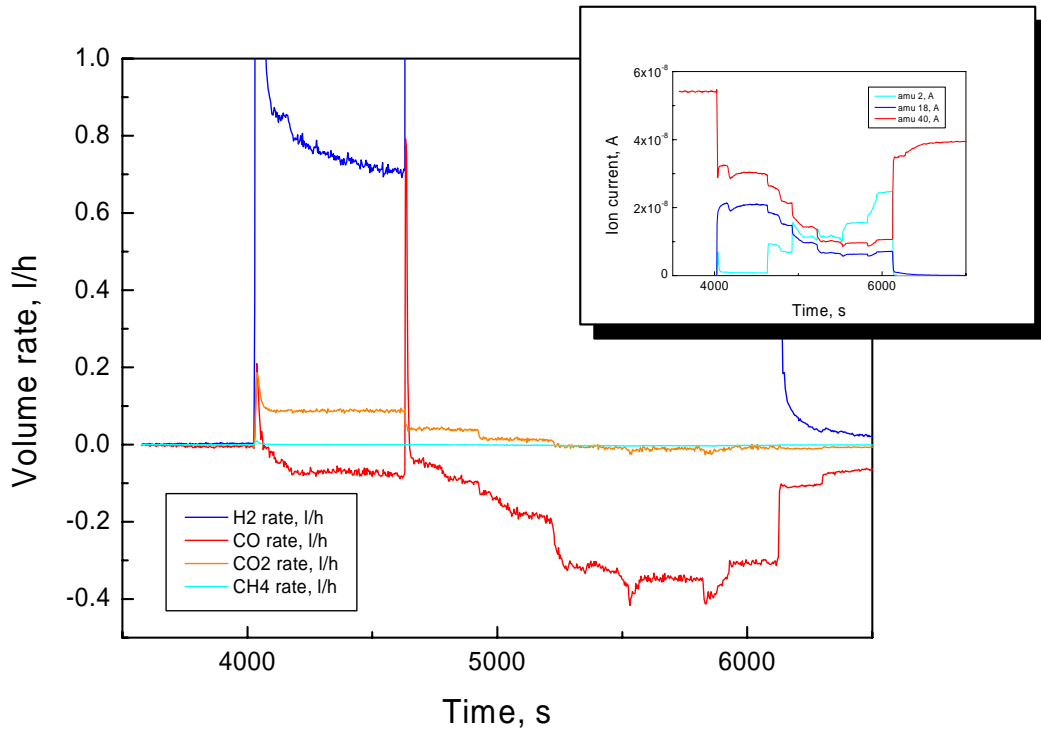
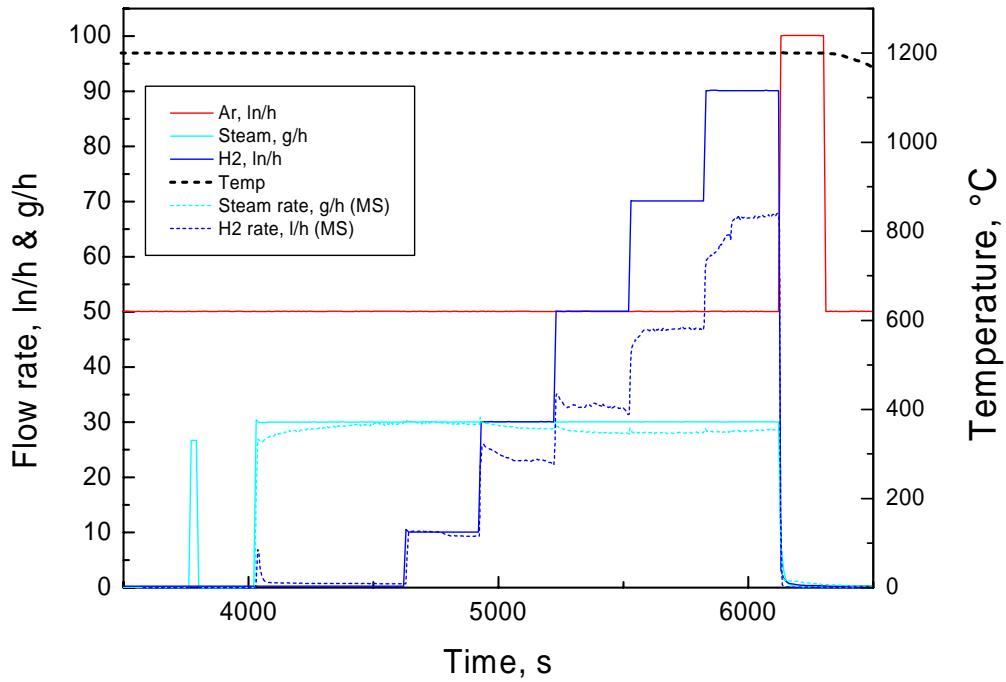
Box10126:

Oxidation of a Framatome B₄C Pellet at 1200 °C under Ar/steam; Variation of the argon flow rate



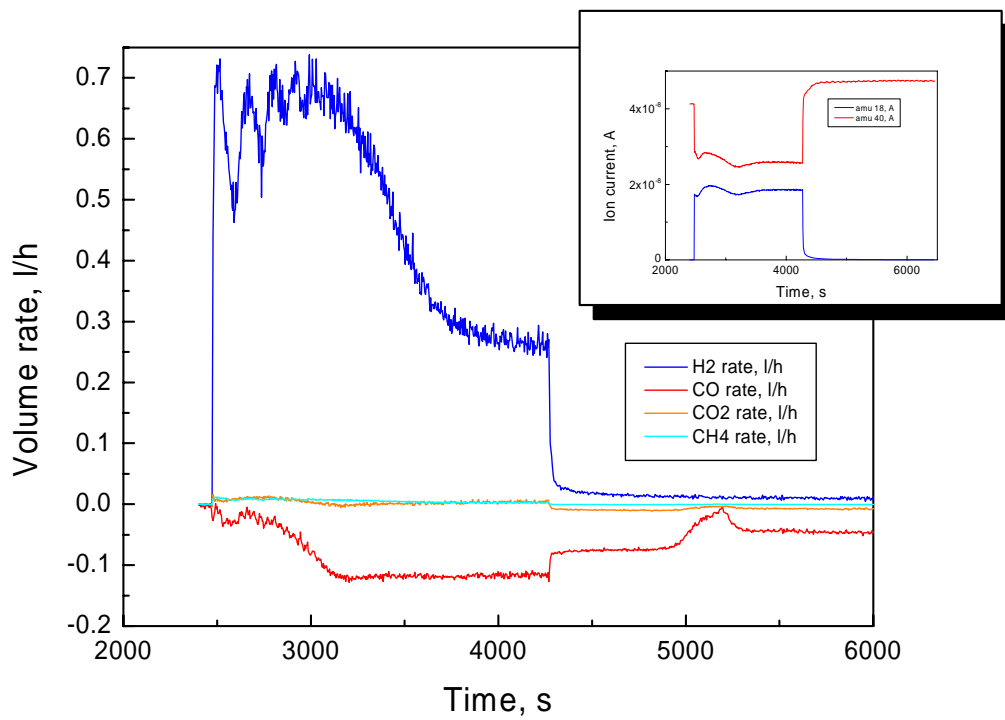
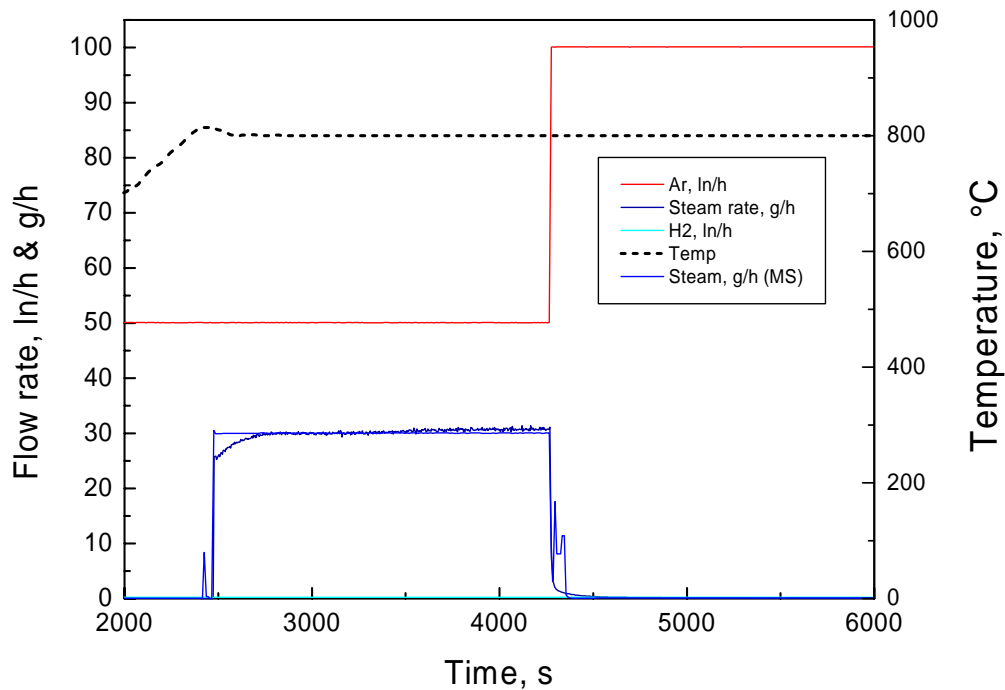
Test Box10213:

Oxidation of a Framatome B₄C Pellet at 1200 °C under argon/steam/hydrogen; Variable hydrogen rate



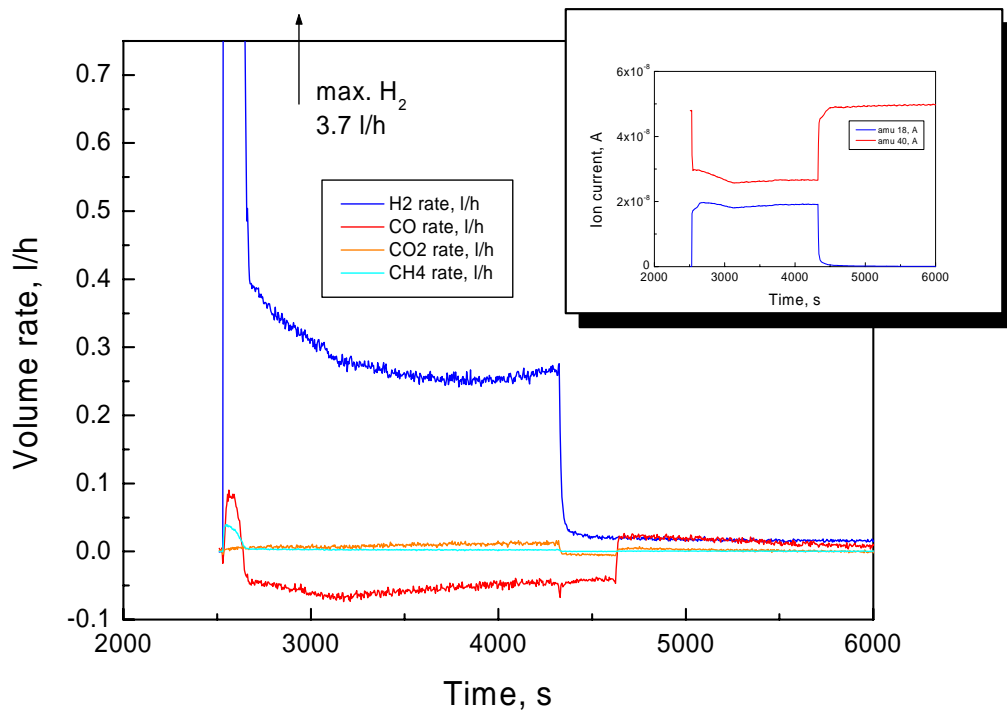
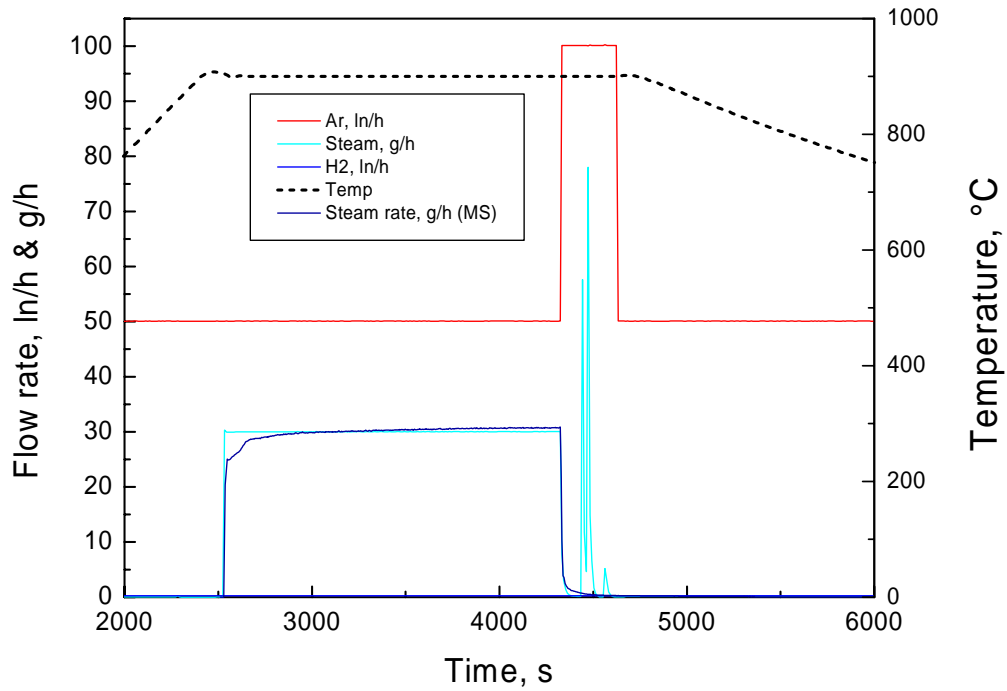
Test Box10214:

Isothermal oxidation of a Framatome B₄C pellet
in Ar/steam at 800 °C



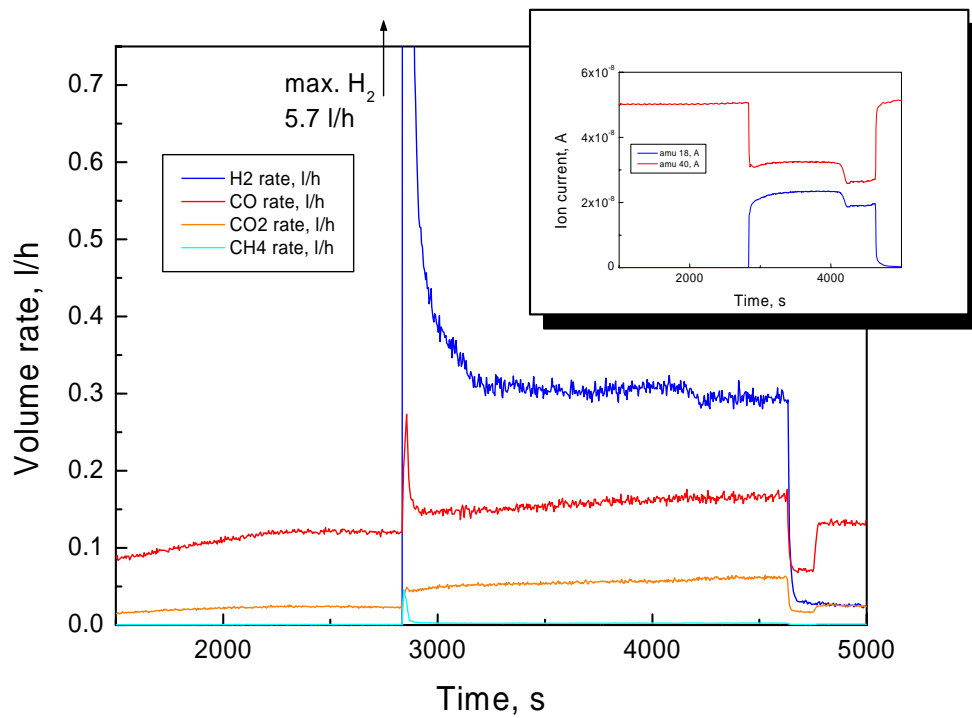
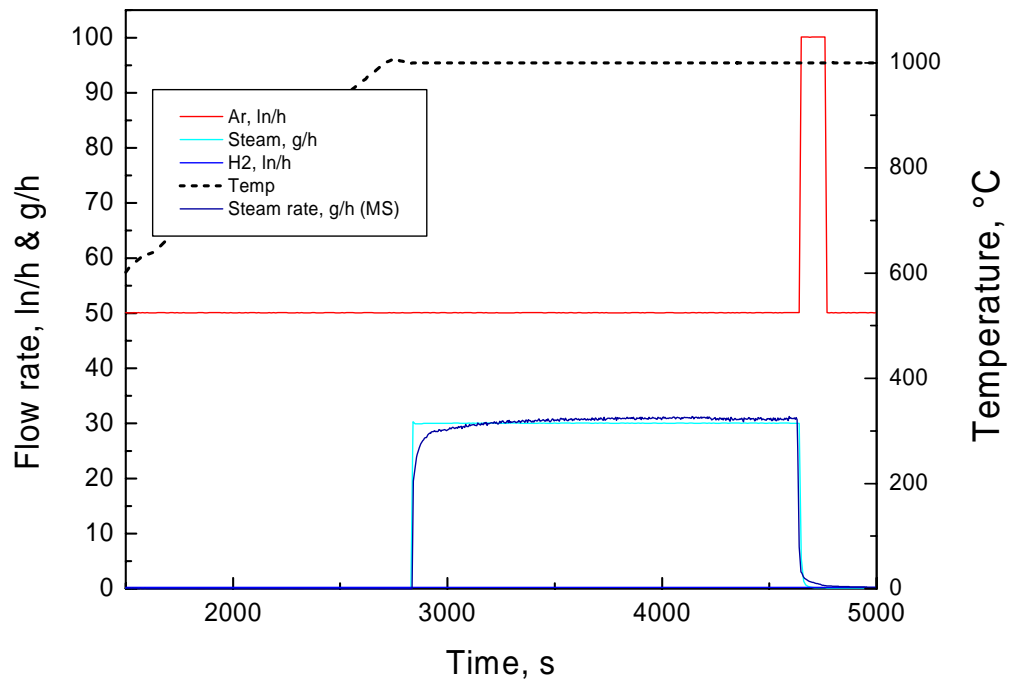
Test Box10216:

Isothermal oxidation of a Framatome B₄C pellet in Ar/steam at 900 °C



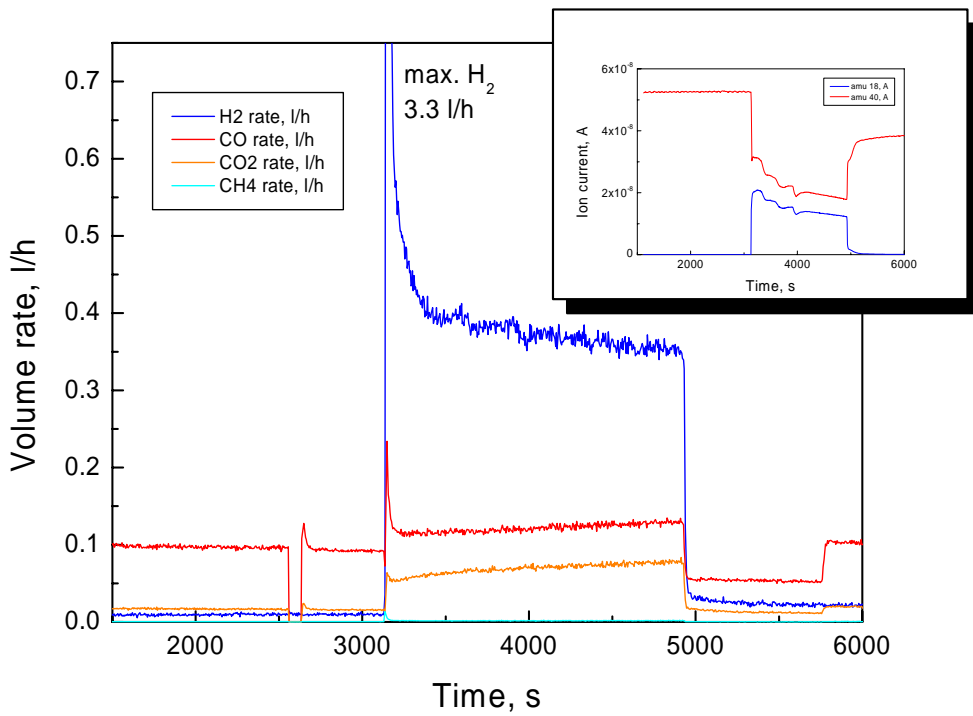
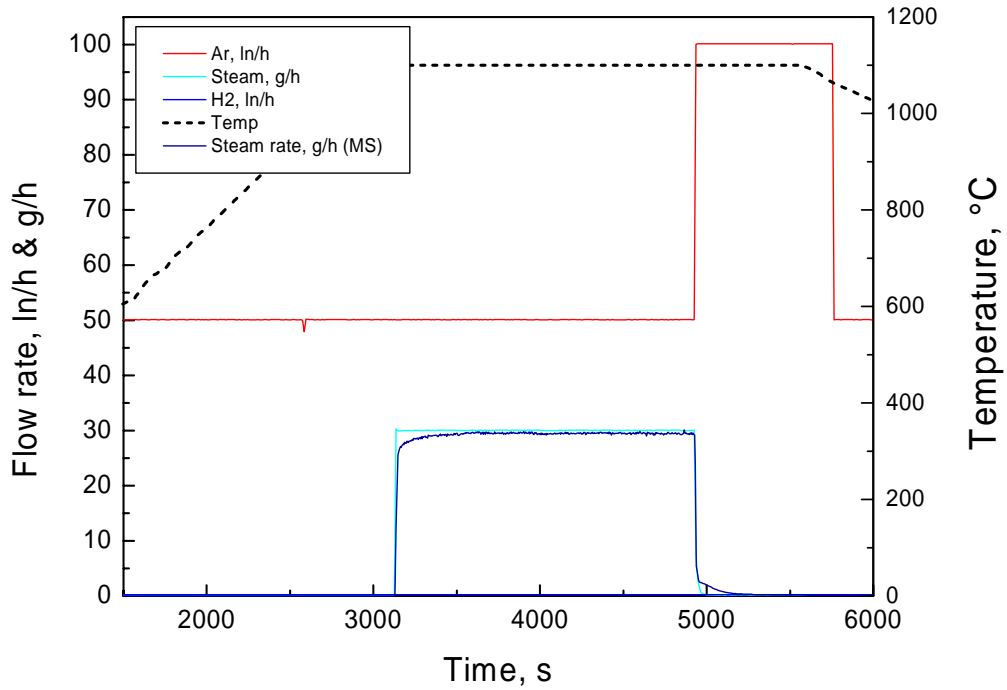
Test Box10219:

Isothermal oxidation of a Framatome B₄C pellet
in Ar/steam at 1000 °C



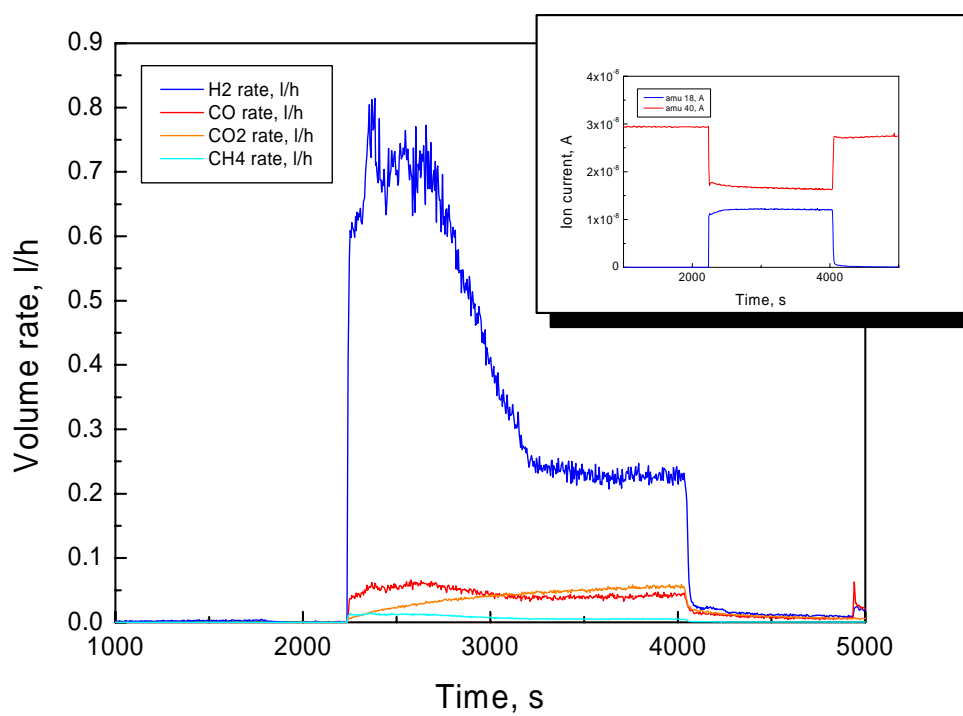
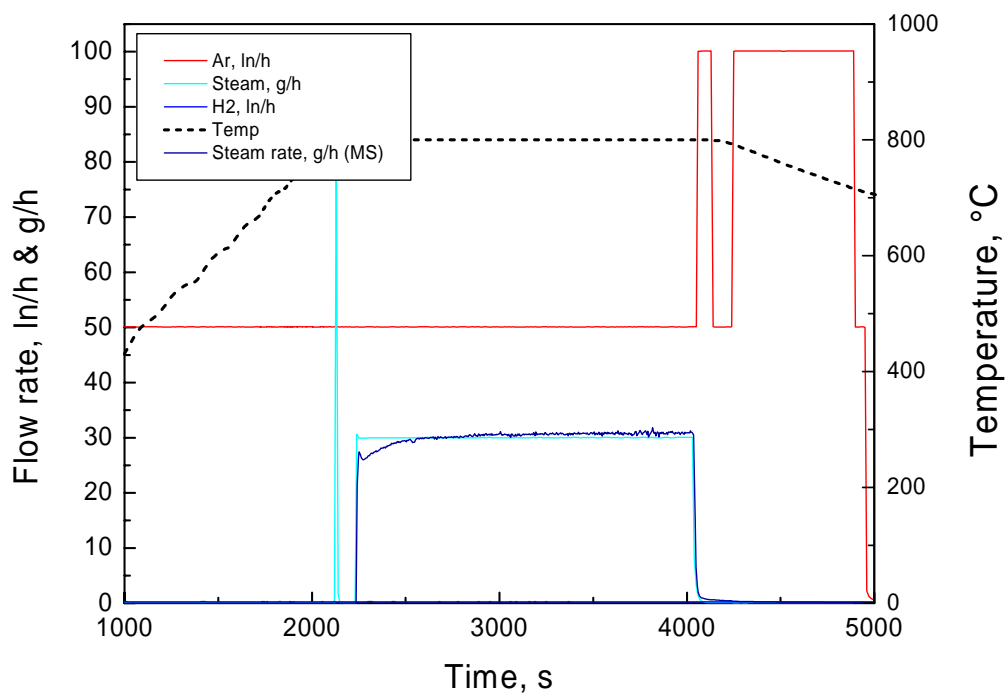
Test Box10220:

Isothermal oxidation of a Framatome B₄C pellet in Ar/steam at 1100 °C



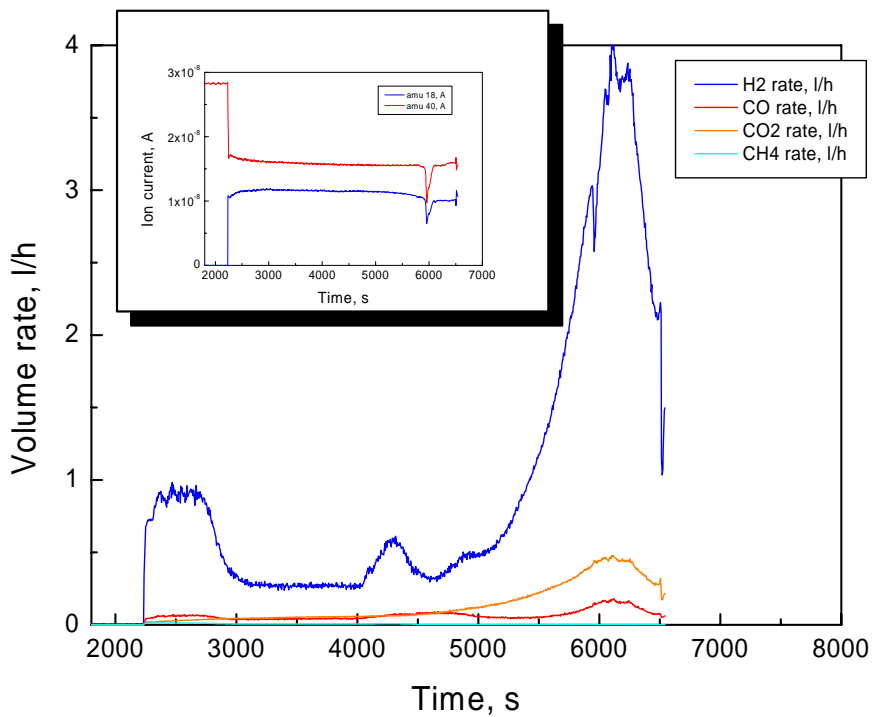
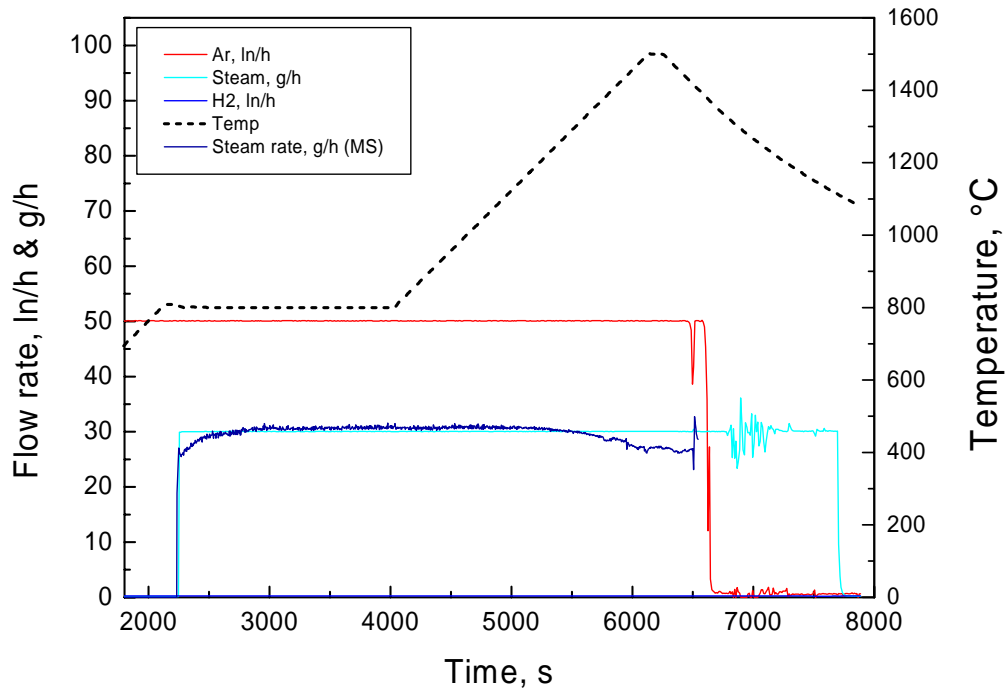
Test Box10405:

Isothermal oxidation of a Framatome B₄C pellet
in Ar/steam at 800 °C

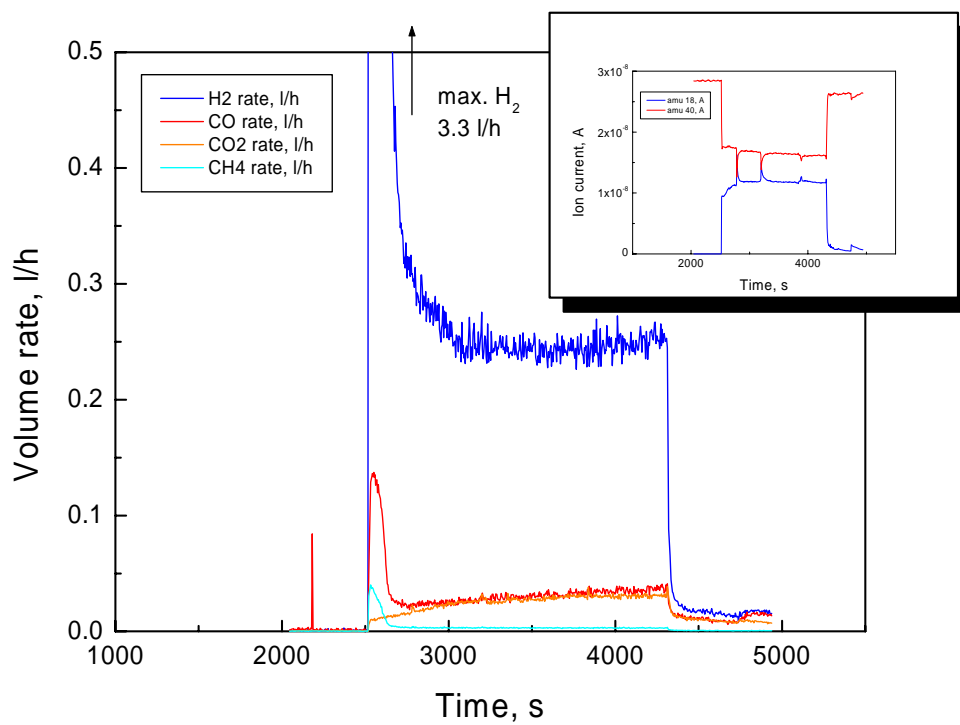
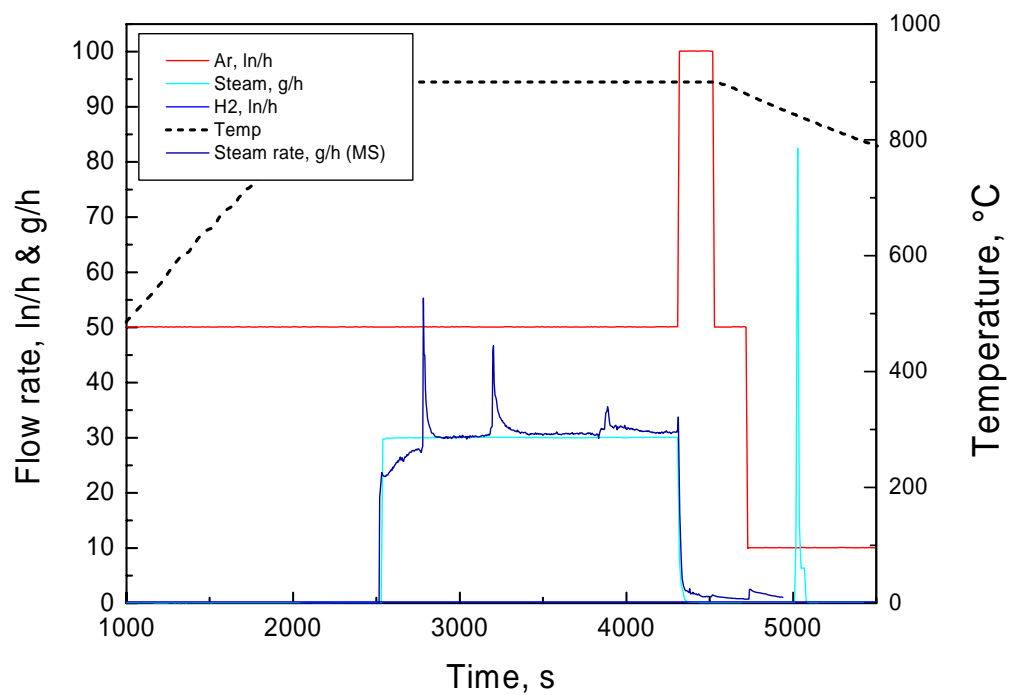


Test Box10406:

Transient oxidation between 800 and 1500 °C of
a Framatome B₄C pellet in Ar/steam

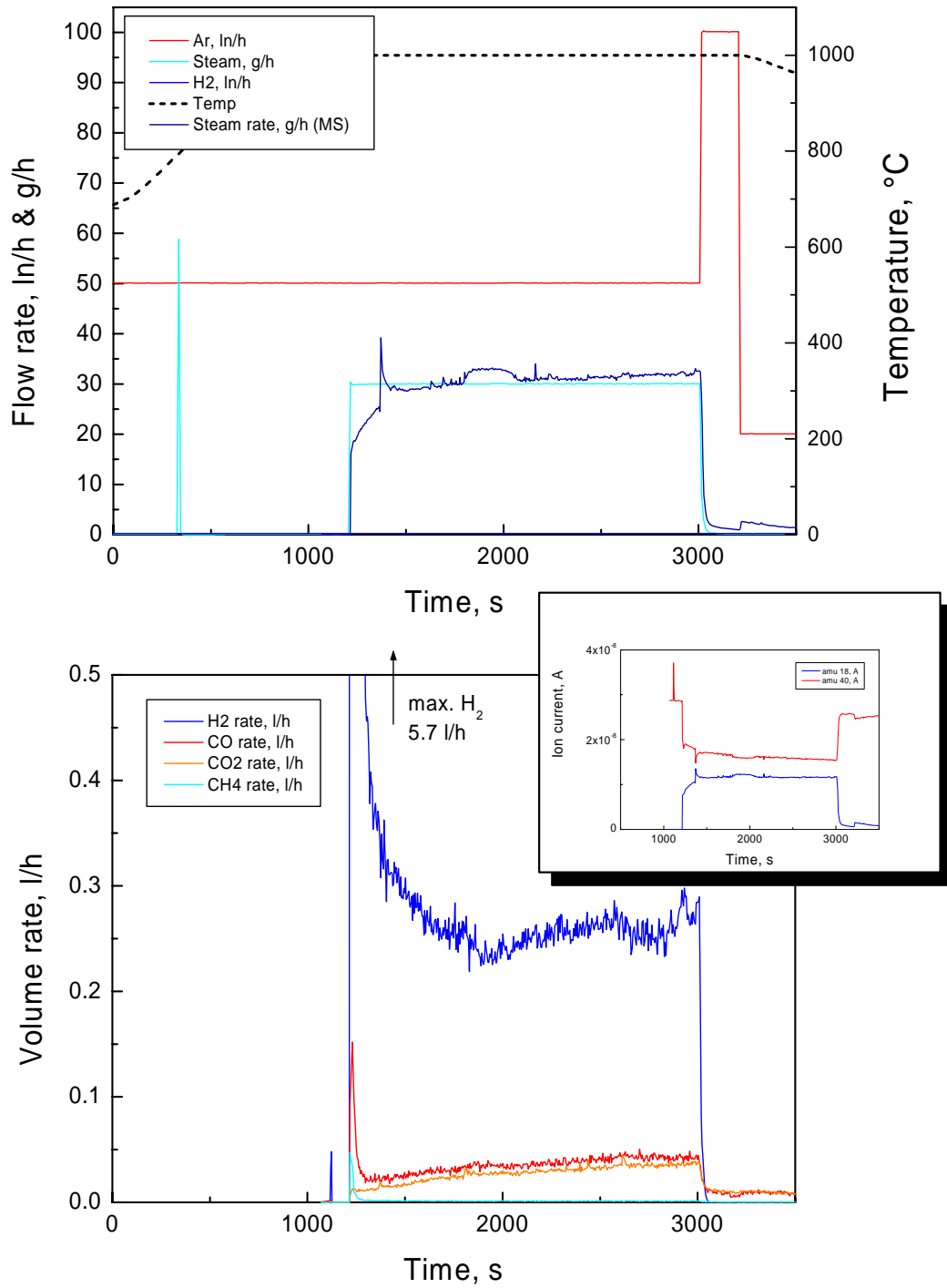


Test Box10511: Isothermal oxidation of a Framatome B₄C pellet in Ar/steam at 900 °C



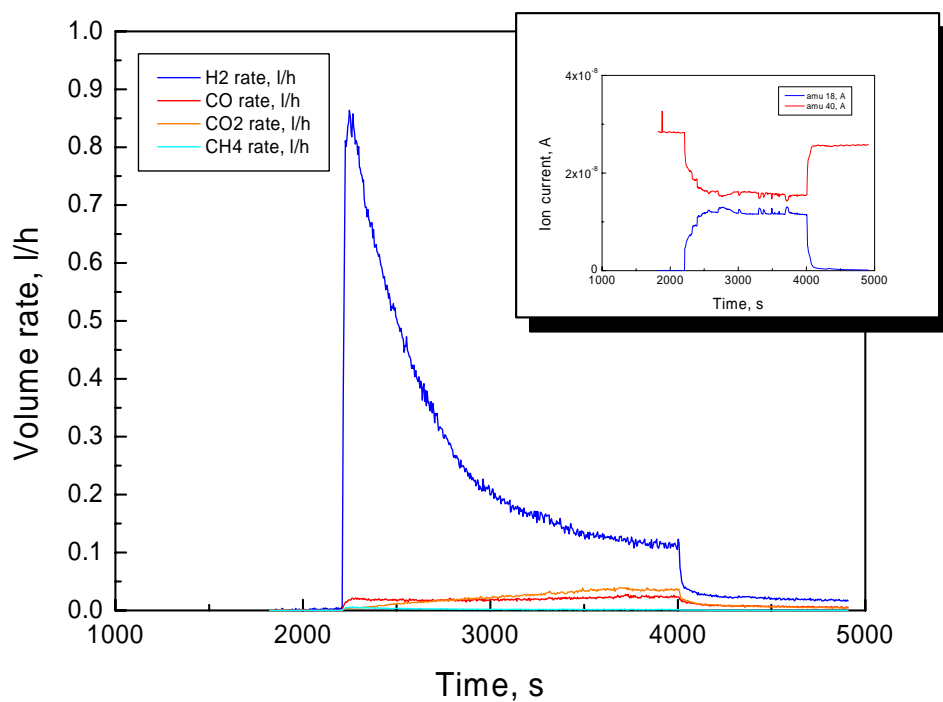
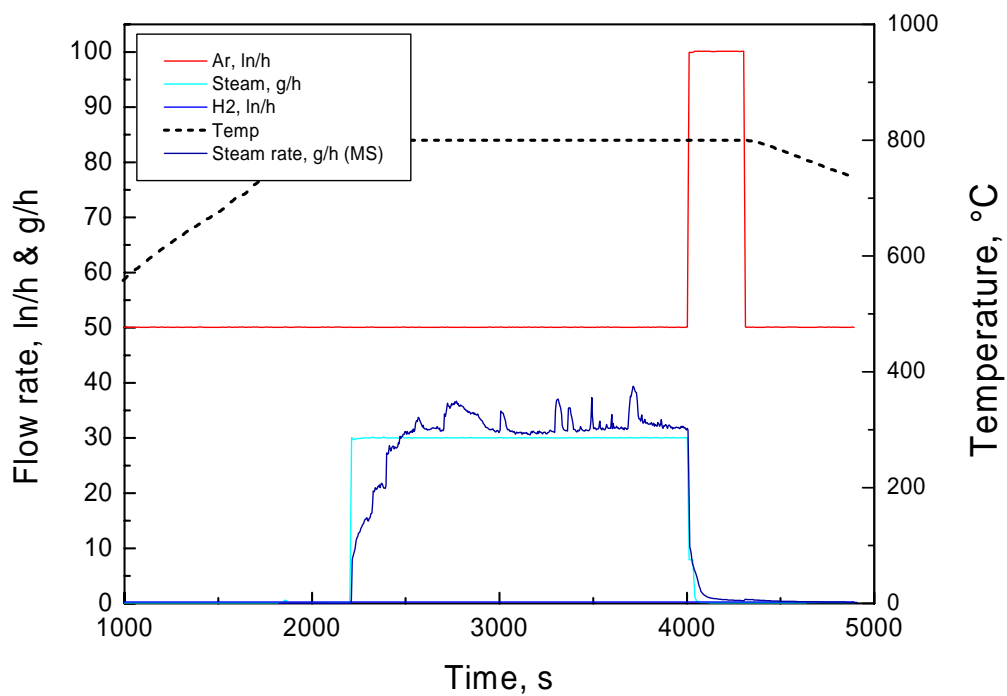
Test Box10514:

Isothermal oxidation of a Framatome B₄C pellet
in Ar/steam at 1000 °C



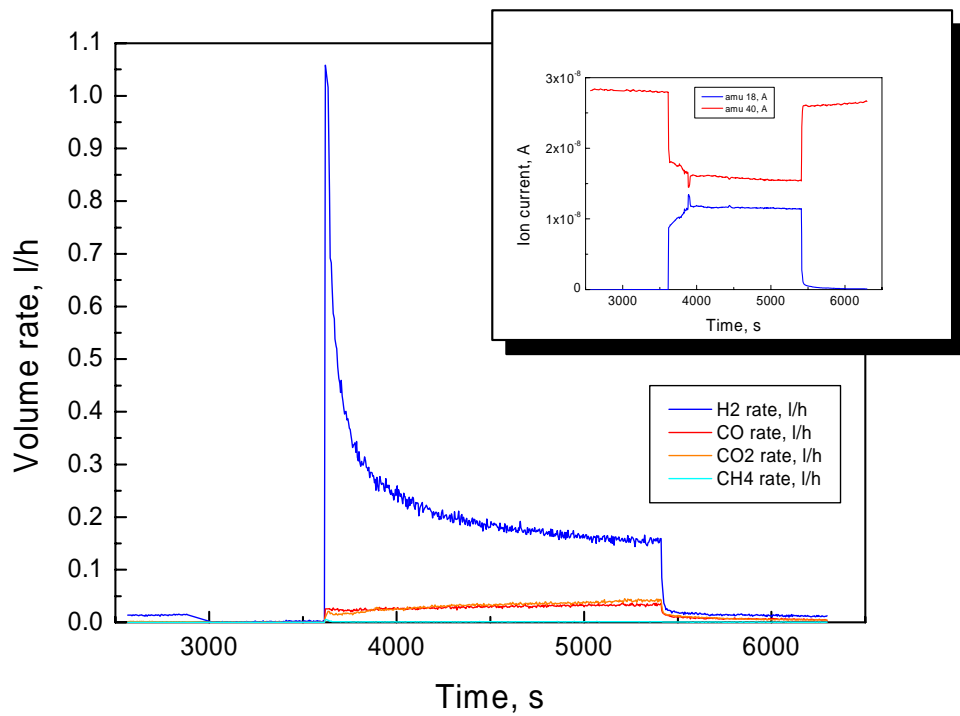
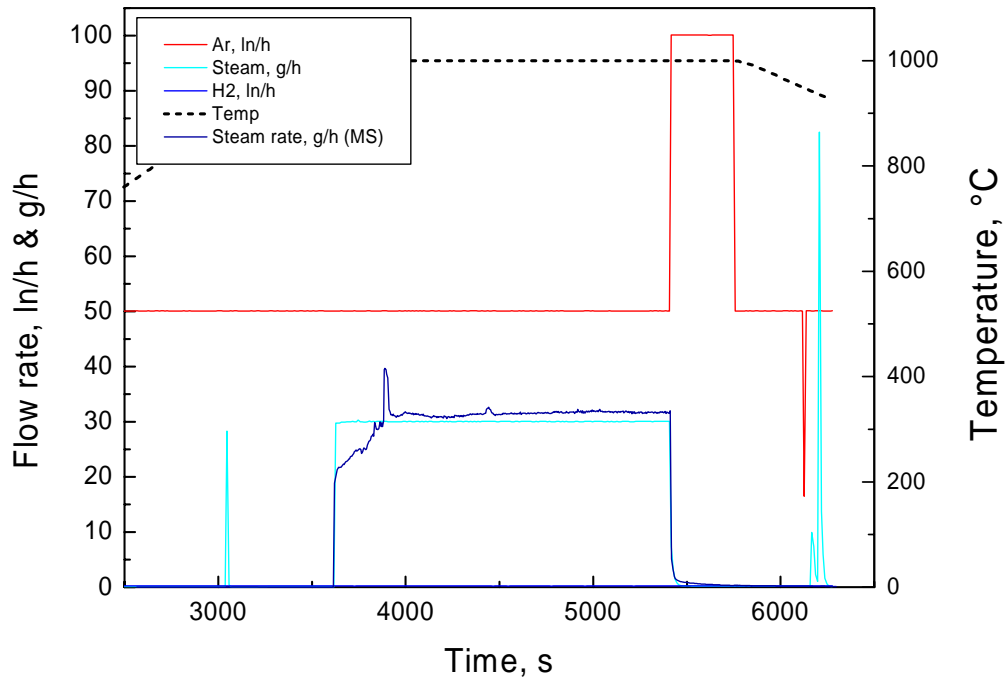
Test Box10516:

Isothermal oxidation of a ESK B₄C powder
in Ar/steam at 800 °C



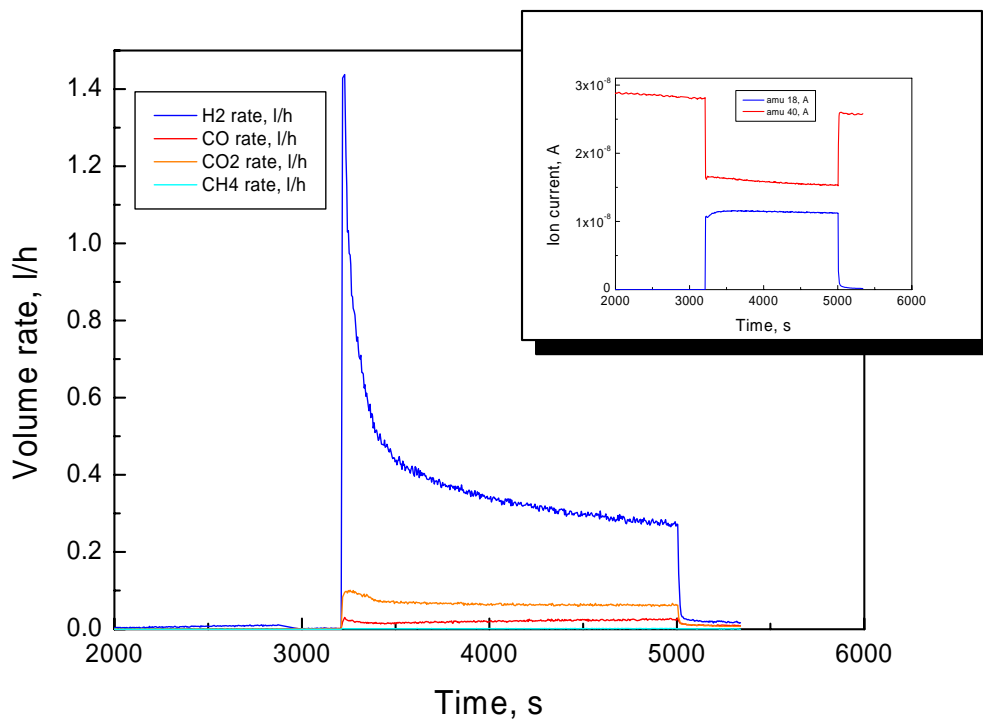
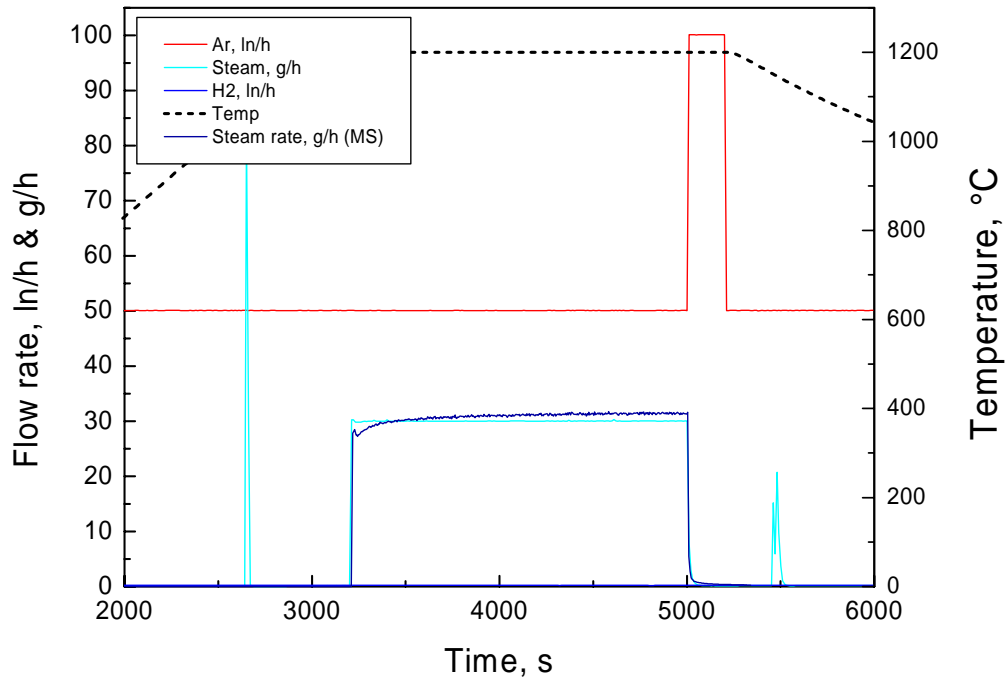
Test Box10529:

Isothermal oxidation of a ESK B₄C powder in Ar/steam at 1000 °C



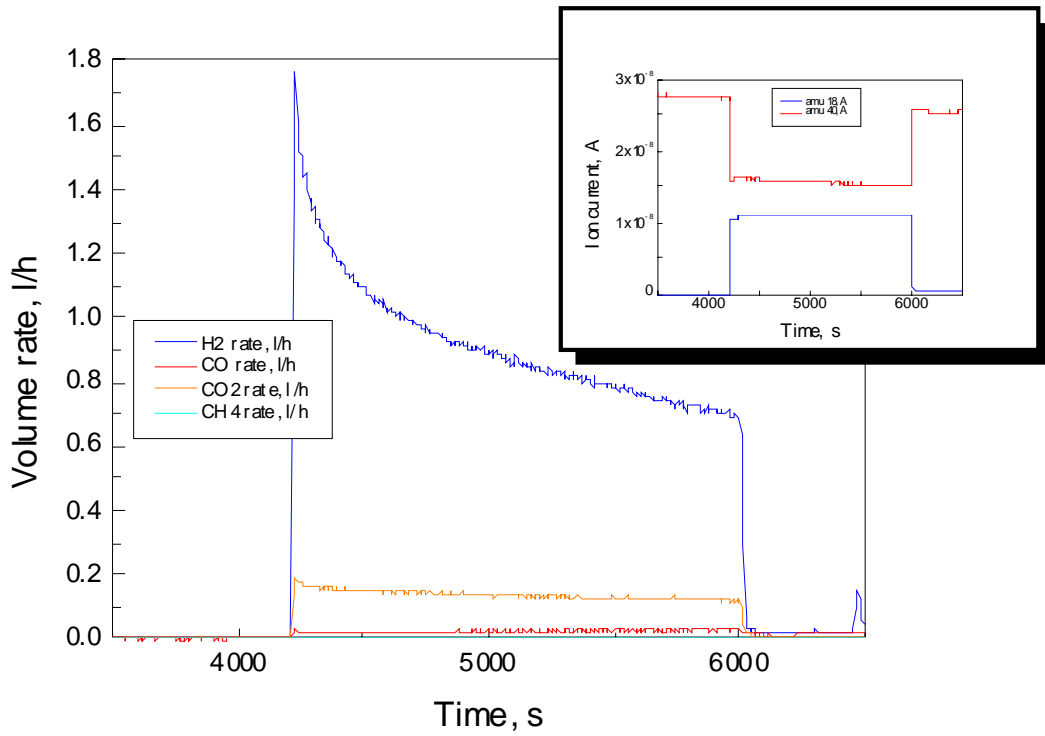
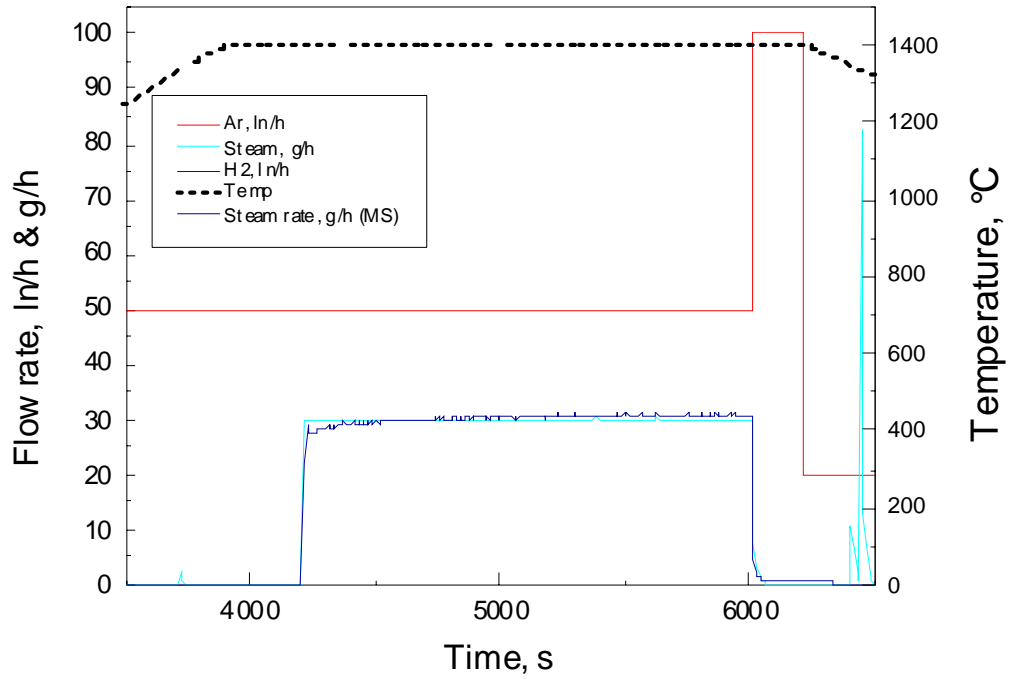
Test Box10530:

Isothermal oxidation of a ESK B₄C powder in Ar/steam at 1200 °C



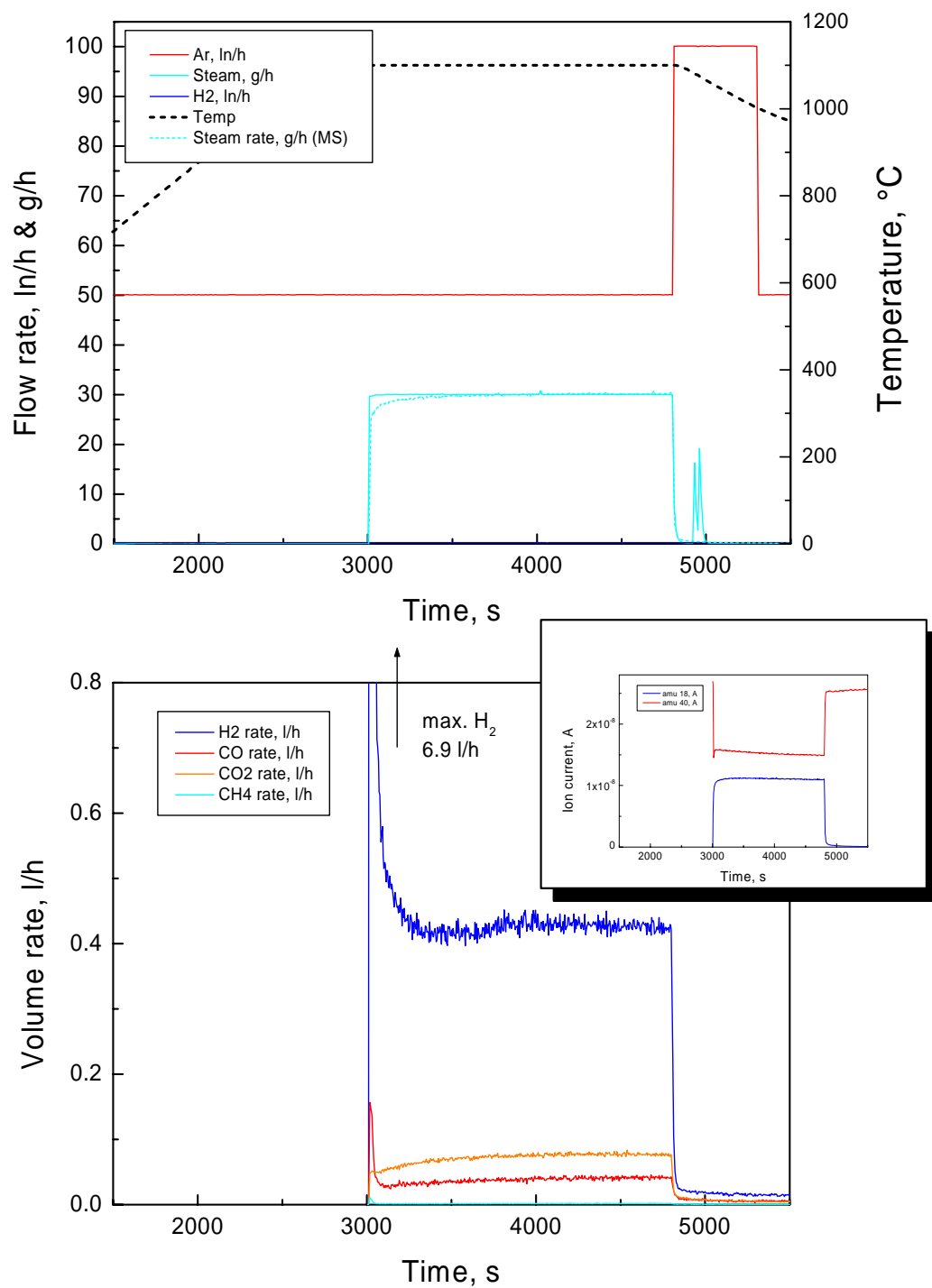
Test Box10531:

Isothermal oxidation of a ESK B₄C powder in Ar/steam at 1400 °C



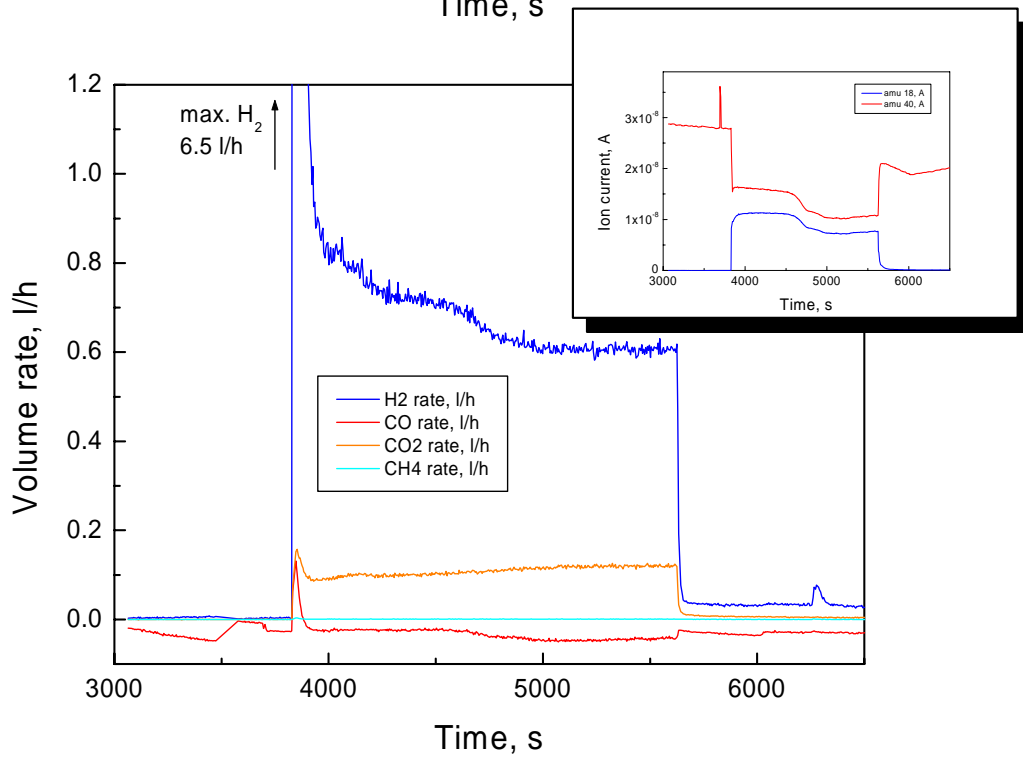
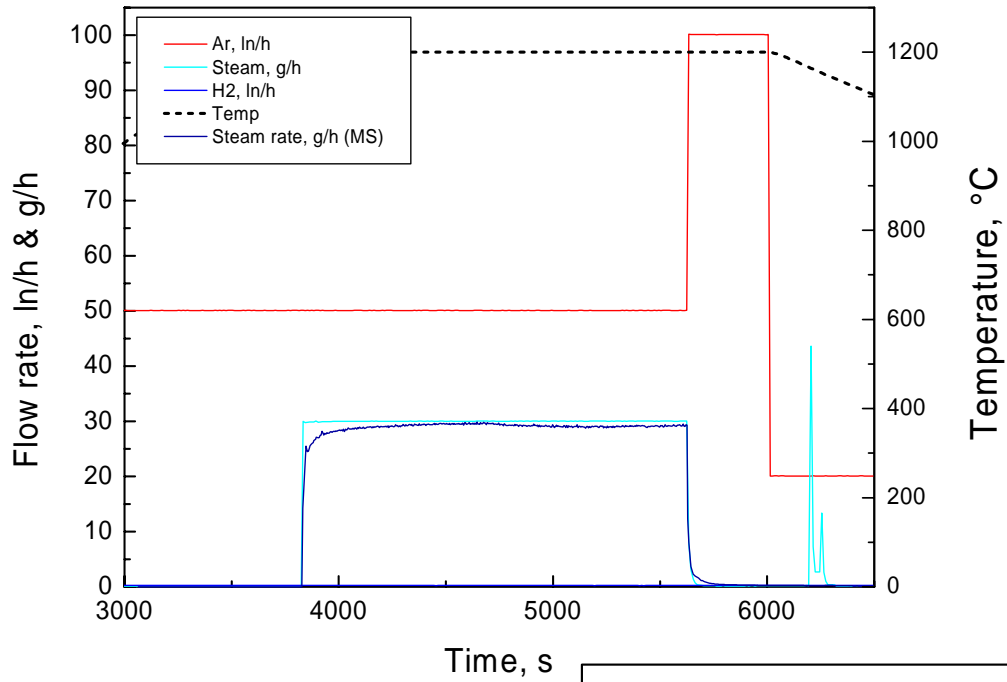
Test Box10605a:

Isothermal oxidation of a Framatome B₄C pellet
in Ar/steam at 1100 °C



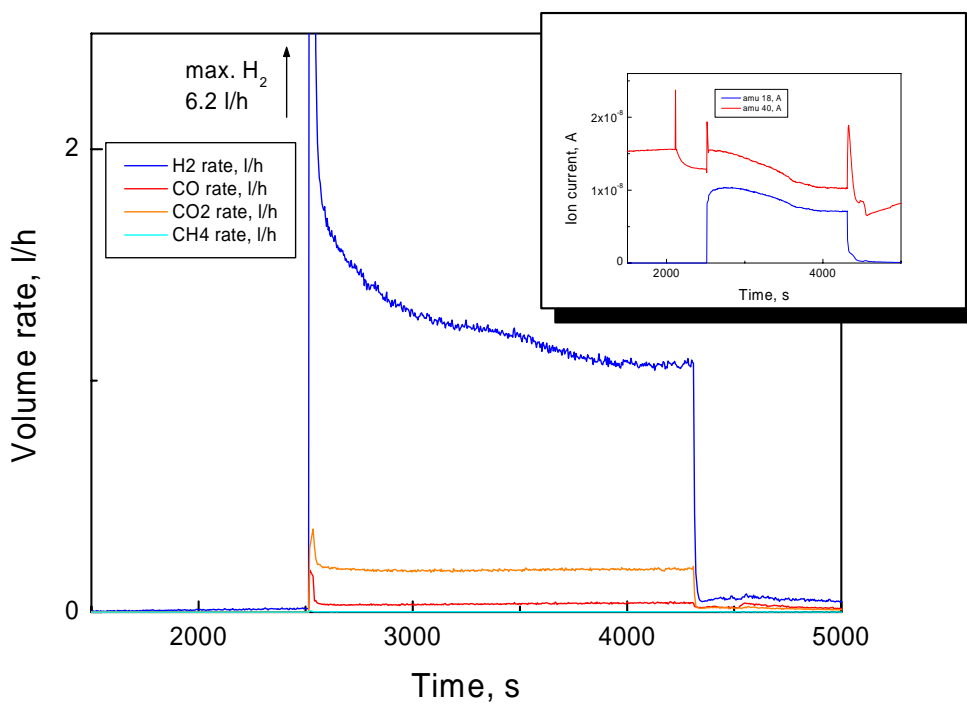
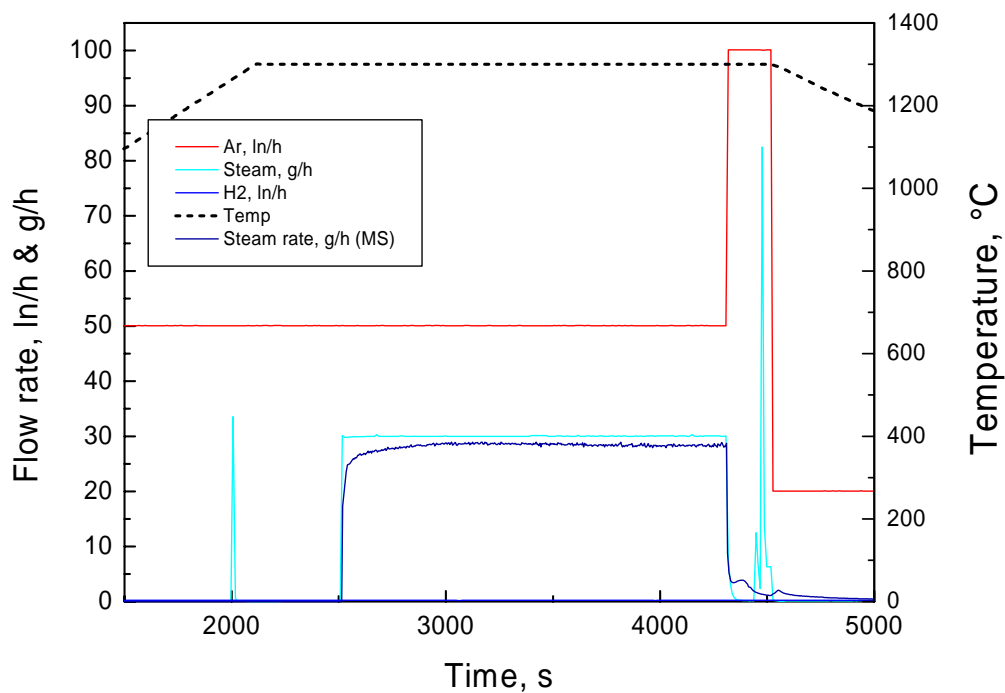
Test Box10606:

Isothermal oxidation of a Framatome B₄C pellet in Ar/steam at 1200 °C



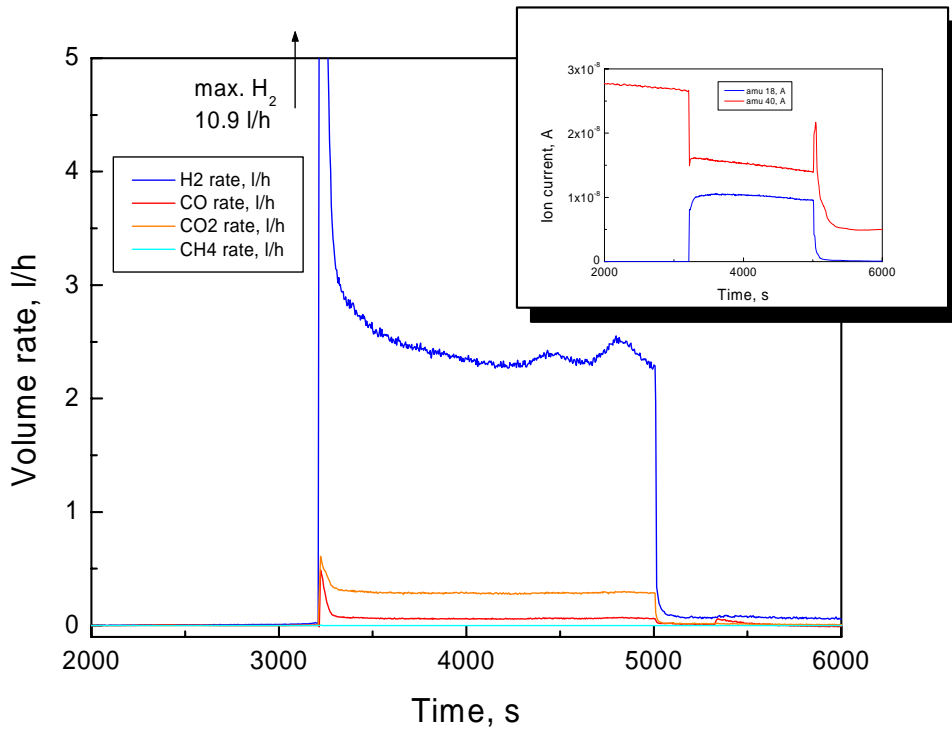
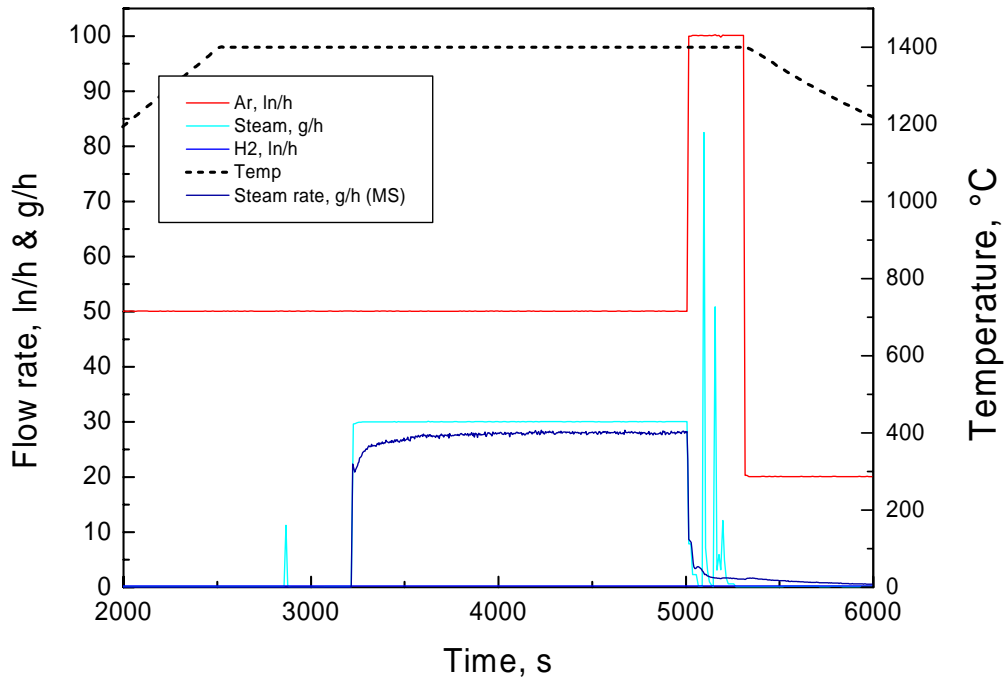
Test Box10607:

Isothermal oxidation of a Framatome B₄C pellet
in Ar/steam at 1300 °C



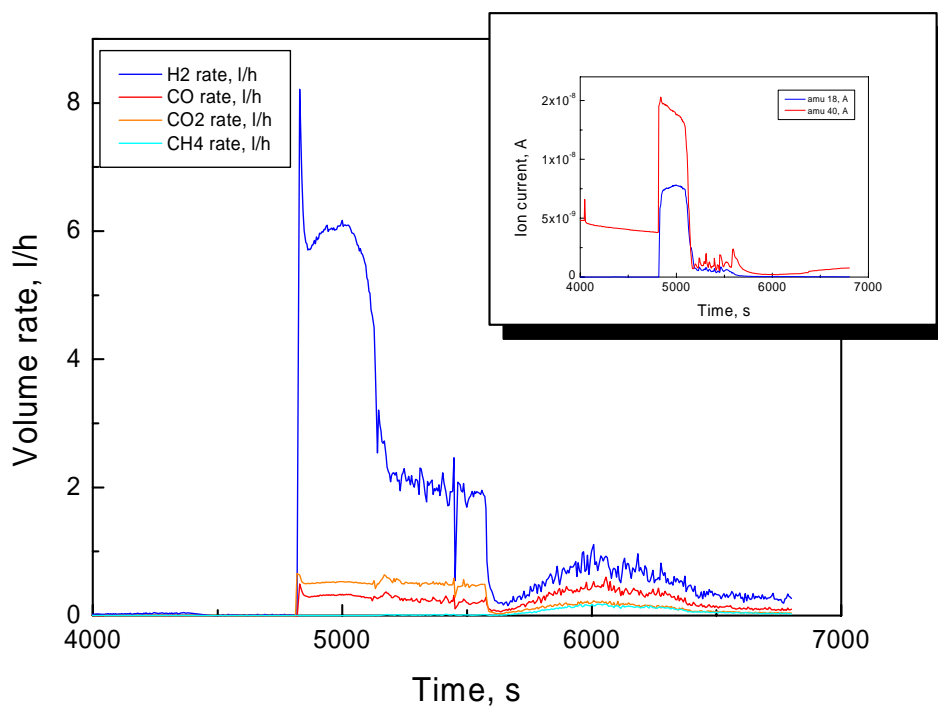
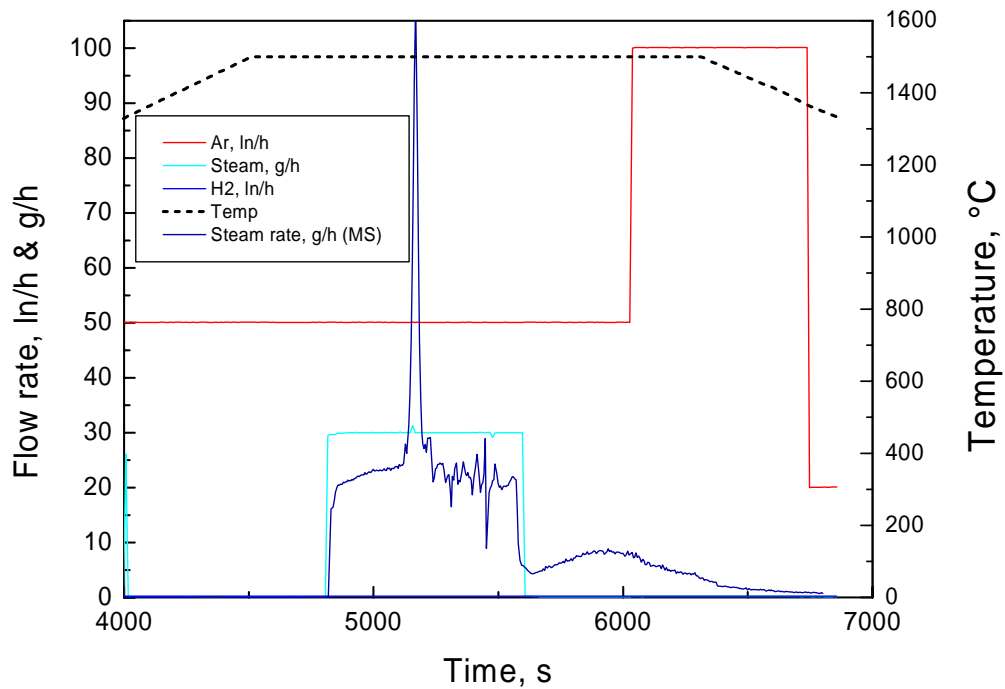
Test Box10611:

Isothermal oxidation of a Framatome B₄C pellet in Ar/steam at 1400 °C

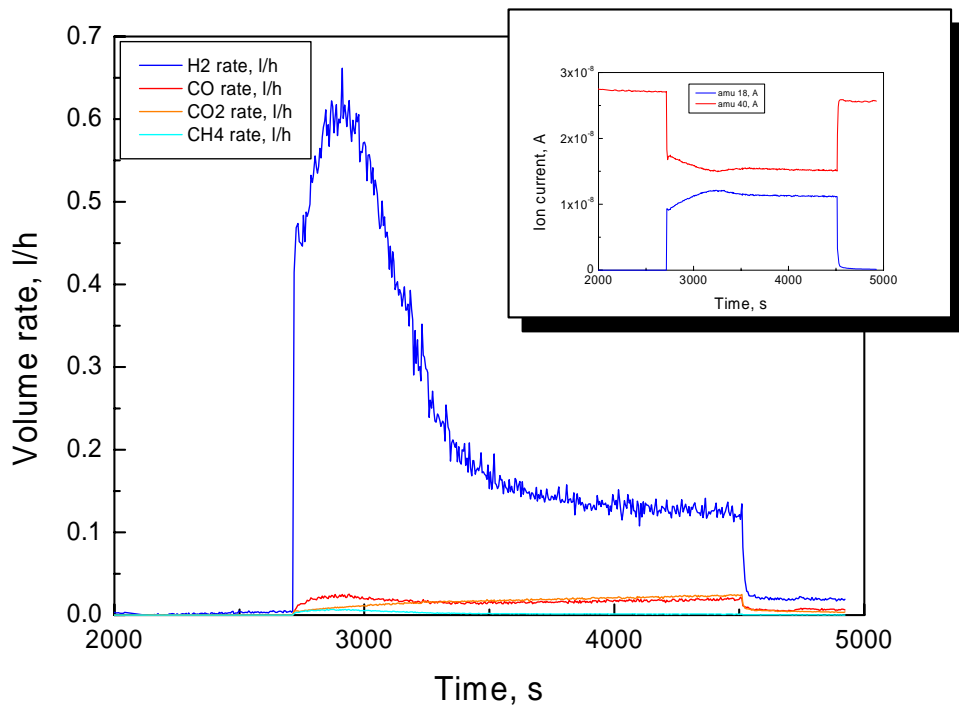
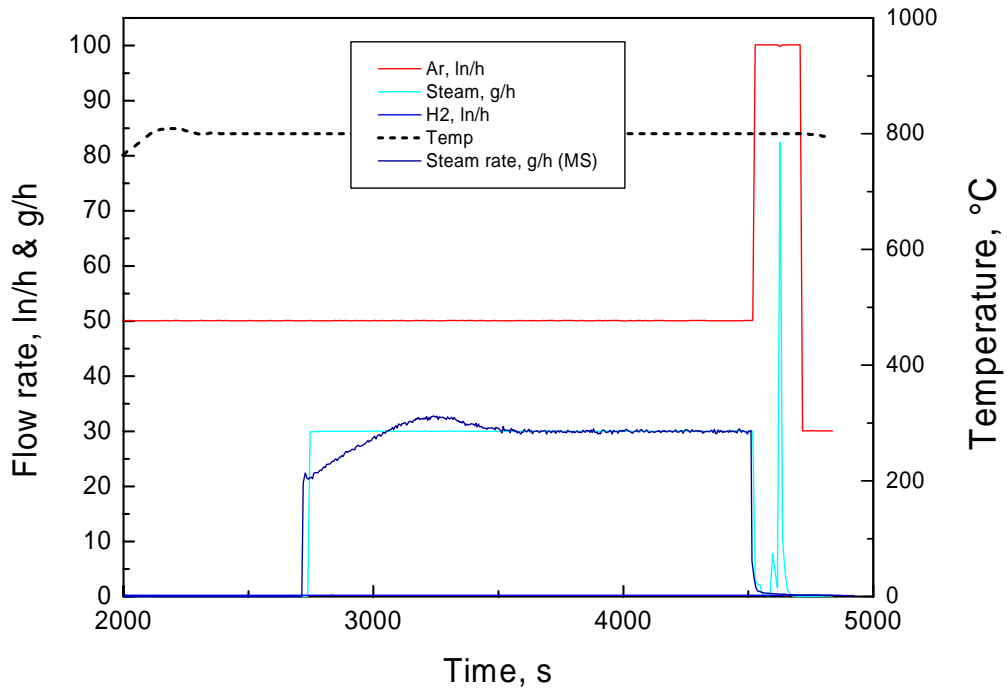


Test Box10612:

Isothermal oxidation of a Framatome B₄C pellet
in Ar/steam at 1500 °C

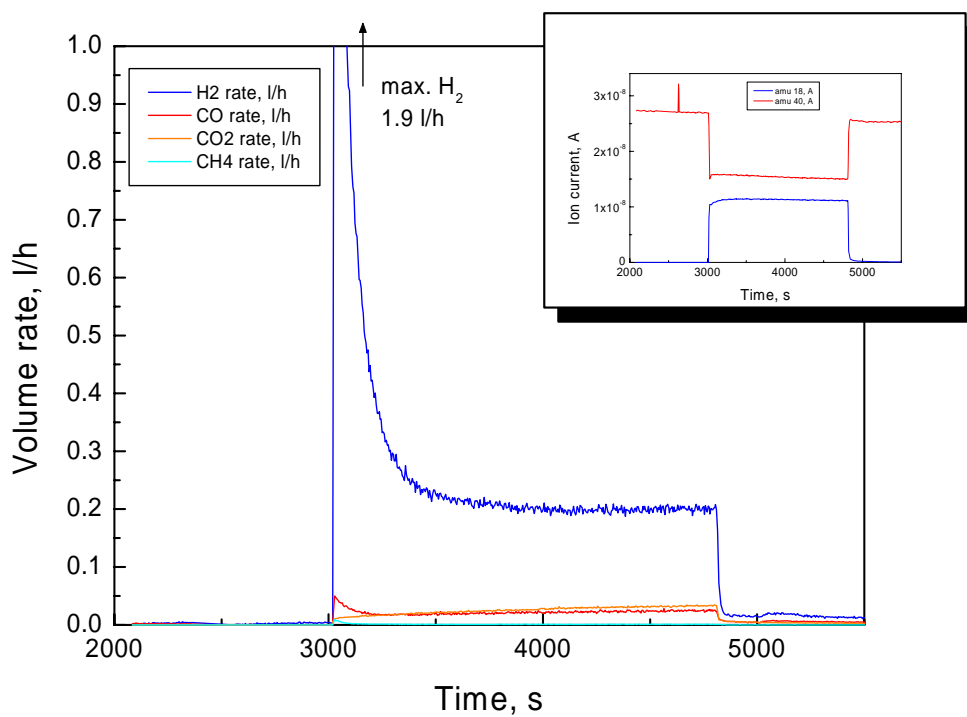
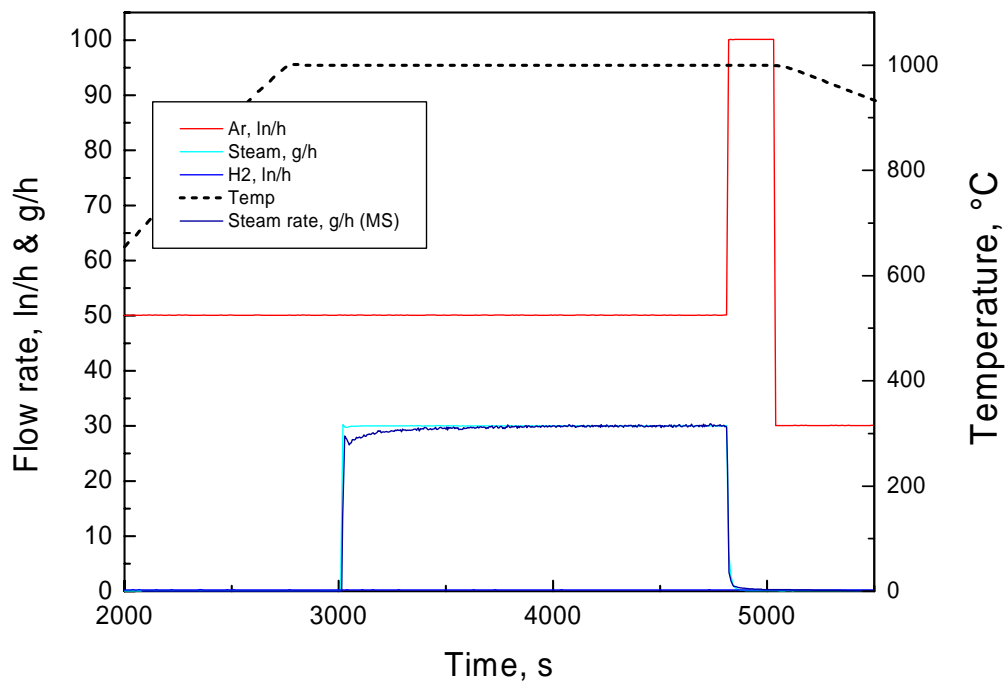


Test Box10907:
 Isothermal oxidation of a CODEX B₄C pellet
 in Ar/steam at 800 °C

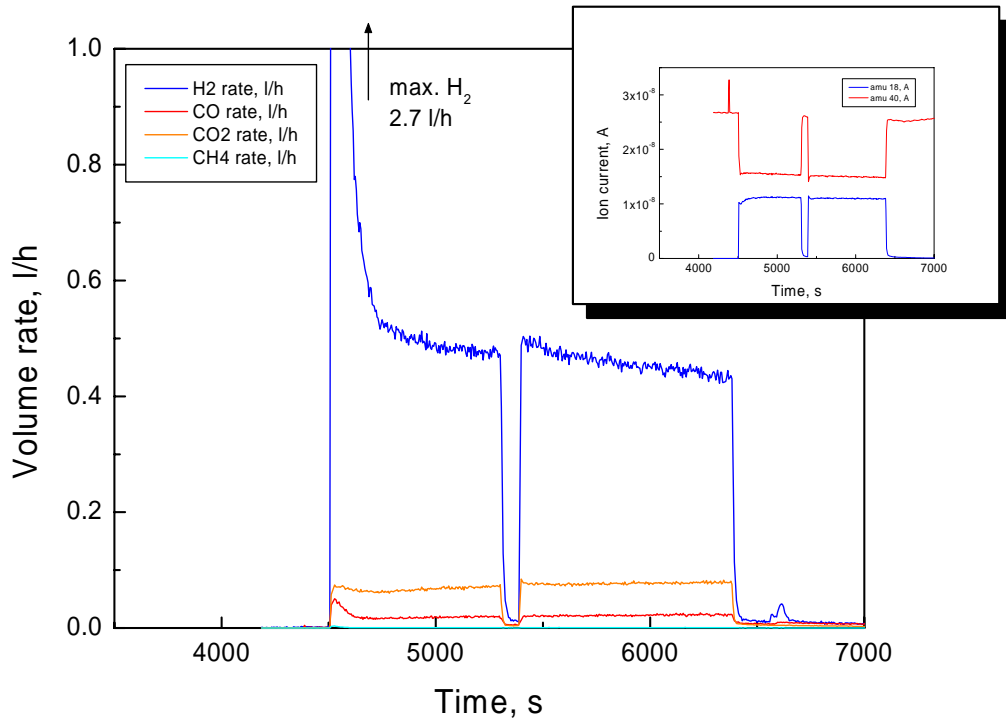
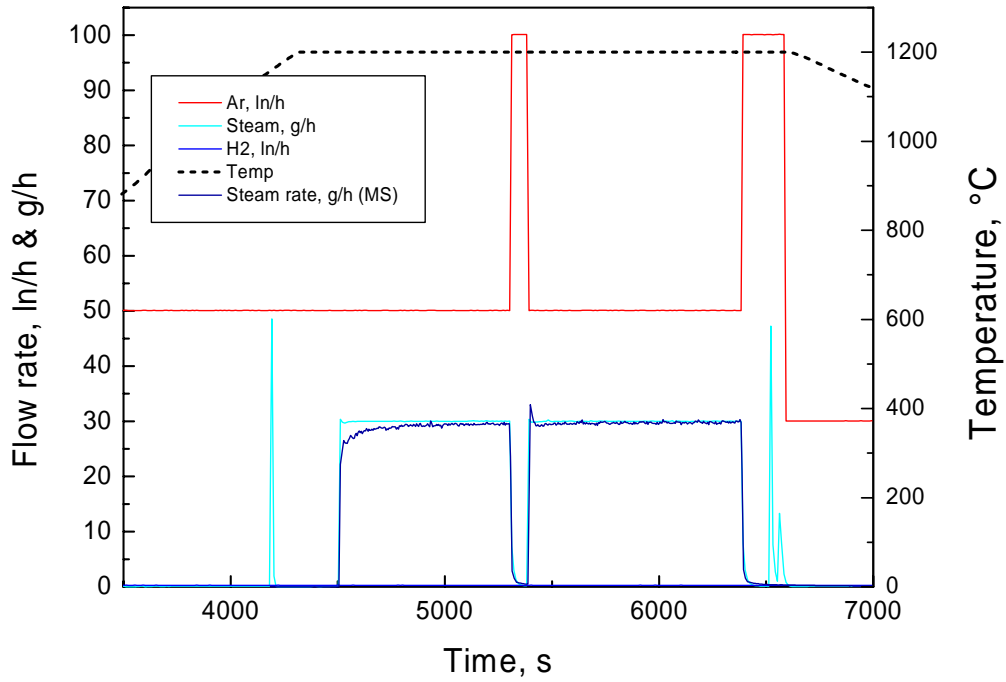


Test Box10910:

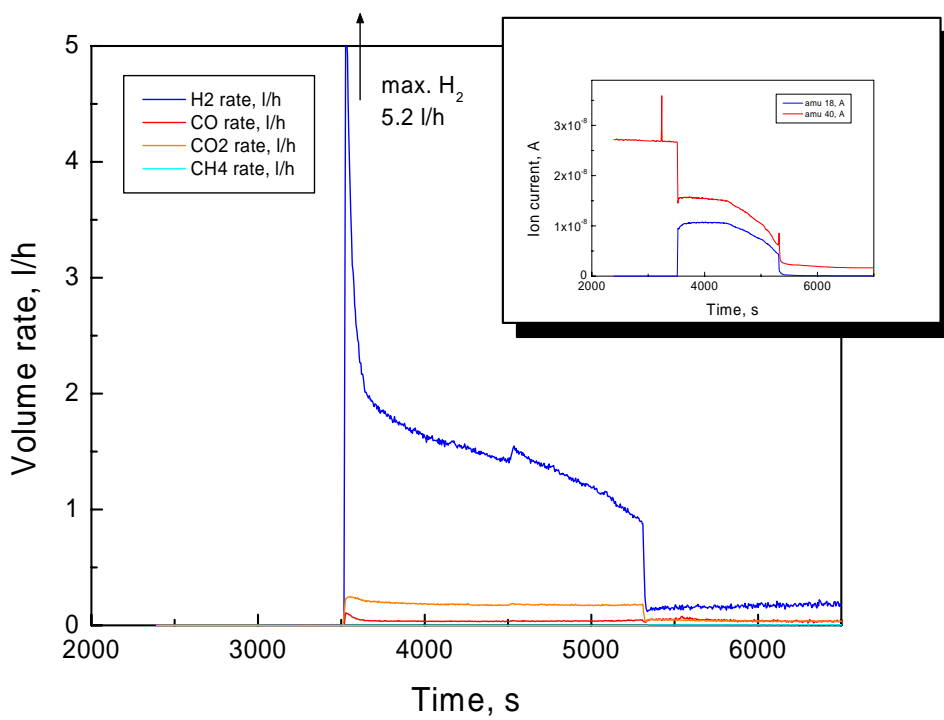
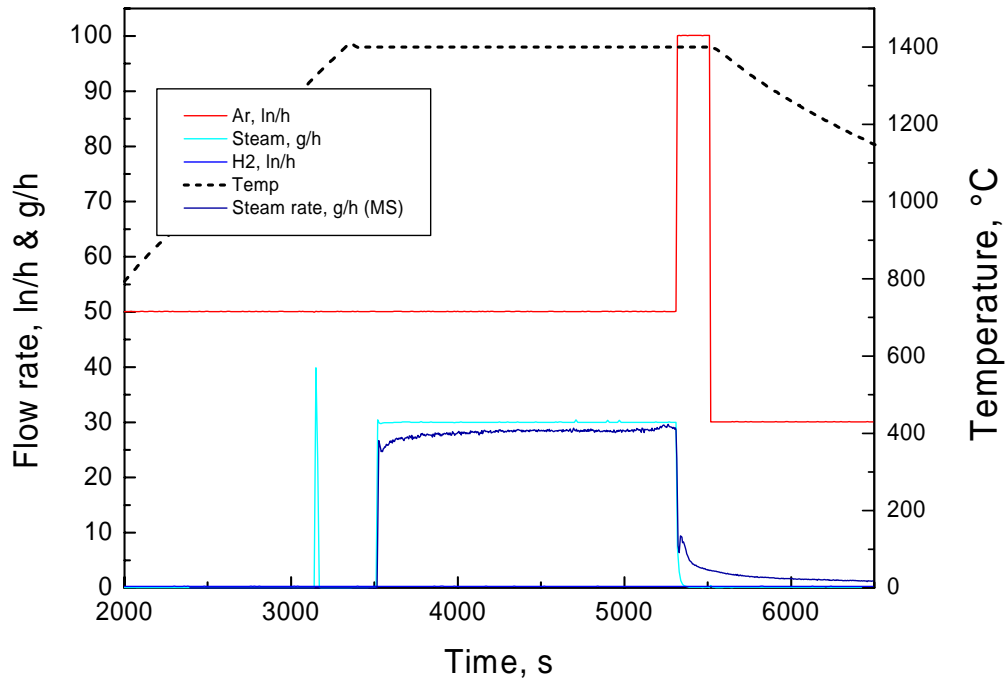
Isothermal oxidation of a CODEX B₄C pellet
in Ar/steam at 1000 °C



Test Box10911: Isothermal oxidation of a CODEX B₄C pellet in Ar/steam at 1200 °C

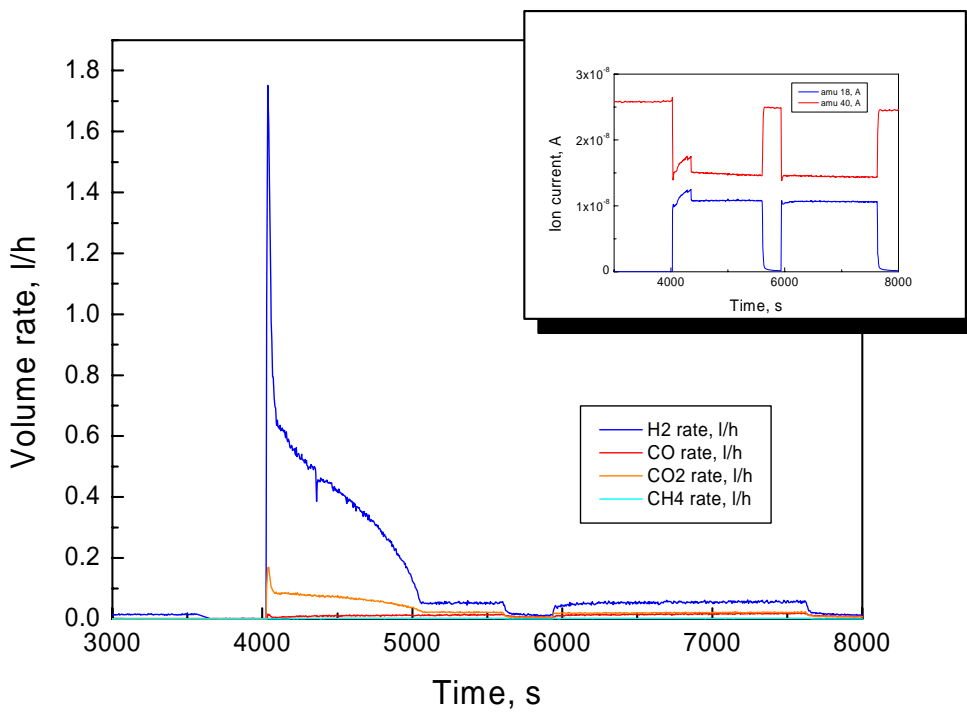
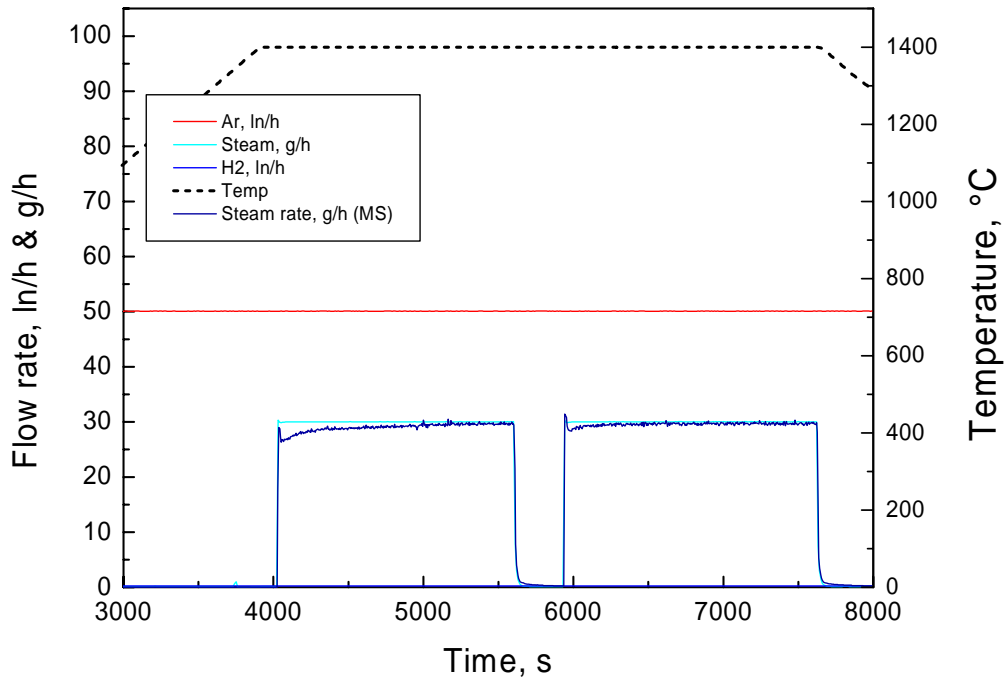


Test Box10912:
 sothermal oxidation of a CODEX B₄C pellet
 in Ar/steam at 1400 °C



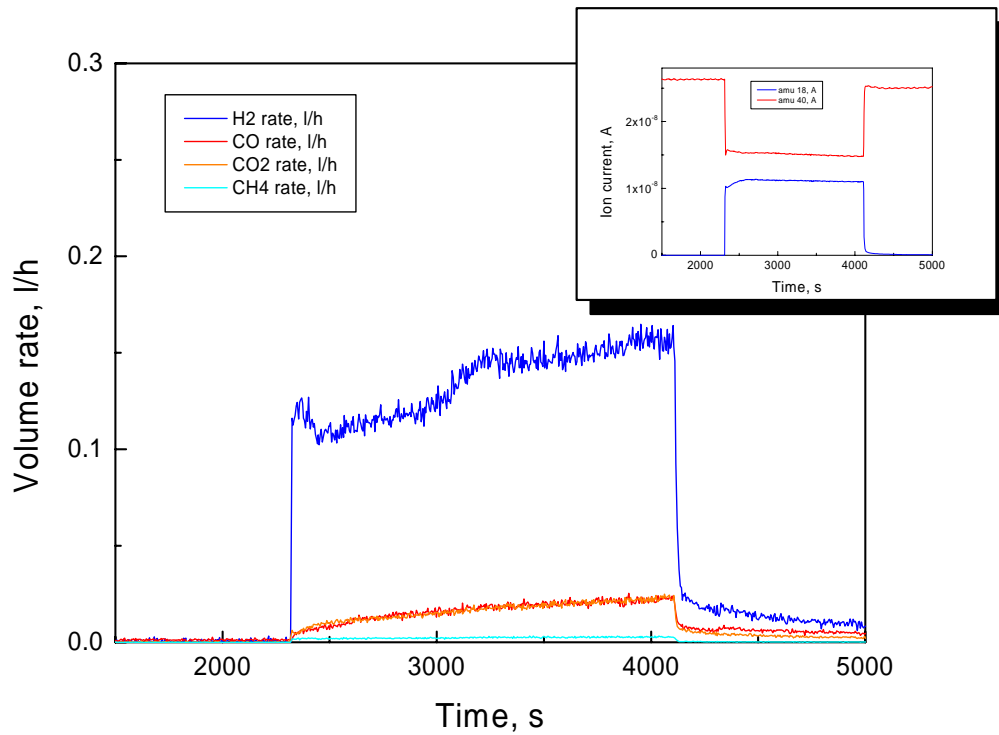
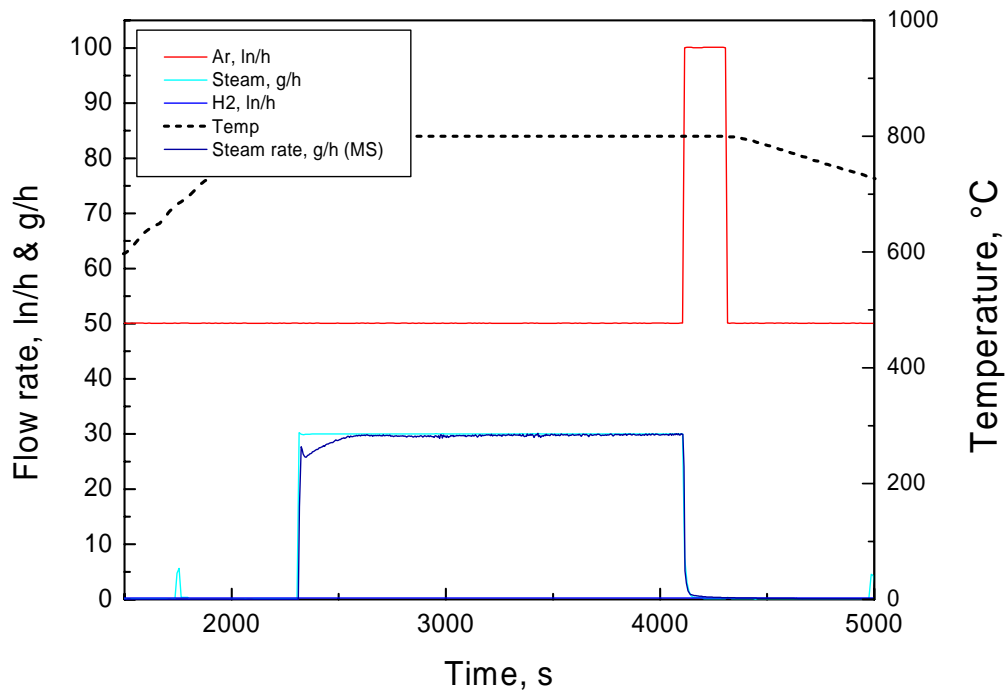
Test Box10914:

Complete oxidation of a small B_4C specimen in Ar/steam at 1400 °C

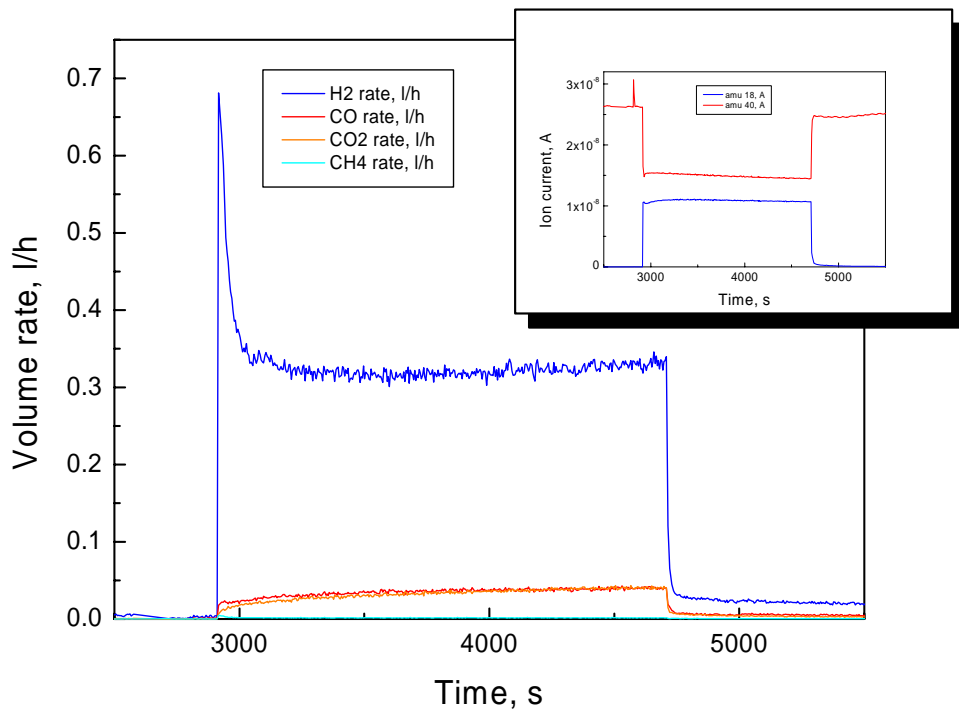
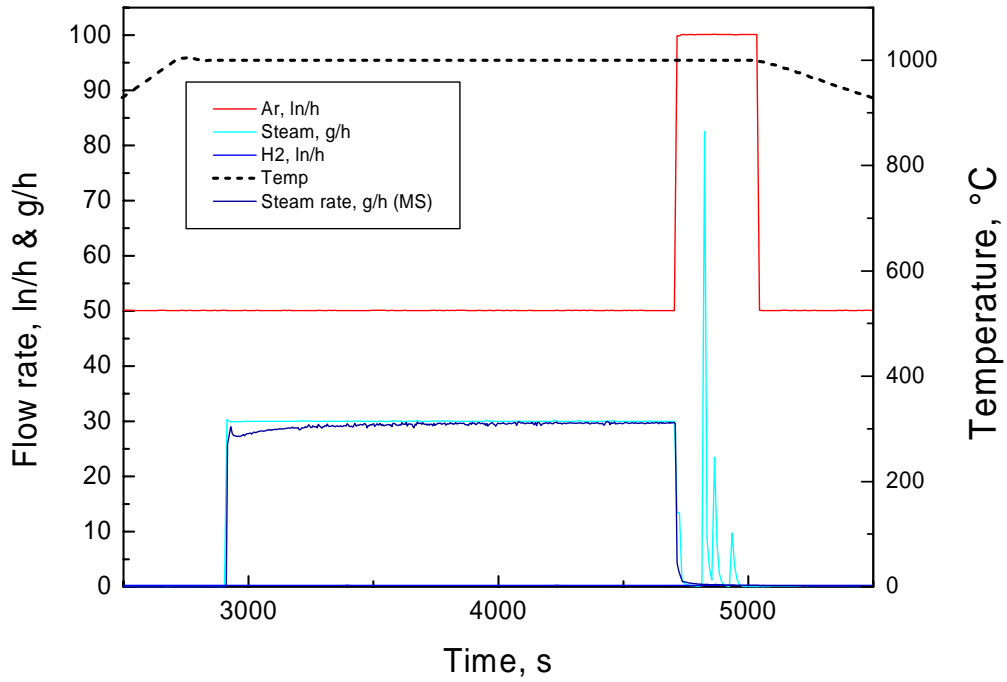


Test Box10927:

Isothermal oxidation of a ESK B₄C pellet in Ar/steam at 800 °C

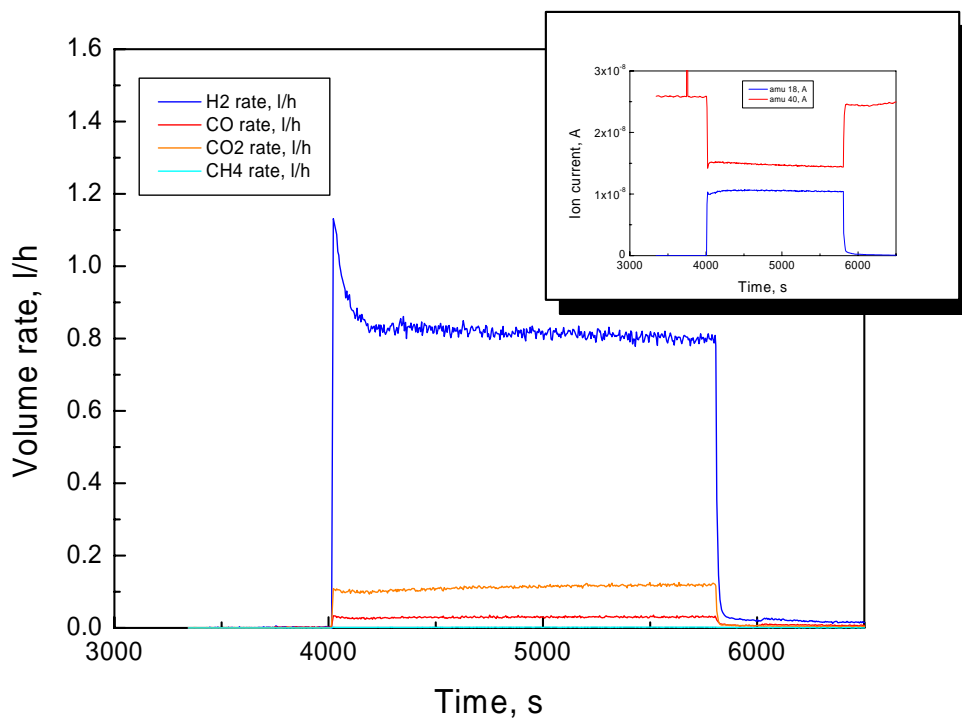
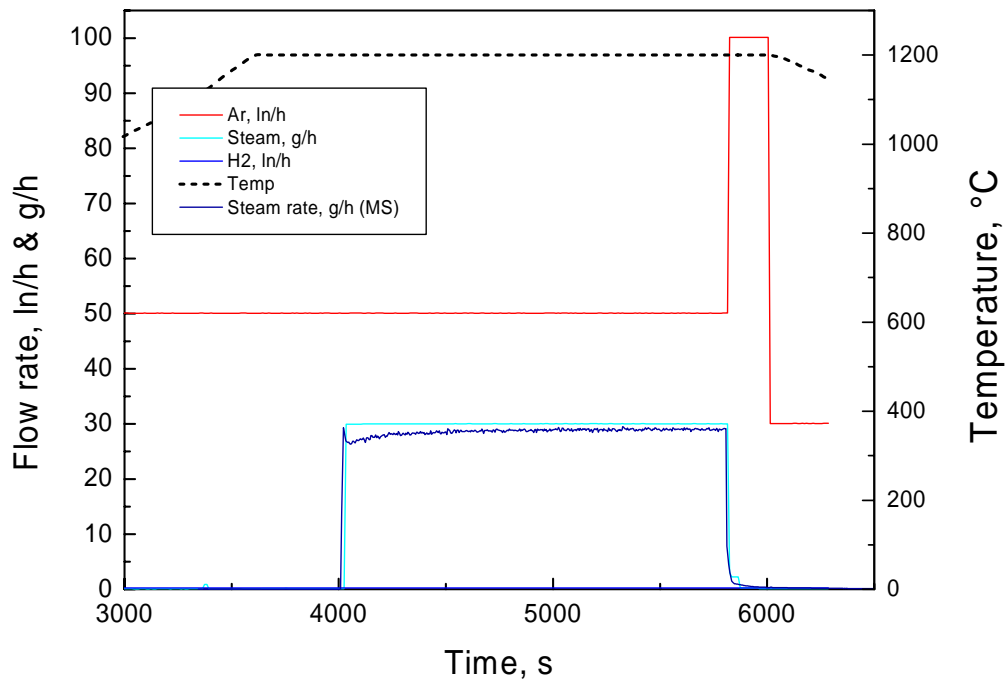


Test Box11001: Isothermal oxidation of a ESK B₄C pellet in Ar/steam at 1000 °C

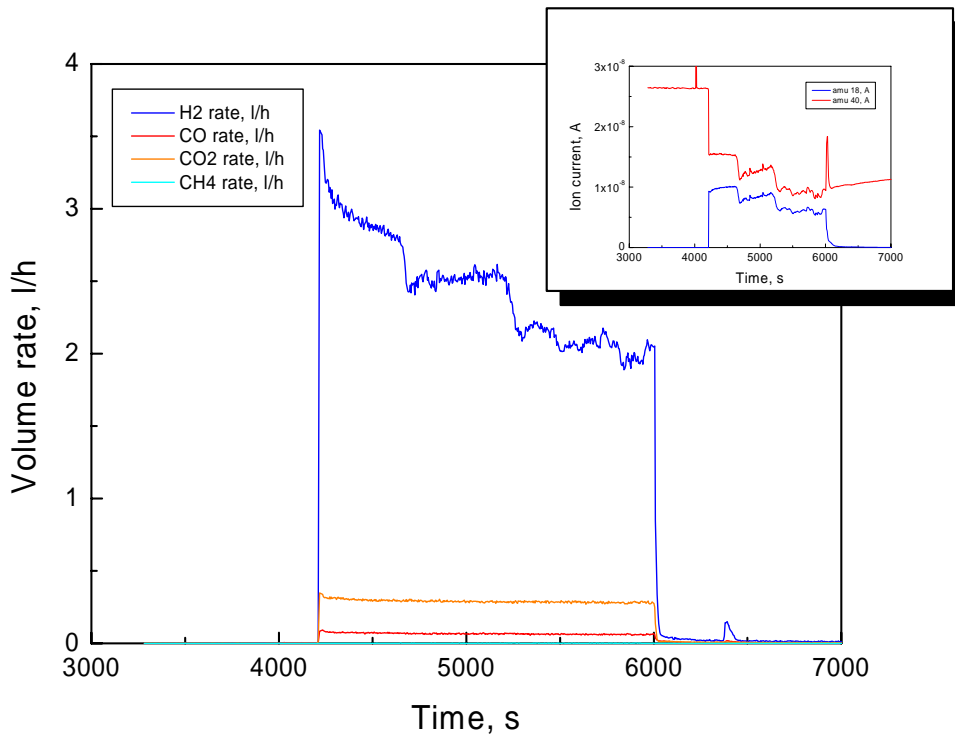
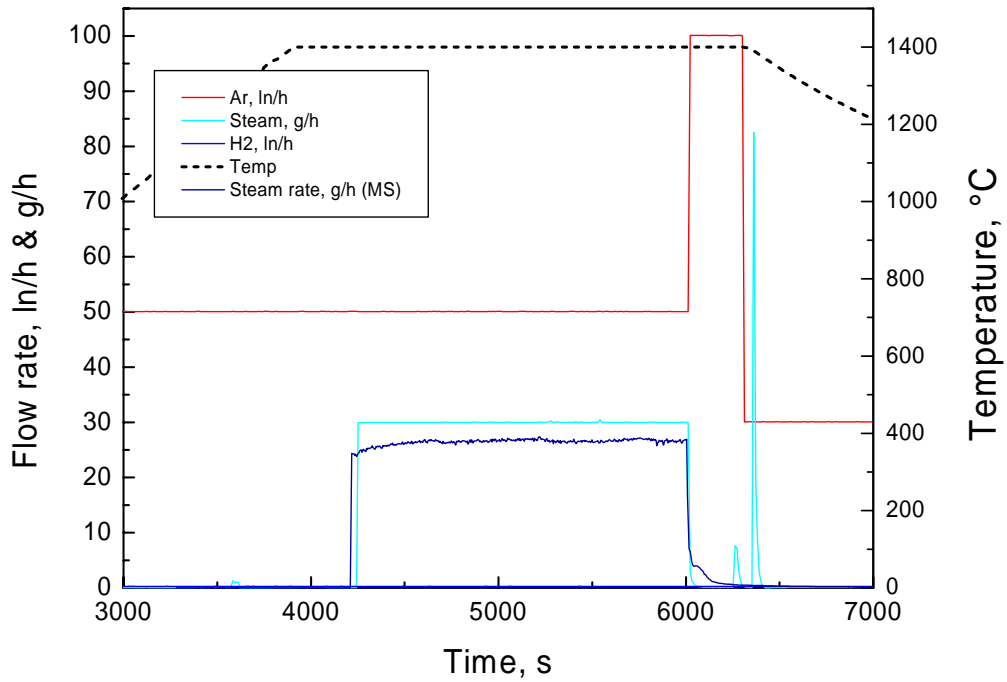


Test Box11002:

Isothermal oxidation of a ESK B₄C pellet in Ar/steam at 1200 °C

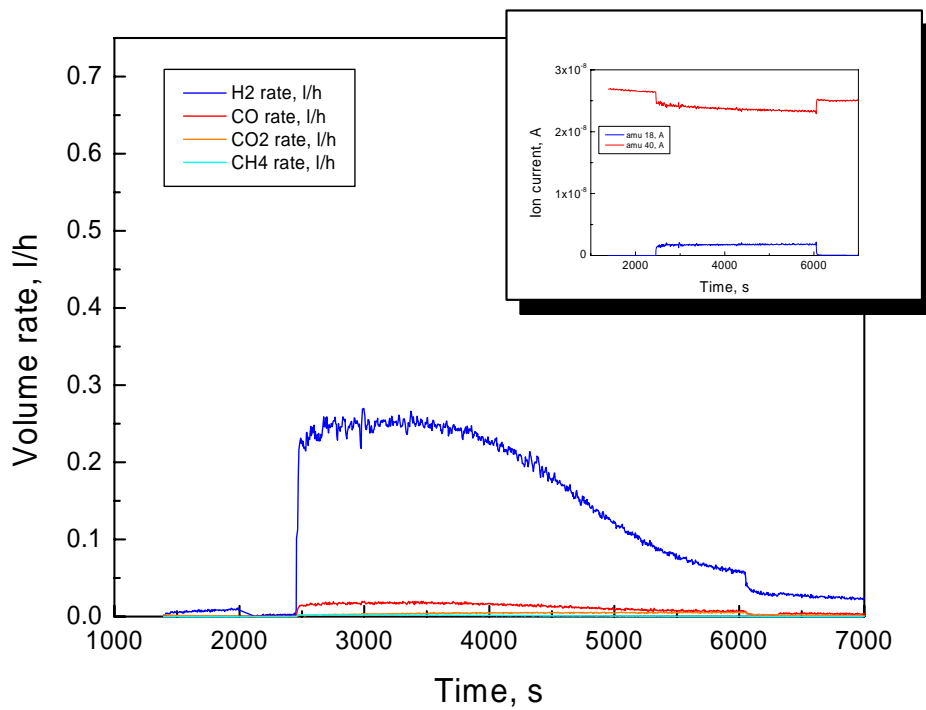
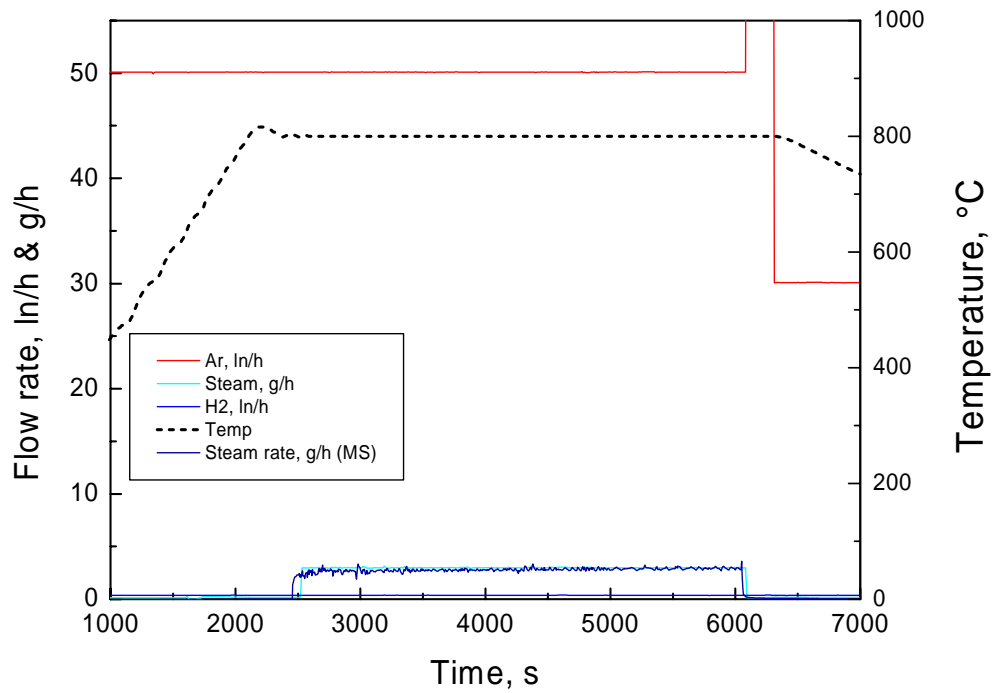


Test Box11004: Isothermal oxidation of a ESK B₄C pellet in Ar/steam at 1400 °C



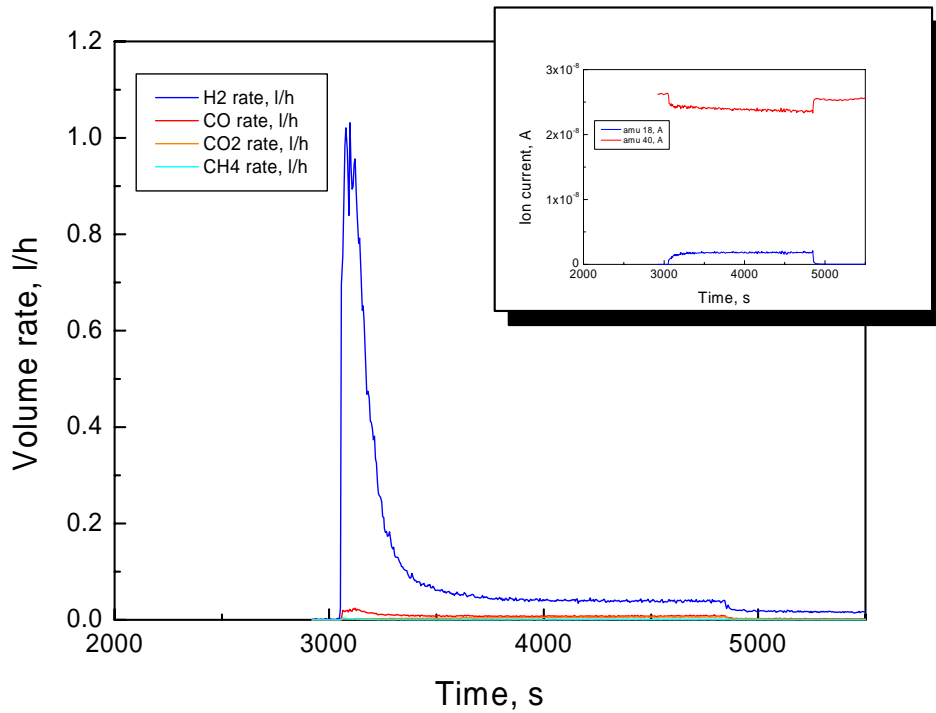
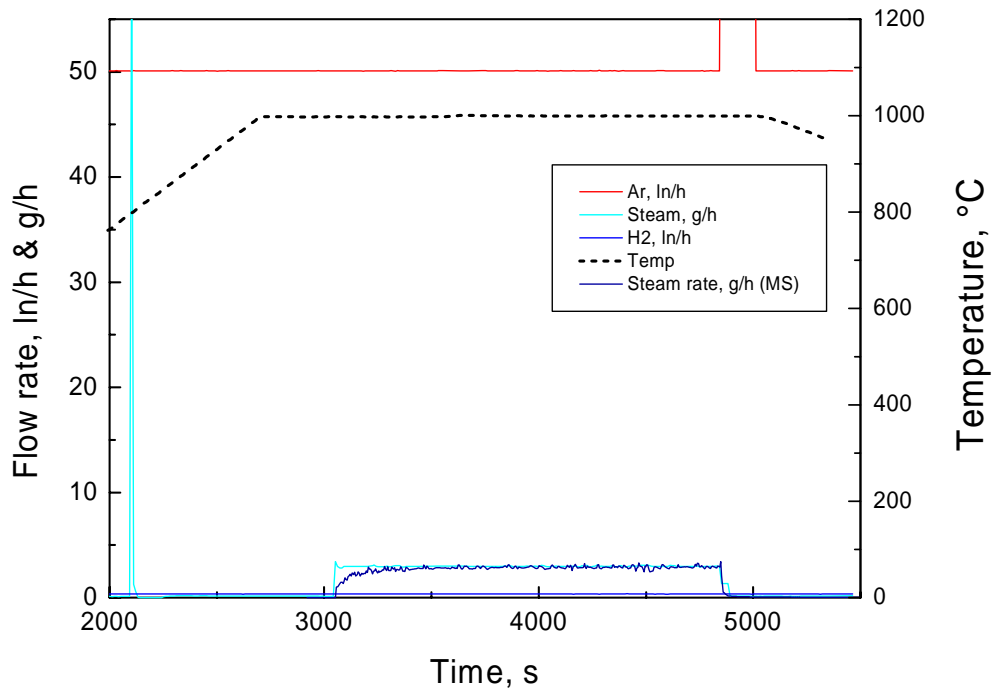
Test Box20304:

Isothermal oxidation of a Framatome B₄C pellet in Ar/steam at 800 °C (low steam)



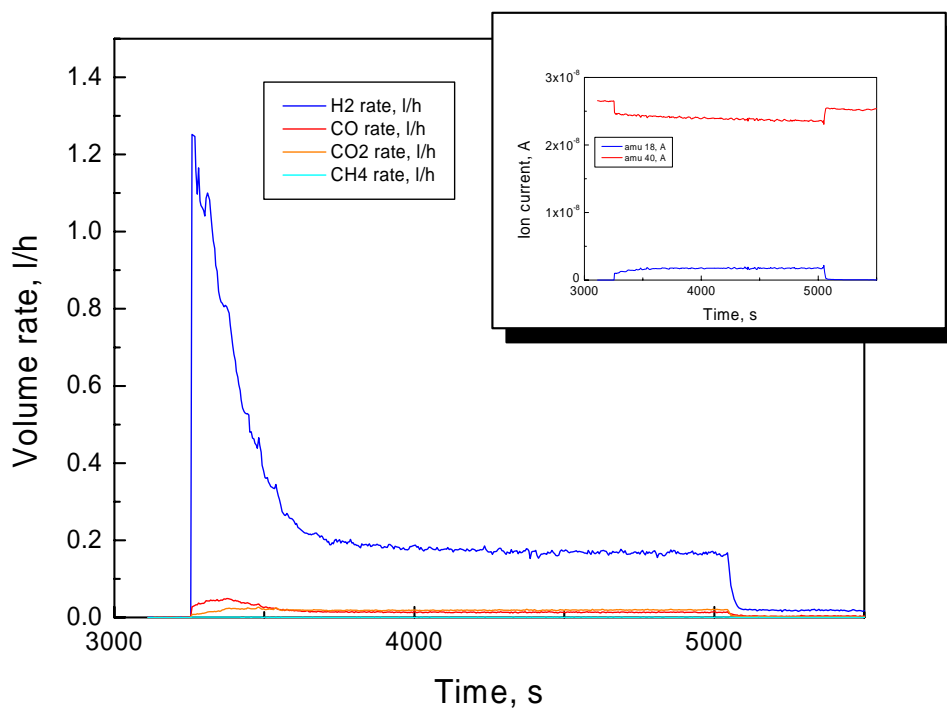
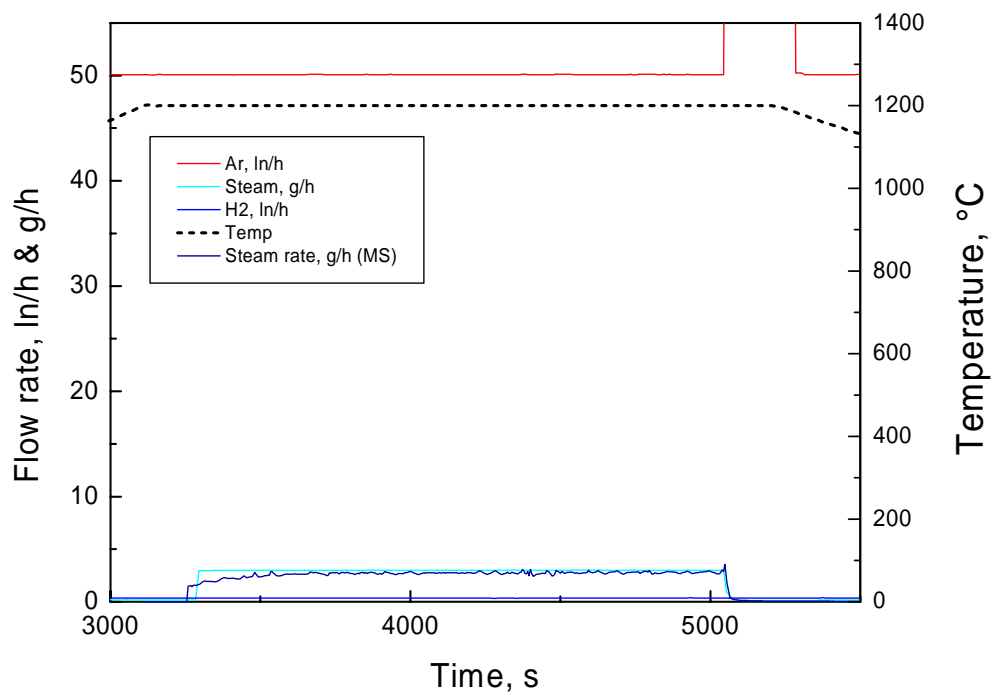
Test Box20305:

Isothermal oxidation of a Framatome B₄C pellet in Ar/steam at 1000 °C (low steam)



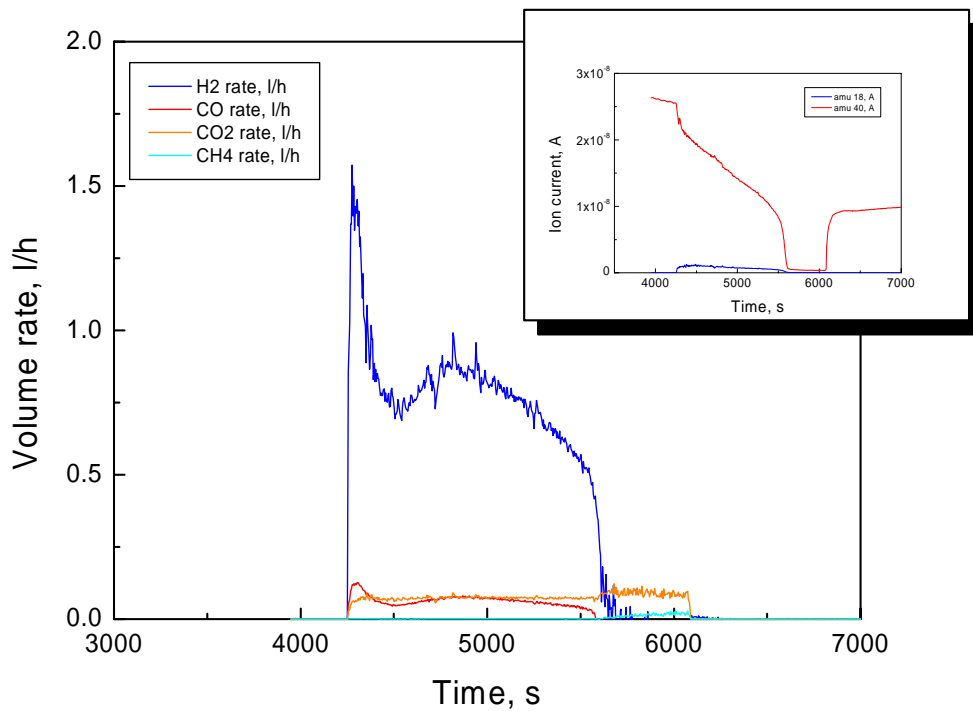
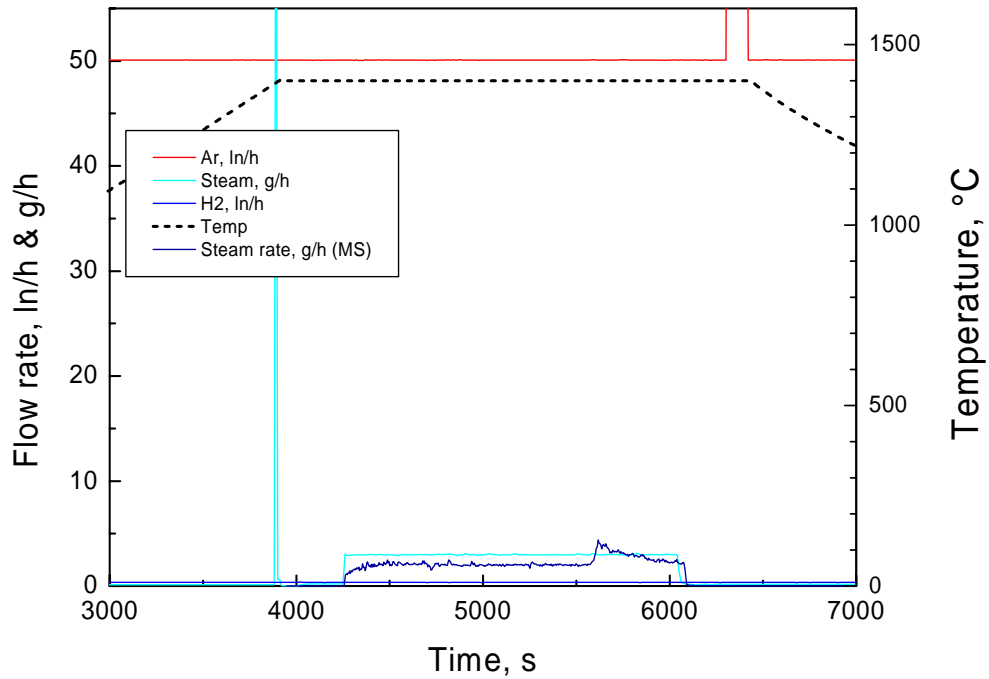
Test Box20306:

Isothermal oxidation of a Framatome B₄C pellet
in Ar/steam at 1200 °C (low steam)



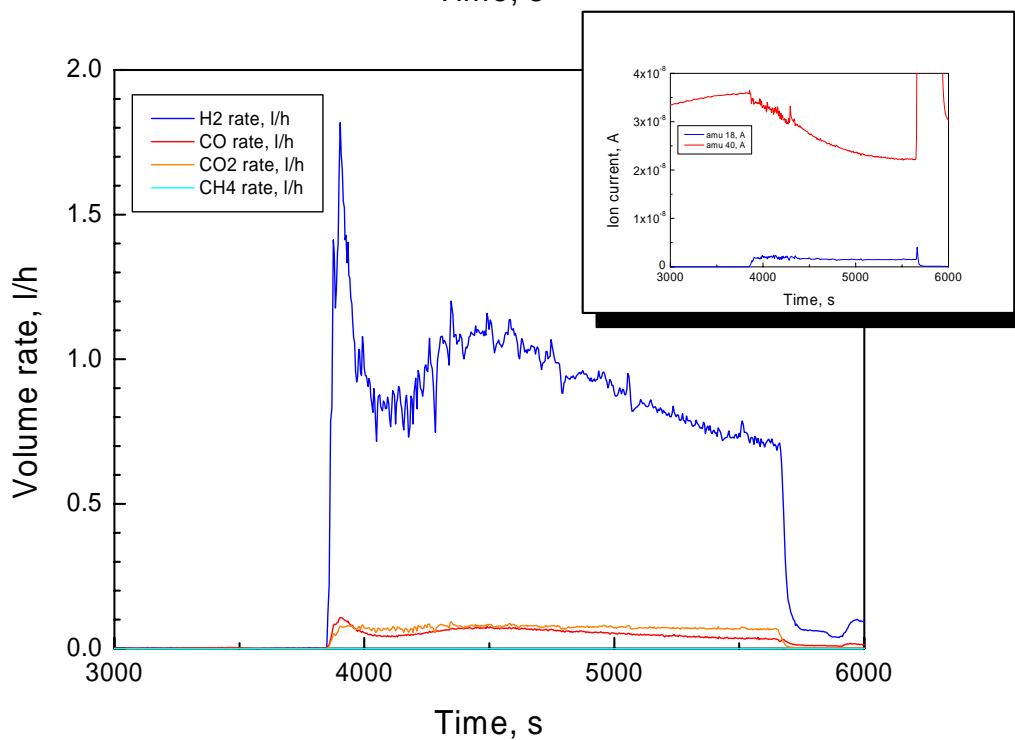
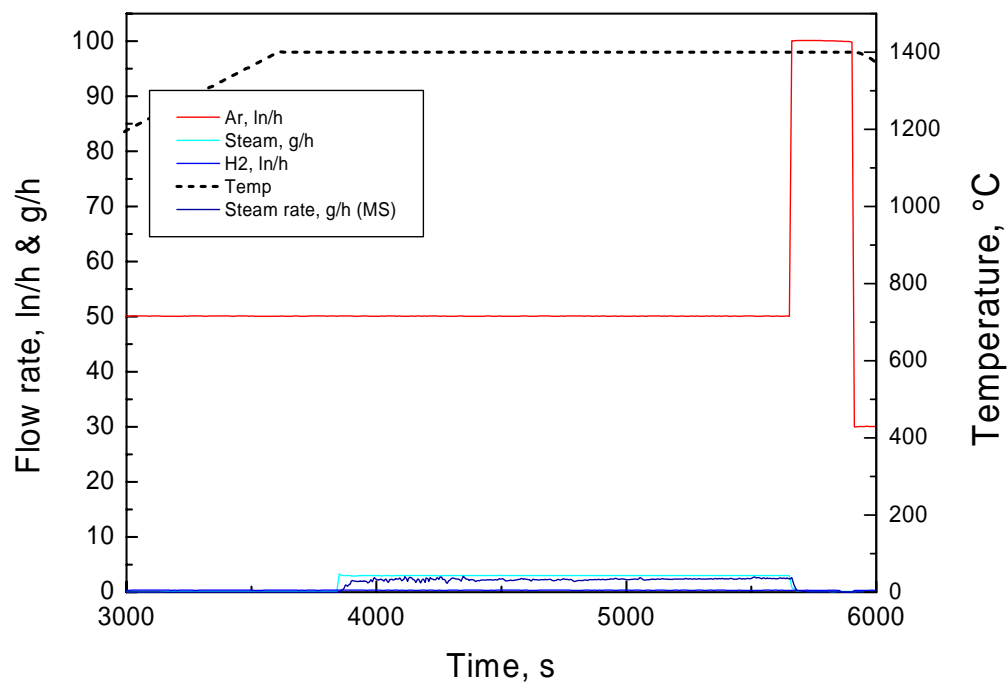
Test Box20307:

Isothermal oxidation of a Framatome B₄C pellet
in Ar/steam at 1400 °C (low steam)



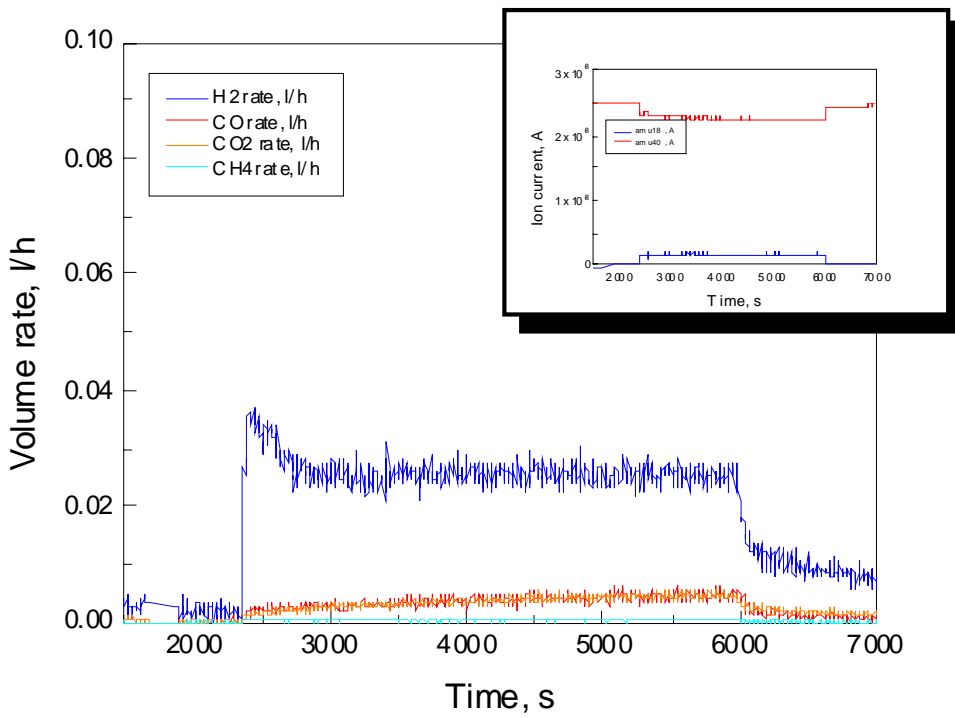
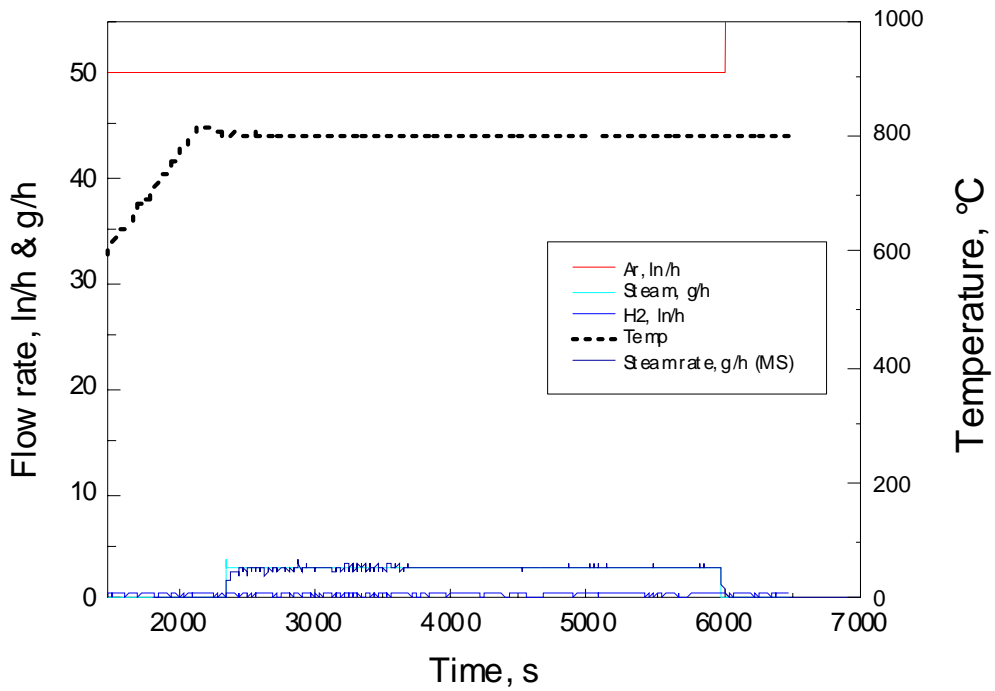
Test Box20313:

Isothermal oxidation of a Framatome B₄C pellet
in Ar/steam at 1400 °C (low steam)



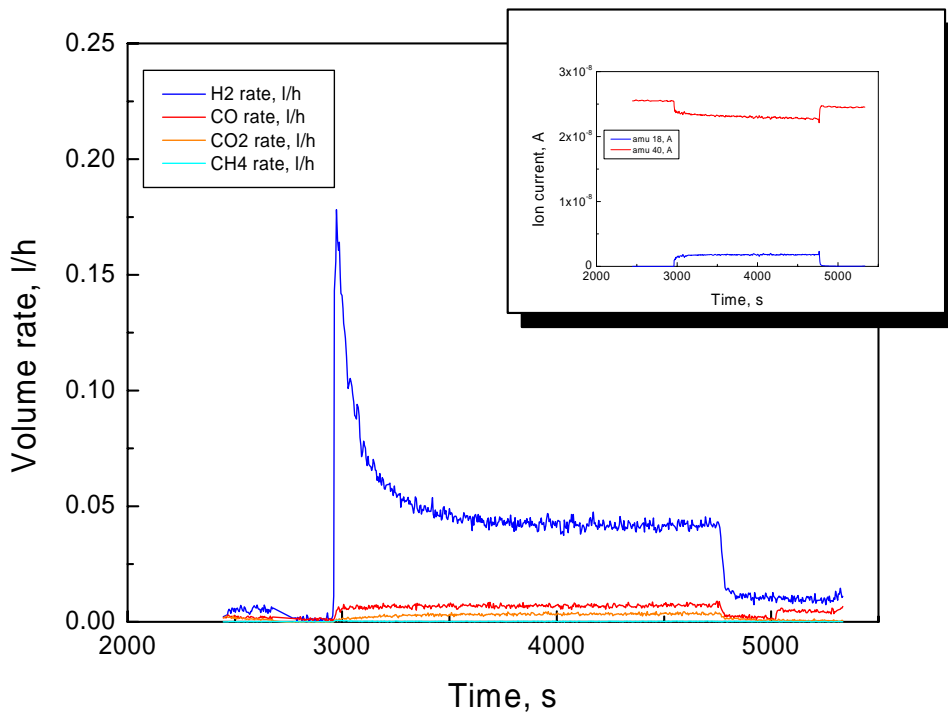
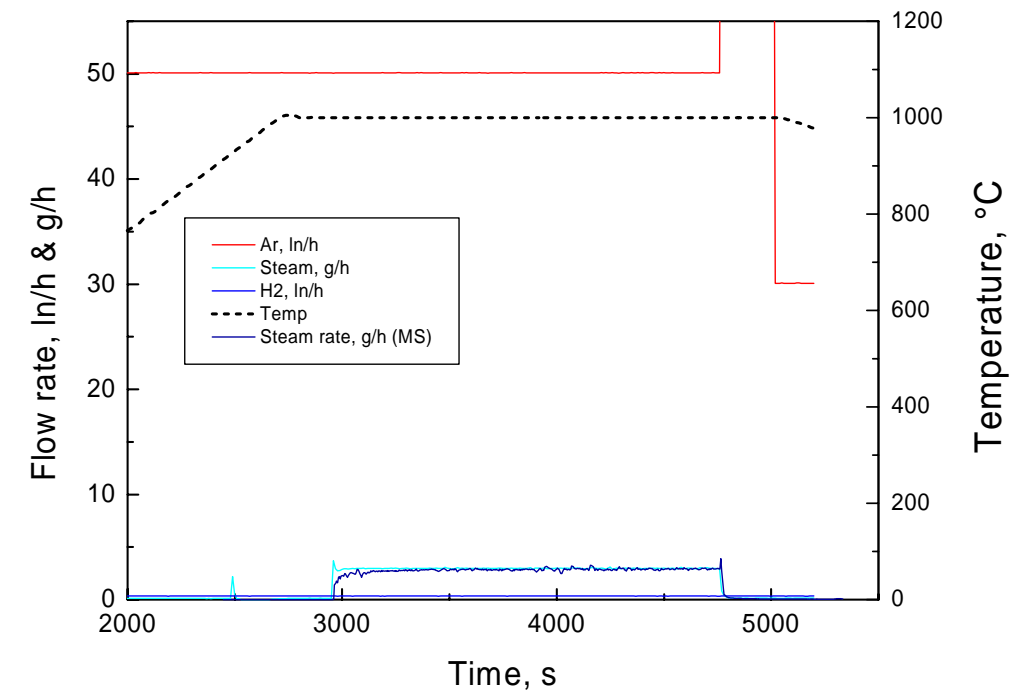
Test Box20409:

Isothermal oxidation of a ESK B₄C pellet in Ar/steam at 800 °C (low steam)



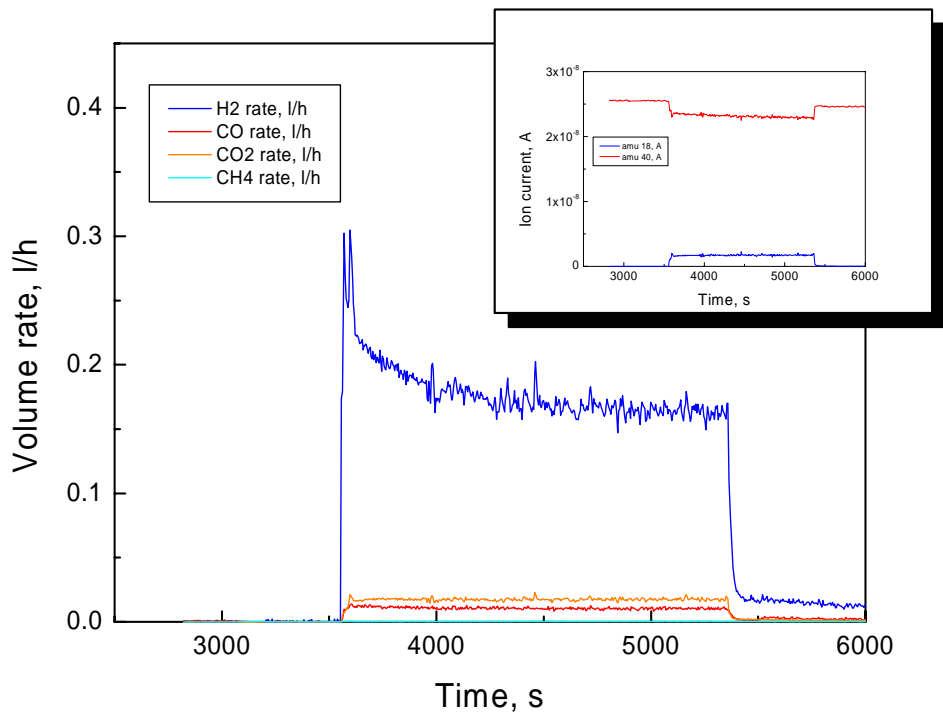
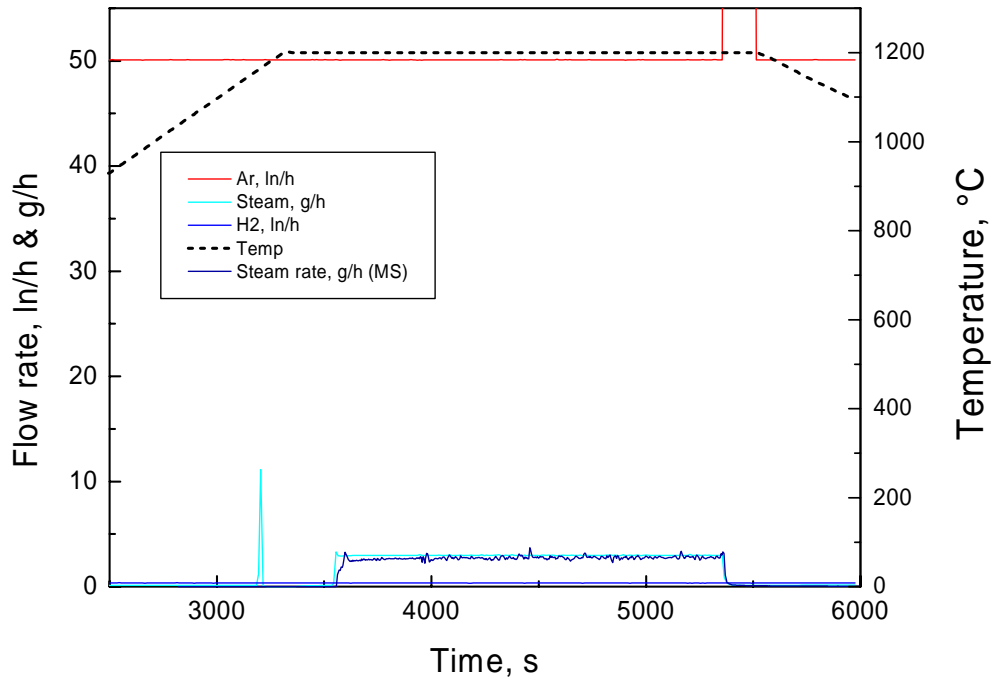
Test Box20410:

Isothermal oxidation of a ESK B₄C pellet
in Ar/steam at 1000 °C (low steam)



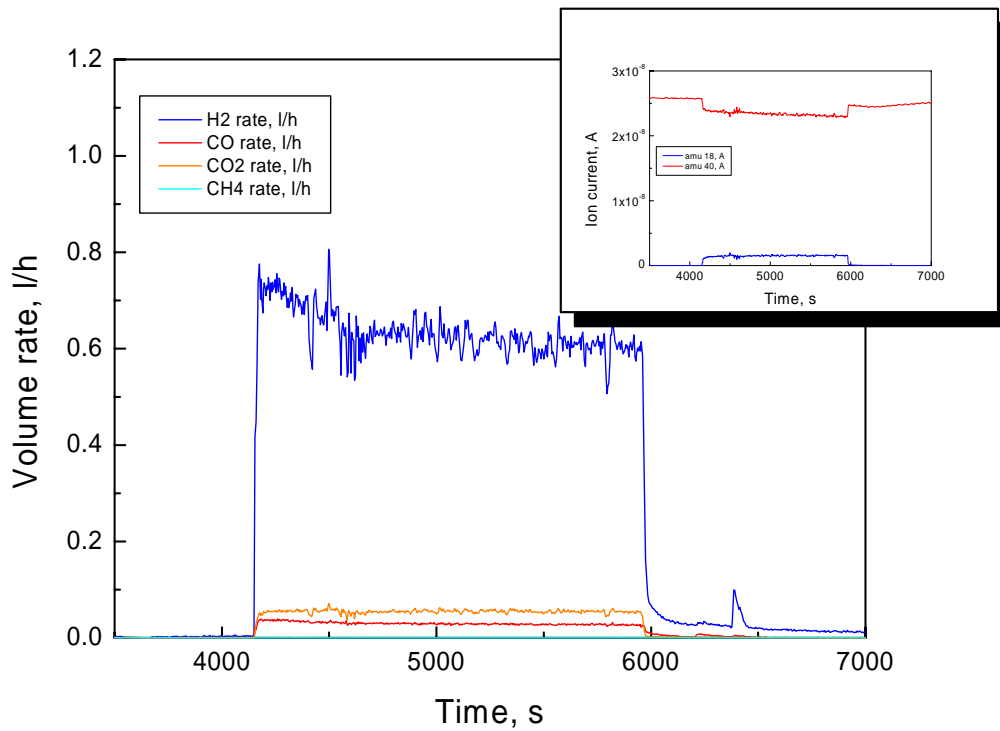
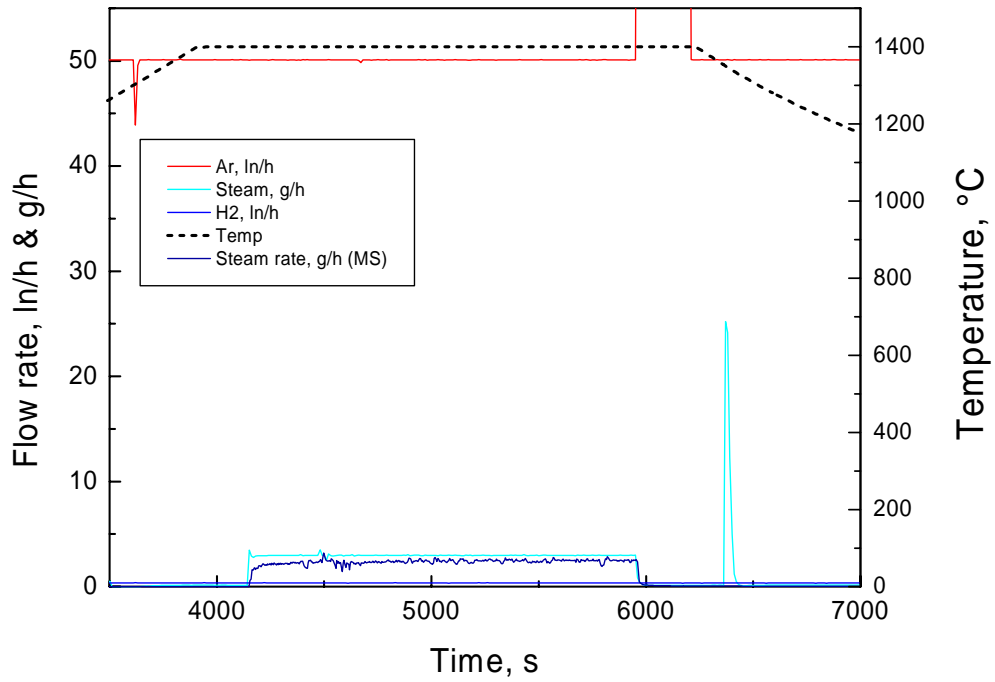
Test Box20411:

Isothermal oxidation of a ESK B₄C pellet
in Ar/steam at 1200 °C (low steam)



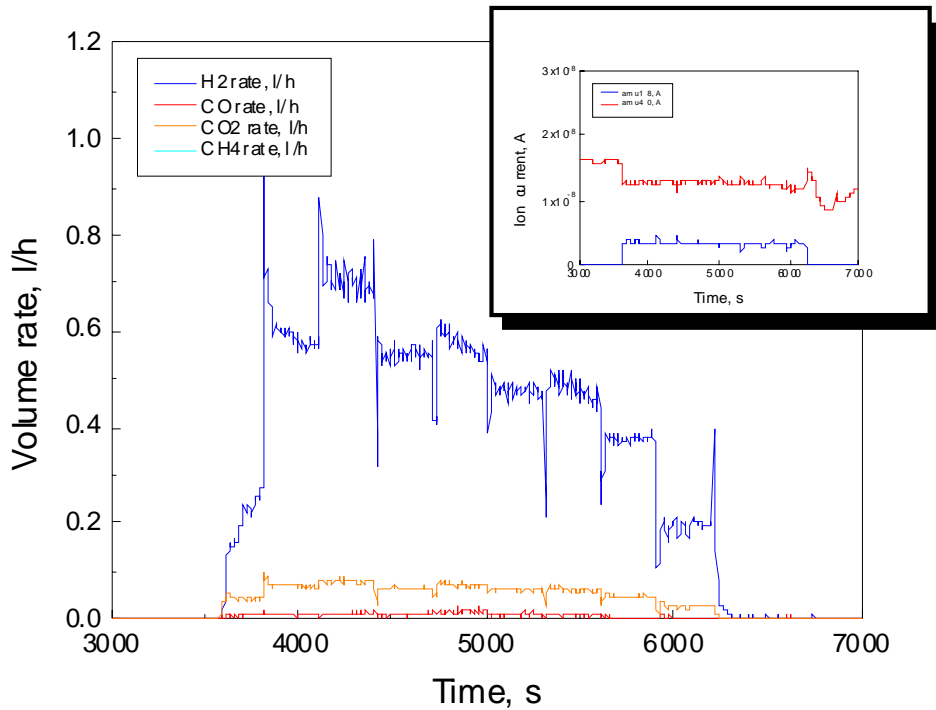
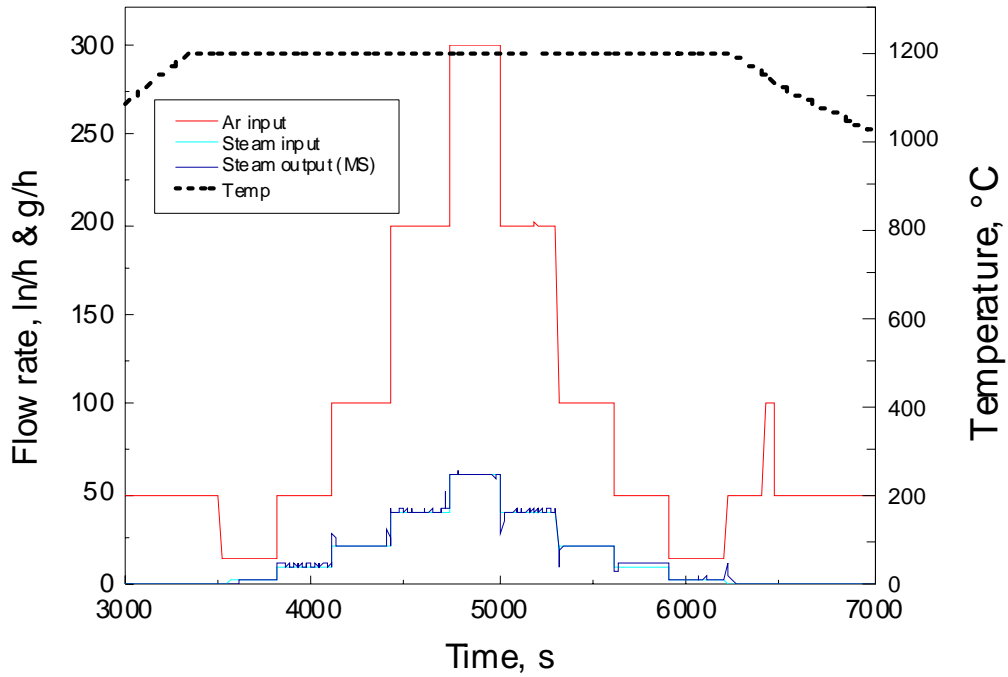
Test Box20416:

Isothermal oxidation of a ESK B₄C pellet in Ar/steam at 1400 °C (low steam)



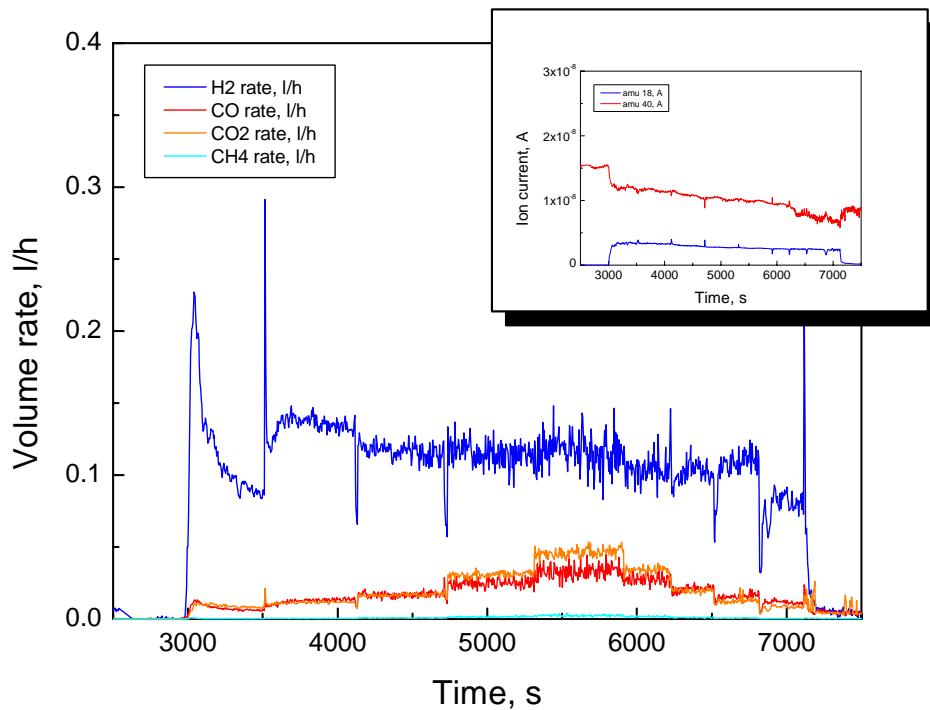
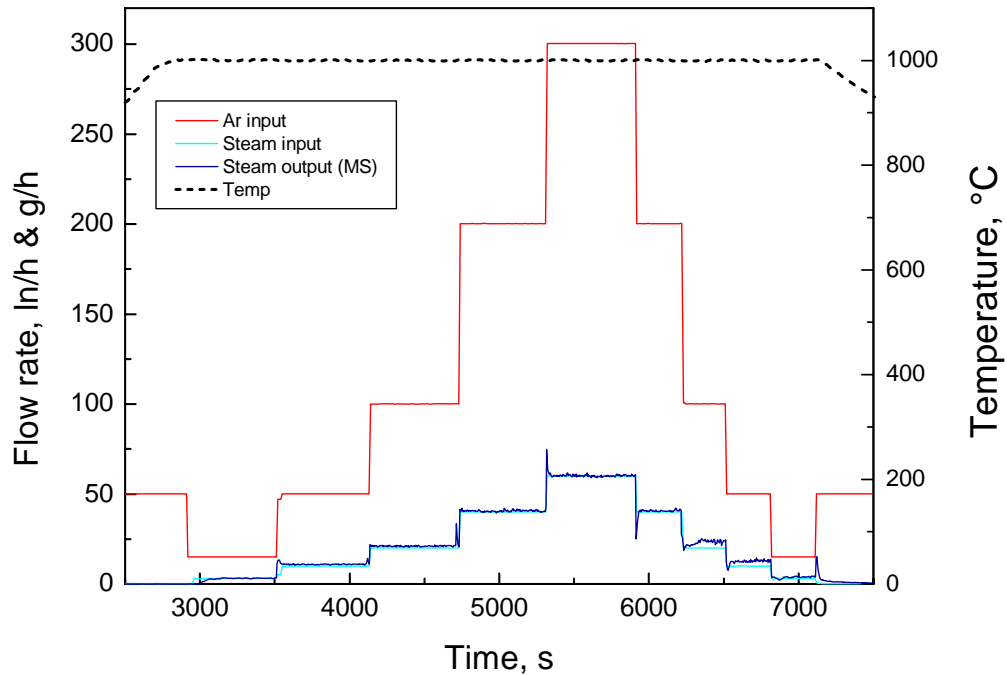
Test Box30509:

Isothermal oxidation of a ESK B₄C pellet at 1200 °C under varying gas flow rates (IBRAE proposal)



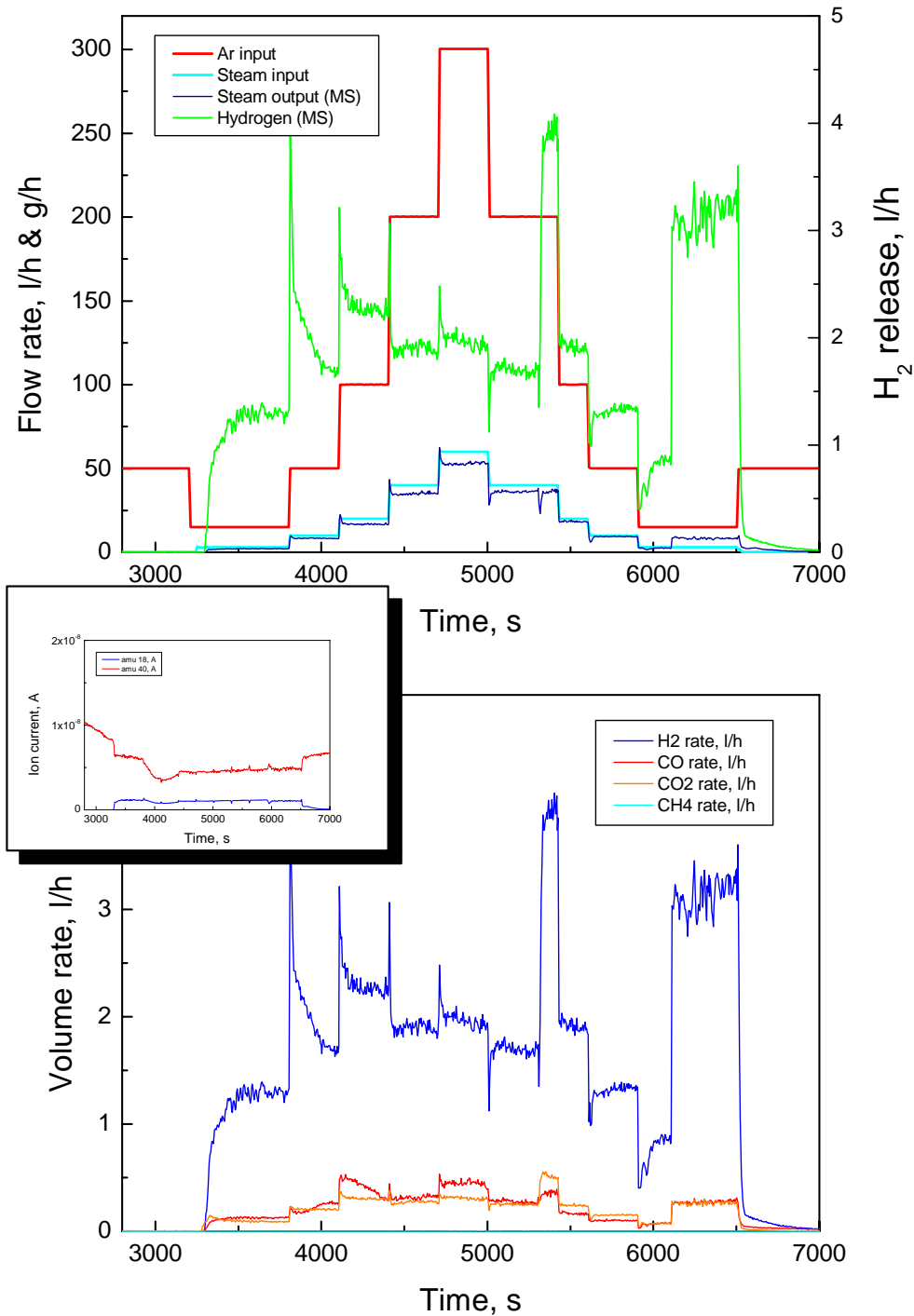
Test Box30512a:

Isothermal oxidation of a ESK B₄C pellet at 1000 °C under varying gas flow rates (IBRAE proposal)



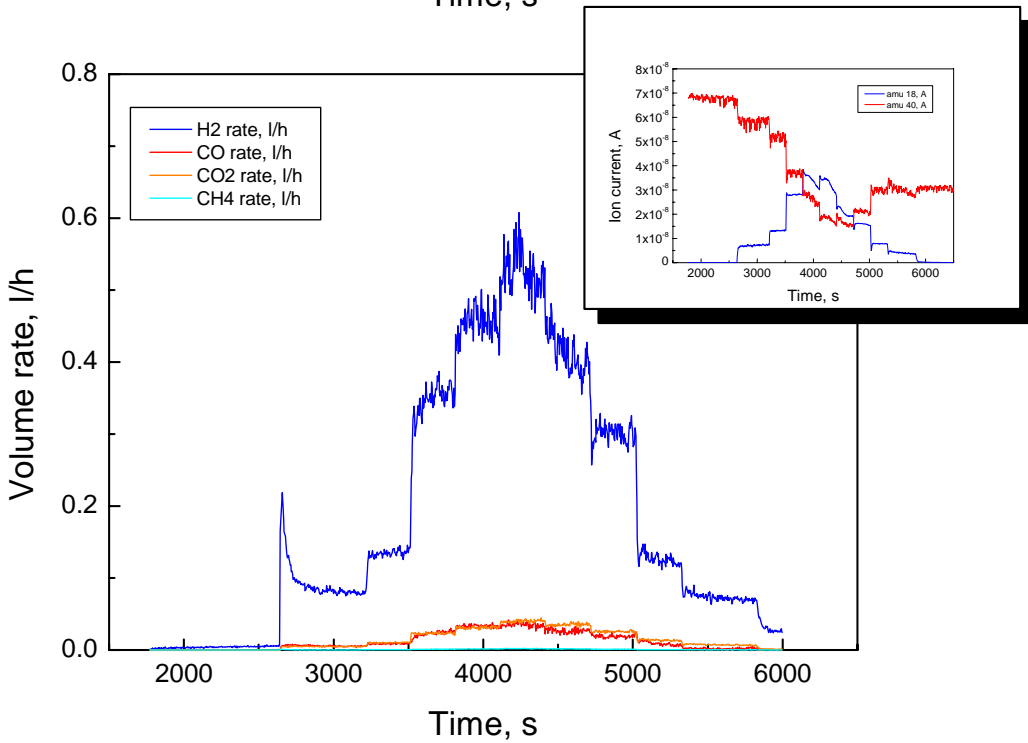
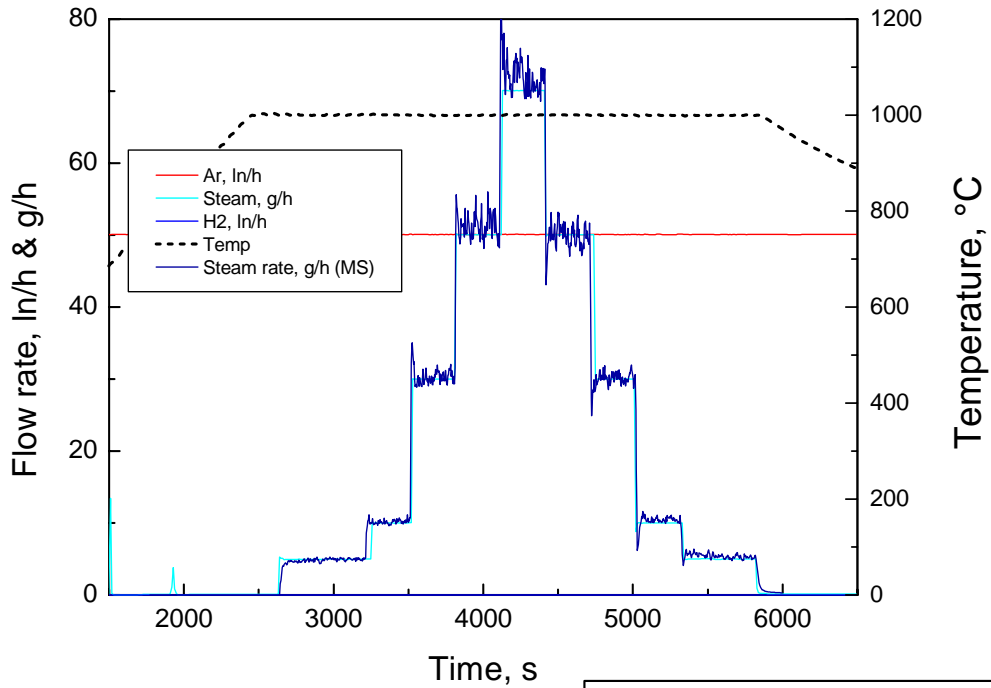
Test Box30512c:

Isothermal oxidation of a ESK B₄C pellet at 1400 °C under varying gas flow rates (IBRAE proposal)



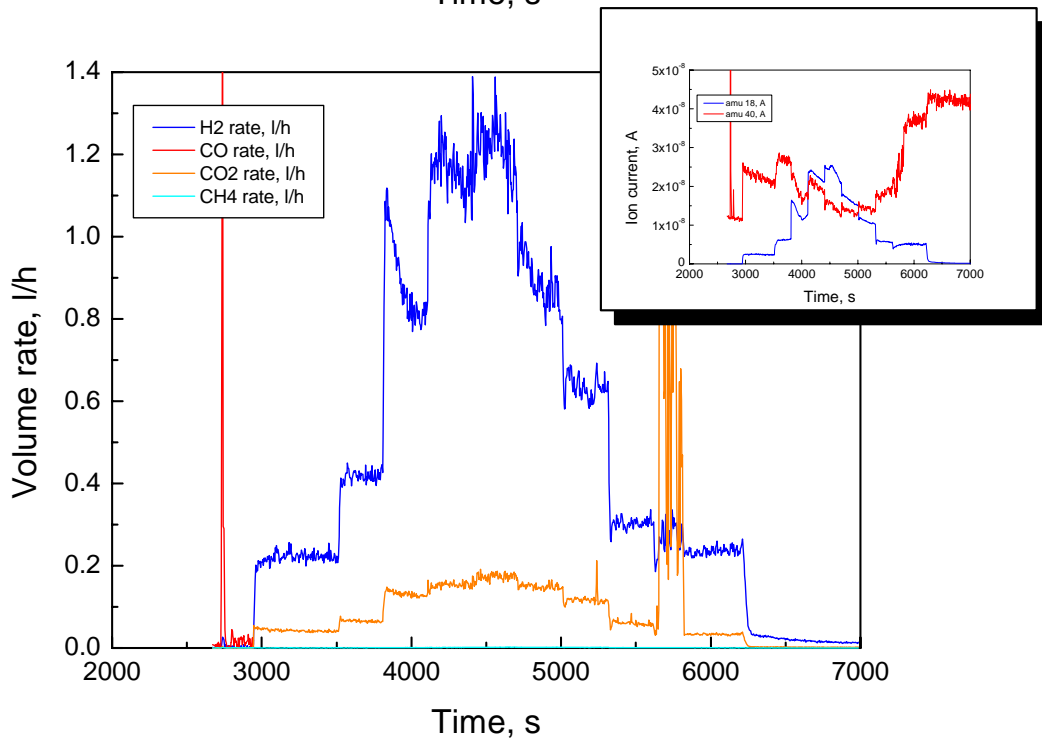
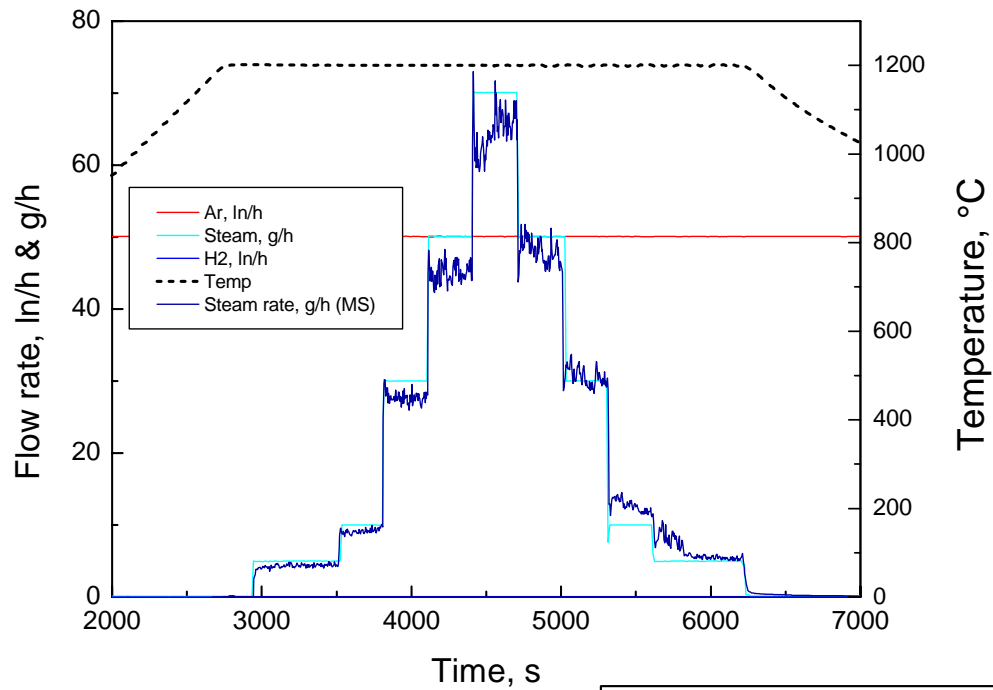
Test Box30520:

Isothermal oxidation of a ESK B₄C pellet in Ar/steam at 1000 °C. Variation of the steam flow rate



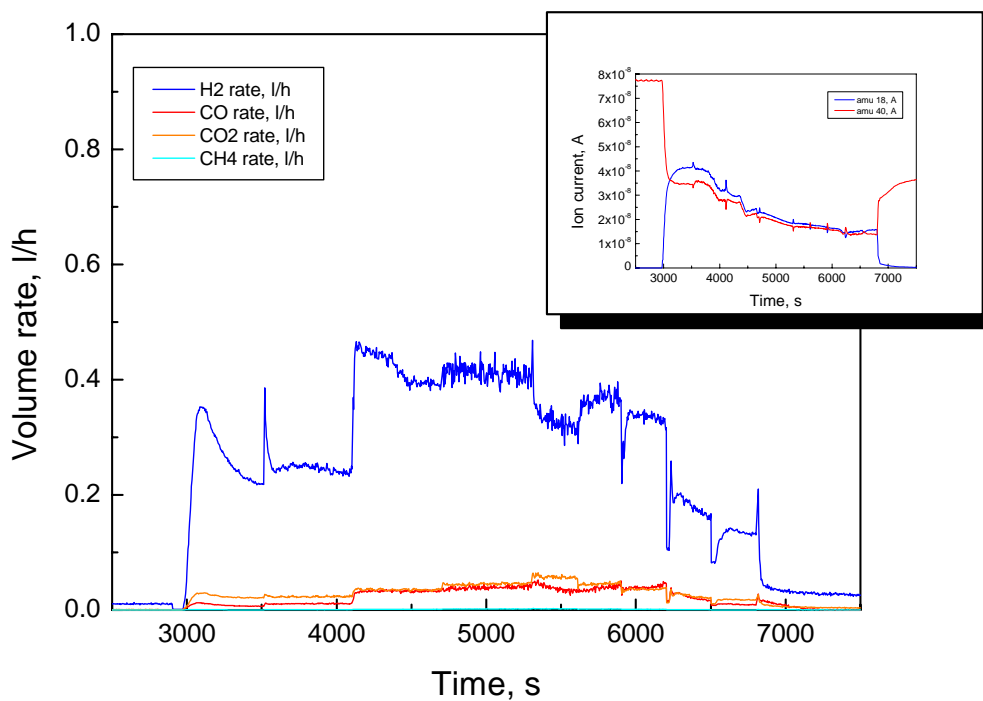
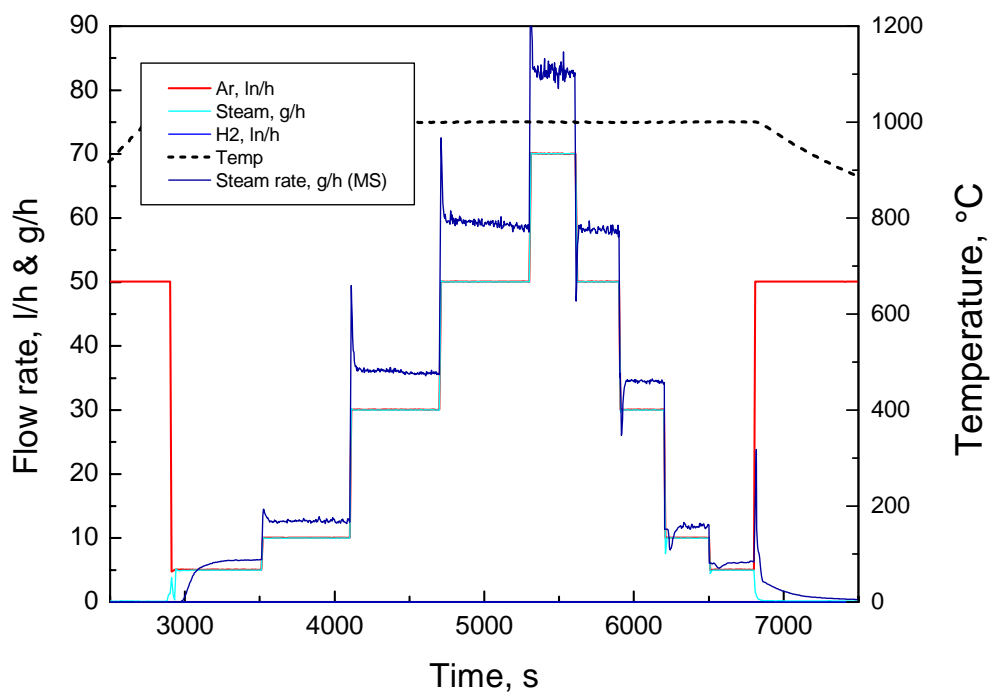
Test Box30521:

Isothermal oxidation of a ESK B₄C pellet in Ar/steam at 1200 °C. Variation of the steam flow rate



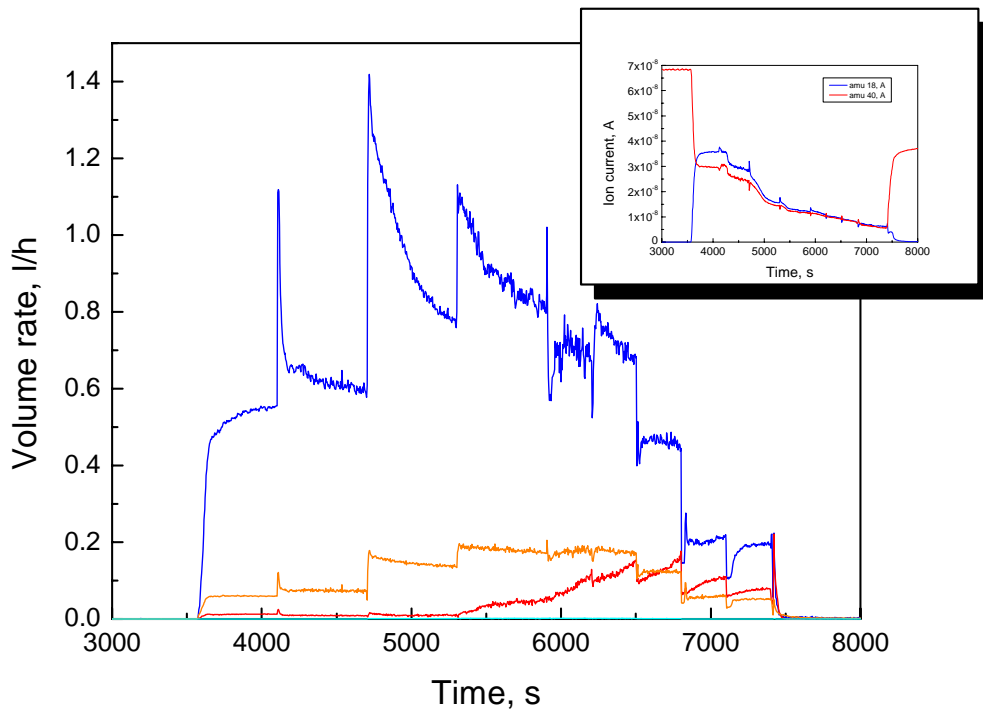
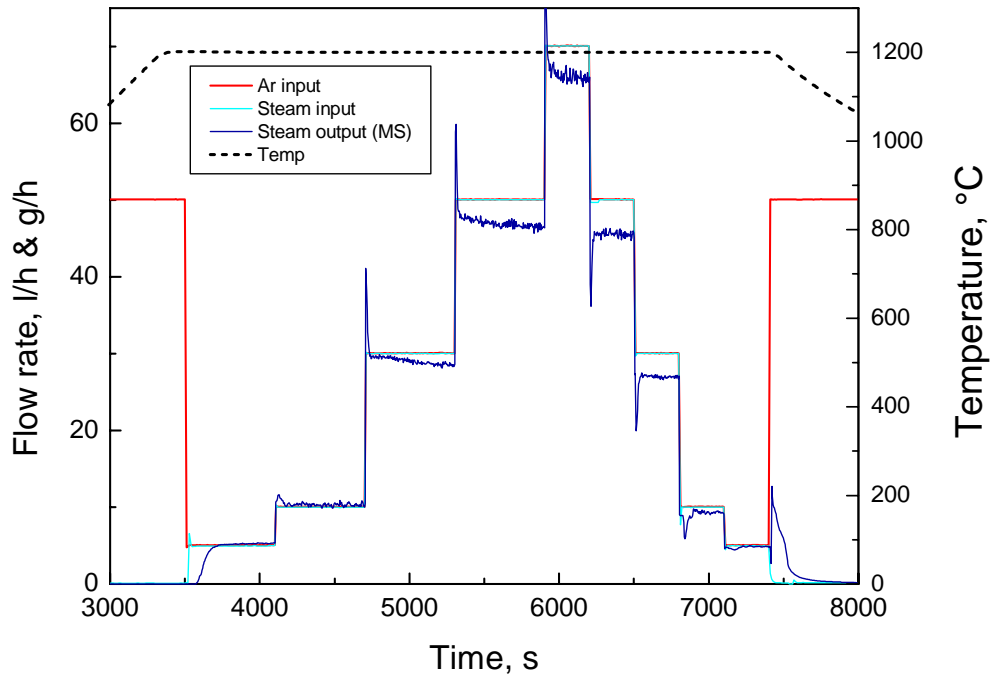
Test Box30916:Isothermal oxidation of an ESK B₄C pellet

in Ar/steam under varying flow rates at 1000 °C



Test Box30917:

Isothermal oxidation of a ESK B₄C pellet at 1200 °C under varying gas flow rates (IBRAE proposal)



Test Box30924:Isothermal oxidation of an ESK B₄C pellet

under varying steam partial pressure at 1000 °C

